

Silicon Detectors in High Energy Physics

Thomas Bergauer (HEPHY Vienna)

Semiconductor Basics

- Introduction
- Basics
 - Material properties
 - Doping of Silicon
 - The pn-junction
 - Detector characteristics
- Manufacturing of Silicon Detectors
 - The Planar Process
- Signal Generation

INTRODUCTION

Where are semiconductor detector used?

- **Nuclear Physics**

- Energy measurement of charged particles (MeV range),
- Gamma spectroscopy (precise determination of photon energy)

- **Particle Physics**

- Tracking or vertex detectors, precise determination of particle tracks and decay vertices

- **Satellite Experiments**

- Tracking detectors

- **Industrial Applications**

- Security, Medicine, Biology,...

Advantages of semiconductor detectors

- Semiconductor detectors have a **high density**
 - large energy loss in a short distance
 - Diffusion effect is smaller than in gas detectors resulting in achievable position resolution of less than 10 μm
- **Low ionization energy** (few eV per e-hole pair) compared to
 - gas detectors (20-40 eV per e-ion pair) or
 - scintillators (400-1000 eV to create a photon).
- **Large experience in industry** with micro-chip technology (silicon).
- **Easy integration with readout electronics** due to identical materials used (silicon)
- High intrinsic radiation hardness

Disadvantages of semiconductor detectors

- No internal amplification, i.e. small signal
 - with a few exceptions
- High cost per surface unit
 - Not only Silicon itself
 - High number of readout channels
 - Large power consumption → cooling

Semiconductor basics and Detector characteristics

BASICS

Elemental Semiconductors

- **Germanium:**
 - Used in nuclear physics
 - Needs cooling due to small band gap of 0.66 eV (usually done with liquid nitrogen at 77 K)
- **Silicon:**
 - Can be operated at room temperature
 - Synergies with micro electronics industry
 - Standard material for vertex and tracking detectors in high energy physics
- **Diamond (CVD or single crystal):**
 - Allotrope of carbon
 - Large band gap (requires no depletion zone)
 - very radiation hard
 - Disadvantages: low signal and high cost

Compound Semiconductors

- Compound semiconductors consist of
 - two (binary semiconductors) or
 - more than two
 atomic elements of the periodic table.
- Depending on the column in the periodic system of elements one differentiates between
 - IV-IV- (e.g. *SiGe*, *SiC*),
 - III-V- (e.g. *GaAs*)
 - II-VI compounds (*CdTe*, *ZnSe*)

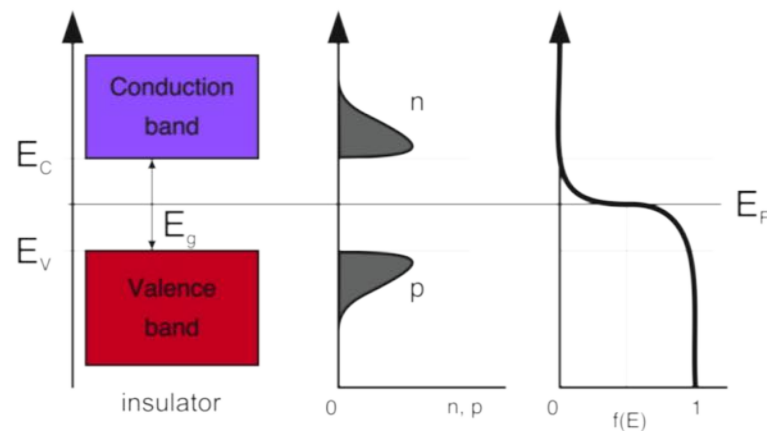
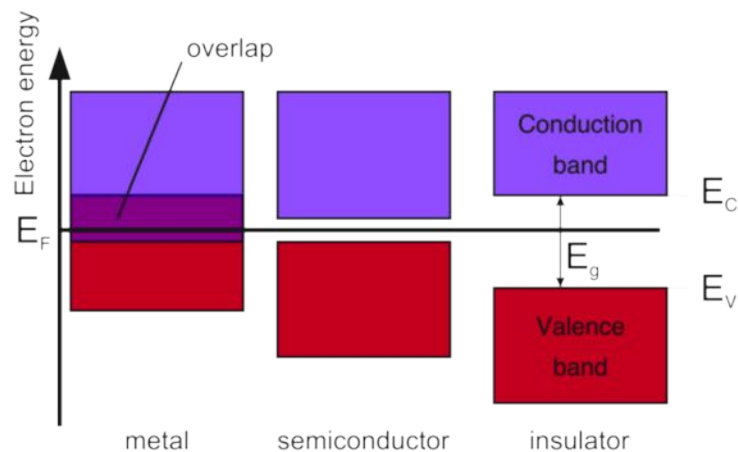
	I	II	III	IV	V	VI	VII	VIII
1	1 H							2 He
2	3 Li	4 Be	5 B	6 C	7 N	8 O	9 F	10 Ne
3	11 Na	12 Mg	13 Al	14 Si	15 P	16 S	17 Cl	18 Ar
4	19 K	20 Ca	31 Ga	32 Ge	33 As	34 Se	35 Br	36 Kr
5	37 Rb	38 Sr	49 In	50 Sn	51 Sb	52 Te	53 I	54 Xe
6	55 Cs	56 Ba	81 Tl	82 Pb	83 Bi	84 Po	85 At	86 Rn
7	87 Fr	88 Ra	113 Uut	114 Uuq	114 Uup	115 Uuh	117 Uus	118 Uuo

Compound Semiconductors (cont.)

- important III-V compounds:
 - **GaAs**: Faster and probably more radiation resistant than Si.
Drawback is less experience in industry and higher costs.
 - GaP, GaSb, InP, InAs, InSb, InAlP
- important II-VI compounds:
 - **CdTe**: High atomic numbers (48+52) hence very efficient to detect photons.
 - ZnS, ZnSe, ZnTe, CdS, CdSe, $\text{Cd}_{1-x}\text{Zn}_x\text{Te}$, $\text{Cd}_{1-x}\text{Zn}_x\text{Se}$

Why Silicon?

- Semiconductor
- Moderate bandgap $E_g = 1.12\text{eV}$
- Energy to create e/h pair = 3.6eV
 - Low compared to gases used for ionization chambers or proportional counters (e.g. Argon gas = 15eV)
- High density and atomic number
 - Higher specific energy loss \rightarrow Thinner detectors
- High carrier mobility \rightarrow Fast!
 - Less than 30ns to collect entire signal
- Industrial fabrication techniques

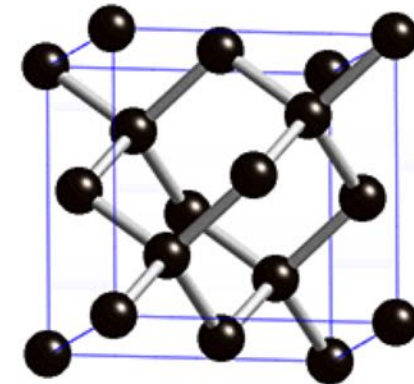


Crystal structure of semiconductors

Si, Ge and diamond

- Group IV elements
- Crystal structure: *diamond lattice*
 - 2 nested sub-lattices
 - shifted by one quarter along the diagonal of the cube.
 - Each atom is surrounded by **four equidistant neighbors**.
 - Lattice parameter $a=0.357\text{nm}$

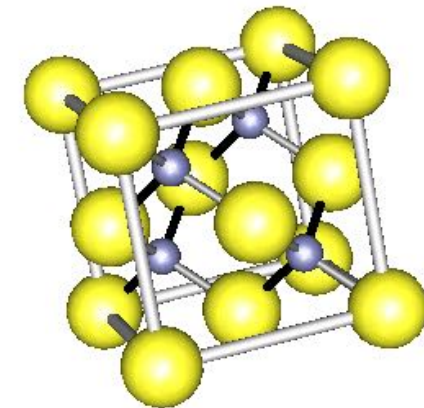
Diamond lattice



Most III-V semiconductors (e.g. GaAs)

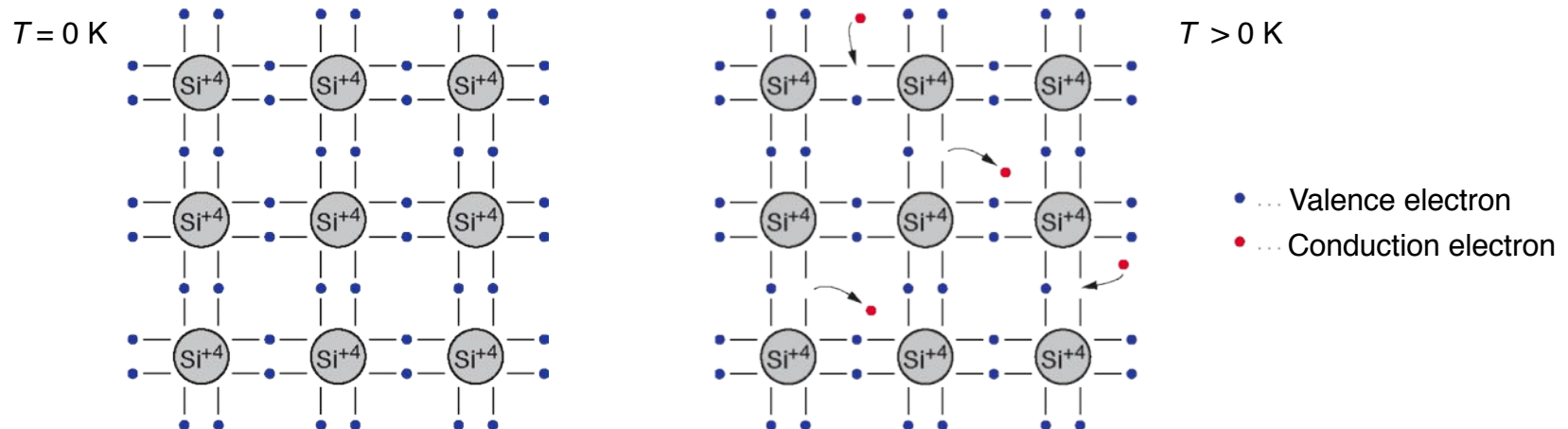
- *zinoblende lattice*
 - similar to the diamond lattice
 - except that each sub-lattice consists of one element.

Zinoblende lattice



Bond model of semiconductors

Example of column IV elemental semiconductor (2-dimensional projection) :

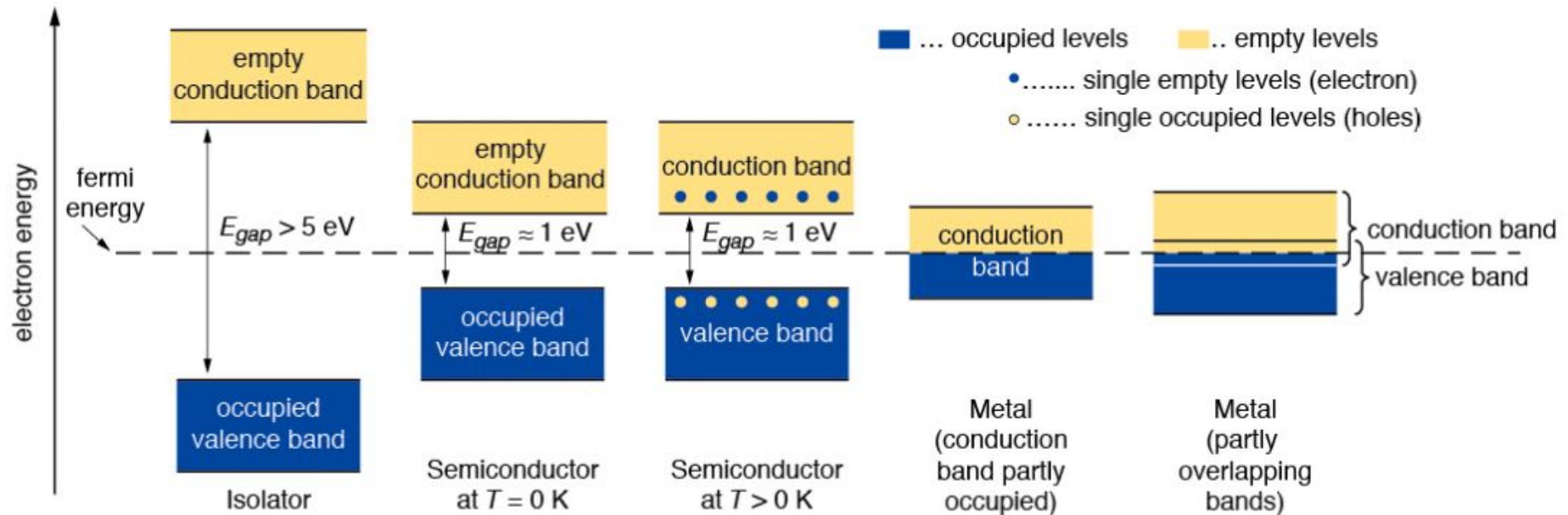


Each atom has 4 closest neighbors, the 4 electrons in the outer shell are shared and form **covalent bonds**.

- At low temperature all electrons are bound
- At higher temperature thermal vibrations break some of the bonds → free e^- cause conductivity (electron conduction)
- The remaining open bonds attract other e^- → The “holes” change position (hole conduction)

Energy bands: isolator–semiconductor–metal

In an isolated atom the electrons have only discrete energy levels. In solid state material the atomic levels merge to energy bands. In **metals** the conduction and the valence band **overlap**, whereas in isolators and semiconductors these levels are **separated** by an energy gap (**band gap**). In isolators this gap is large.



Fermi distribution, Fermi levels

Fermi distribution $f(E)$ describes the **probability that an electronic state with energy E is occupied by an electron.**

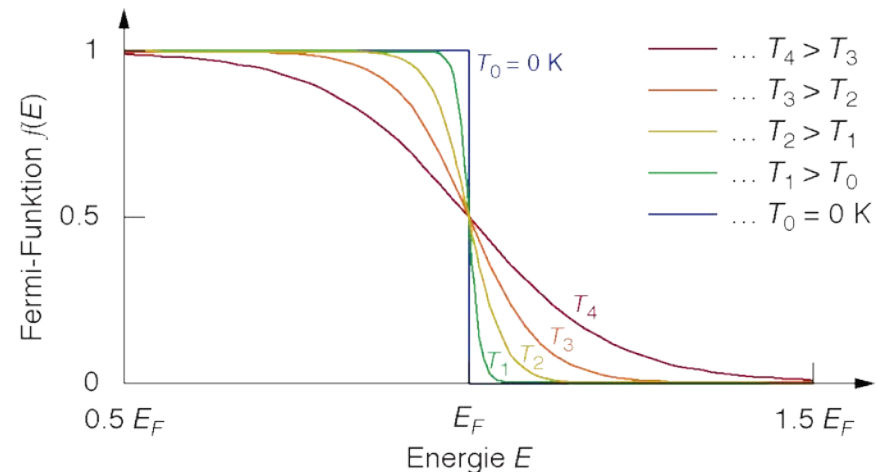
$$f(E) = \frac{1}{1 + e^{\frac{E-E_F}{kT}}}$$

The **Fermi level E_F** is the energy at which the **probability of occupation is 50%**. For metals E_F is in the conduction band, for semiconductors and isolators E_F is in the band gap

Fermi distribution function for different temperatures

$$T_4 > T_3 > T_2 > T_1 > T_0 = 0 \text{ K}$$

$T_0 = 0 \text{ K}$: saltus function



Intrinsic carrier concentration

- Due to the small band gap in semiconductors electrons already occupy the conduction band at room temperature.
- Electrons from the conduction band may recombine with holes.
- A **thermal equilibrium** is reached between **excitation** and **recombination**: Charged carrier concentration $n_e = n_h = n_i$
This is called intrinsic carrier concentration:

$$n_i = \sqrt{N_C N_V} \cdot \exp\left(-\frac{E_g}{2kT}\right) \propto T^{\frac{3}{2}} \cdot \exp\left(-\frac{E_g}{2kT}\right)$$

N_C, N_V ... effective density of states at the conduction, valence band edge

In ultrapure silicon the intrinsic carrier concentration is **$1.45 \cdot 10^{10} \text{ cm}^{-3}$** .

With approximately $10^{22} \text{ Atoms/cm}^3$ about 1 in 10^{12} silicon atoms is ionized.

Drift velocity and mobility

Drift velocity

For electrons:

$$\vec{v}_n = -\mu_n \cdot \vec{E}$$

and for holes:

$$\vec{v}_p = \mu_p \cdot \vec{E}$$

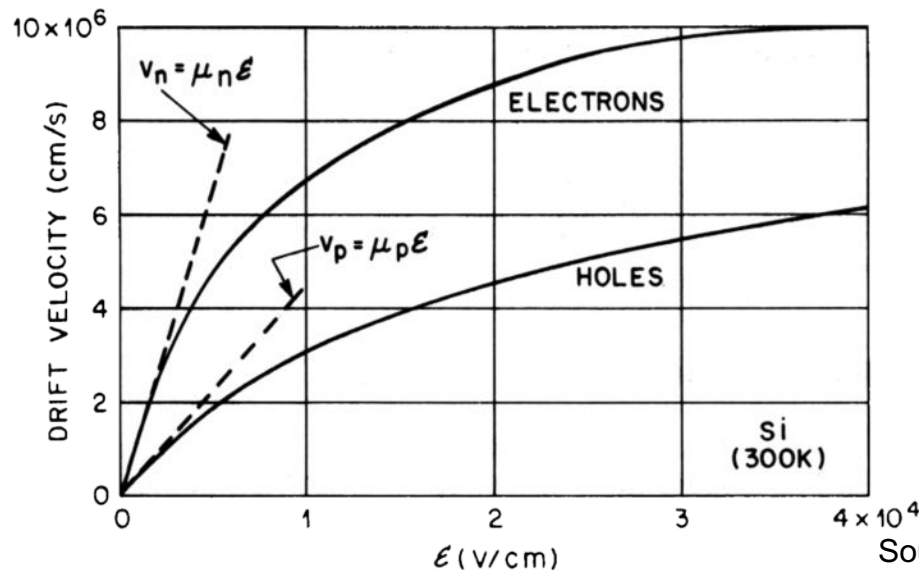
Mobility

For electrons:

$$\mu_n = \frac{e \tau_n}{m_n}$$

and for holes:

$$\mu_p = \frac{e \tau_p}{m_p}$$



- e ... electron charge
- E ... external electric field
- m_n, m_p ... effective mass of e^- and holes
- τ_n, τ_p ... mean free time between collisions for e^- and holes (carrier lifetime)

Source: S.M. Sze, *Semiconductor Devices*, J. Wiley & Sons, 1985

Resistivity

Specific resistivity is a measure of silicon purity:

$$\rho = \frac{1}{e(\mu_n n_e + \mu_p n_h)}$$

n_e, n_h ... Charge carrier density for electrons and holes
 μ_n, μ_p ... Mobility for electrons and holes
 e ... elementary charge

Carrier mobilities: $\mu_p(\text{Si}, 300 \text{ K}) \approx 450 \text{ cm}^2/\text{Vs}$
 $\mu_n(\text{Si}, 300 \text{ K}) \approx 1450 \text{ cm}^2/\text{Vs}$

The charge carrier concentration in pure silicon (i.e. intrinsic Si) for $T = 300 \text{ K}$ is:

$$n_e = n_h \approx 1.45 \cdot 10^{10} \text{ cm}^{-3}$$

This yields an intrinsic resistivity of:

$$\rho \approx 230 \text{ k}\Omega\text{cm}$$

Comparison of different semiconductor materials

Material	Si	Ge	GaAs	GaP	CdTe	Diamond*
Atomic number Z	14	32	31+33	31+15	48+52	6
Mass Number A (amu)	28.086	72.61	69.72+74.92	69.72+30.97	112.4+127.6	12.011
Lattice constant a (Å)	5.431	5.646	5.653	5.451	6.482	3.567
Density ρ (g/cm ³)	2.328	5.326	5.32	4.13	5.86	3.52
E_g (eV) bei 300 K	1.11	0.66	1.42	2.26	1.44	5.47–5.6
E_g (eV) bei 0 K	1.17	0.74	1.52	2.34	1.56	≈ 6
rel. permittivity $\epsilon_r = \epsilon/\epsilon_0$	11.9	16.0	12.8	11.1	10.9	5.7
Melting point (°C)	1415	938	1237	1477	1040	3527
eff. e ⁻ -mass (m_n/m_e)	0.98, 0.19	1.64, 0.08	0.067	0.82	0.11	0.2
eff. hole mass ⁺ (m_h/m_e)	0.16	0.044	0.082	0.14	0.35	0.25

*usually considered an isolator

Source: <http://www.ioffe.rssi.ru/SVA/NSM/Semicond/> ; S.M.Sze, *Physics of Semicon. Devices* , J. Wiley & Sons, 1981,
 J. Singh, *Electronic & Optoelectronic Properties of Semiconductor Structures*, Cambridge University Press, 2003

Comparison of different semiconductor materials

Material	Si	Ge	GaAs	GaP	CdTe	Diamond*
eff. density of states in conduction band n_{CB} (cm ⁻³)	$3 \cdot 10^{19}$	$1 \cdot 10^{19}$	$4.7 \cdot 10^{17}$	$2 \cdot 10^{19}$		$\approx 10^{20}$
eff. Density of states in valence band n_{VB} (cm ⁻³)	$1 \cdot 10^{19}$	$6 \cdot 10^{18}$	$7 \cdot 10^{18}$	$2 \cdot 10^{19}$		$\approx 10^{19}$
Electron mobility μ_e bei 300 K (cm ² /Vs)	~1450	3900	8500	< 300	1050	1800
Hole mobility μ_h bei 300 K (cm ² /Vs)	~450	1900	400	< 150	100	1200
instrins. charge carrier density at 300 K (cm ⁻³)	$1.45 \cdot 10^{10}$	$2.4 \cdot 10^{13}$	$2 \cdot 10^6$	2		$\approx 10^{-27}$
instrins. resistivity at 300 K (Ω cm)	$2.3 \cdot 10^5$	47	$\approx 10^8$		$\approx 10^9$	$\geq 10^{42}$
Breakdown field (V/cm)	$3 \cdot 10^5$	$\approx 10^5$	$4 \cdot 10^5$	$\approx 10^6$		$3 \cdot 10^7$
Mean E to create an e ⁻ h ⁺ pair (eV), 300 K	3.62	2.9	4.2	≈ 7	4.43	13.25

*usually considered an isolator

Source: <http://www.ioffe.rssi.ru/SVA/NSM/Semicond/> ; S.M.Sze, *Physics of Semicon. Devices* , J. Wiley & Sons, 1981, J. Singh, *Electronic & Optoelectronic Properties of Semiconductor Structures*, Cambridge University Press, 2003

Constructing a Detector

One of the most important parameter of a detector is the **signal-to-noise-ratio** (SNR). A good detector should have a large SNR.

However this leads to **two contradictory requirements**:

- **Large signal**
 - low ionization energy -> small band gap
- **Low noise**
 - very few intrinsic charge carriers -> large band gap

An optimal material should have $E_g \approx 6 \text{ eV}$.

In this case the conduction band is almost empty at room temperature and the band gap is small enough to create a large number of e^-h^+ pairs through ionization.

Such a material exist, it is **Diamond**. However even artificial diamonds (e.g. CVD diamonds) are too expensive for large area detectors.

Constructing a Detector (cont.)

Let's make a simple calculation for silicon:

- Mean ionization energy $I_0 = 3.62 \text{ eV}$,
- mean energy loss per flight path of a mip $dE/dx = 3.87 \text{ MeV/cm}$

Assuming a detector with a thickness of $d = 300 \mu\text{m}$ and an area of $A = 1 \text{ cm}^2$.

- **Signal of a mip in such a detector:**

$$\frac{dE/dx \cdot d}{I_0} = \frac{3.87 \cdot 10^6 \text{ eV/cm} \cdot 0.03 \text{ cm}}{3.62 \text{ eV}} \approx 3.2 \cdot 10^4 \text{ e}^- \text{h}^+ \text{-pairs}$$

- **Intrinsic charge carrier in the same volume ($T = 300 \text{ K}$):**

$$n_i d A = 1.45 \cdot 10^{10} \text{ cm}^{-3} \cdot 0.03 \text{ cm} \cdot 1 \text{ cm}^2 \approx 4.35 \cdot 10^8 \text{ e}^- \text{h}^+ \text{-pairs}$$

Result: The number of thermal created e⁻h⁺-pairs (noise) is four orders of magnitude larger than the signal.

We have to remove the charge carriers

-> Depletion zone in reverse biased **pn junctions**

Doping

A pn junction consists of n and p doped substrates:

- Doping is the **replacement of a small number of atoms** in the lattice by atoms of **neighboring columns** from the periodic table
- These doping atoms create **energy levels within the band gap** and therefore alter the conductivity.

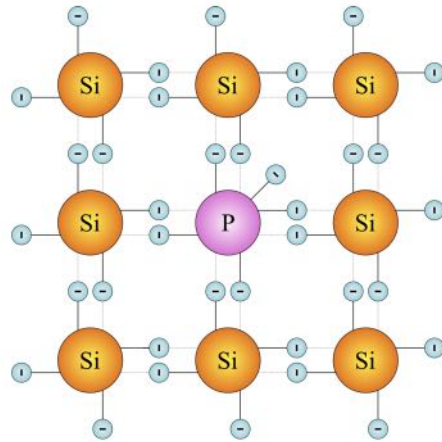
Definitions:

- An un-doped semiconductor is called an **intrinsic semiconductor**
 - For each conduction electron exists the corresponding hole.
- A doped semiconductor is called an **extrinsic semiconductor**.
 - Extrinsic semiconductors have a abundance of electrons or holes.

Doping: n- and p-type Silicon

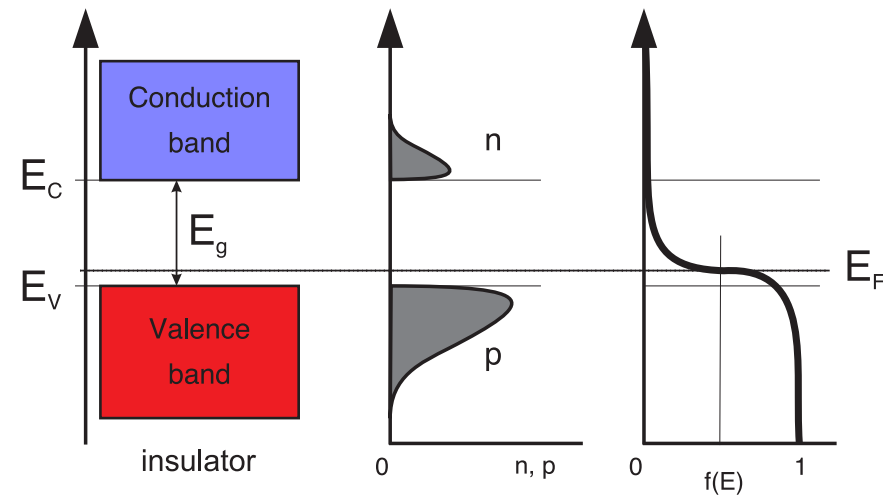
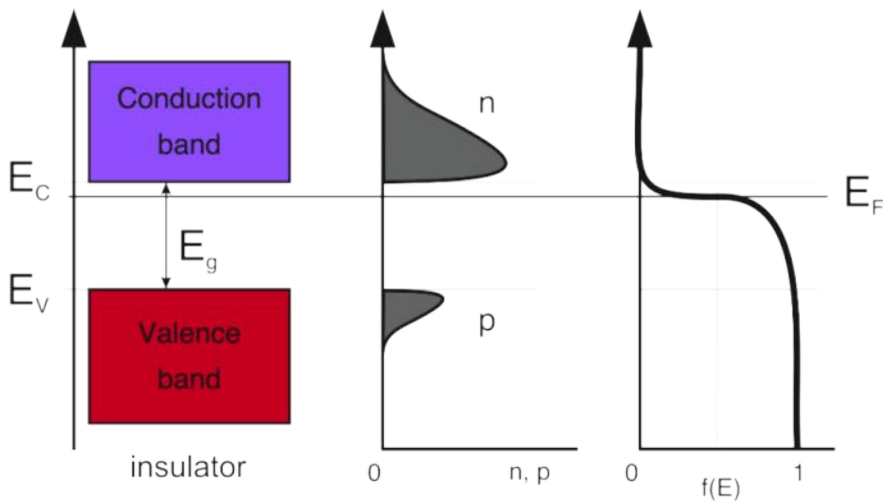
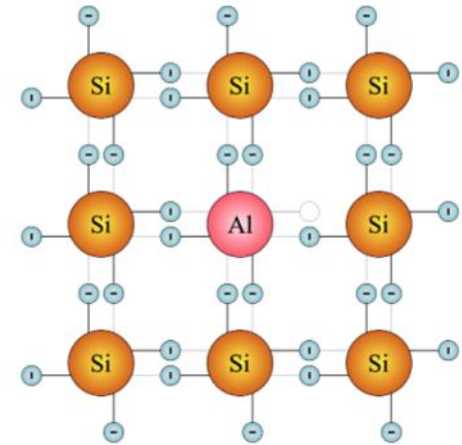
n-type:

- Dopants: Elements with 5 valence electrons, e.g. Phosphorus
- Donators
- Electron abundance



p-type:

- Dopants: Elements with 3 valence electrons, e.g. Aluminum
- Acceptors
- Electron shortage

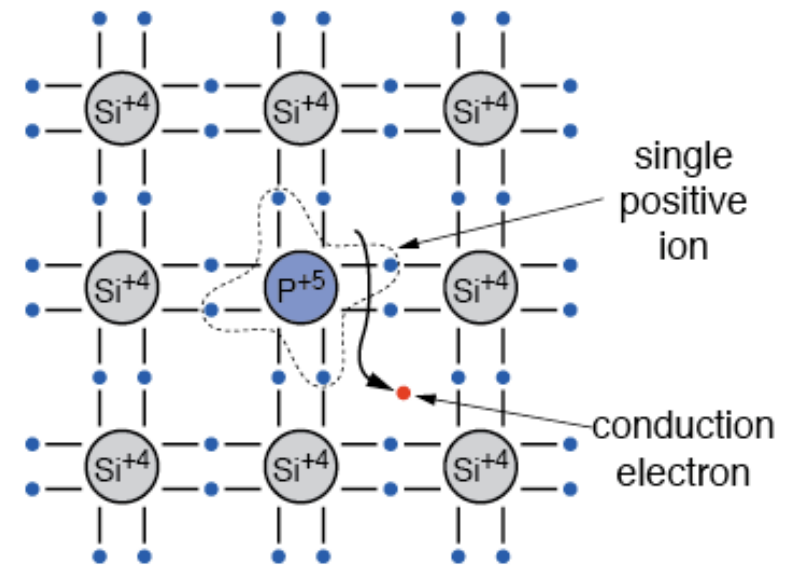
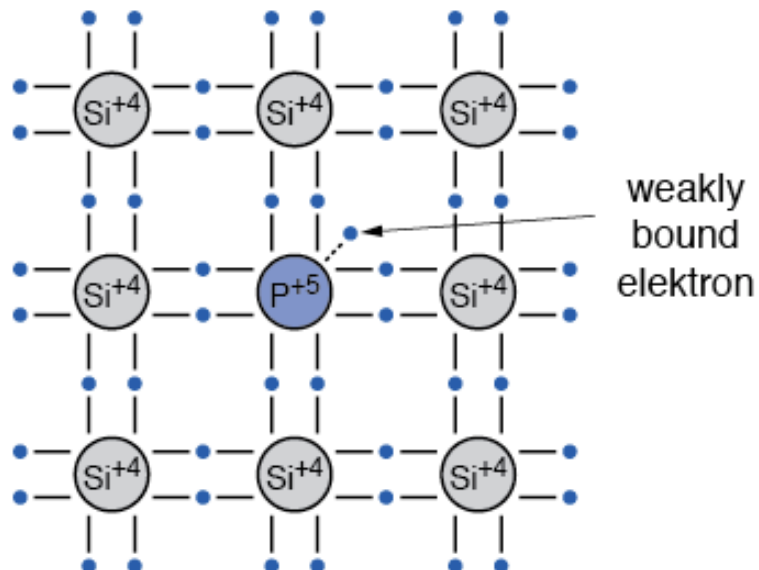


Bond model: n-doping in Si

Doping with an element 5 atom (e.g. P, As, Sb). The 5th valence electrons is weakly bound.

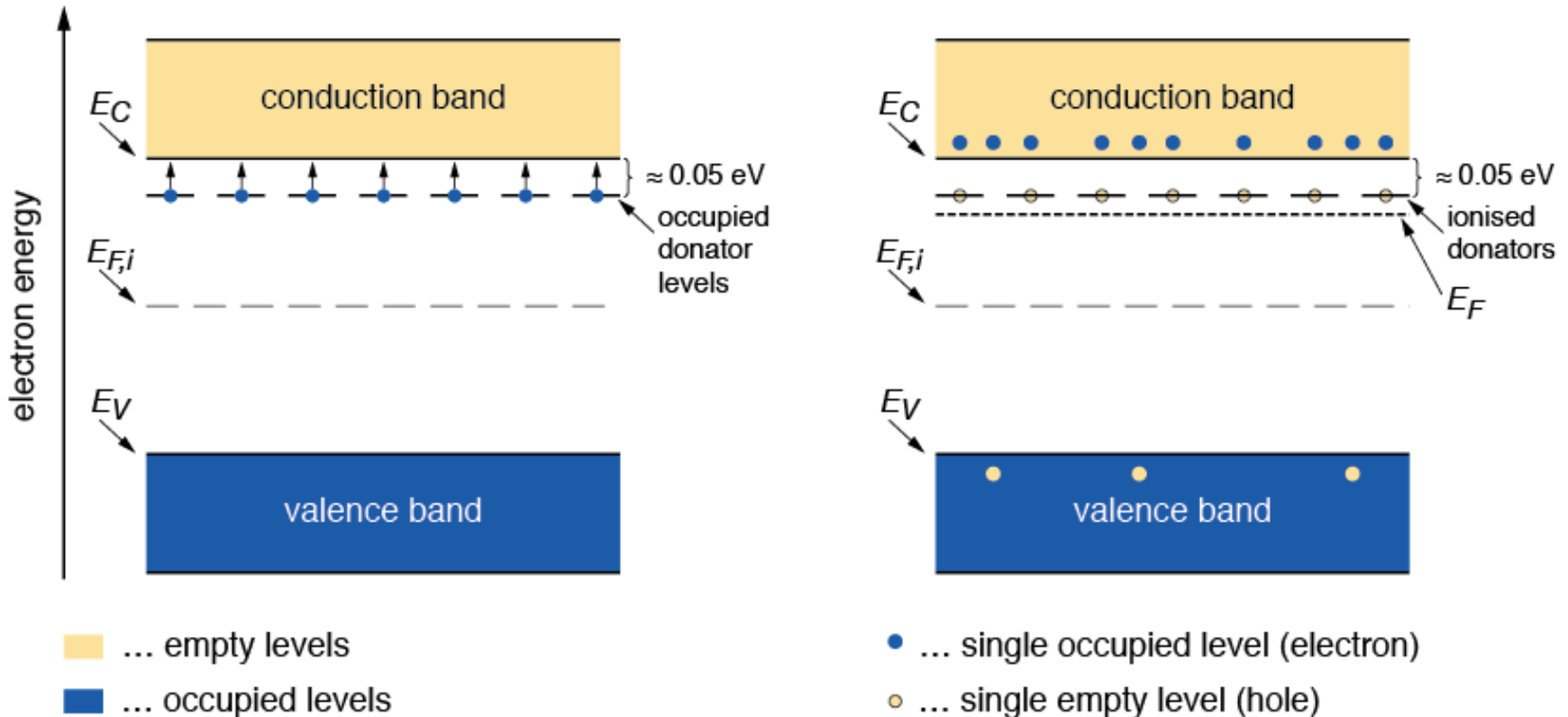
The doping atom is called **donor**

The released conduction electron leaves a positively charged ion



Band model: n-doping in Si

The energy level of the donor is just below the edge of the conduction band. At room temperature most electrons are raised to the conduction band. The Fermi level E_F moves up.

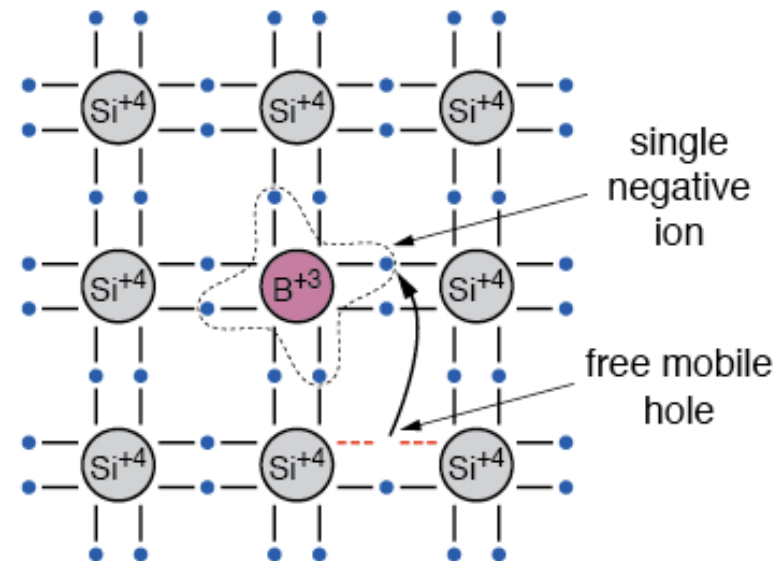
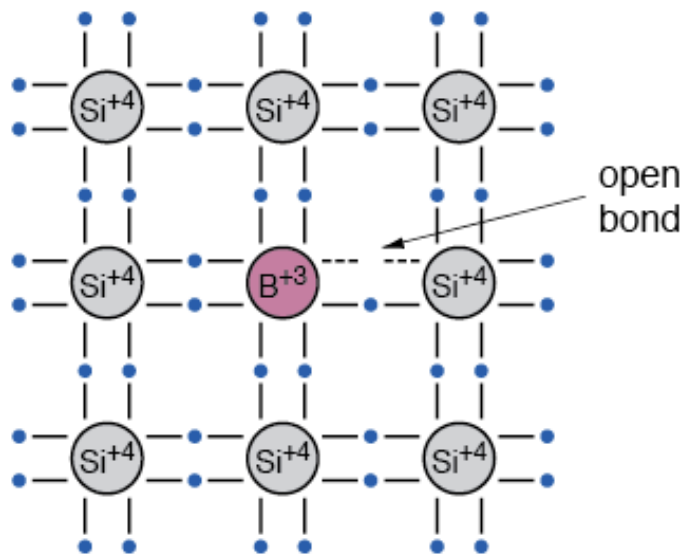


Bond model: p-doping in Si

Doping with an element 3 atom (e.g. B, Al, Ga, In). One valence bond remains open. This open bond attracts electrons from the neighbor atoms.

The doping atom is called **acceptor**.

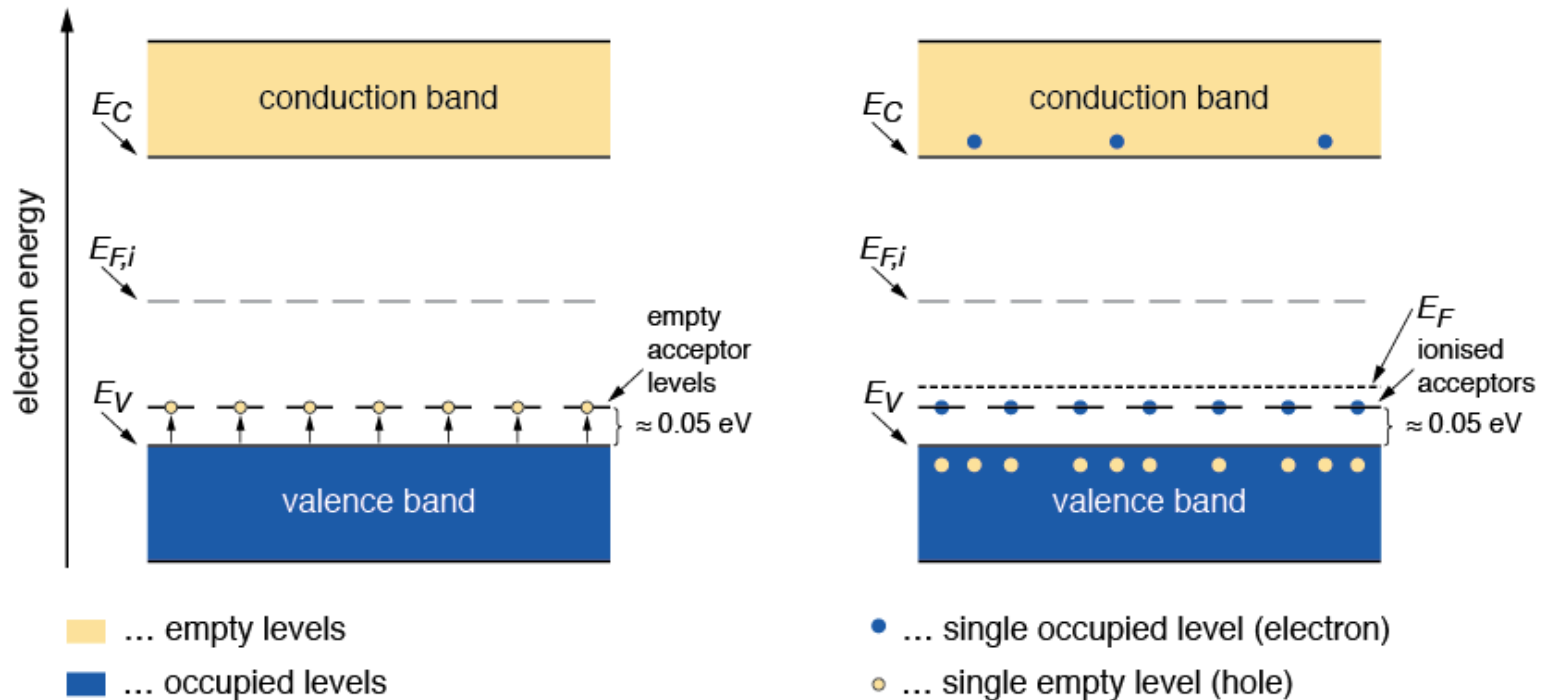
The acceptor atom in the lattice is negatively charged.



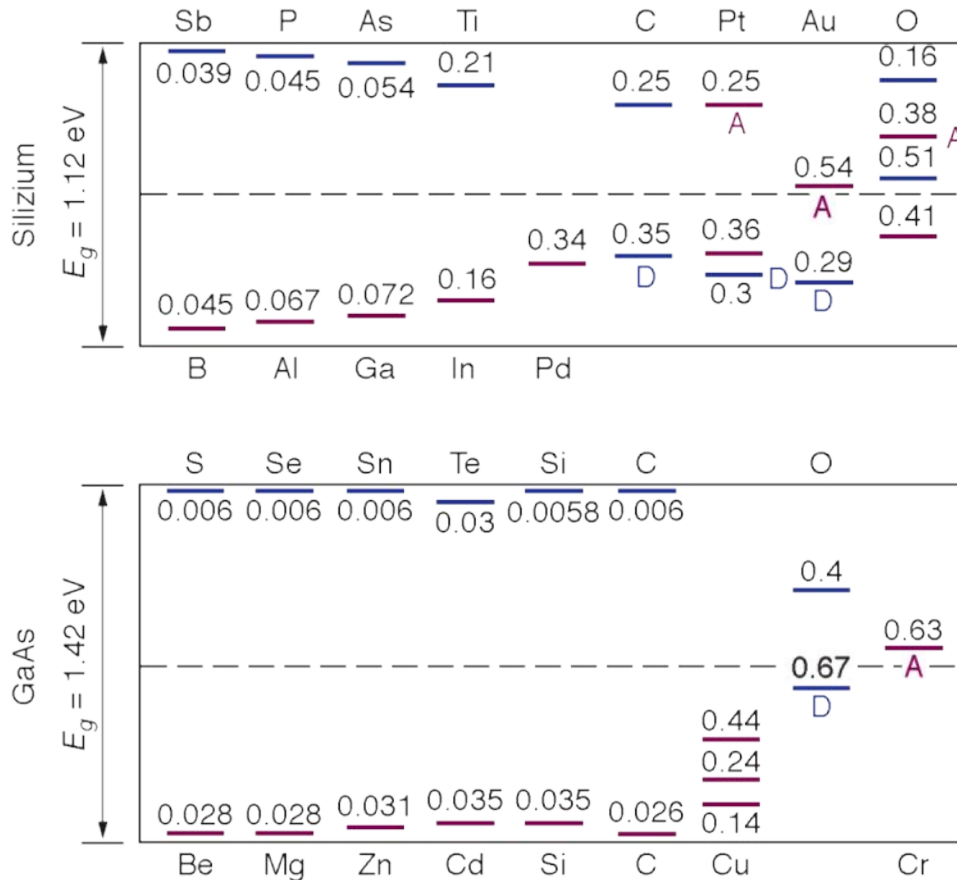
Band model: p-doping in Si

The energy level of the acceptor is just above the edge of the valence band. At room temperature most levels are occupied by electrons leaving holes in the valence band.

The Fermi level E_F moves down.



Donor and acceptor levels in Si und GaAs



Measured ionization energies for doping atoms in *Si* and *GaAs*.

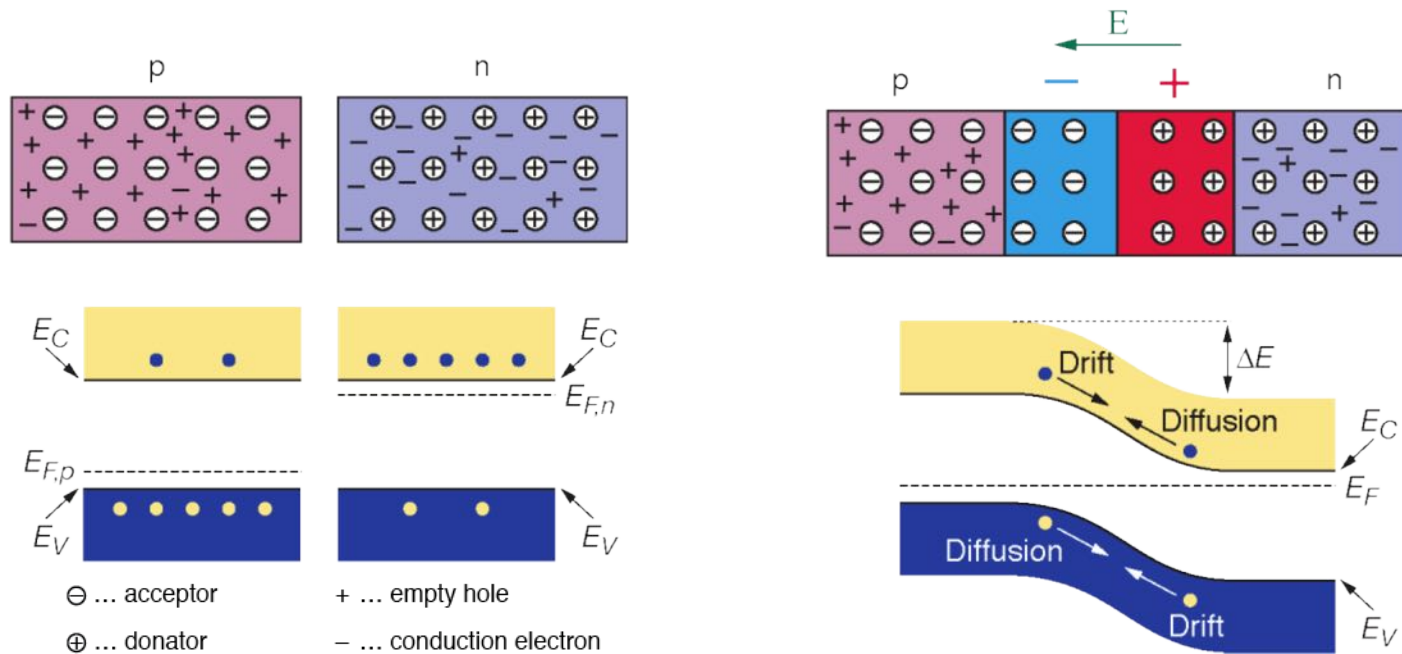
Levels **above band gap middle** are **donators** and are measured from the edge of the conduction band (exceptions denoted D).

Levels **below band gap middle** are **acceptors** and are measured from the edge of the valence band (exceptions denoted A).

Source: S.M. Sze, *Semiconductor Devices*, J. Wiley & Sons, 1985

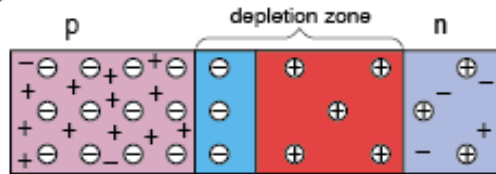
Creating a p-n junction

At the interface of an n-type and p-type semiconductor the difference in the Fermi levels cause diffusion of excessive carries to the other material until thermal equilibrium is reached. At this point the Fermi level is equal. The remaining ions create a **space charge region** and an electric field stopping further diffusion. The stable space charge region is free of charge carries and is called the **depletion zone**.

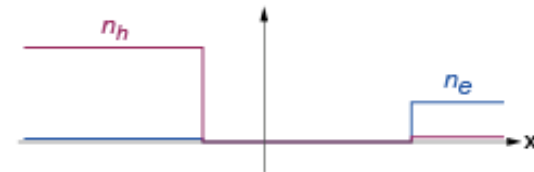


Electrical characteristics of pn junctions

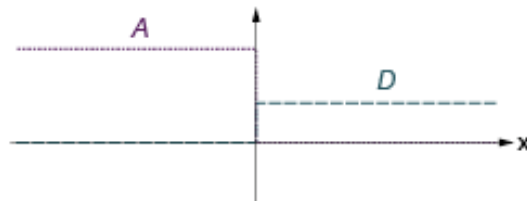
pn junction scheme



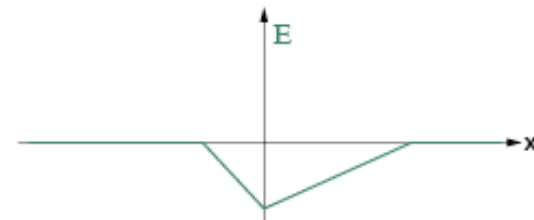
concentration of free charge carriers



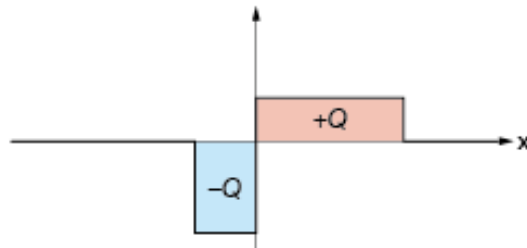
acceptor and donator concentration



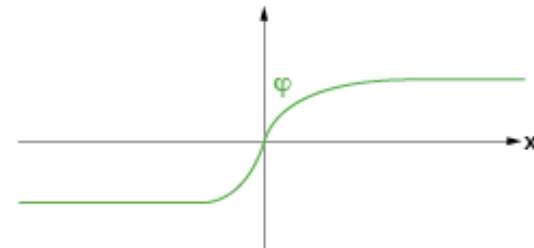
electric field



space charge density



electric potential



- ⊖ ... acceptor
- ⊕ ... donator
- + ... empty hole
- ... conduction electron

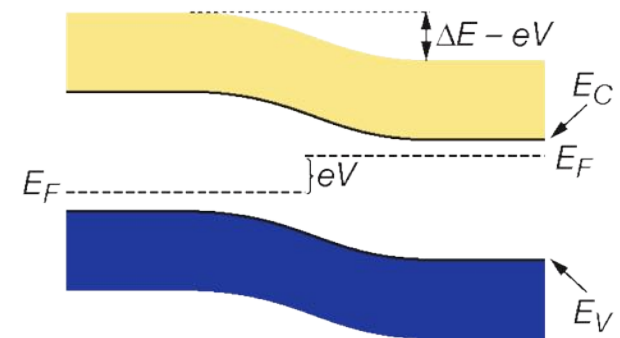
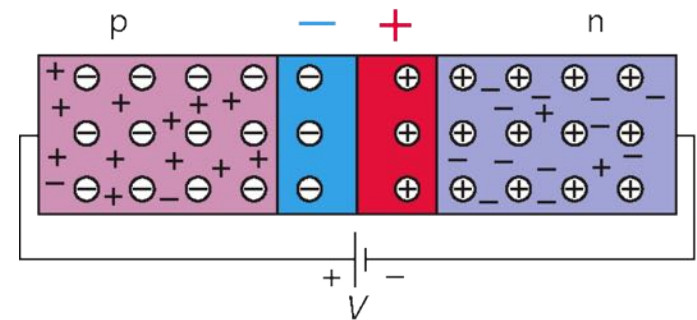
Operation of a pn-junction with forward bias

Applying an external voltage V with the anode to p and the cathode to n e- and holes are refilled to the depletion zone. The **depletion zone becomes narrower** (forward biasing)

Consequences:

- The potential barrier becomes smaller by eV
- Diffusion across the junction becomes easier
- The current across the junction increases significantly.

p-n junction with forward bias

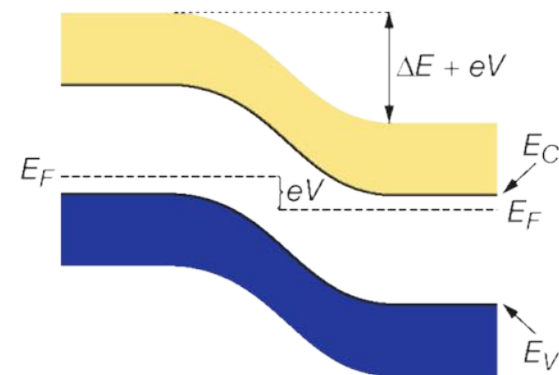
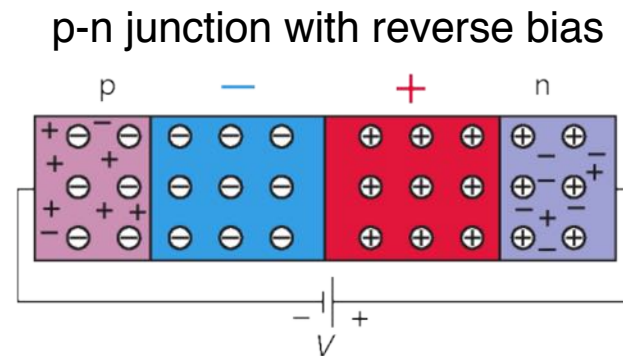


Operation a pn-junction with reverse bias

Applying an external voltage V with the cathode to p and the anode to n e- and holes are pulled out of the depletion zone. The **depletion zone becomes larger** (reverse biasing).

Consequences:

- The potential barrier becomes higher by eV
- Diffusion across the junction is suppressed.
- The current across the junction is very small ("leakage current")



➤ This is the way we operate our semiconductor detector!

Width of the depletion zone

Effective doping concentration in typical silicon detector with p⁺-n junction

- $N_a = 10^{15} \text{ cm}^{-3}$ in p⁺ region
- $N_d = 10^{12} \text{ cm}^{-3}$ in n bulk.

Without external voltage:

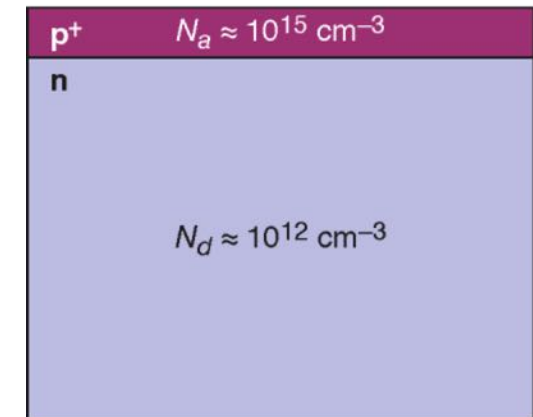
$$W_p = 0.02 \mu\text{m}$$

$$W_n = 23 \mu\text{m}$$

Applying a reverse bias voltage of 100 V:

$$W_p = 0.4 \mu\text{m}$$

$$W_n = 363 \mu\text{m}$$



p⁺n junction

Width of depletion zone in n bulk:

$$W \approx \sqrt{2\varepsilon_0\varepsilon_r\mu\rho|V|}$$

with $\rho = \frac{1}{e\mu N_{eff}}$

- V ... External voltage
- ρ ... specific resistivity
- μ ... mobility of majority charge carriers
- N_{eff} ... effective doping concentration

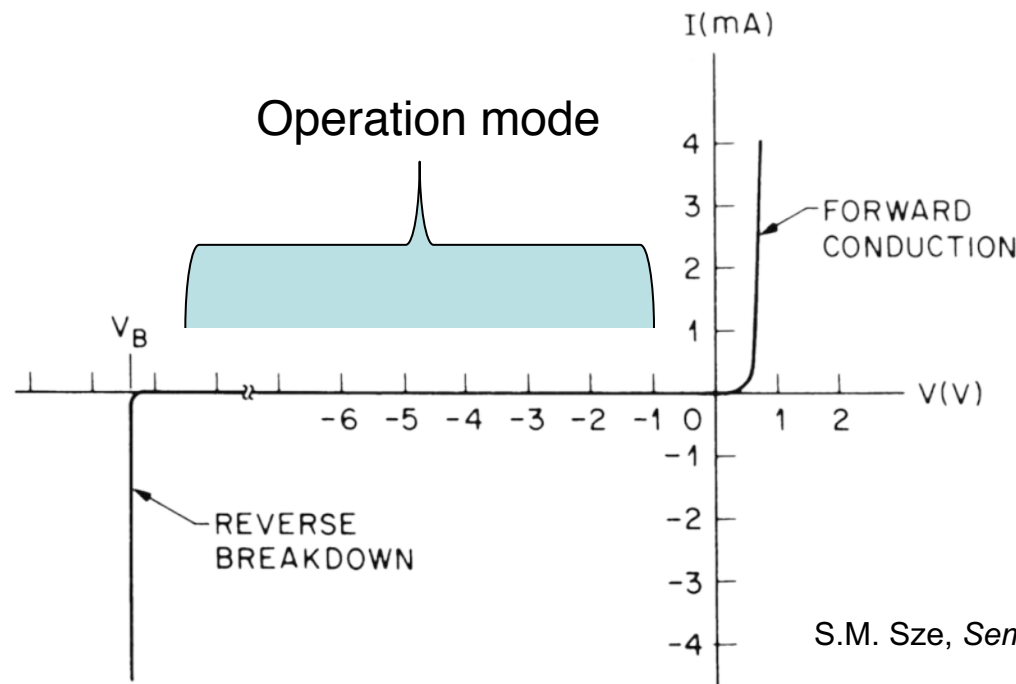
Current-voltage characteristics

Typical current-voltage of a p-n junction (diode): exponential current increase in forward bias, small saturation in reverse bias.

Ideal diode equation:
(Shockley-equation)

$$I = I_0 \cdot \left[\exp\left(\frac{eV}{kT}\right) - 1 \right]$$

I_0 ... reverse saturation current



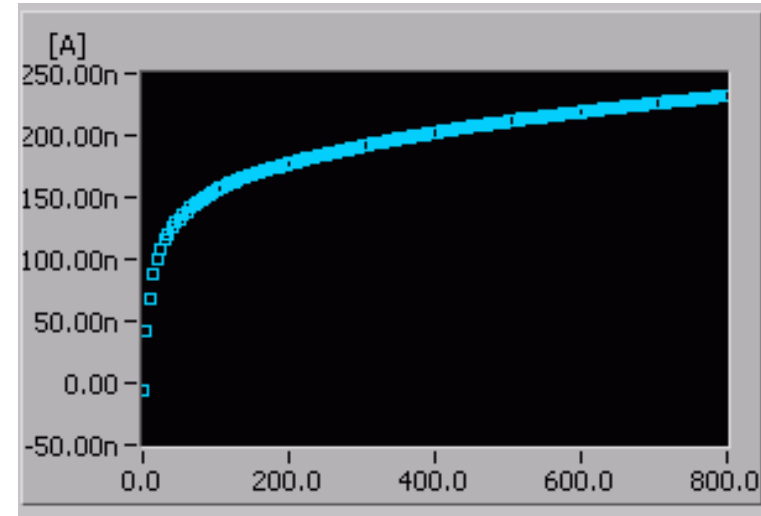
S.M. Sze, *Semiconductor Devices*, J. Wiley & Sons, 1985

Reverse current

- **Diffusion current**
 - From generation at edge of depletion region
 - Negligible for a fully depleted detector

- **Generation current**
 - From thermal generation in the depletion region
 - Reduced by using pure and defect free material
 - high carrier lifetime
 - Must keep temperature low & controlled

IV curve of diode in reverse mode:



$$j_{gen} = \frac{1}{2} q \frac{n_i}{\tau_0} W \quad j_{gen} \propto T^{3/2} \exp\left(\frac{1}{2kT}\right)$$

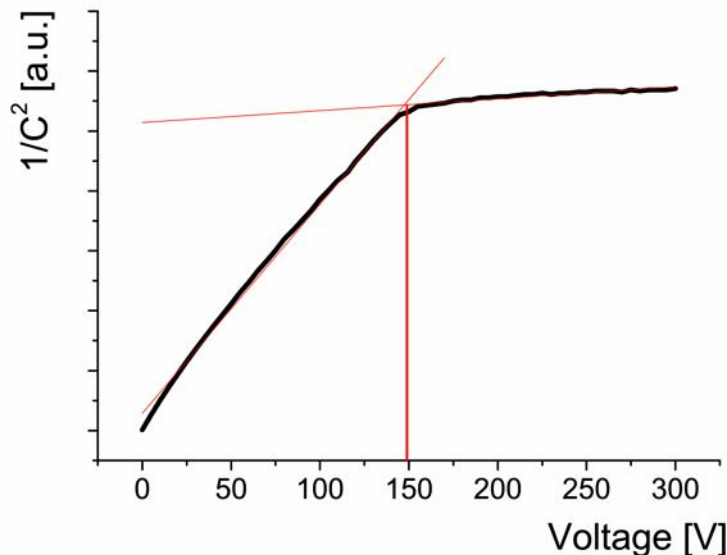
$$j_{gen} \times 2 \text{ for } \Delta T = 7K$$

Detector Capacitance and Full Depletion

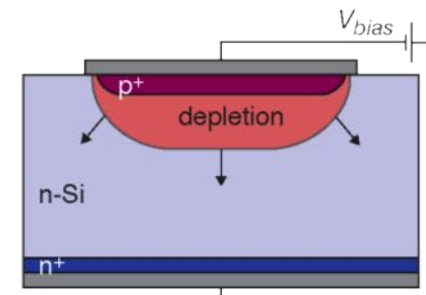
- Capacitance is similar to parallel-plate capacitor
- Fully depleted detector capacitance defined by geometric capacitance

$$C = \frac{\epsilon_0 \epsilon_r \cdot A}{W} = \sqrt{\frac{e \epsilon_0 \epsilon_r N_a N_d}{2(N_a + N_d) \cdot |V|}} \cdot A$$

$$C = \sqrt{\frac{\epsilon_0 \epsilon_r}{2\mu\rho|V|}} \cdot A$$



ρ ... bulk resistivity
 μ ... charge mobility
 V ... voltage
 A ... junction area

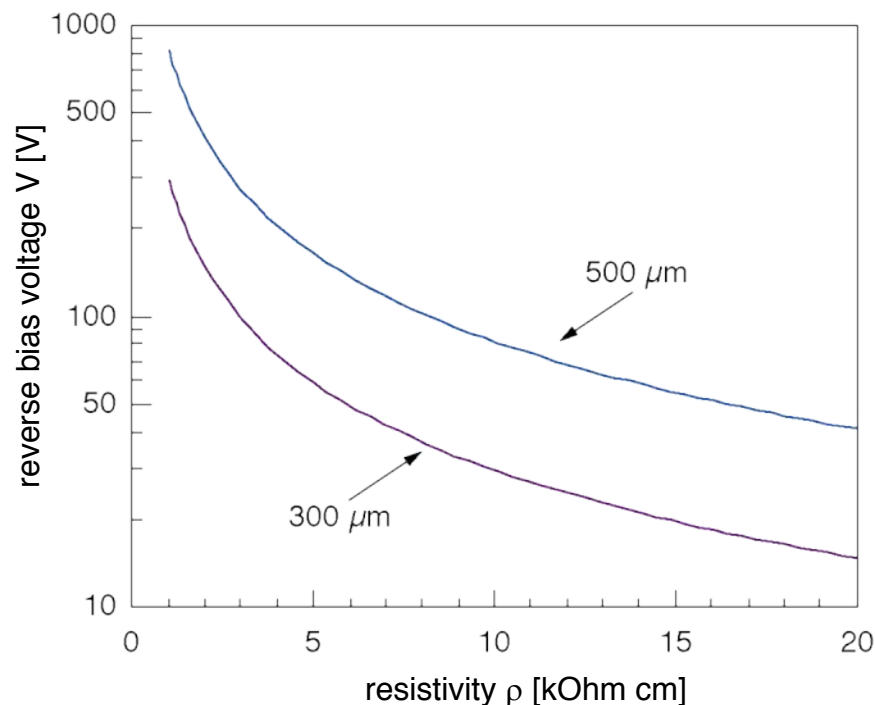


Full Depletion Voltage

The full depletion voltage is the minimum voltage at which the bulk of the sensor is fully depleted. The operating voltage is usually chosen to be slightly higher (over depletion).

High-resistivity material (i.e. low doping) requires low depletion voltage.

Depletion voltage as a function of the material resistivity for two different detector thicknesses (300 μm , 500 μm).

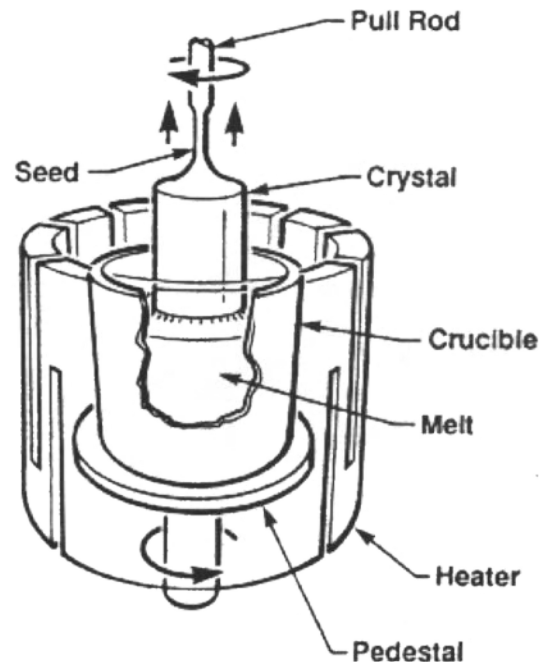


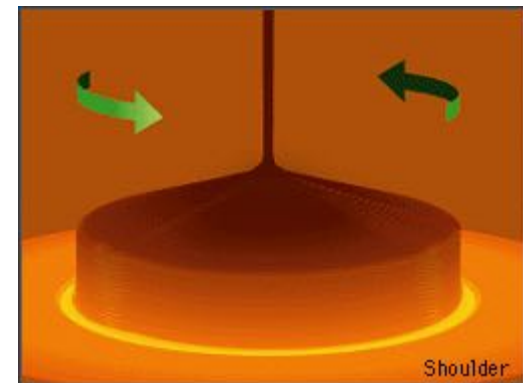
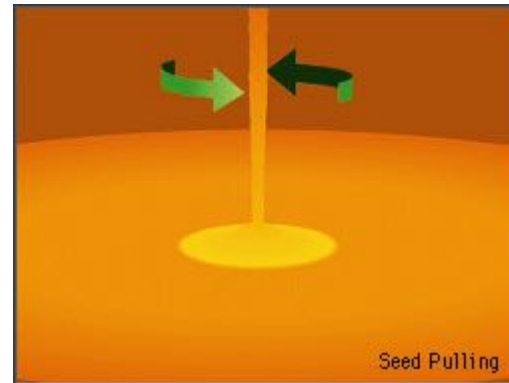
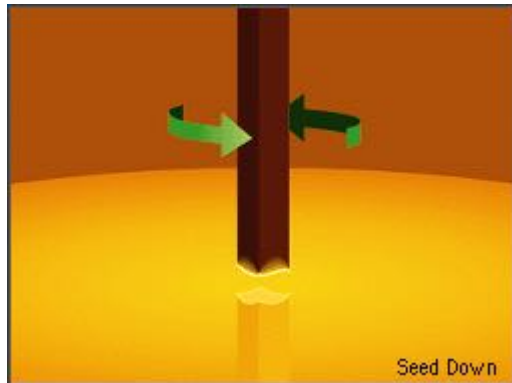
Manufacturing of Silicon Detectors

THE PLANAR PROCESS

The Ingot

- Czochralski process
 - Melt silicon at 1425 °C
 - Add impurities (dopants)
 - Spin and pull crystal
- Slice into wafers
 - 0.25mm to 1.0mm thick
- Polish one side



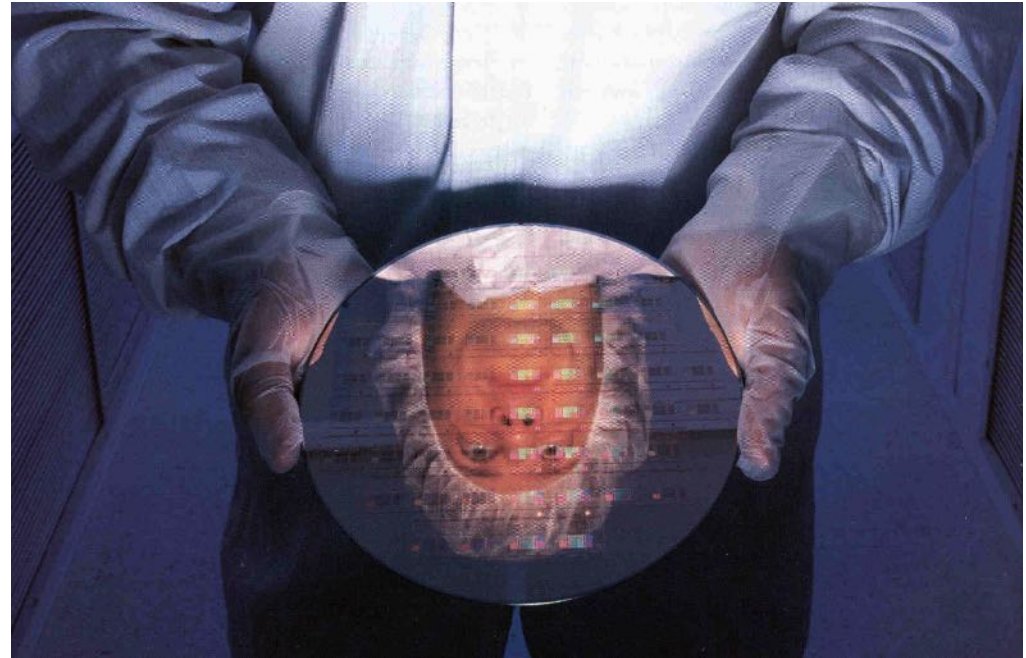


Crystal and wafer



© Kay Chernush

Wand
(a finished 250lb crystal)



A polished wafer

Float-Zone Silicon

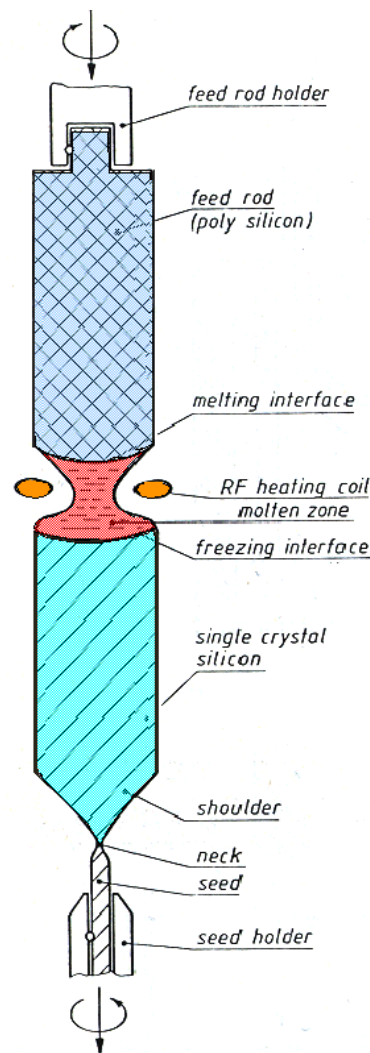
Properties of Si bulk required for detectors:

- Diameter: 4, 6 or 8 inches
- Lattice orientation $\langle 111 \rangle$ or $\langle 100 \rangle$
- Resistivity 1–10 k Ω cm

Therefore, float-zone technique for ingot production is used

- technique moves a liquid zone through the mater
- Result: **single-crystal ingot**

Chip industry: Czochralski process
(less purity)



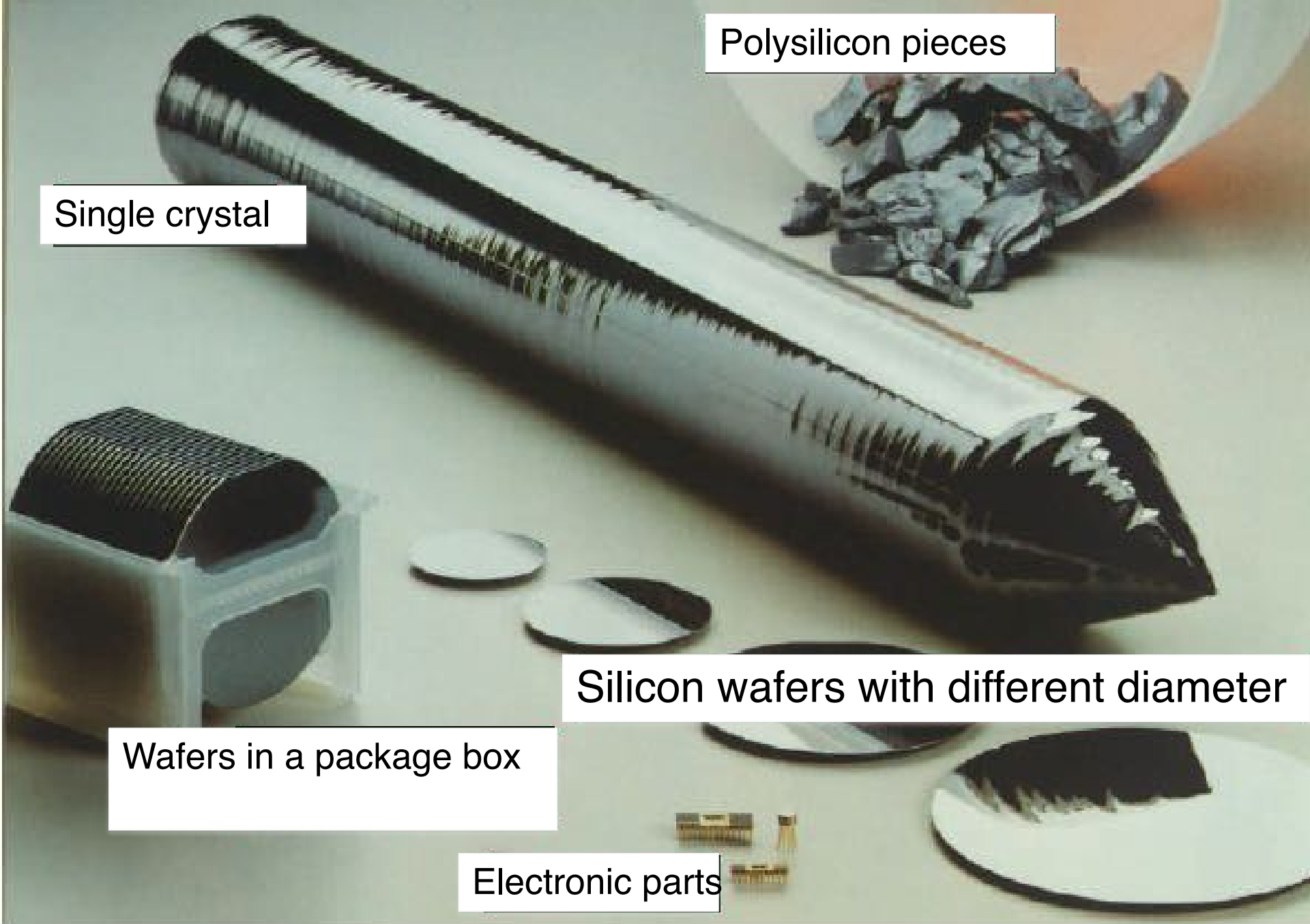
Polysilicon pieces

Single crystal

Silicon wafers with different diameter

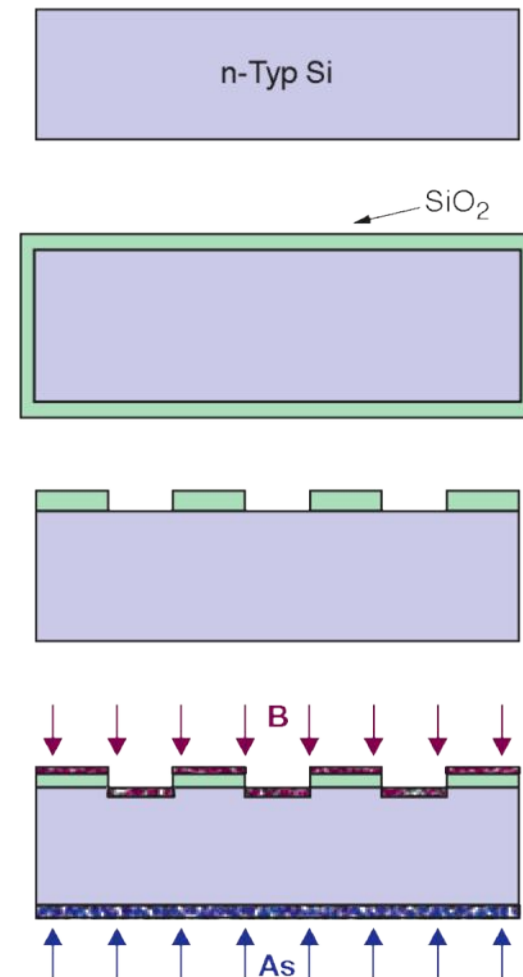
Wafers in a package box

Electronic parts



Planar process

1. Starting Point: single-crystal n-doped wafer ($N_D \approx 1-5 \cdot 10^{12} \text{ cm}^{-3}$)
2. Surface passivation by SiO_2 -layer (approx. 200 nm thick). E.g. growing by (dry) thermal oxidation at 1030° C .
3. Window opening using **photolithography technique** with etching, e.g. for strips
4. Doping using either
 - **Thermal diffusion** (furnace)
 - **Ion implantation**
 - p⁺-strip: Boron, 15 keV, $N_A \approx 5 \cdot 10^{16} \text{ cm}^{-2}$
 - Ohmic backplane: Arsenic, 30 keV, $N_D \approx 5 \cdot 10^{15} \text{ cm}^{-2}$



Planar process

5. After ion implantation: **Curing** of damage via thermal annealing at approx. 600°C , (activation of dopant atoms by incorporation into silicon lattice)
6. **Metallization** of front side: sputtering or CVD
7. Removing of excess metal by photolithography: **etching** of non-covered areas
8. Full-area metallization of backplane with annealing at approx. 450°C for better adherence between metal and silicon

Last step: wafer **dicing** (cutting)

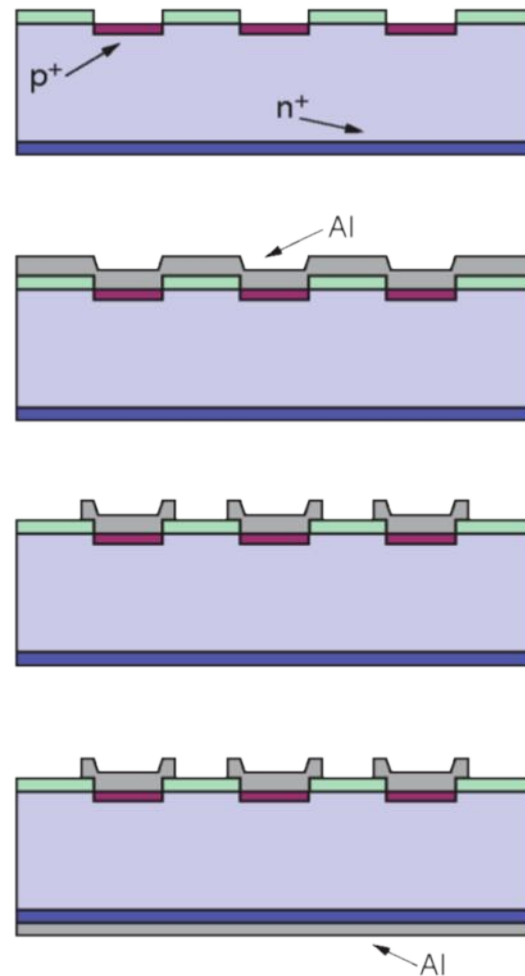
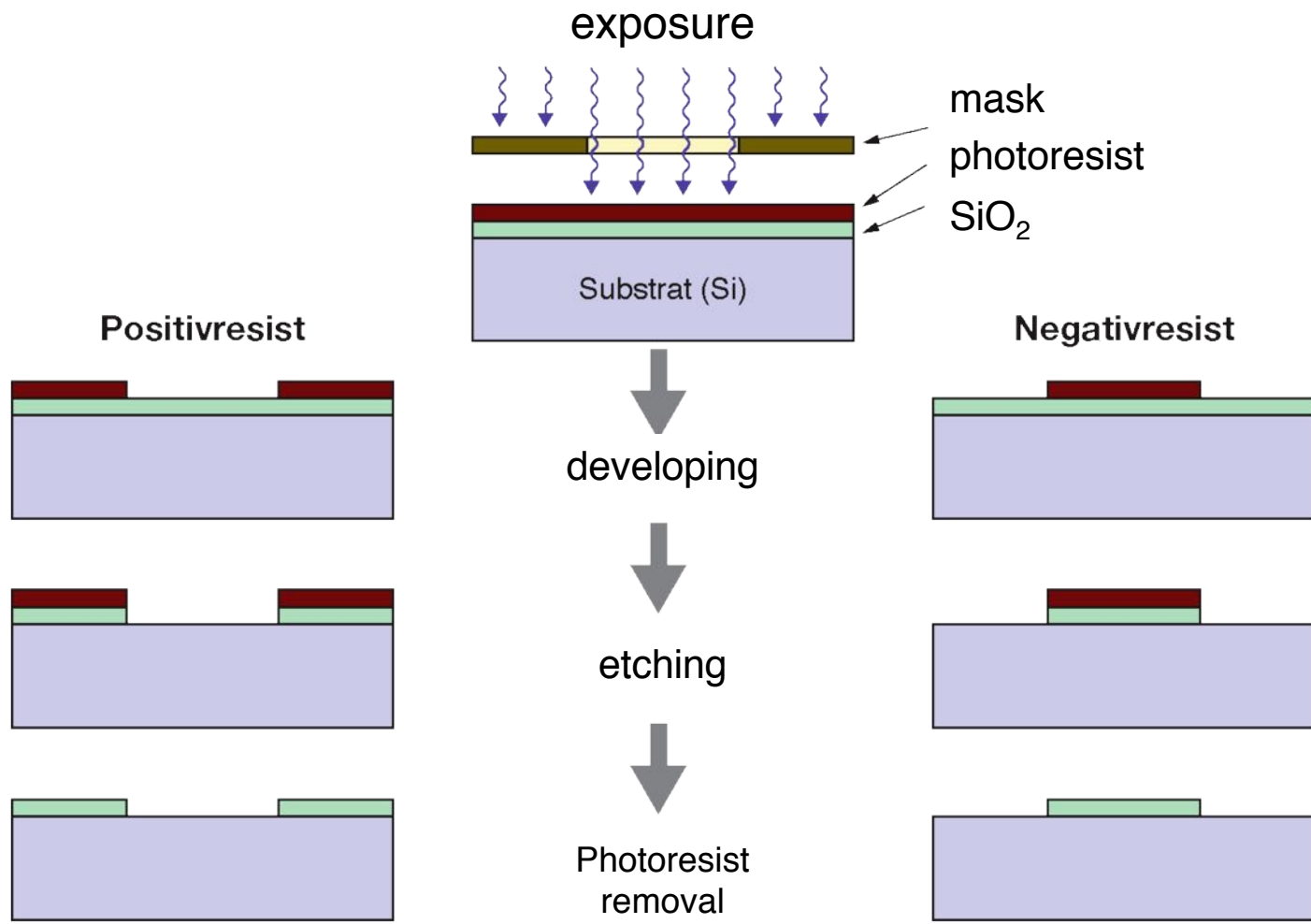


Photo-Lithography



Sensor mask design

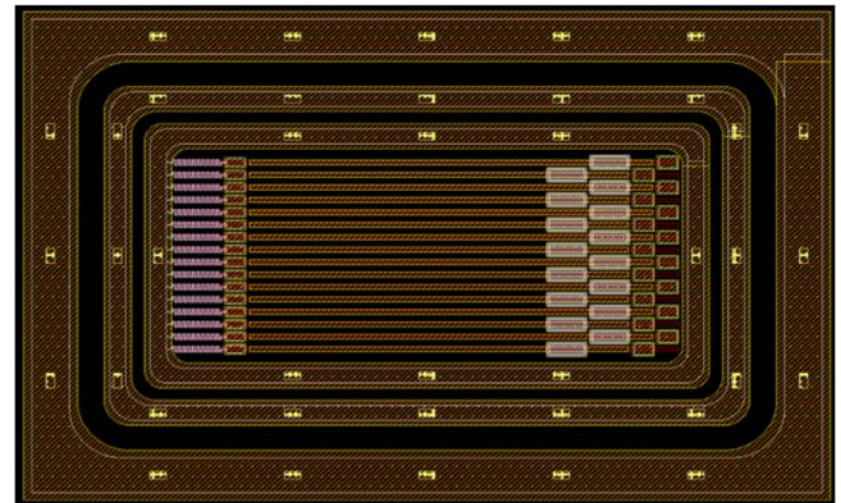
- Design tools like in commercial chip industry
 - ICStation from Mentor Graphics
 - Cadence
- Design is not drawn but actually “programmed”
 - using simple programming language (C like)
- Therefore, it is easy to change any parameter and re-create the full sensor within minutes
 - e.g. width of strips

```

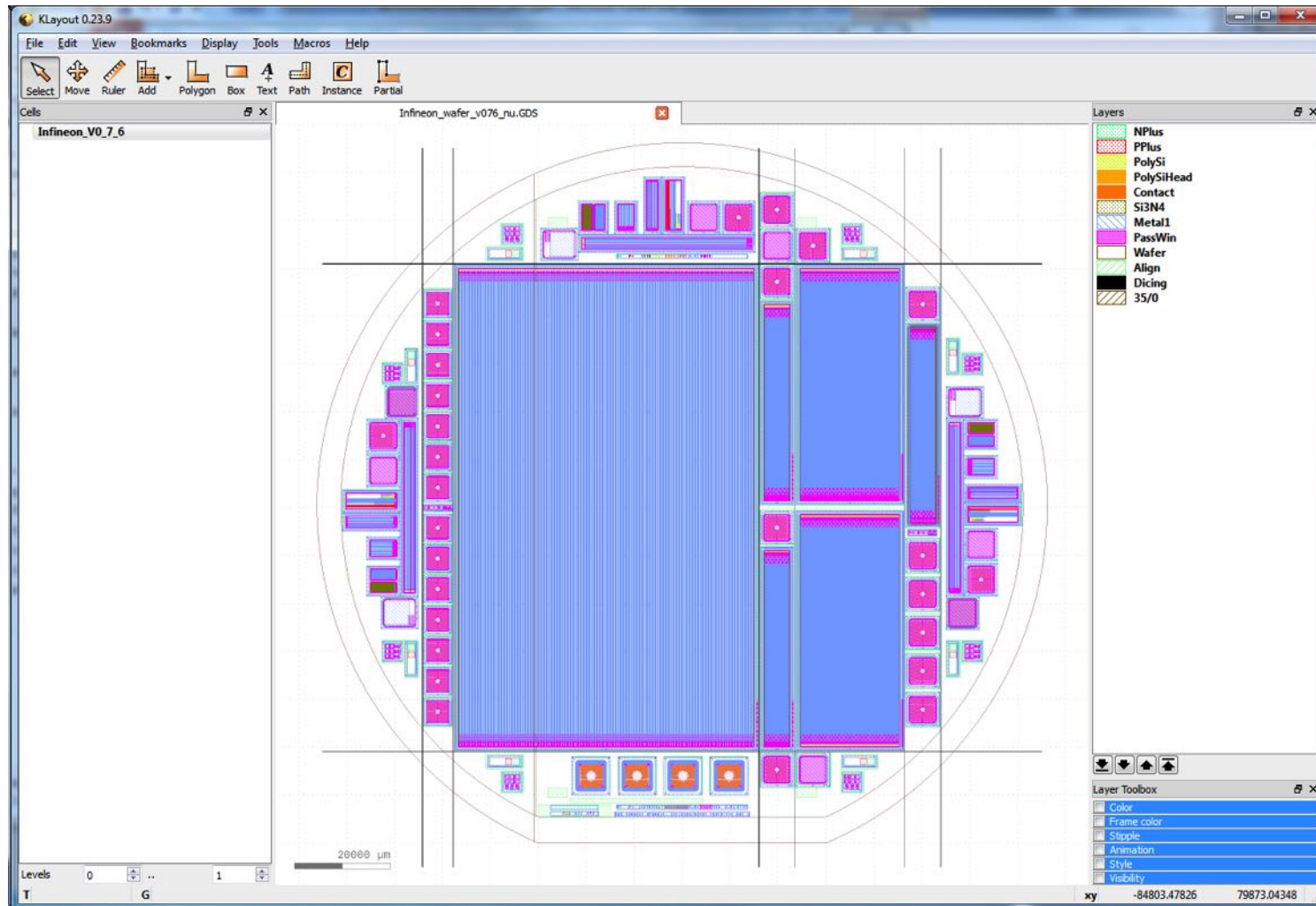
mentor@idobserver:~/SAMPLE/ONSEMI/FUNCTIONS
// Sensor
extern SensorPitch=50;
extern SensorSizeX=10000;
extern SensorSizeY=100000;
extern SensorCutMargin=100;
extern SensorGuardSpacing=50;
extern SensorGuardBiasSpacing=100;
extern SensorBiasStripSpacing=50;

// GuardRing
extern GuardNRings=10;
extern GuardWidth=100;
extern GuardCornerRadius=30;
extern GuardCornerPoints=20;

// BiasRing
extern BiasWidth=100;
extern BiasCornerRadius=30;
    
```

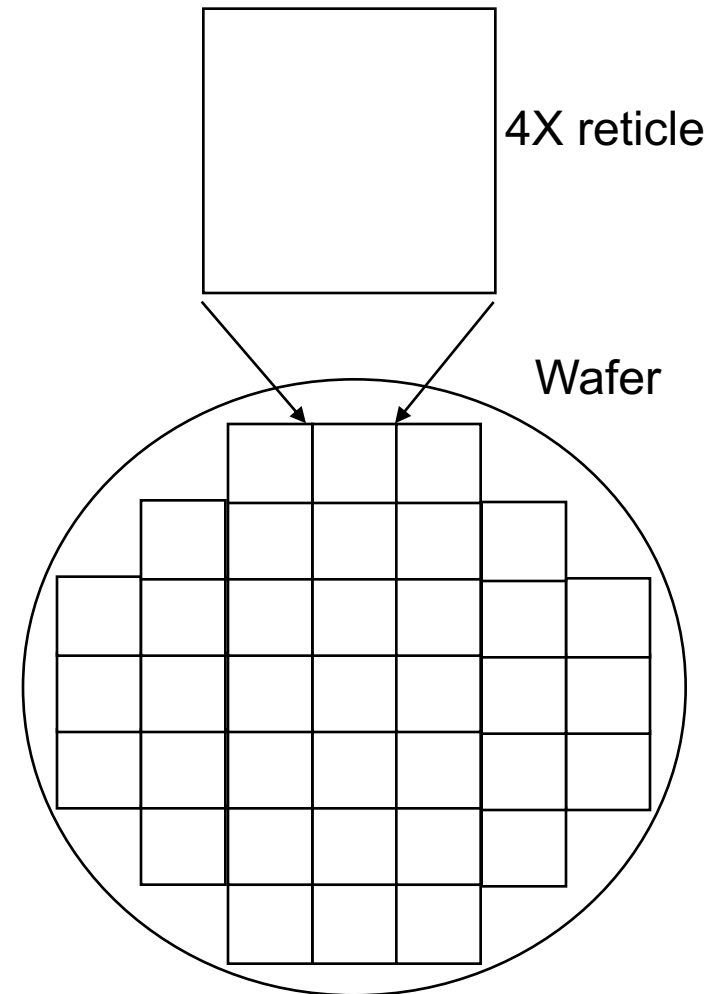


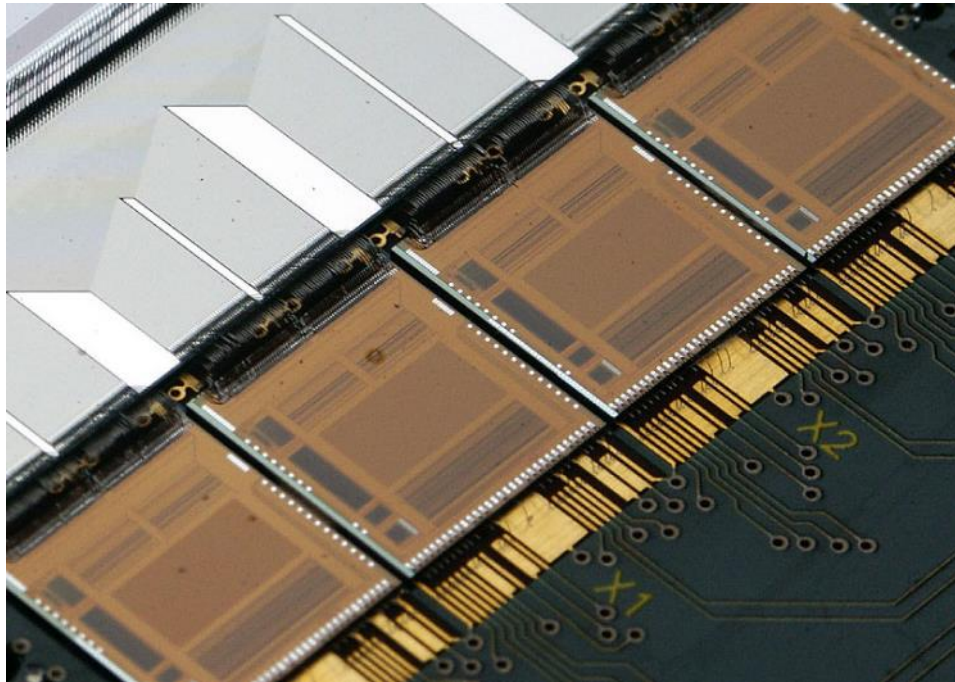
Sensor Mask Design: GDS Files



Stepper vs. full mask lithography

- Illuminate reticle on wafer
 - Typically 4× reduction
- Typical image is 25×25mm
 - Limited by focus
- Step-and repeat across wafer
 - Limited by mechanical alignment





Silicon Detectors in High Energy Physics

Thomas Bergauer (HEPHY Vienna)

Detector concepts: Pixels and Strips

- Single-sided Strip Detectors
- Two-dimensional Readout

- Pixel Detectors

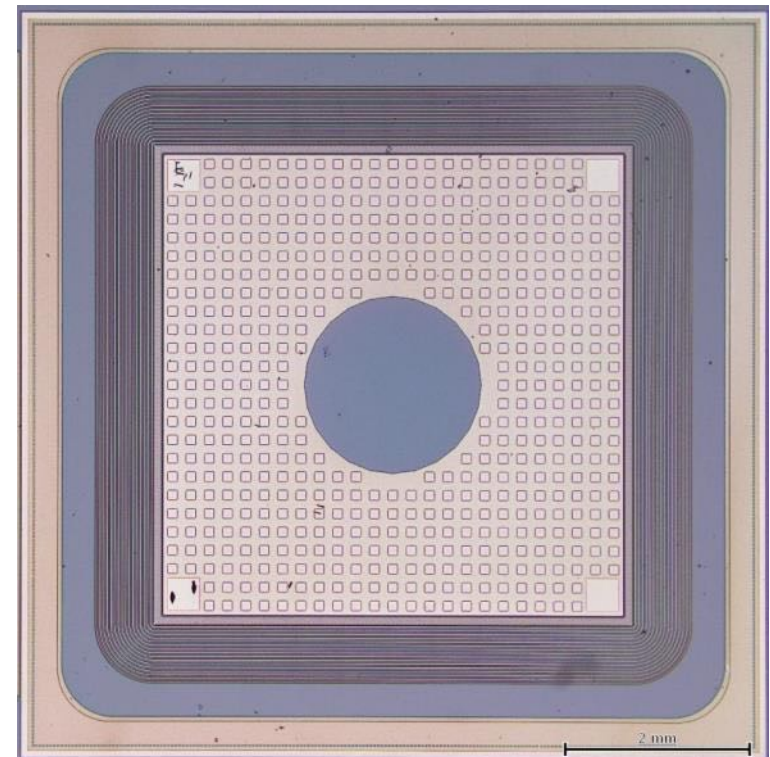
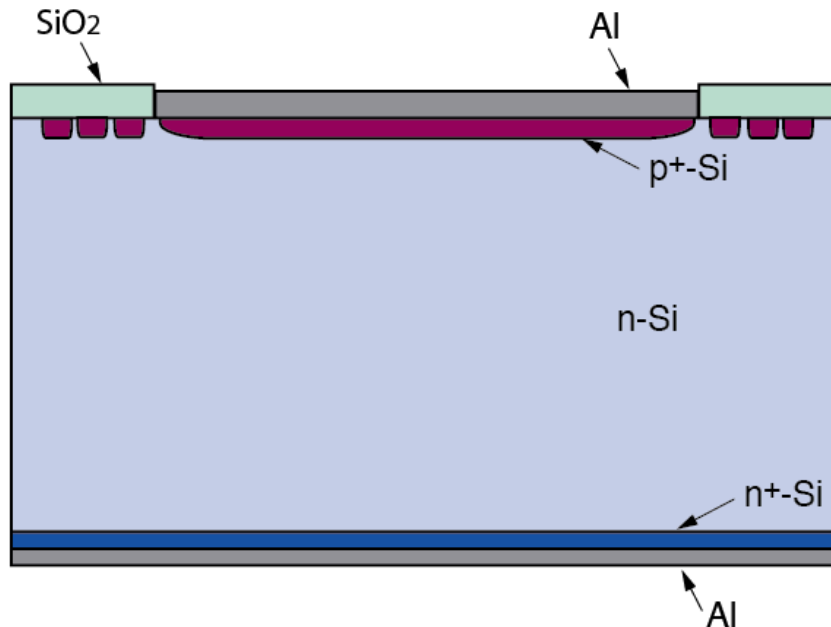
- Other Silicon Detector Structures
 - CCD, Drift Detectors, APD and SiPM, MAPS, DEPFET, SOI, 3D-detectors

SINGLE SIDED STRIP DETECTORS

Pad Detector

The most simple detector is a large surface diode with guard ring(s).

- no position resolution
- Good for basic tests (IV, CV)

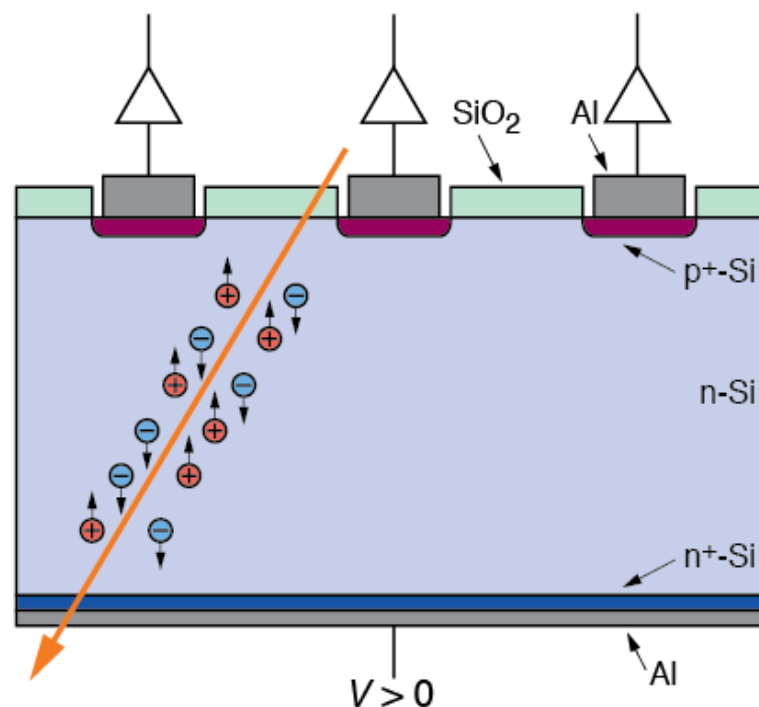


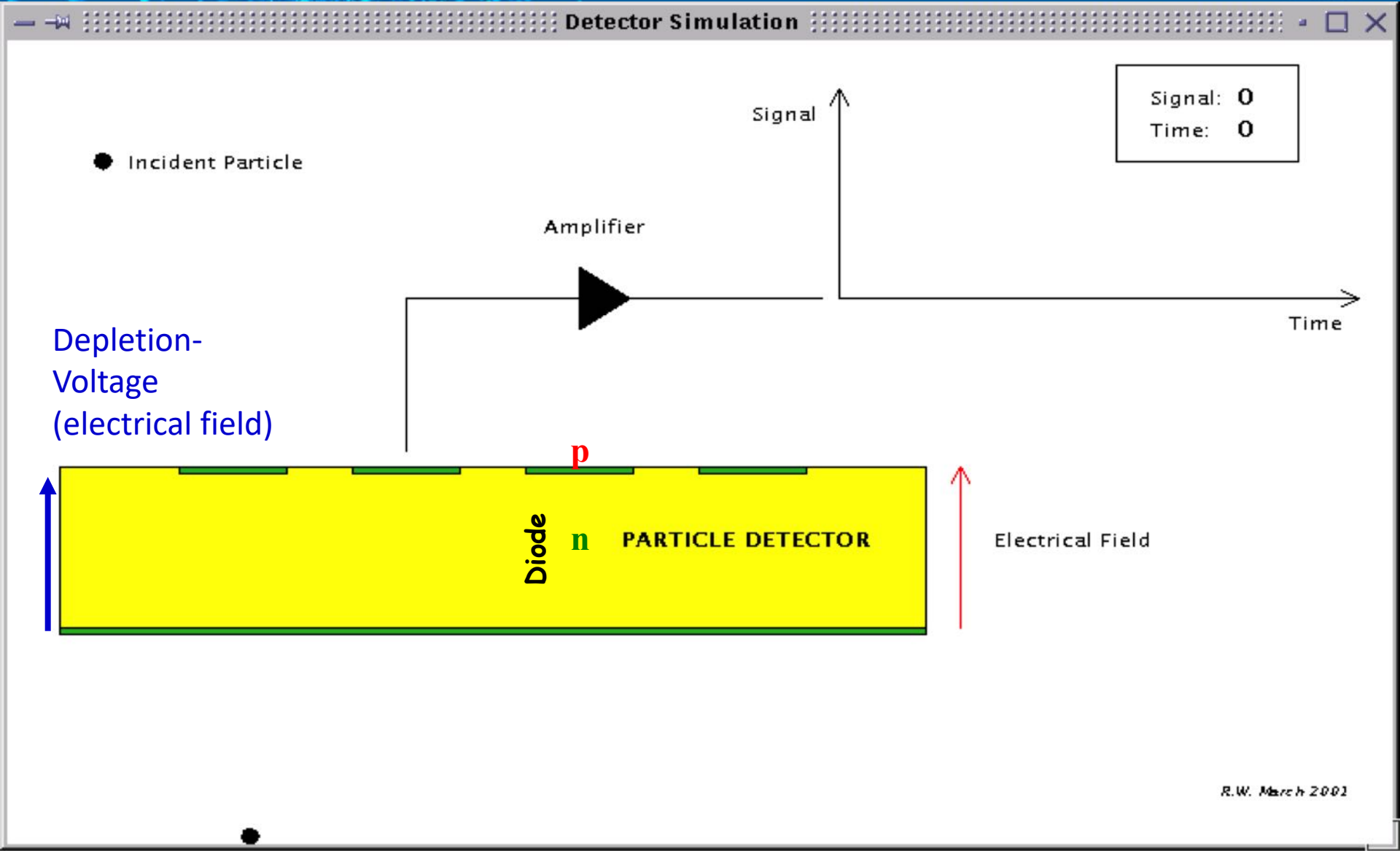
DC coupled strip detector

- Charged particles traversing sensor create e^-/h^+ pairs in the depletion region
- These charges drift to the electrodes.
- The drift (current) creates the signal which is amplified by an amplifier connected to each strip.
- From the signals on the individual strips the position of the through going particle is deduced.

Typical n-type Si strip detector:

- n-type bulk: $\rho > 2 \text{ k}\Omega\text{cm}$
- thickness $300 \mu\text{m}$
- Operating voltage $< 200 \text{ V}$.
- n^+ layer on backplane to avoid Schottky contact and improve ohmic contact
- Aluminum metallization



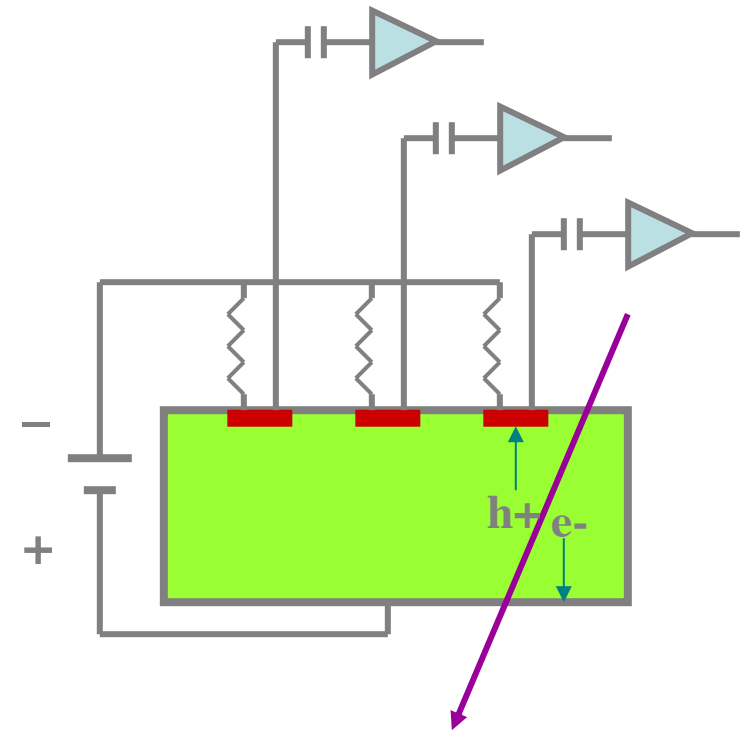


R.W. March 2001

Biassing Methods

- AC-coupled sensors create two electrical circuits on the sensor:
 - Readout circuit into amplifier (AC current)
 - Biasing circuit (DC current)

- Method to connect readout strips to bias voltage source:
 - Poly-silicon resistor
 - Punch-through
 - FOXFET

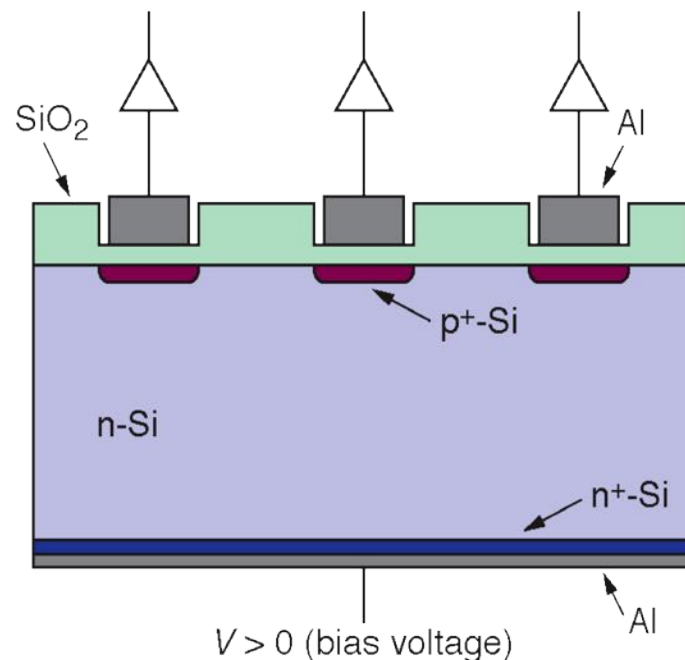


AC coupled strip detector

AC coupling blocks leakage current from the amplifier.

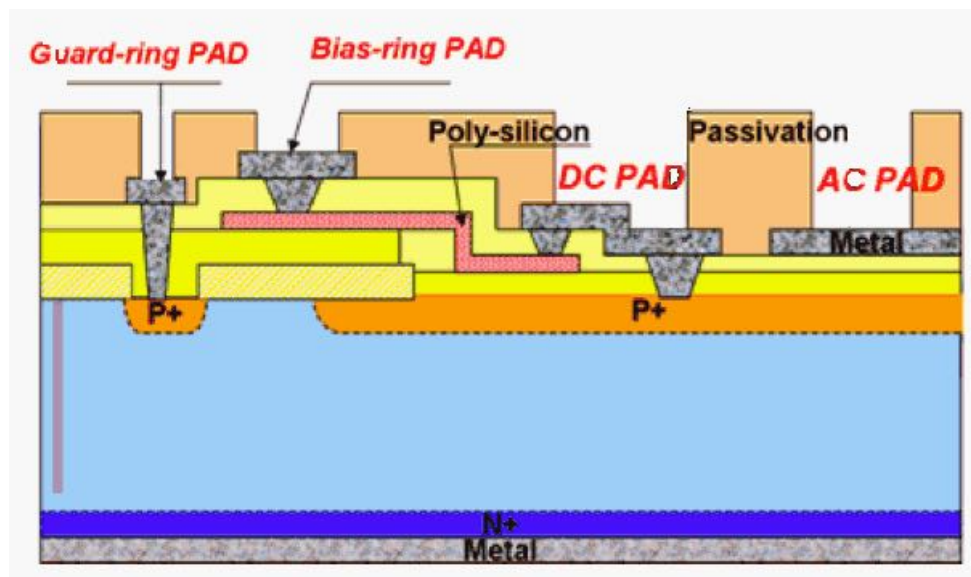
- Integration of coupling capacitances in standard planar process.
- Deposition of SiO_2 with a thickness of **100–200 nm** between p+ and aluminum strip
- Increase quality of dielectric by a second layer of Si_3N_4 .

AC coupled strip detector:



Biassing Methods: Poly-Silicon

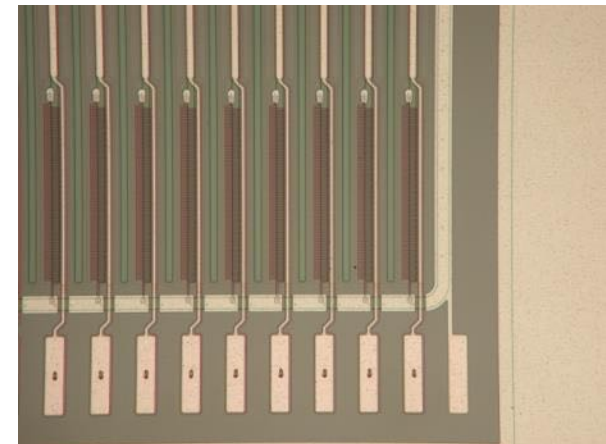
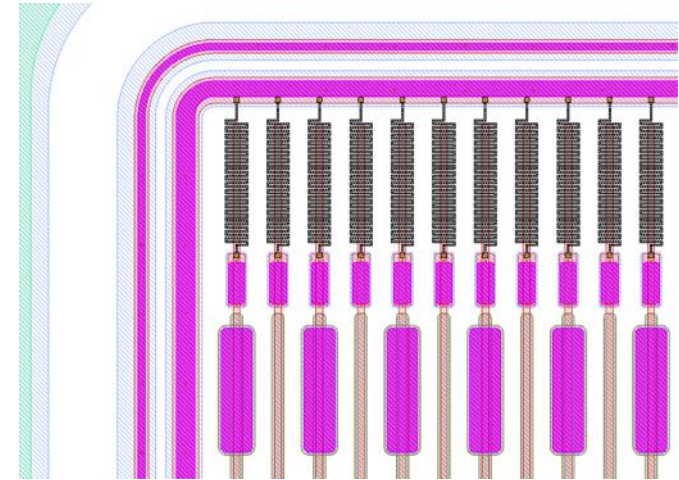
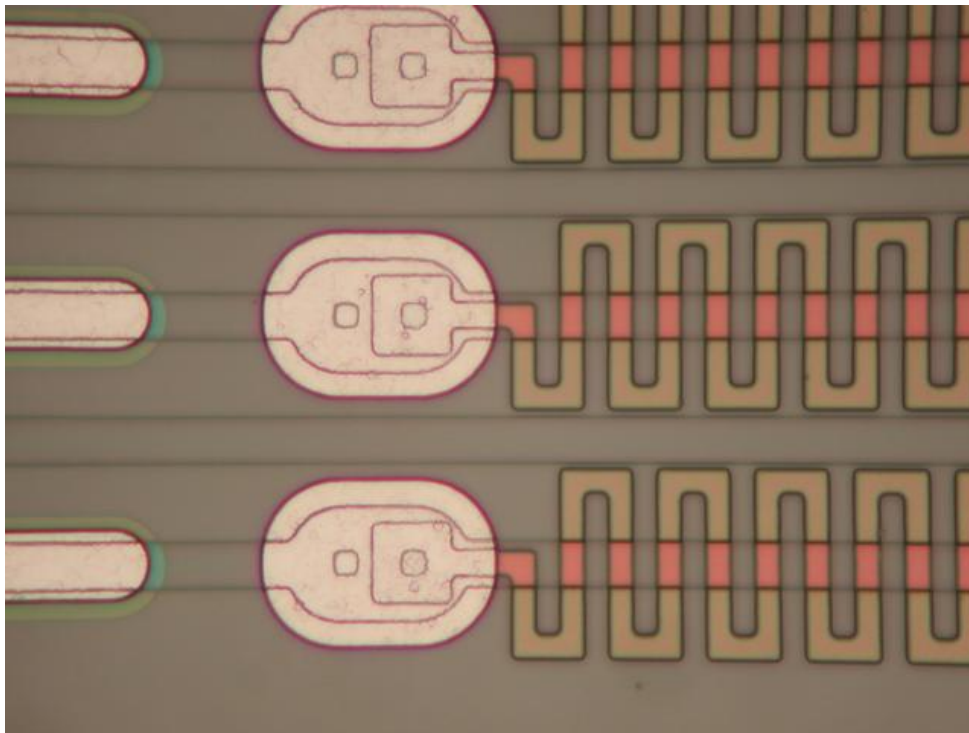
- Deposition of poly-crystalline silicon between p⁺ implants and a common bias line.
- Typical sheet resistance of up to $R_s \approx 4 \text{ k}\Omega/\text{square}$. Depending on width and length a resistor of up to $R \approx 20 \text{ M}\Omega$ is achieved ($R = R_s \cdot \text{length}/\text{width}$).
- To achieve high resistor values meandering poly structures are deposited.
- Drawback: Additional production steps and photo lithographic masks required.



Cross section of AC coupled strip detector with integrated poly resistors:

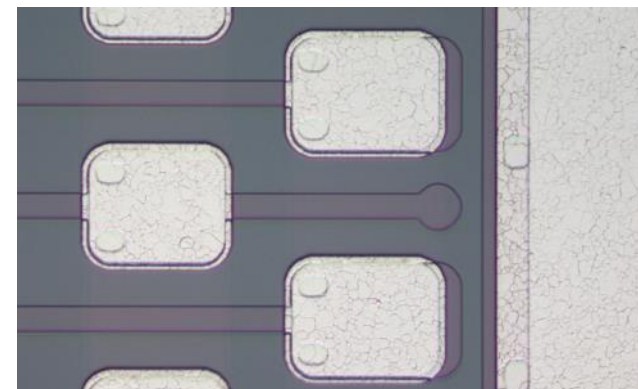
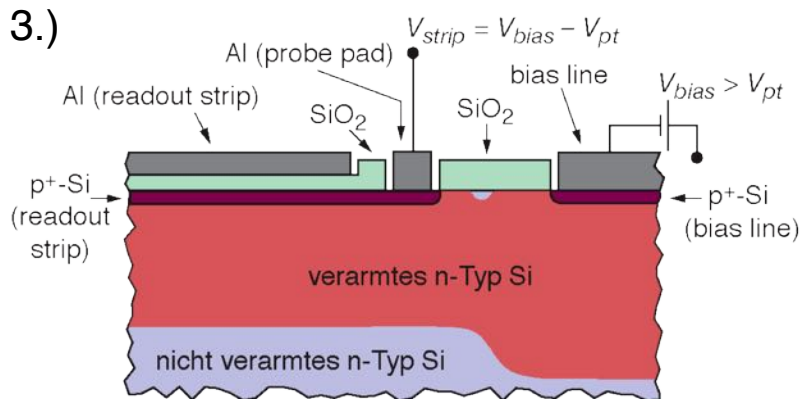
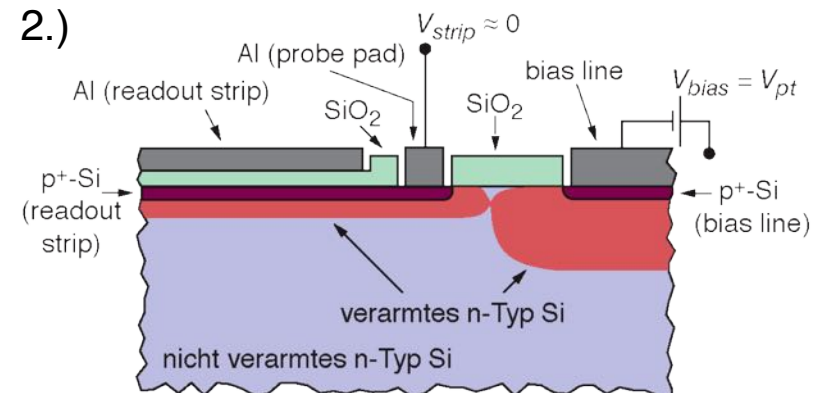
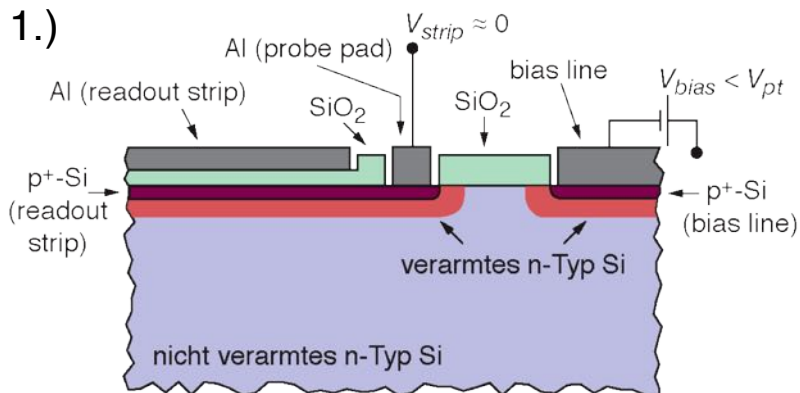
Biasing Methods: Poly-Silicon (2)

Top view of a strip detector with poly-silicon resistors:



Biassing Methods: Punch through

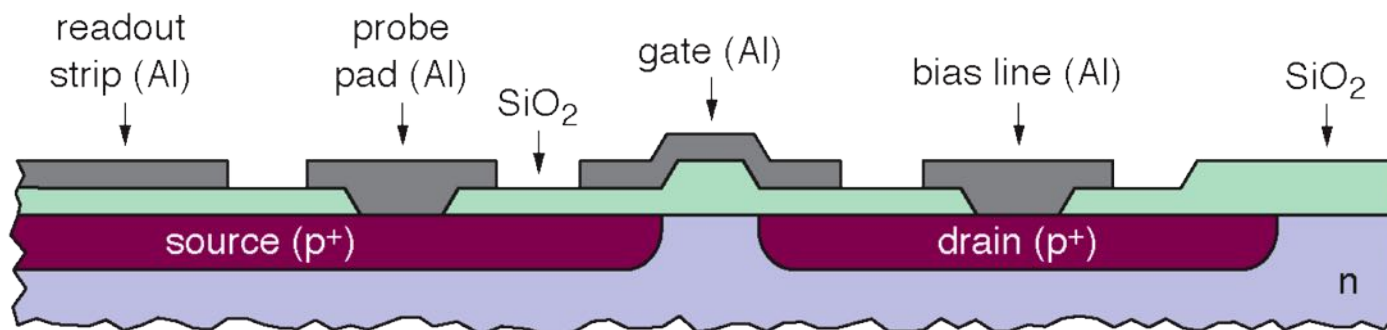
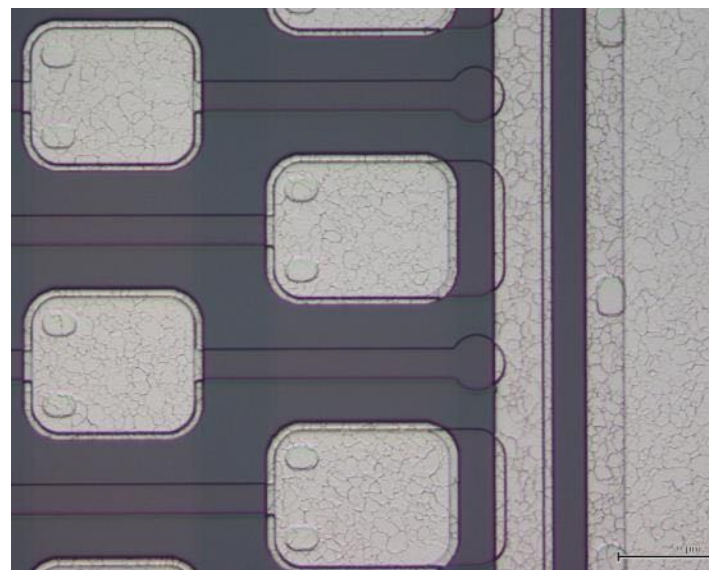
Punch through effect: Figures show the increase of the depletion zone with increasing bias voltage (V_{pt} = punch through voltage).



Advantage: No additional production steps required.

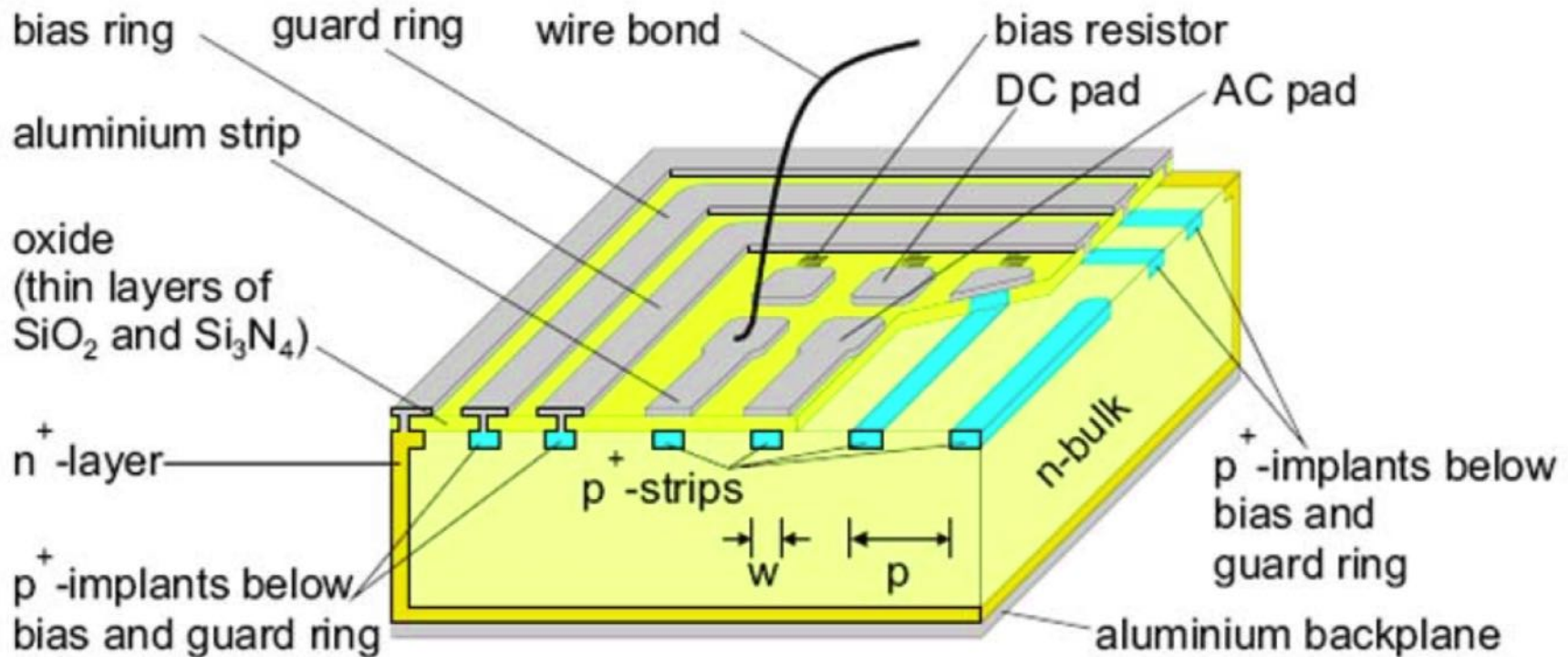
Biasing Methods: FOXFET

- Strip p⁺ implant and bias line p⁺ implant are source and drain of a field effect transistor
→ FOXFET (**Field OXide Field Effect Transistor**).
- A gate is implemented on top of a SiO₂ isolation.
- Dynamic resistor between drain and source can be adjusted with gate voltage.



Summary: Typical AC-coupled Sensor

Most commonly used scheme using poly-Si bias resistor



TWO-DIMENSIONAL-READOUT

Stereo Modules

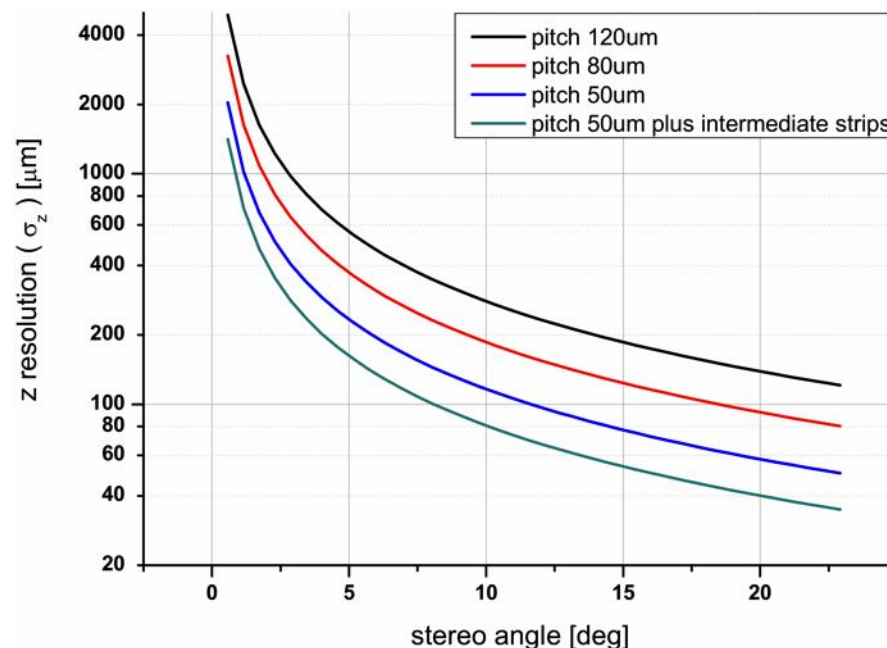
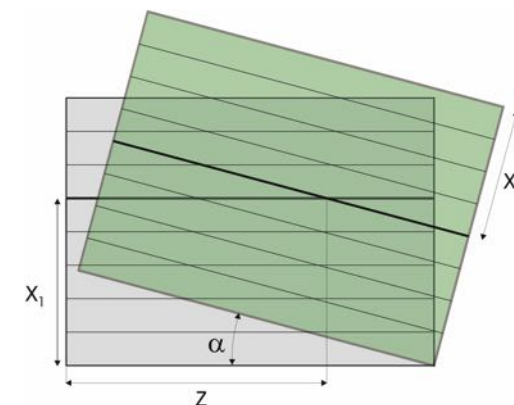
2nd coordinate requires second detector underneath

→ double the material

- Acceptable for hadron colliders like LHC
- Not acceptable for e⁺/e⁻ colliders with tighter material budget

Tilt angle defines z-resolutions (usually along beam axis)

- CMS uses ~6 degrees



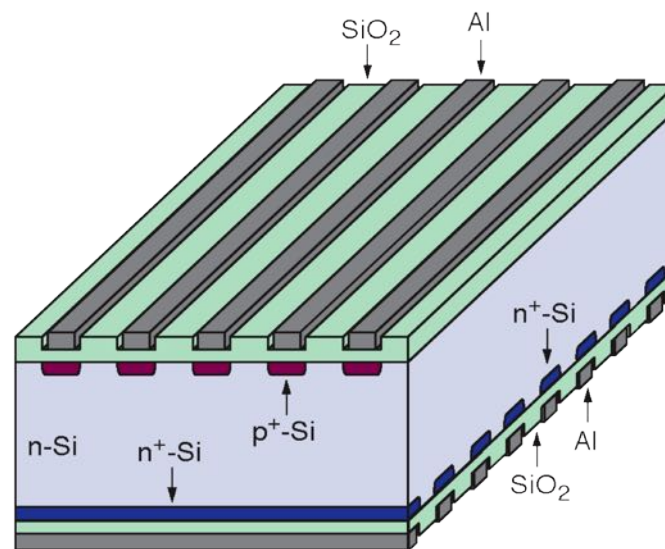
Double Sided Silicon Detectors (DSSDs)

Advantages:

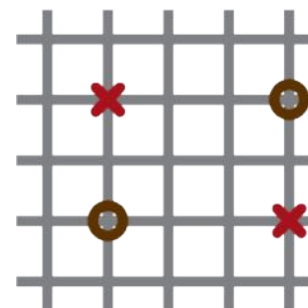
- More elegant way for measuring 2 coordinates
- Saves material



Disadvantages:

- Needs special strip insulation of n-side (p-stop, p-spray techniques)
- Very complicated manufacturing and handling procedures → expensive
- Ghost hits at high occupancy



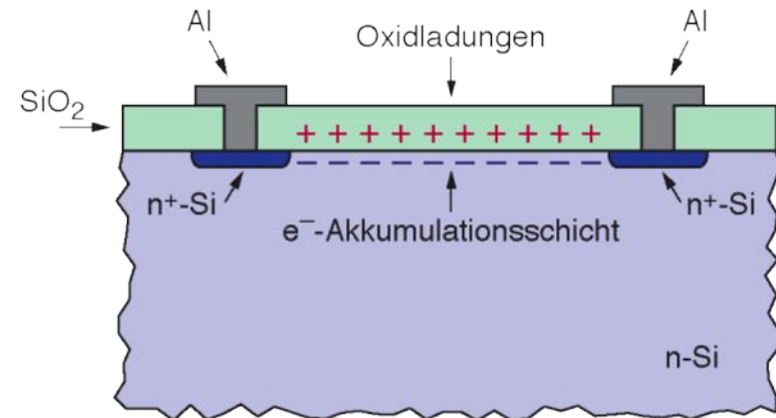
Scheme of a double sided strip detector (biasing structures not shown)



 real hits
 "Ghosts"

Strip Isolation on n-Side

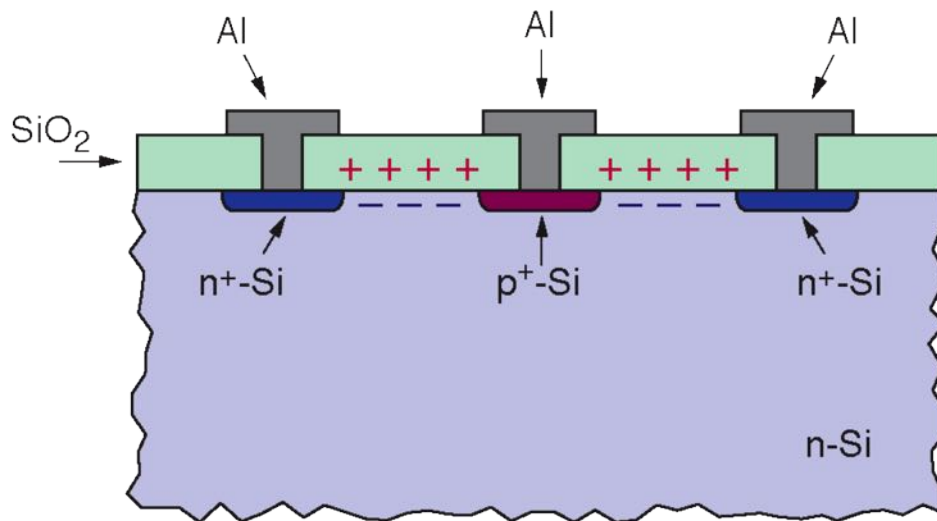
- Problem with n^+ segmentation: Static, positive oxide charges in the Si-SiO_2 interface.
- These positive charges attract electrons. The electrons form an accumulation layer underneath the oxide.
- n^+ strips are no longer isolated from each other (resistance $\approx \text{k}\Omega$).
- Charges generated by through going particle spread over many strips.
- **No position measurement possible.**
- Solution: Interrupt accumulation layer using p^+ -stops, p^+ -spray or field plates.



Positive oxide charges cause electron accumulation layer.

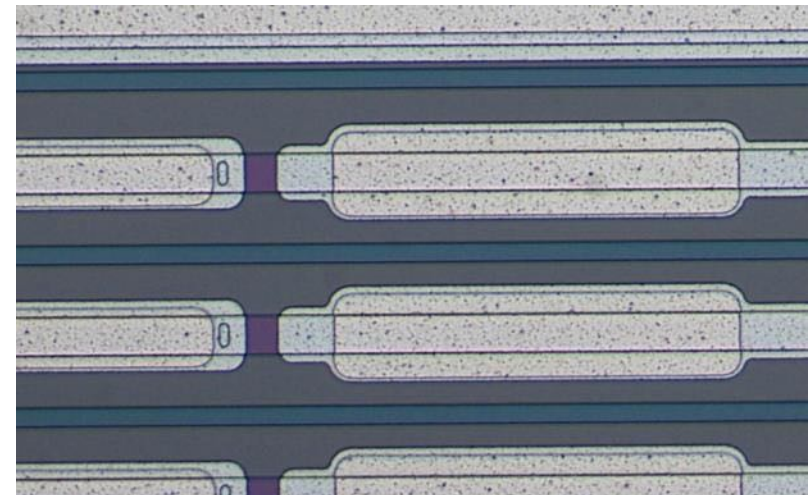
Strip Isolation using p-stop

- p⁺-implants (p⁺-stops, blocking electrodes) between n⁺-strips interrupt the electron accumulation layer.
- Inter-strip resistance reach again O(GΩ).



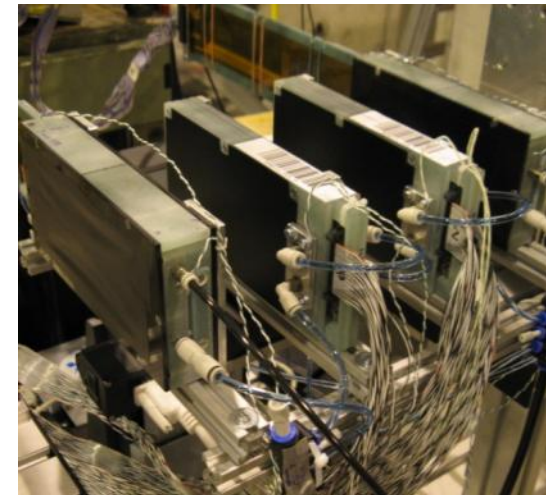
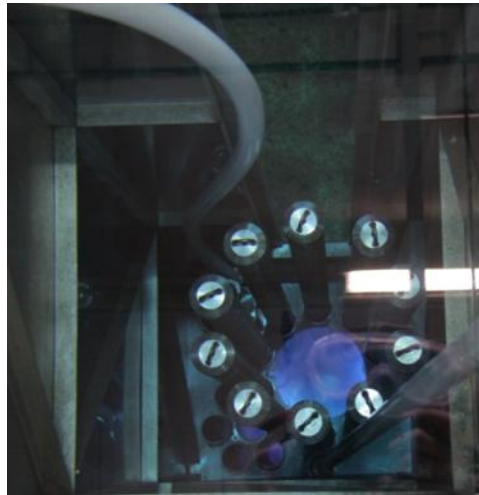
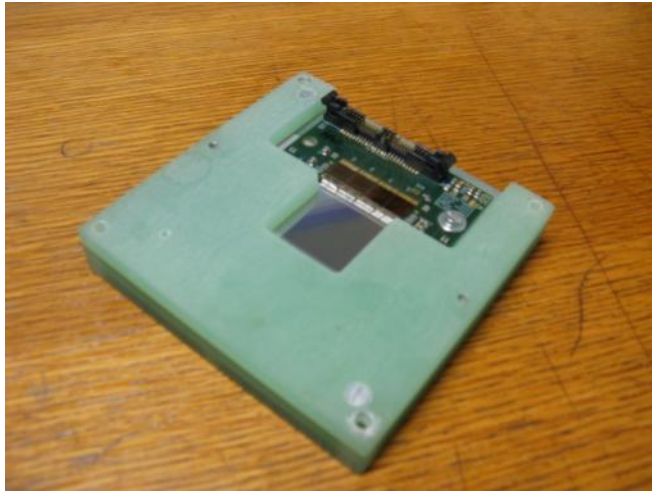
A. Peisert, *Silicon Microstrip Detectors*, DELPHI 92-143 MVX 2, CERN, 1992

Picture showing the n⁺-strips and the p⁺-stop structure:



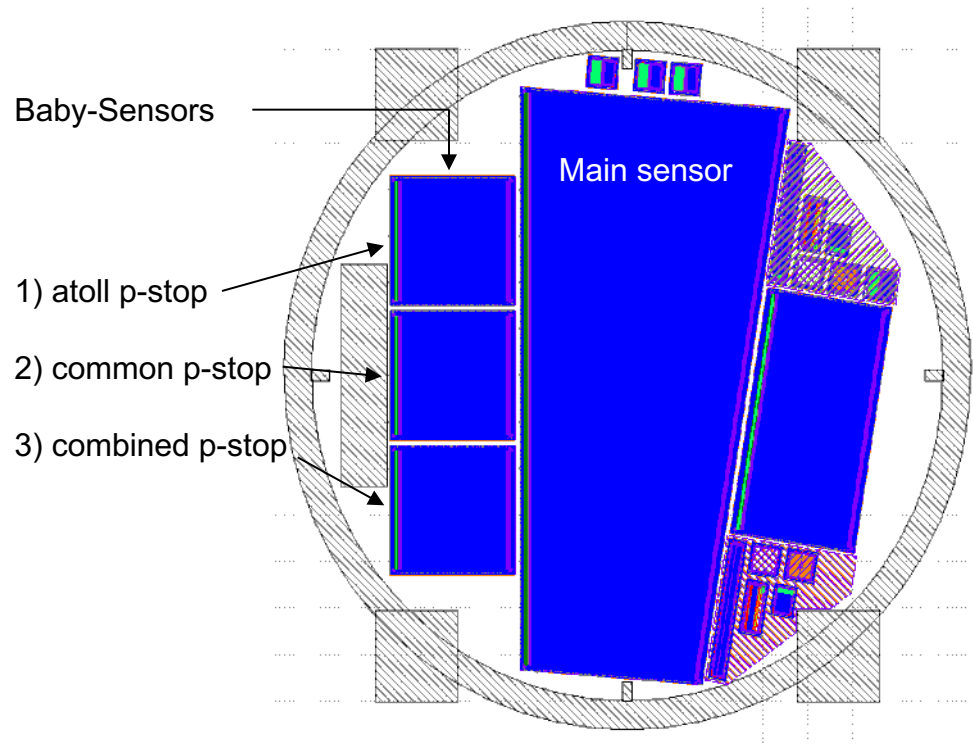
Prototype sensors for Belle II SVD

P-stop performance before/after irradiation



DSSD Sensor design

- Belle II sensors
- Double sided
 - Structures for strip separation on n-side needed → „p-stop“
 - 3 design with 4 different layouts



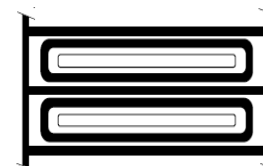
Muster 1: atoll p-stop



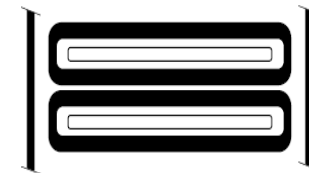
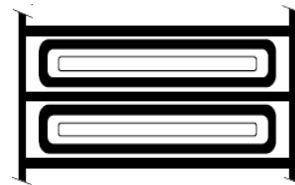
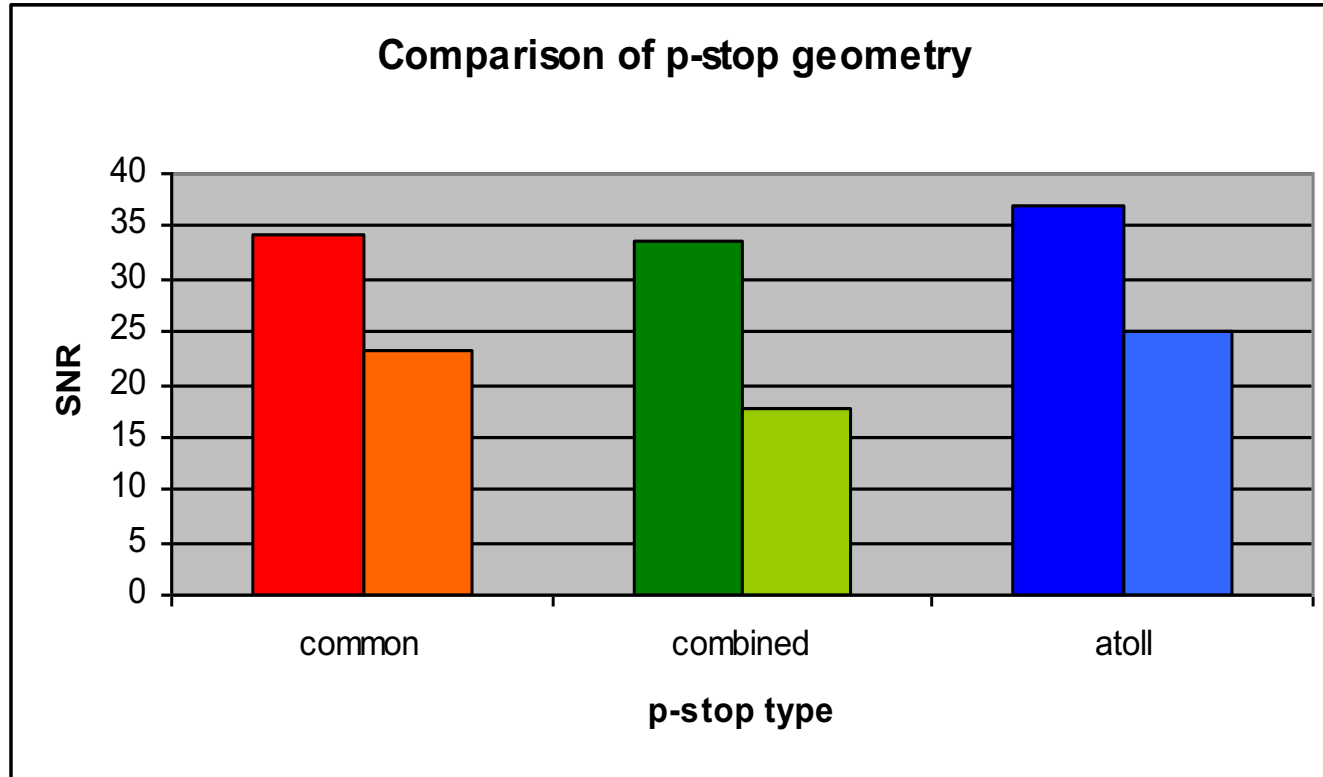
Muster 2: common p-stop



Muster 3: combined p-stop

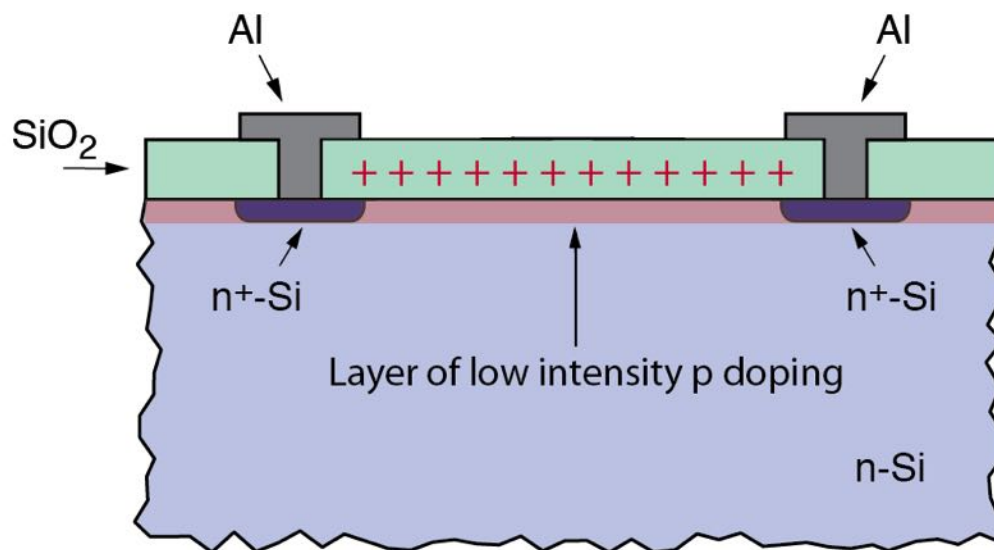


Example 2 (cont.): Analysis of data



Strip Isolation using p-spray

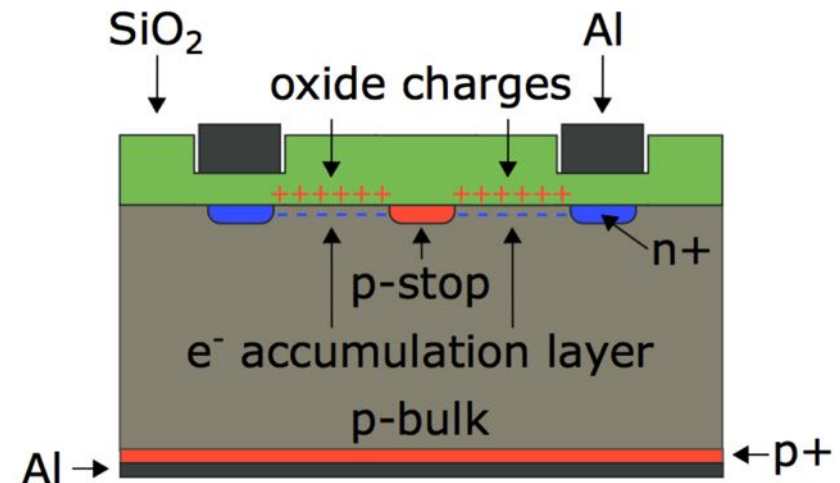
- p doping as a layer over the whole surface.
- disrupts the e^- accumulation layer.



- Often, a combination of p⁺ stops and p spray is being used

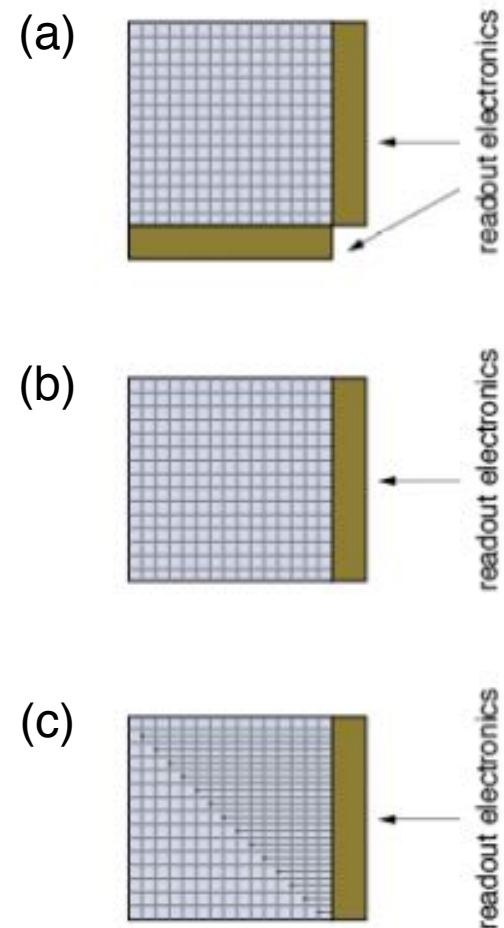
Strip Isolation in single-sided p-type detector

- Single-sided detector using p-type substrate and n-type strips would NOT give working detector.
 - Fixed oxide charges are always positive and create e⁻ accumulation layer in silicon
 - Electrons create short between
- For tradition and production reasons most detectors used are n-type detectors. p-type detectors have some advantages in high radiation environment (see later).



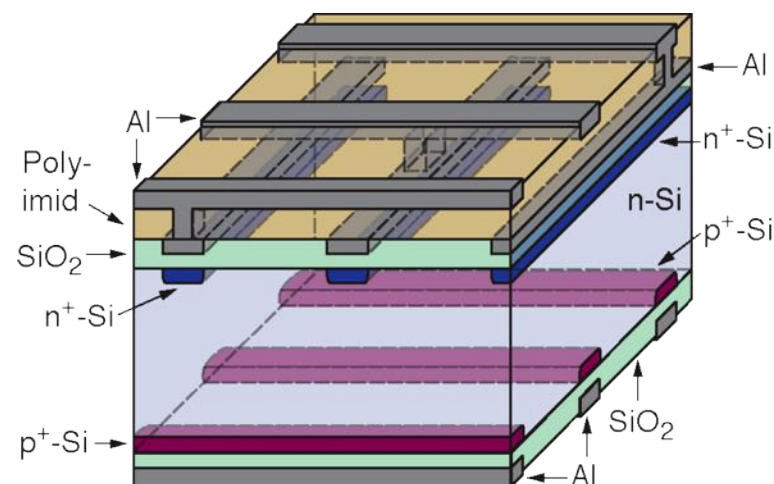
Routing using 2nd metal layer

- In the case of double sided strip detectors with orthogonal strips the readout electronics is located on at least two sides (fig. a).
- Many drawbacks for construction and material distribution, especially in collider experiments.
- Electronics only on one side is a preferred configuration (fig. b).
- Possible by introducing a second metal layer. Lines in this layer are orthogonal to strips and connect each strips with the electronics (fig. c). The second metal layer can be realized by an external printed circuit board, or better integrated into the detector.



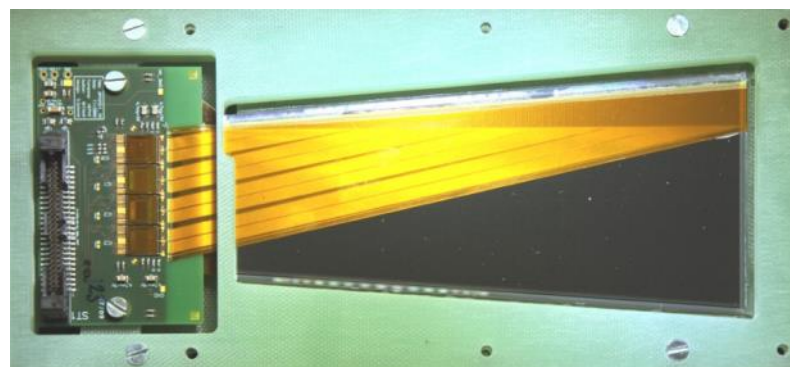
Routing using 2nd metal layer

- **DSSD with double metal**
 - Most complex detector
 - 16 layers
 - The isolation between the two metal layers is either SiO_2 or polyimide (common name Kapton)
 - Has been used by DELPHI experiment at LEP



3D scheme of an AC coupled double sided strip detector with 2nd metal readout lines (bias structure not shown).

- **Alternative**
 - Discrete pitch adapter using Kapton flex circuit



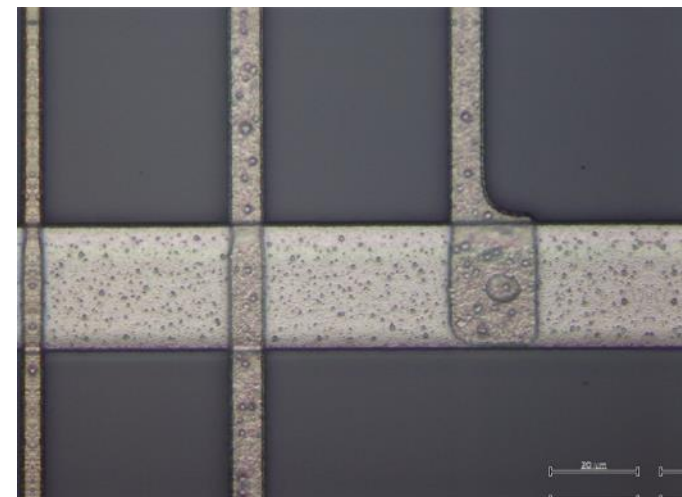
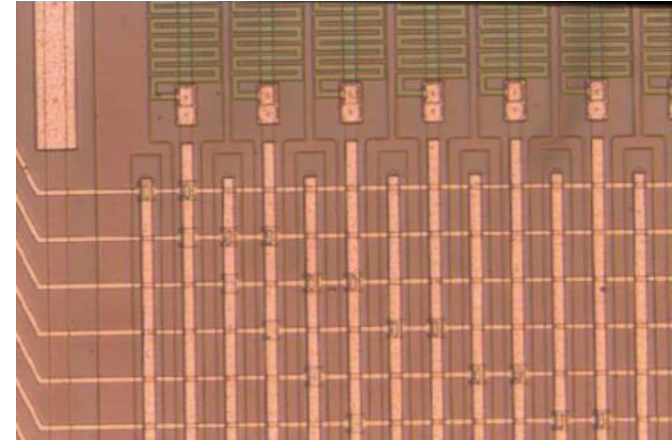
Double Metal Layer

Advantages:

- routing integrated into sensor

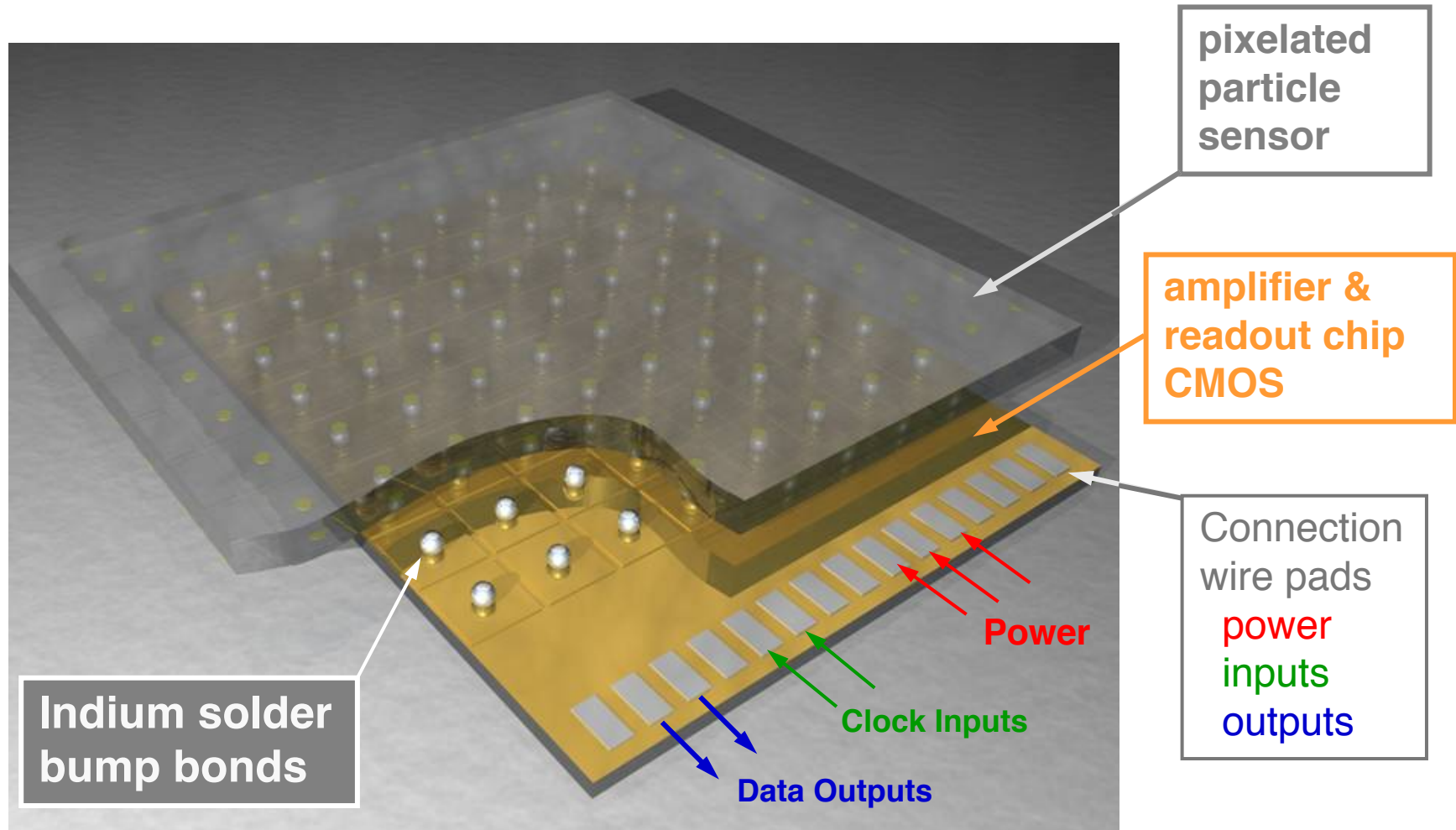
Disadvantages:

- Two more layers on wafer increase complexity
 - Via's
 - Metal
- Increased coupling and crosstalk between readout and routing lines
 - Thickness of isolation between metal layers is crucial



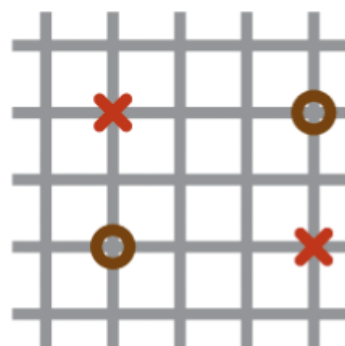
HYBRID PIXEL DETECTORS



Hybrid Pixel Detectors Principle




Pixel Detectors Advantages

- Double sided strip sensors produce ghost hits
 - Problematic for high occupancies
- Pixel detectors produce unambiguous hits



 real tracks
 "ghosts"

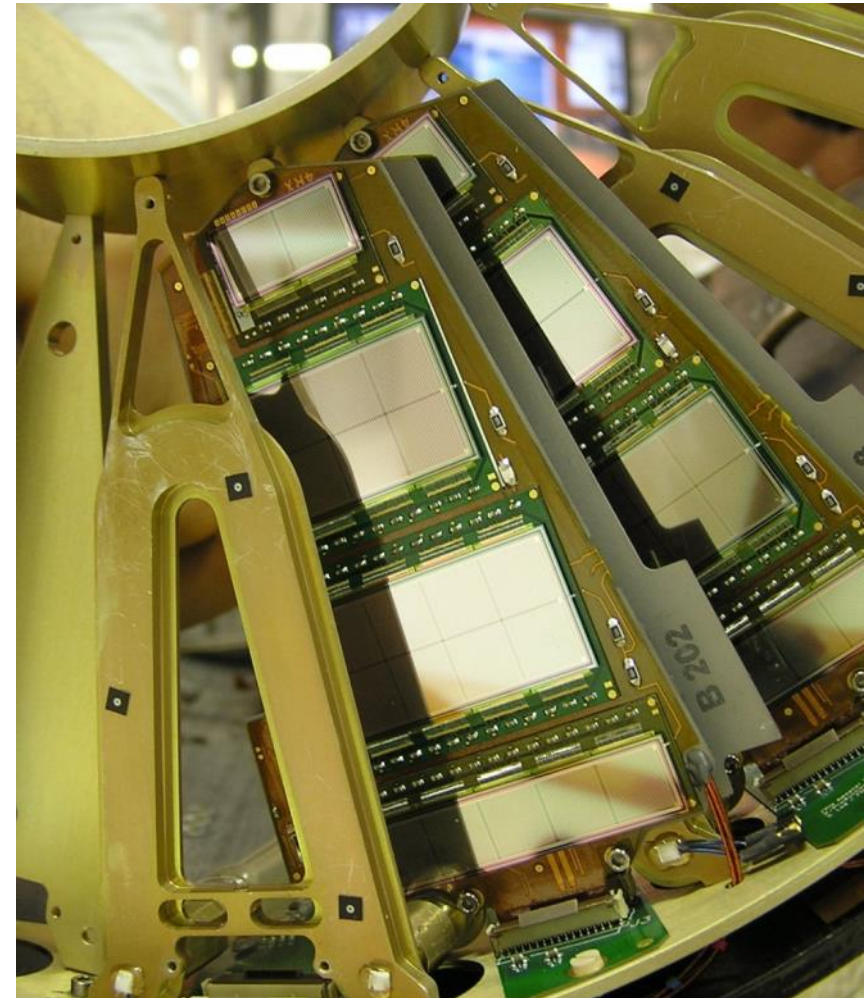


 real tracks

- **Small pixel area** → low detector capacitance (≈ 1 fF/Pixel)
→ large signal-to-noise ratio (e.g. 150:1).
- **Small pixel volume** → low leakage current (≈ 1 pA/Pixel)

Disadvantages of pixel detectors

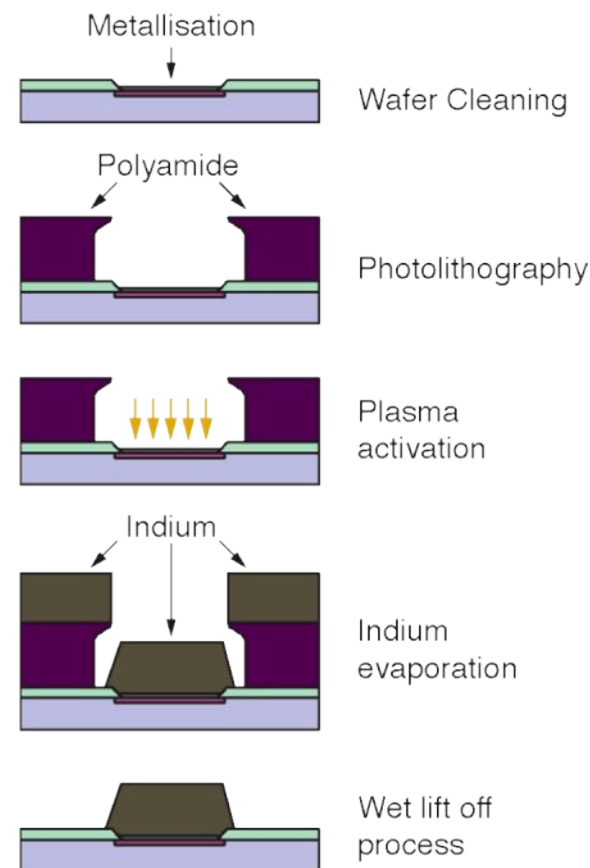
- Large number of readout channels
 - Large number of electrical connections in case of hybrid pixel detectors.
 - Large power consumption of electronics
- Expensive to cover large areas
 - Suitable for innermost region near collision region



Bump bonding process

A typical bump bonding process (array bump bonding) is the following:

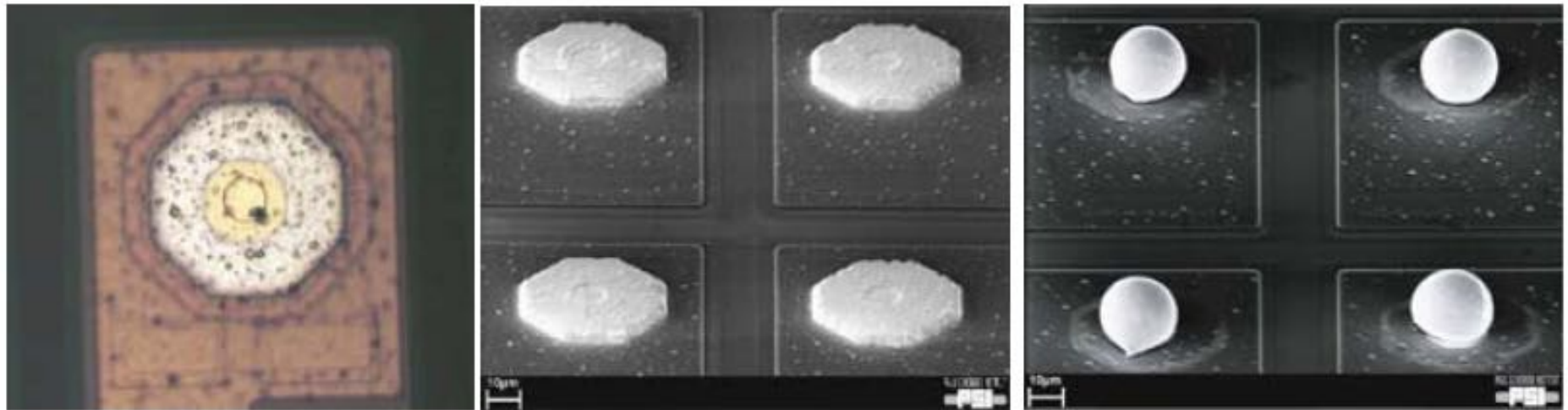
1. Deposition of an “under-bump metal layer”, plasma activated, for a better adhesion of the bump material.
2. Photolithography to precisely define areas for the deposition of the bond material.
3. Deposition, by evaporation, of the bond material (e.g. In or SnPb) producing little “bumps” ($\approx 10 \mu\text{m}$ height).
4. Edging of photolithography mask leaves surplus of bump metal on pads.
5. Reflow to form balls.



L. Rossi, Pixel Detectors Hybridisation,
Nucl. Instr. Meth. A 501, 239 (2003)

Bump bonding process

Electron microscope pictures before and after the reflow production step.
In bump, The distance between bumps is $100\ \mu\text{m}$, the deposited indium is $50\ \mu\text{m}$ wide while the reflowed bump is only $20\ \mu\text{m}$ wide.



C. Broennimann, F. Glaus, J. Gobrecht, S. Heising, M. Horisberger, R. Horisberger, H. Kästli, J. Lehmann, T. Rohe, and S. Streuli, *Development of an Indium bump bond process for silicon pixel detectors at PSI*, *Nucl. Inst. Met. Phys. Res. A565(1)* (2006) 303–308 82

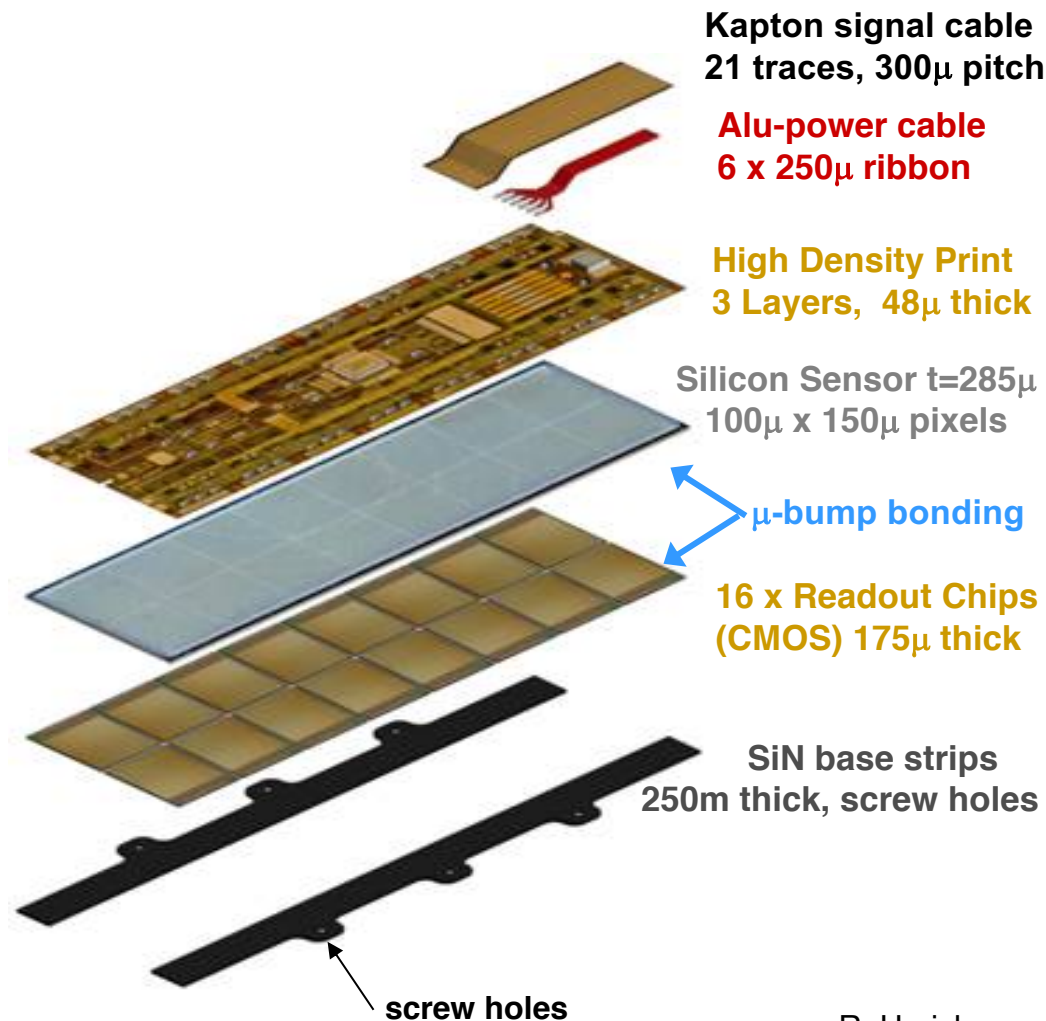
Hybrid Pixel Module for CMS

Sensor:

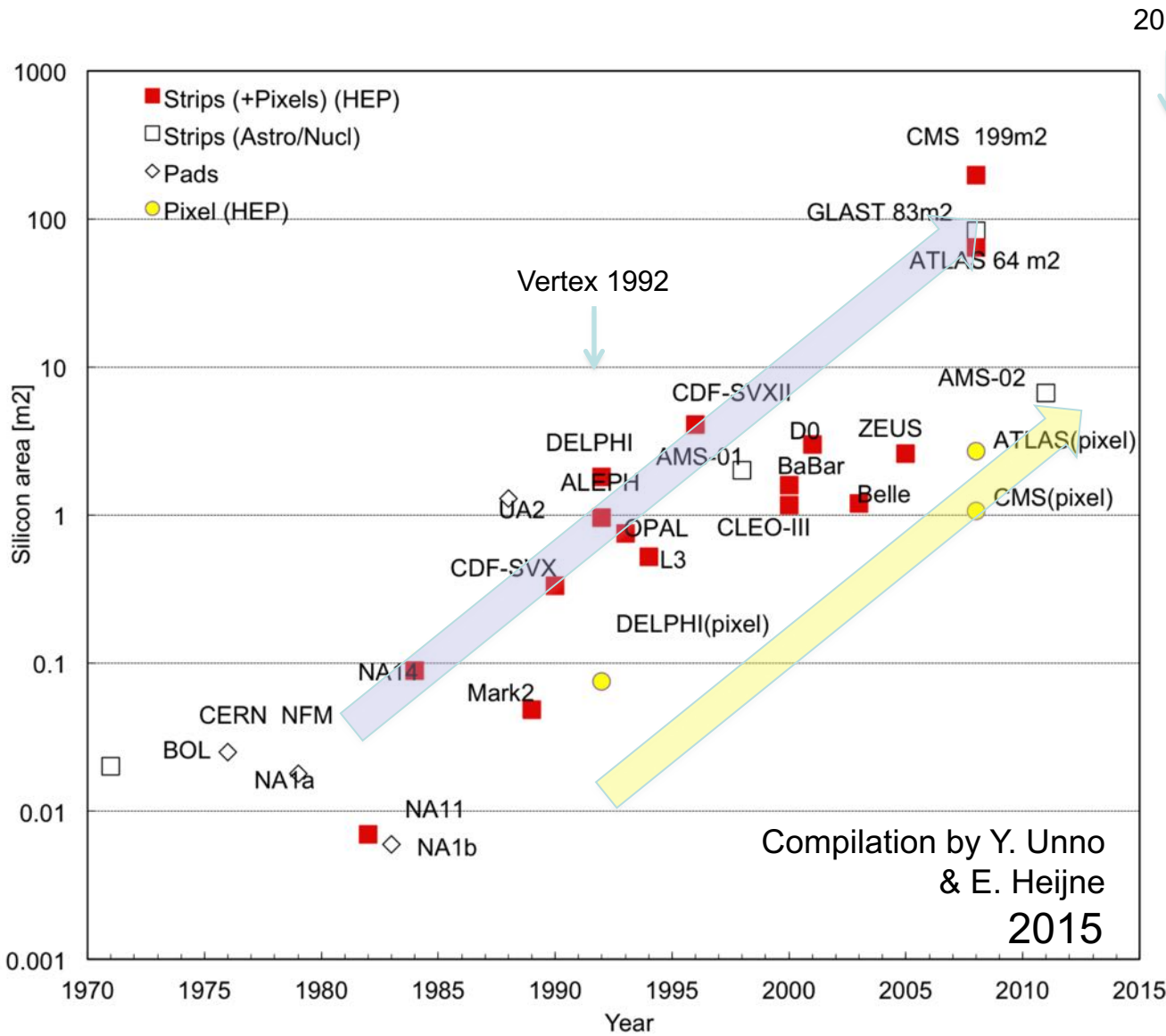
- Pixel Size: 150mm x 100mm
 - Resolution $\sigma_{r-\phi} \sim 15\mu\text{m}$
 - Resolution $\sigma_z \sim 20\mu\text{m}$
- n+-pixel on n-silicon design
 - Moderated p-spray \rightarrow HV robustness

Readout Chip:

- Thinned to 175 μm
- 250nm CMOS IBM Process
- 8" Wafer



R. Horisberger



- Evolution of the silicon area from $O(1 \text{ cm}^2)$ to $O(100 \text{ m}^2)$
- The front of the 1st “wave” has been “Strip” detectors.
- We may see the 2nd “wave” of the “pixel-like” detectors now...

2017



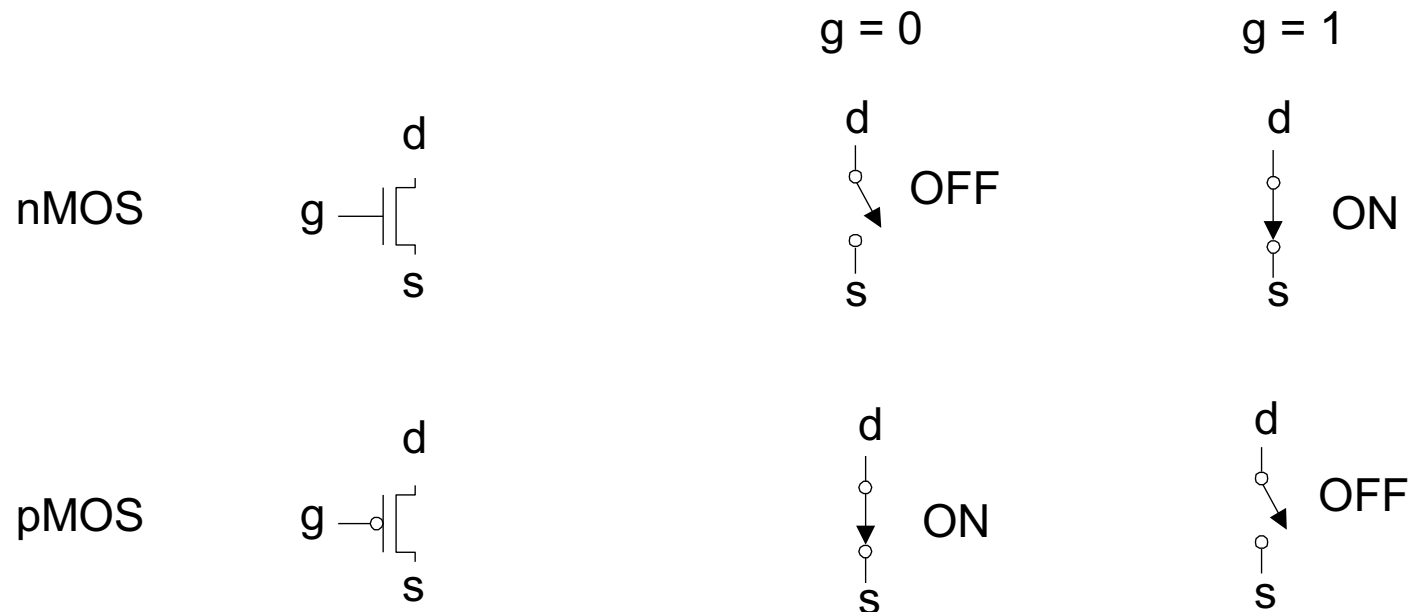
CMOS Sensors

MAPS AND HV/HR-CMOS^{*)}

^{*)} High-Voltage/High Resistivity CMOS

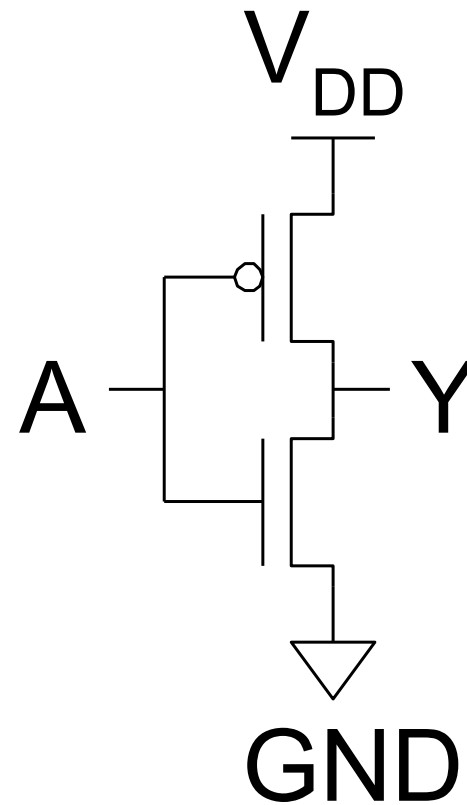
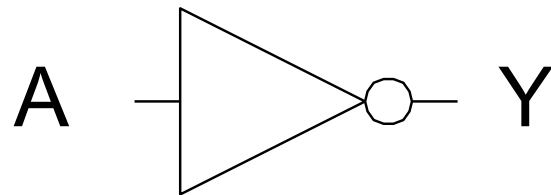
Transistors as Switches

- We can view MOS transistors as electrically controlled switches
- Voltage at gate controls path from source to drain



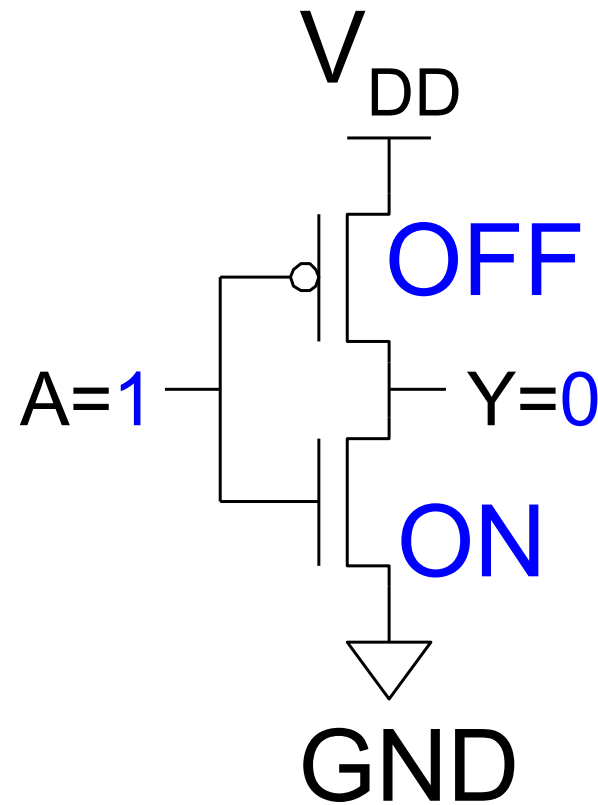
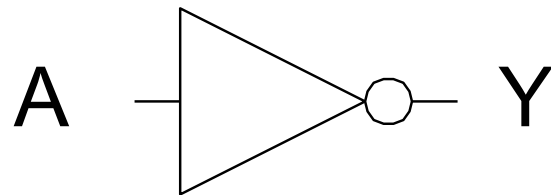
CMOS Inverter

A	Y
0	
1	



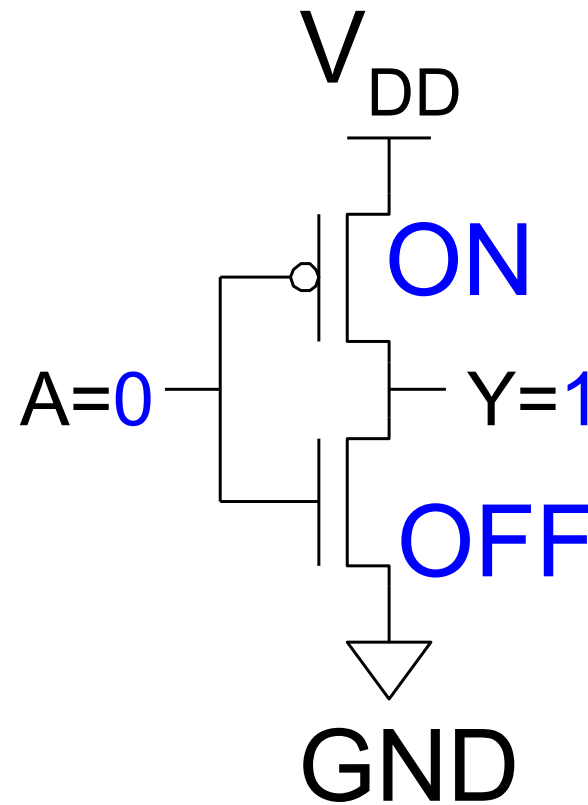
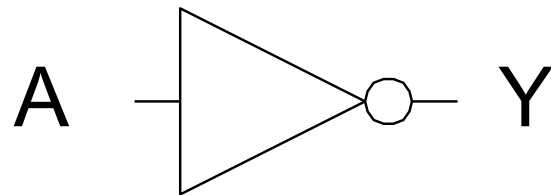
CMOS Inverter

A	Y
0	
1	0



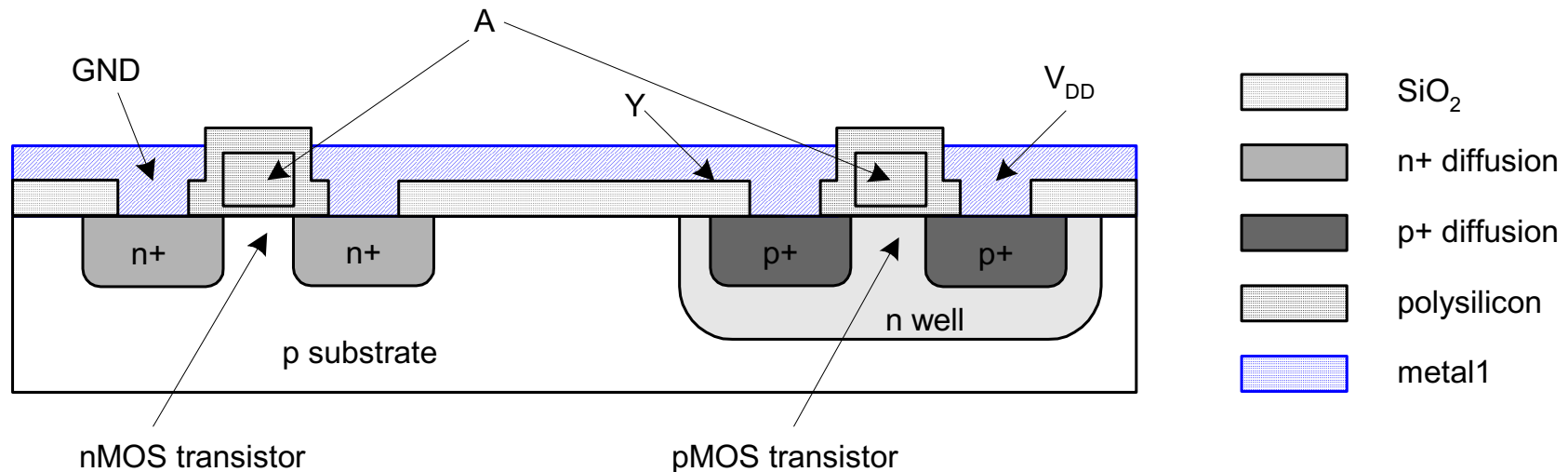
CMOS Inverter

A	Y
0	1
1	0



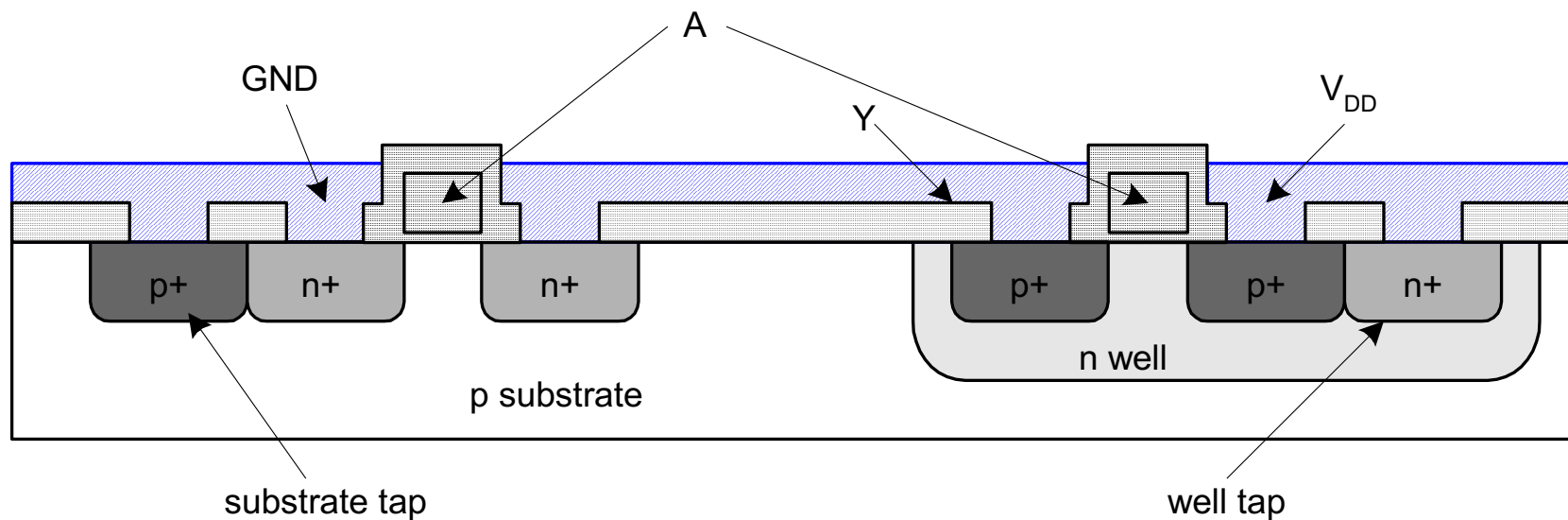
Inverter Cross-section

- Typically use p-type substrate for nMOS transistor
 - Requires n-well for body of pMOS transistors
 - Several alternatives: SOI, twin-tub, etc.



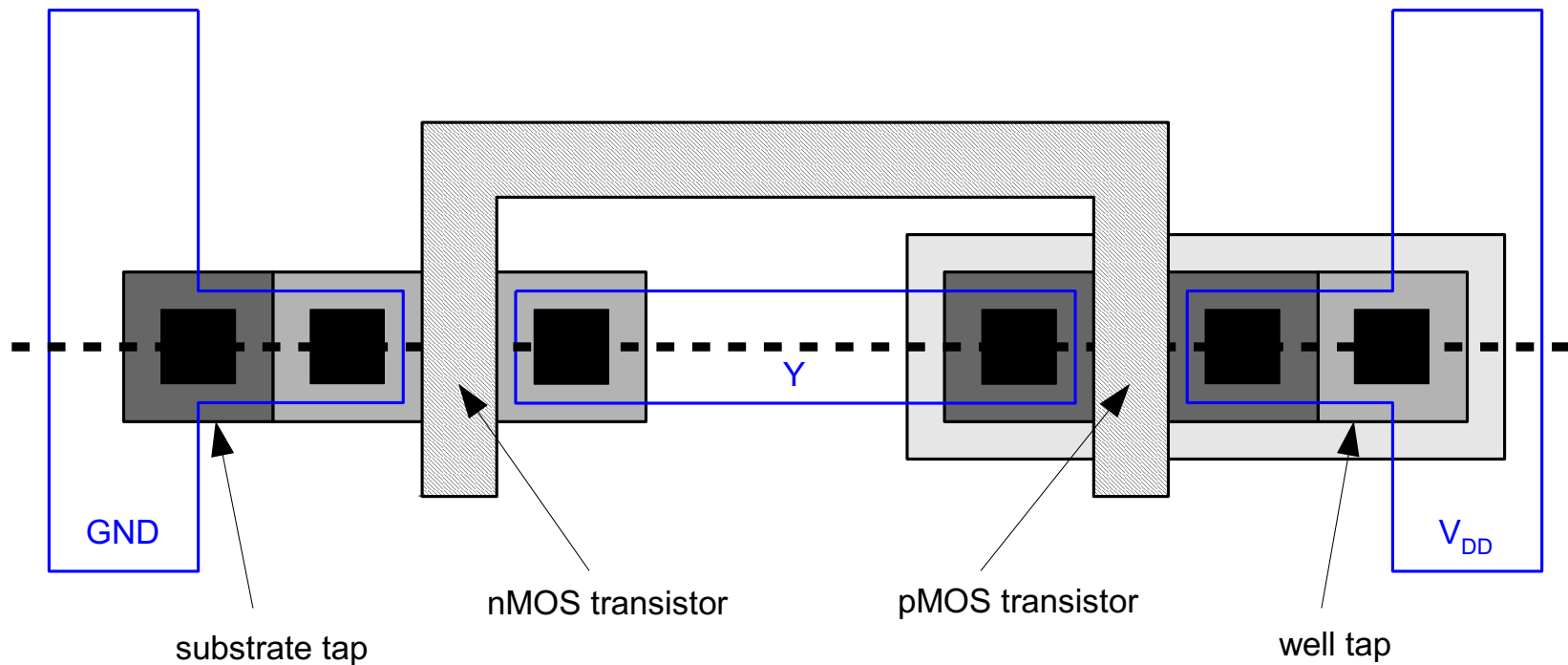
Well and Substrate Taps

- Substrate must be tied to GND and n-well to V_{DD}
- Metal to lightly-doped semiconductor forms poor connection called Schottky Diode
- Use heavily doped well and substrate contacts / taps



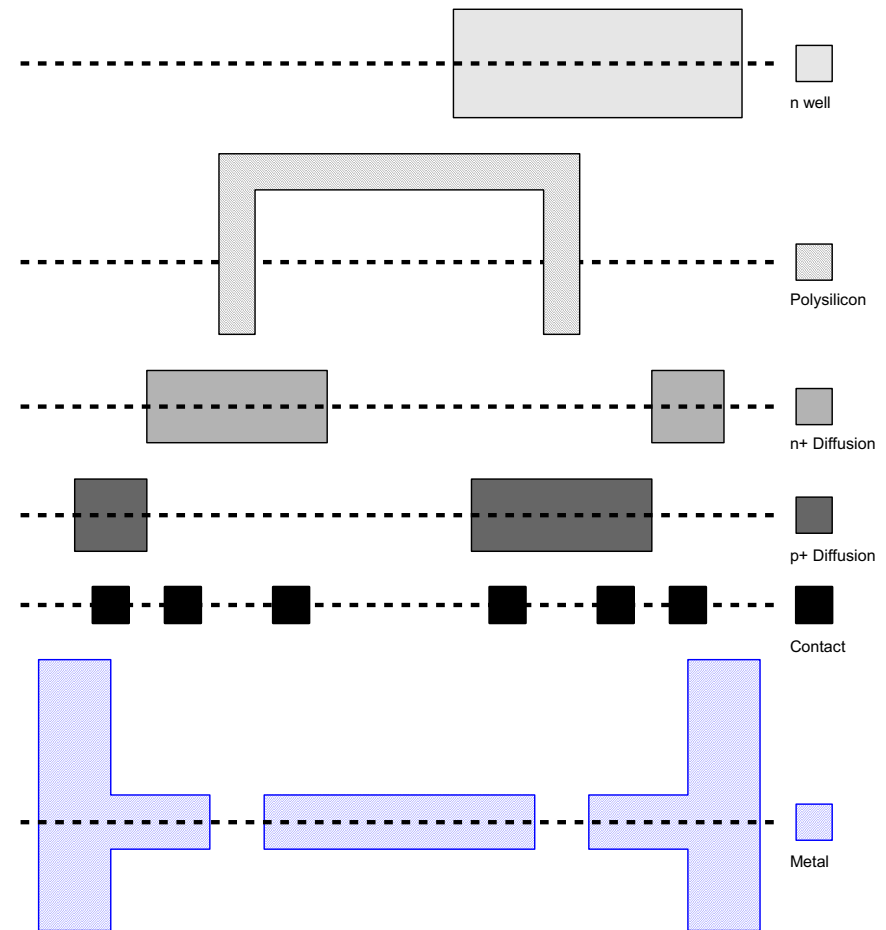
Inverter Mask Set

- Transistors and wires are defined by *masks*
- Cross-section taken along dashed line



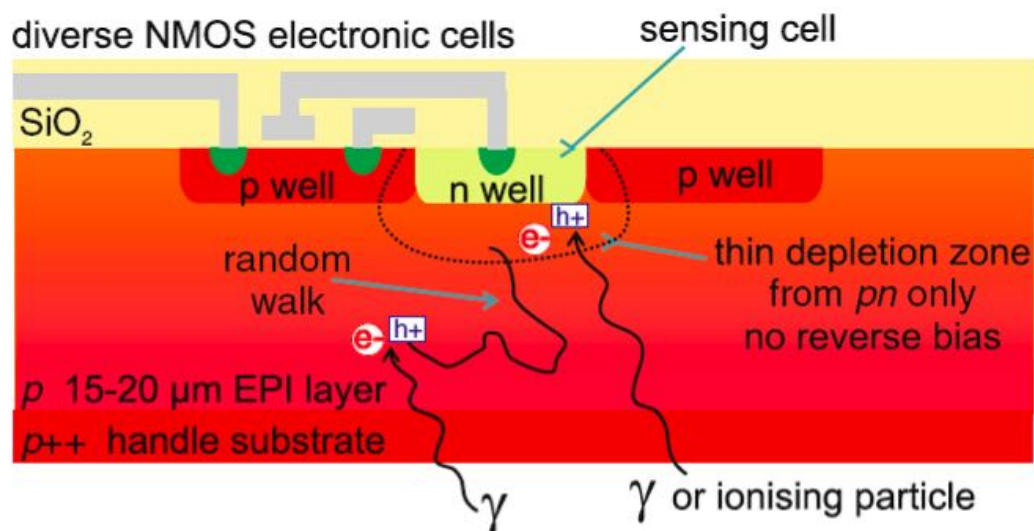
Detailed Mask Views

- Six masks
 - n-well
 - Polysilicon
 - n+ diffusion
 - p+ diffusion
 - Contact
 - Metal



Monolithic Active Pixels (MAPS)

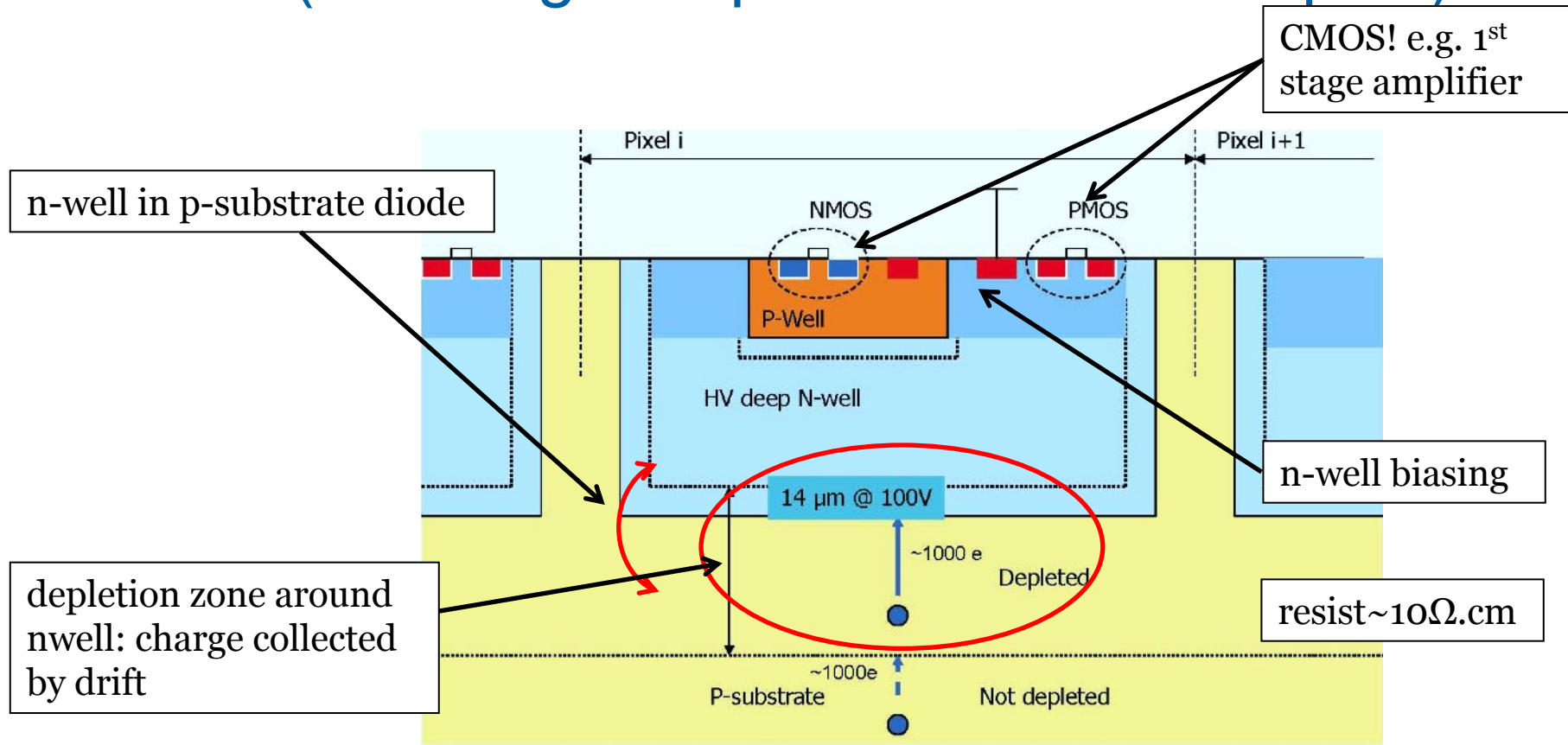
Scheme of a CMOS monolithic active pixel cell with an NMOS transistor. The N-well collects electrons from both ionization and photo-effect. Charge collection due to diffusion (and tiny intrinsic space charge region due to built in voltage)



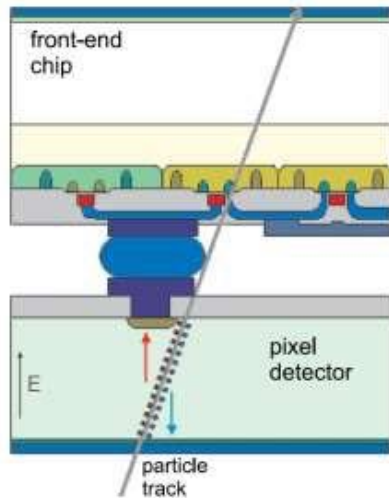
Evolution of Silicon Sensor Technology in Particle Physics,
 F. Hartmann, Springer Volume 231, 2009

Principle of HV-CMOS process

- An n-well in p-substrate diode, populated with CMOS (first stage amplifier or more complex).

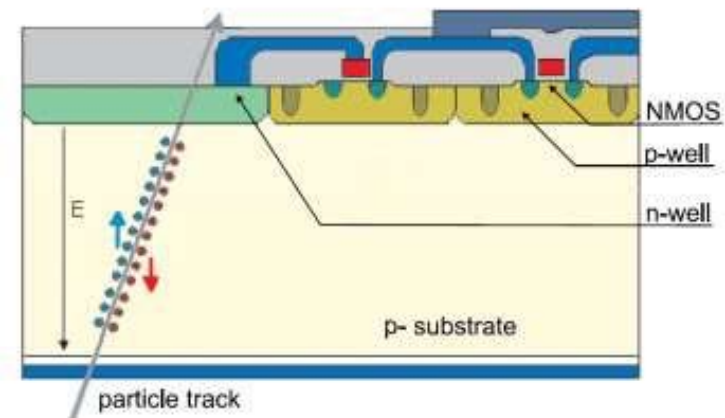
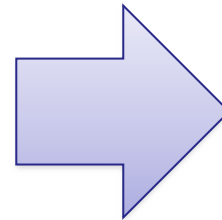


Hybrid Pixel Detectors:

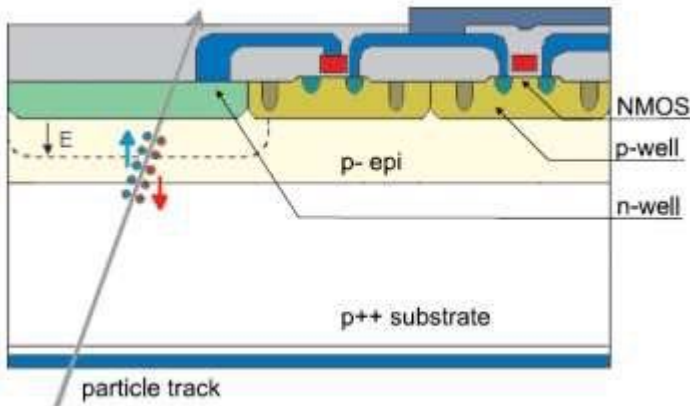


Pixel Detectors

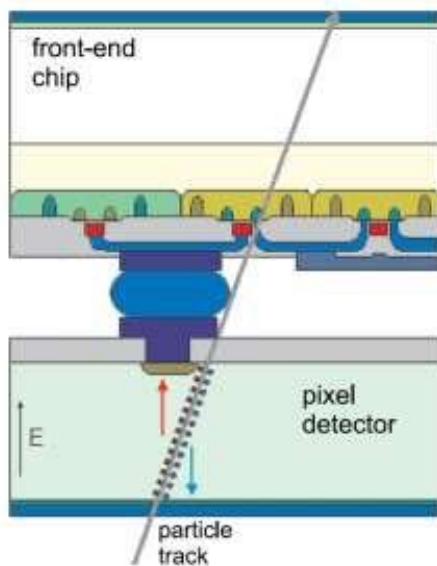
Depleted Monolithic Pixels with everything integrated into one “thing”:



MAPS (Monolithic Active Pixel Sensors):



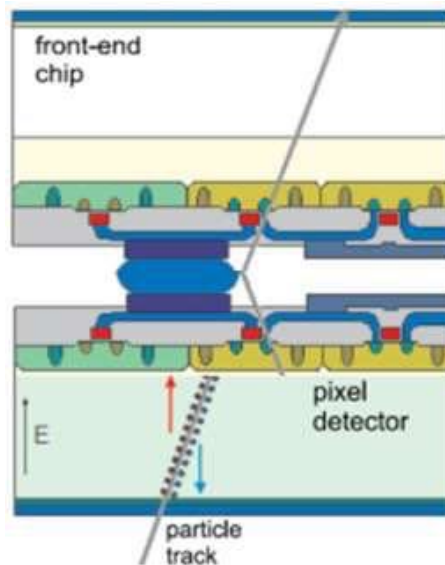
“passive Hybrid Pixel”:



Classic Hybrid pixel with

- Classic sensor
- **passive CMOS sensor** (Bonn Univ, ATLAS)

“Active Pixel sensor”:



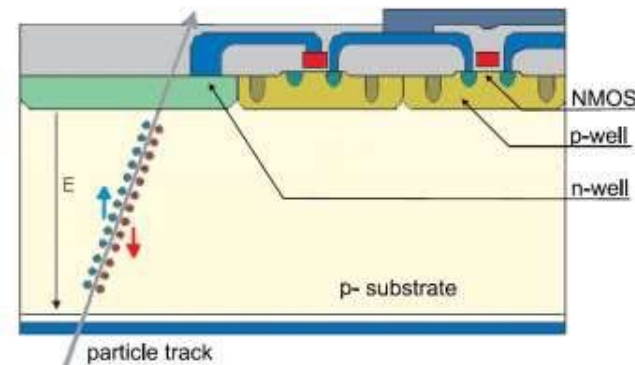
different levels of hybridization:

- Analog part (amplifier) in detector, digital part (comparator) in chip

Different connection methods:

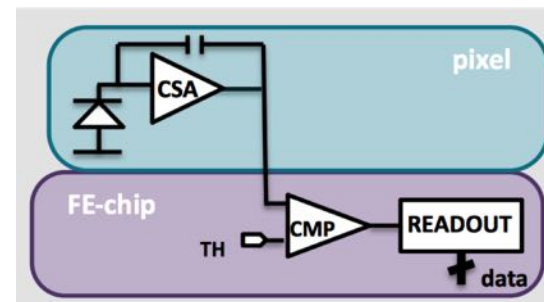
- bumping,
- gluing (capacitive)
- bonding

HV/HR-MAPS:



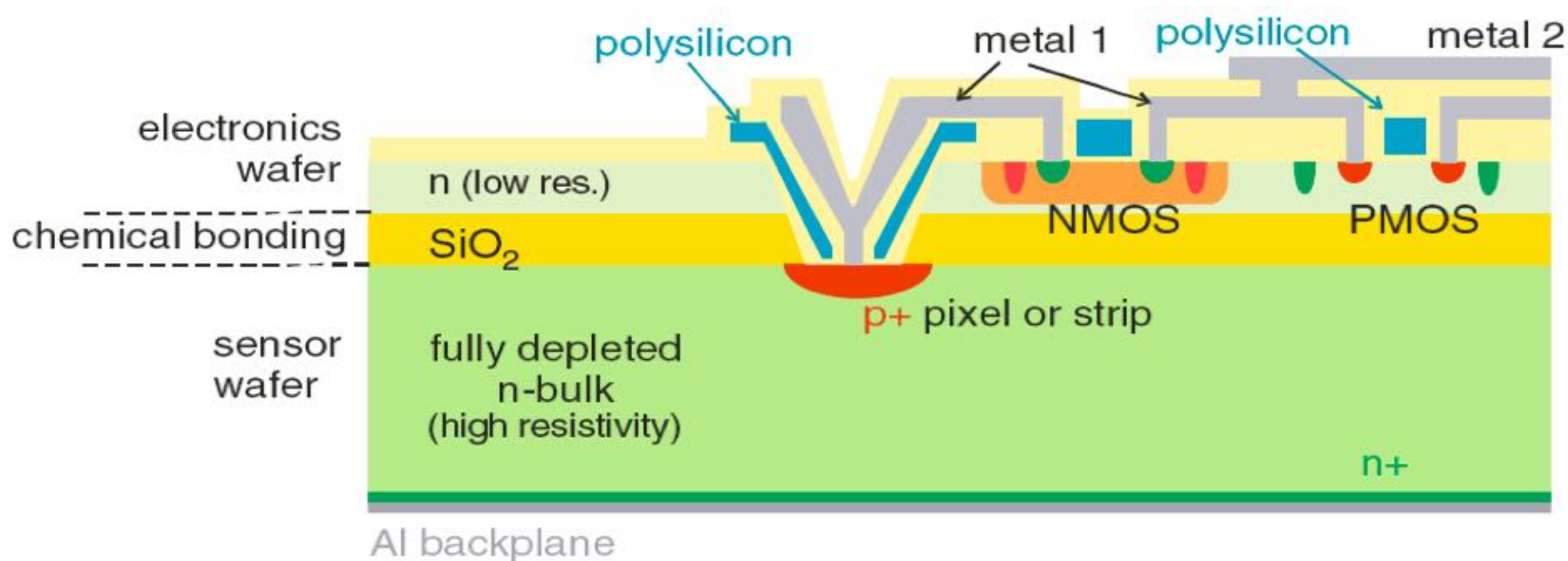
different other levels of hybridization:

- CMOS
- Readout in FPGA



Silicon on isolator (SOI)

A SOI detector consists of a thick fully depleted high resistivity bulk and separated by a layer of SiO_2 a low resistivity n-type material. NMOS and PMOS transistors are implemented in the low resistivity material using standard IC methods.



Evolution of Silicon Sensor Technology in Particle Physics, F. Hartmann, Springer Volume 231, 2009

OTHER SILICON DETECTOR STRUCTURES

Other Silicon Detector Structures

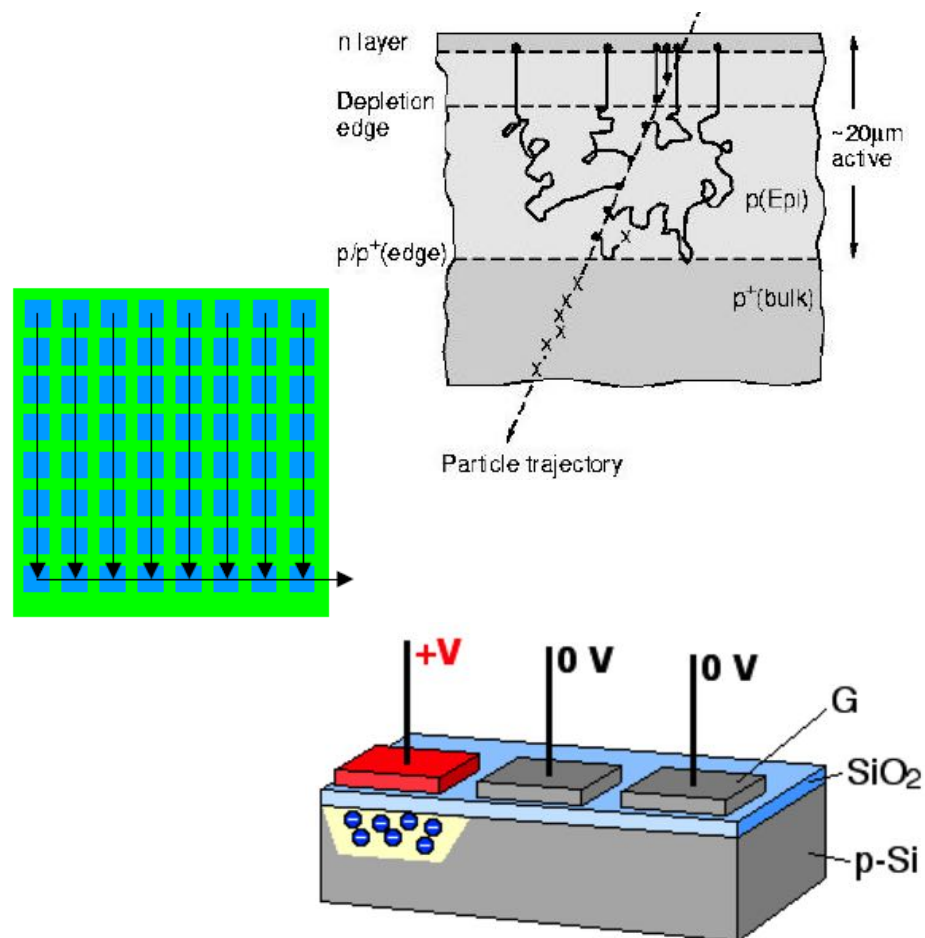
Strip and hybrid pixel detectors are mature technologies employed in almost every experiment in high energy physics.

Additional interesting silicon detector structures are:

- **Charged Coupled Devices (CCD)**
- **Silicon Drift Detectors (SDD)**
- **3D detectors**
- **Depleted Field Effect detectors (DEPFET)**
- **Low Gain Avalanche Detectors (LGAD)**
- **Avalanche Photo Diodes (APD) and Silicon Photo Multiplier (SiPM)**

Charge Coupled Devices (CCD)

- Shallow depletion layer (typically $15\ \mu\text{m}$)
- relatively small signal
- charge is kept in the pixel
- shifted during readout through the columns
- final row to a single signal readout channel:
 - Slow device, hence not suitable for fast detectors.
 - Improvements are under development, e.g. parallel column readout.



Silicon Drift Detectors

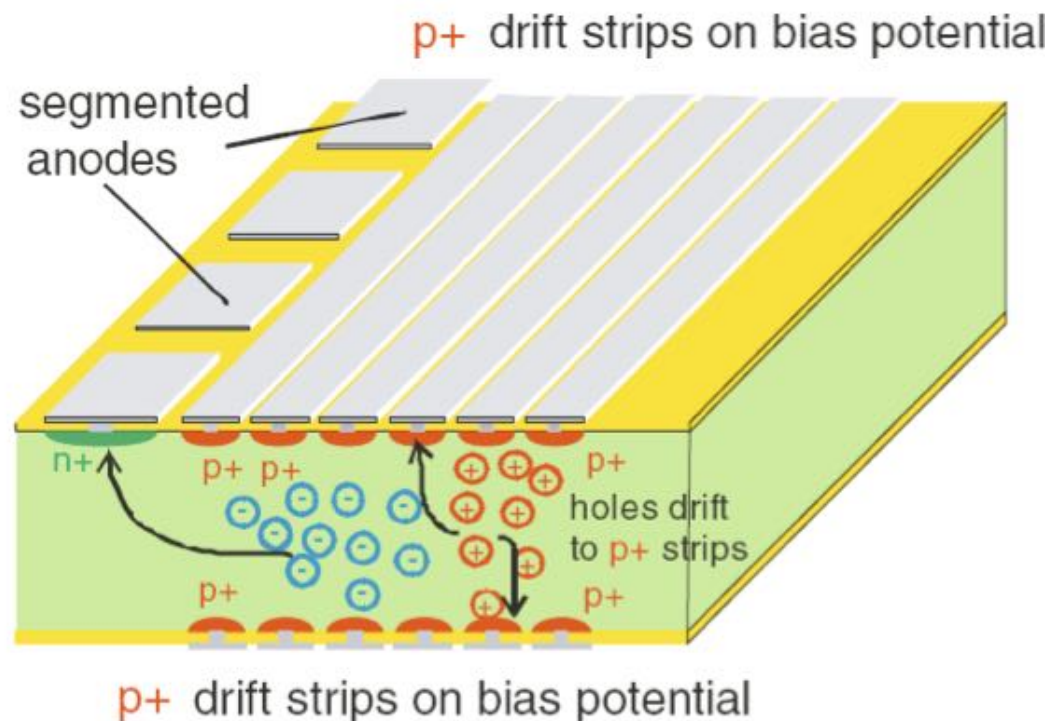
- Bulk fully depleted by p^+ strips and backplane p^+ implantation

Used for example in the experiment ALICE (CERN)

- Ionizing particle produces e/h-pairs
 - Holes swept out
 - Electrons move towards collecting anodes (n^+).

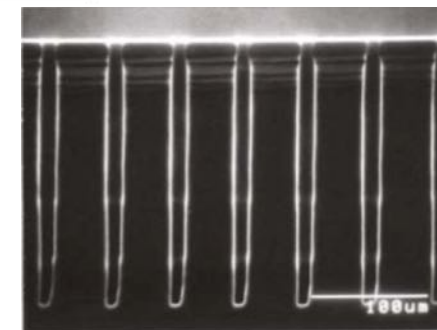
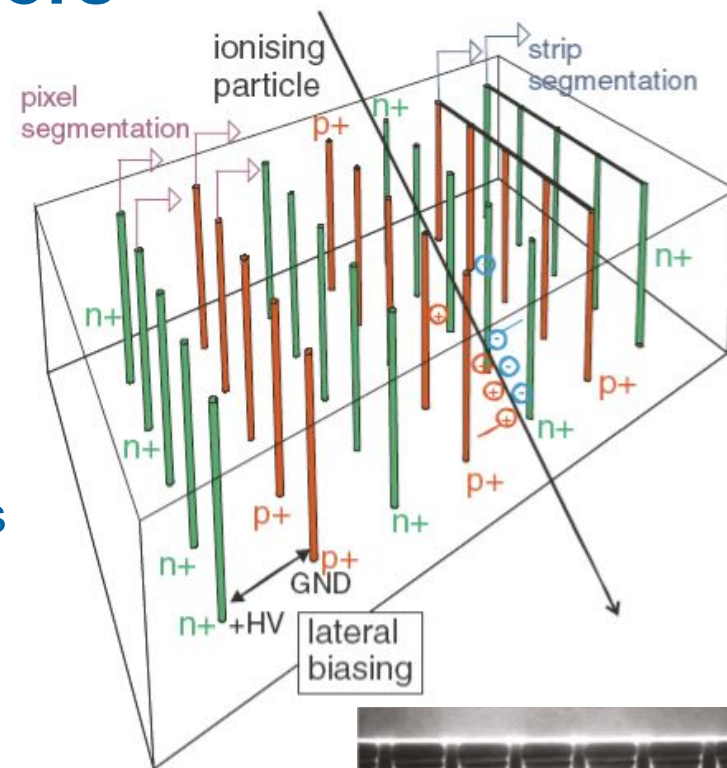
Evolution of Silicon Sensor Technology in Particle Physics, F. Hartmann, Springer Volume 231, 2009

- 2-dimensional readout
 - Segmentation of collection anodes
 - Drift time



3D Detectors

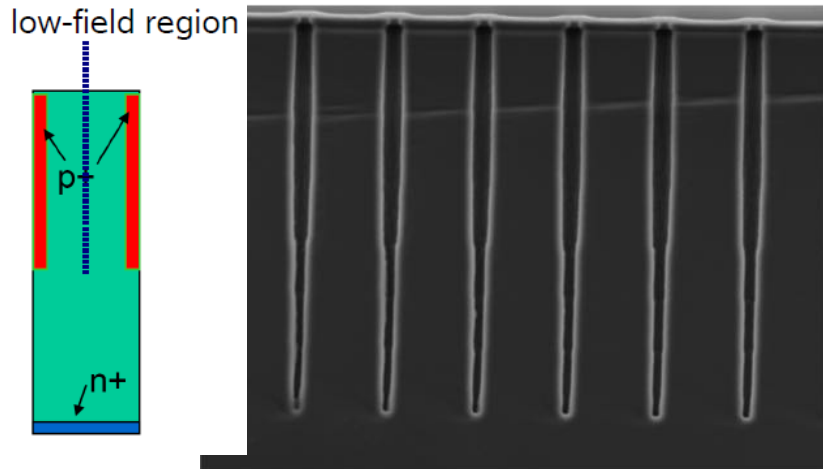
- Non planar detectors
- Deep holes are etched into the silicon
 - filled with n^+ and p^+ material.
 - Voltage is applied between
 - Depletion is sideways
- Small distances between the electrodes
- Very low depletion voltages
- Very fast, since charge carriers travel shorter distances
- Very radiation tolerant detectors, in discussion for inner detector layers at SLHC.



Picture from CNM-IMB (CSIC), Barcelona

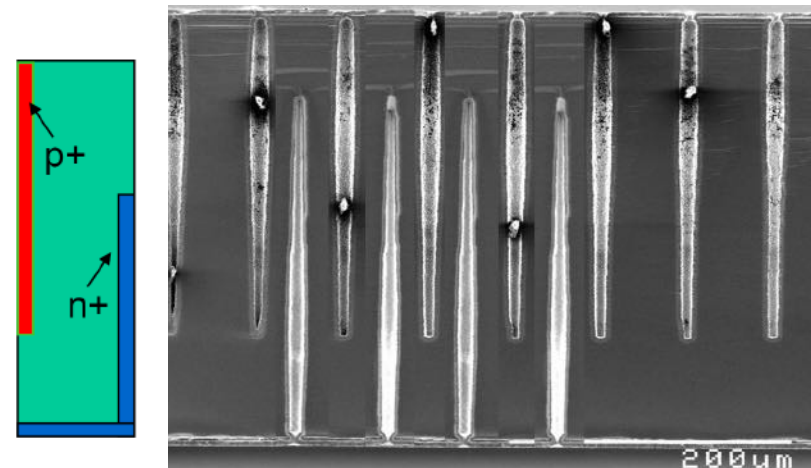
3D Detectors (cont.)

Single column:



Low field region between columns

Double-sided double column:

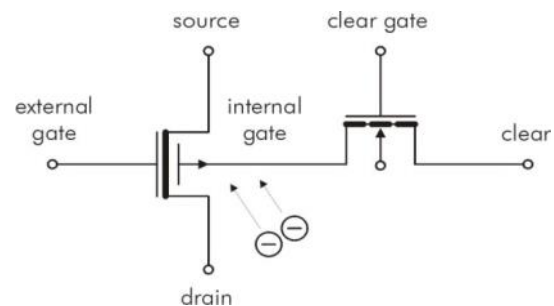
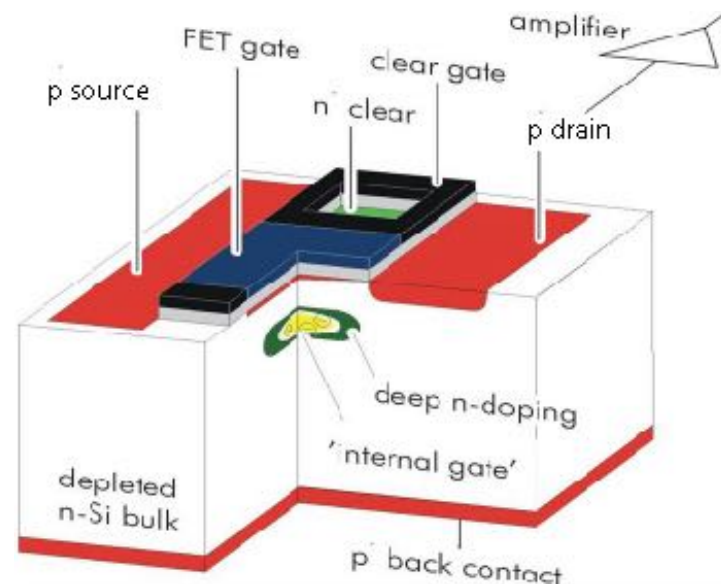


High field, but more complicated

Depleted Field Effect Transistor (DEPFET)

Function principle

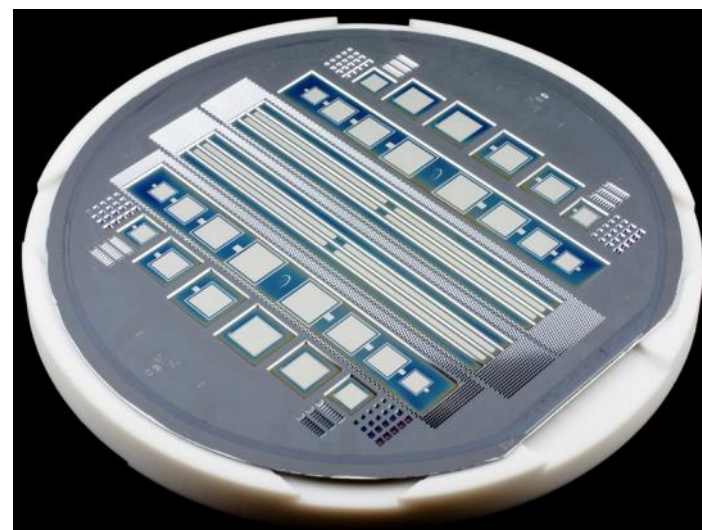
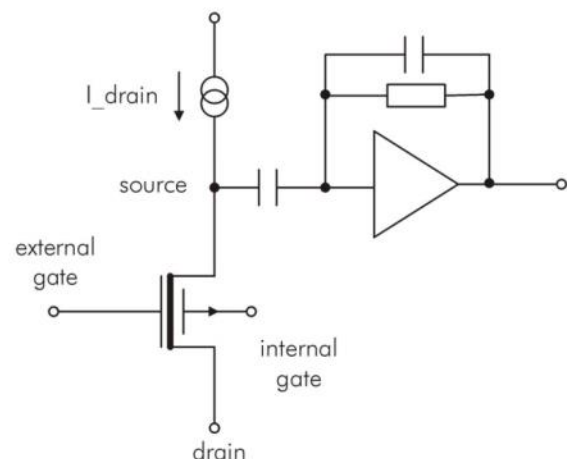
- Field effect transistor on top of fully depleted bulk
- All charge generated in fully depleted bulk
 - assembles underneath the transistor channel
 - steers the transistor current
 - Results in **amplification of signal**
- Clearing by positive pulse on clear electrode
- Combined function of sensor and amplifier
- Used for Belle II and candidate for ILC



Depleted Field Effect Transistor (DEPFET)

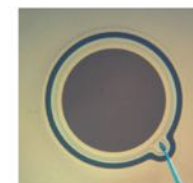
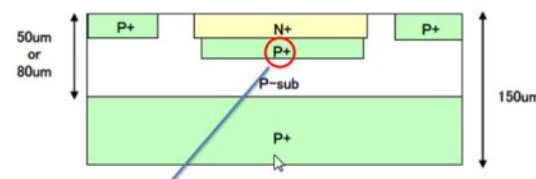
Properties

- low capacitance → low noise
- Signal charge remains undisturbed by readout → repeated readout
- Complete clearing of signal charge → no reset noise
- Full sensitivity over whole bulk → large signal for mip. → X-ray sensitivity
- Thin radiation entrance window on backside → X-ray sensitivity
- Charge collection also in turned off mode → low power consumption



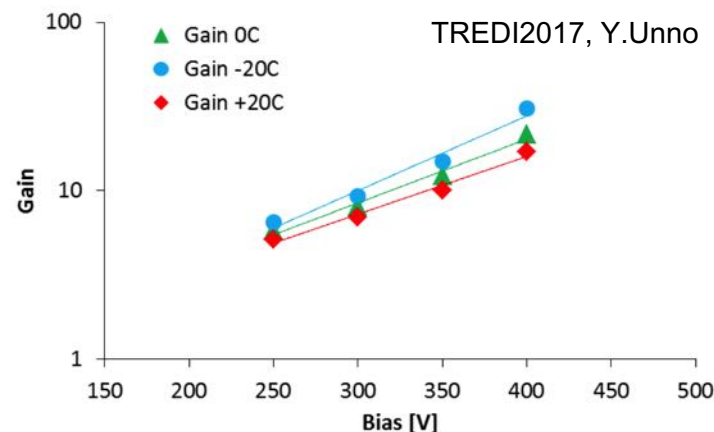
Low Gain Avalanche Detectors (LGAD)

- Deep p+ implantation create high fields which lead to charge amplification similar to gas detectors
- Gain ~ 10 (compared to 10^4 - 10^6 in gas detectors)
- Radiation hardness to be proved since gain significantly depends on implant doses
 - Doping concentration vary with irradiation



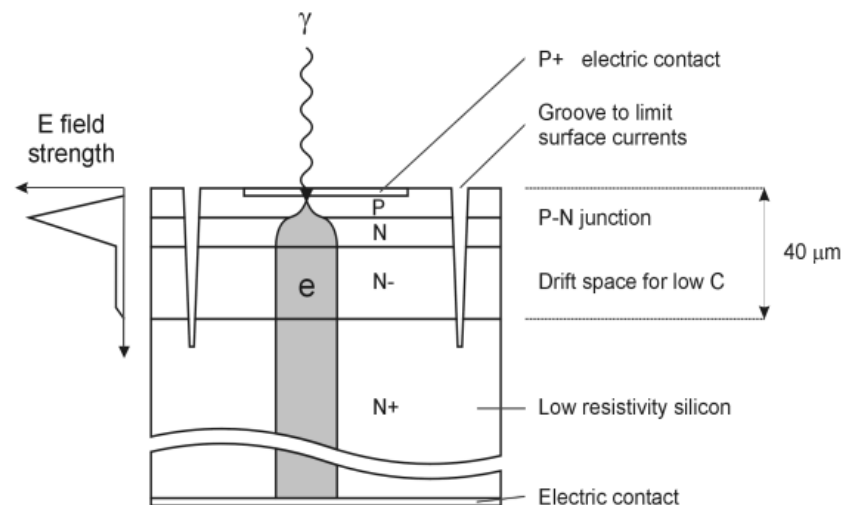
Sample Name	P+ density	Physical Thickness [μm]	Active Thickness [μm]
50A	A low	150	50 (3~8k Ωcm)
50B	B		
50C	C		
50D	D high		
80A	A	150	80 (1k Ωcm)
80B	B		
80C	C		
80D	D		

- Diode
- Chip size:
– $2.5 \times 2.5 \text{ mm}^2$
- Window: $1 \text{ mm } \phi$

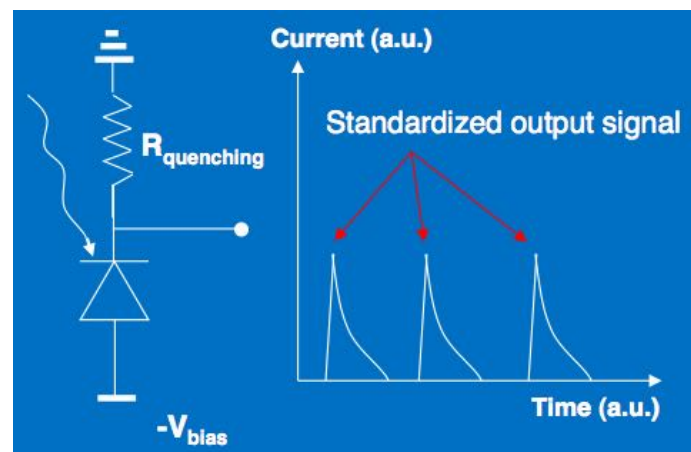


Avalanche Photo Diode (APD)

- Operated in reverse bias mode in the breakdown regime
 - Geiger-mode
- A **single photon** is able to trigger an avalanche breakdown.
 - Very temperature sensitive
- Current increase limited by quenching resistor.
- Used for photon detection in calorimeters (e.g the electromagnetic calorimeter of CMS), in Cherenkov counters, etc.

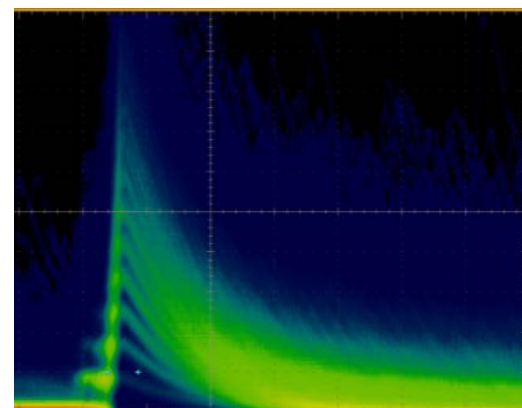
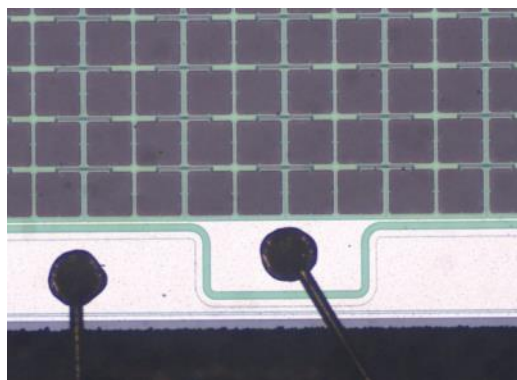
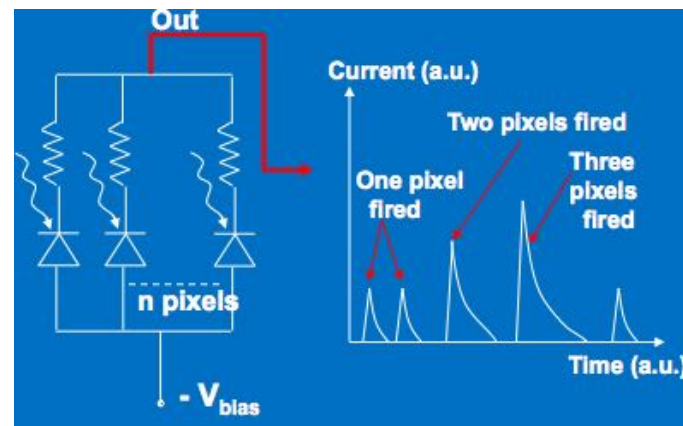
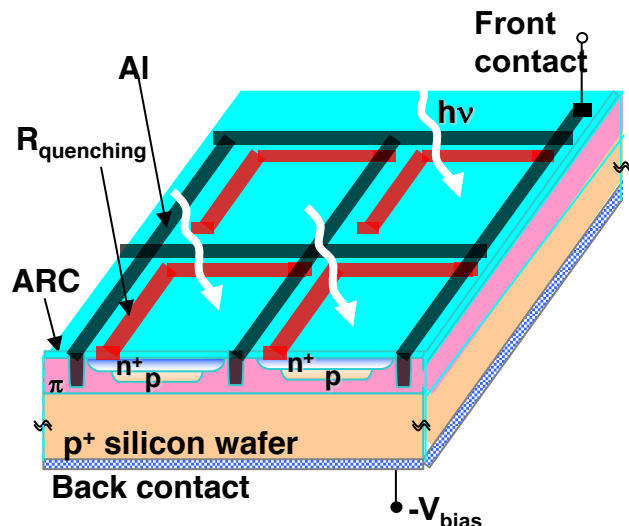


D. Renker, Nucl. Instr. Methods A 571 (2007) 1-6



Silicon photo multiplier (SiPM)

SiPM are matrices of APDs:

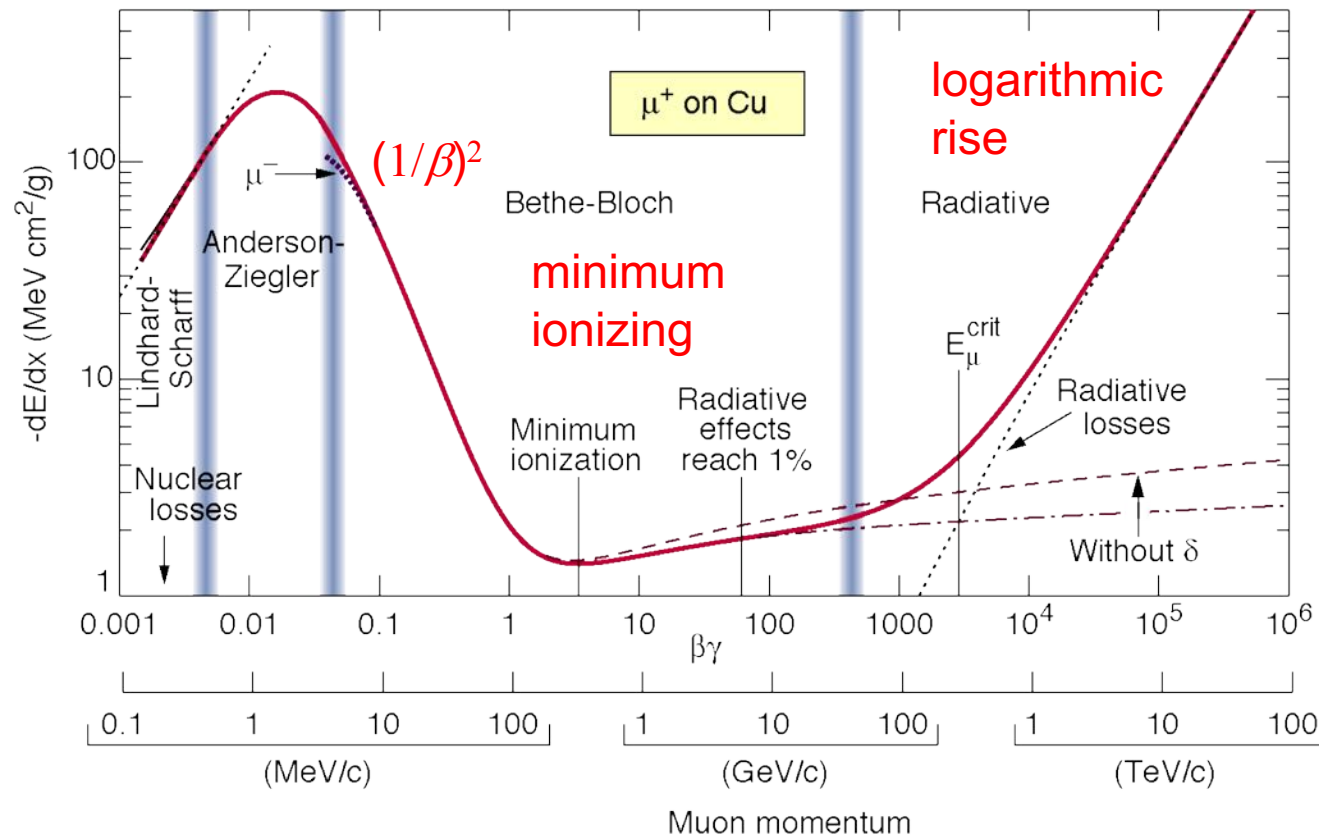


SiPMs become more and more popular as replacement for standard photo multiplier tubes.

SIGNAL-TO-NOISE RATIO

Bethe-Bloch-Equation

$$-\left(\frac{dE}{dx}\right)_{\text{coll}} = 2\pi N_A r_e^2 m_e c^2 \rho \frac{Z z^2}{A \beta^2} \cdot \left[\ln\left(\frac{2m_e c^2 \gamma^2 \beta^2 W_{\text{max}}}{I^2}\right) - 2\beta^2 - \delta - 2\frac{C}{Z} \right]$$



Valid only for thick absorber

Thin absorber (silicon detectors) need cut-off parameter since delta electrons carry energy away

$$-\frac{1}{\rho} \frac{dE}{dx} \approx 1,5 \frac{\text{MeV}}{\text{g cm}^{-2}}$$

Landau Distribution in thin layers

Energy Loss in Silicon Sensors:

- $(dE/dx)_{Si} = 3.88 \text{ MeV/cm}$

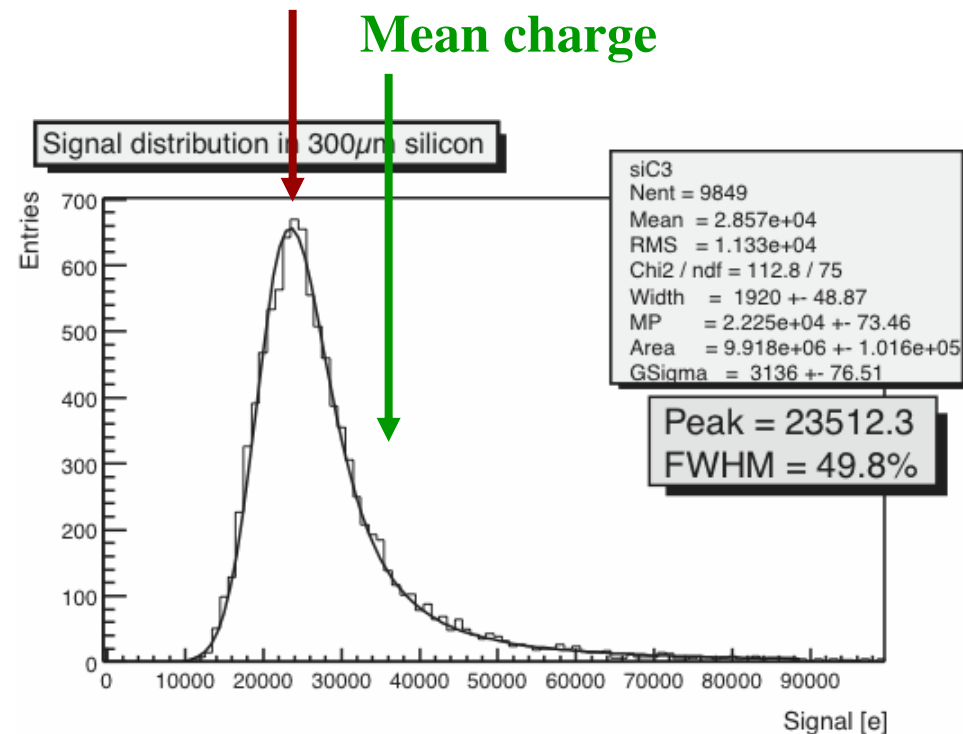
3.6eV needed to make e-h pair:

- **72 e⁻ / μm (most probable)**
- **108 e⁻ / μm (mean)**

Typical sensor thickness
 (300 μm):

- 21600 e⁻ (most probable)
- 32400 e⁻ (mean)

Most probable charge $\approx 0.7 \times$ mean



Landau distribution, convoluted with a narrow Gaussian distribution due to electronic noise and intrinsic detector fluctuations

Signal to Noise Ratio

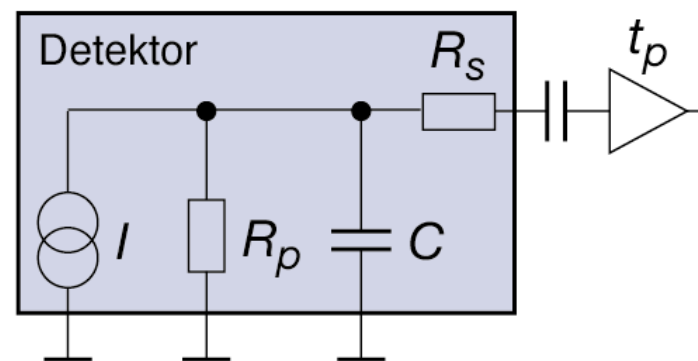
- **The signal** generated in a silicon detector depends essentially only on the thickness of the depletion zone and on the dE/dx of the particle.
- **The noise** in a silicon detector system depends on various parameters: geometry of the detector, the biasing scheme, the readout electronics, etc.

Noise is typically given as “equivalent noise charge” ENC. This is the noise at the input of the amplifier in elementary charges.

Noise contributions

The most important noise contributions are:

1. Leakage current (ENC_I)
2. Detector capacity (ENC_C)
3. Det. parallel resistor (ENC_{R_p})
4. Det. series resistor (ENC_{R_s})



Equivalent circuit diagram of a silicon detector.

The overall noise is the quadratic sum of all contributions:

$$ENC = \sqrt{ENC_C^2 + ENC_I^2 + ENC_{R_p}^2 + ENC_{R_s}^2}$$

Leakage current

- The detector leakage current comes from thermally generated electron holes pairs within the depletion region.
- These charges are separated by the electric field and generate the leakage current.
- The fluctuations of this current are the source of noise.
- In a typical detector system (good detector quality, no irradiation damage) the leakage current noise is usually negligible.

Leakage current (cont.)

Assuming an amplifier with an integration time (“peaking time”) t_p followed by a CR-RC filter the noise contribution by the leakage current I can be written as:

$$\text{ENC}_I = \frac{e}{2} \sqrt{\frac{I t_p}{e}}$$

e Euler number (2.718...)

e Electron charge

Using the physical constants, the leakage current in units of nA and the integration time in μs the formula can be simplified to:

$$\text{ENC}_I \approx 107 \sqrt{I t_p} \quad [I \text{ in nA, } t_p \text{ in } \mu\text{s}]$$

To minimize this noise contribution the detector should be of high quality with small leakage current.

Detector Capacitance

The detector capacitance at the input of a charge sensitive amplifier is usually the **dominant noise source** in the detector system.

This noise term can be written as:

$$\text{ENC}_C = a + b \cdot C$$

The parameter a and b are given by the design of the (pre)-amplifier. C is the detector capacitance at the input of the amplifier channel.

Integration time t_p is crucial, short integration time leads usually to larger a and b values. Integration time is depending on the accelerator time structure.

Typical values are (amplifier with $\sim 1 \mu\text{s}$ integration time):

$$a \approx 160 \text{ e und } b \approx 12 \text{ e/pF}$$

To reduce this noise component segmented detectors with short strip or pixel structures are preferred.

Parallel resistor

The parallel resistor R_p in the alternate circuit diagram is the **bias resistor**. The noise term can be written as:

$$\text{ENC}_{R_p} = \frac{e}{e} \sqrt{\frac{kTt_p}{2R_p}}$$

e Euler number (2.718...)
 e Electron charge

Assuming a temperature of $T=300\text{K}$, t_p in μs and R_p in $\text{M}\Omega$ the formula can be simplified to:

$$\text{ENC}_{R_p} \approx 772 \sqrt{\frac{t_p}{R_p}} \quad [R_p \text{ in } \text{M}\Omega, t_p \text{ in } \mu\text{s}]$$

To achieve low noise the parallel (bias) resistor should be large!

However the value is limited by the production process and the voltage drop across the resistor (high in irradiated detectors).

Series resistor

The series resistor R_s in the alternate circuit diagram is given by the resistance of the connection between strips and amplifier input (e.g. aluminum readout lines, hybrid connections, etc.). It can be written as:

$$\text{ENC}_{R_s} \approx 0.395 C \sqrt{\frac{R_s}{t_p}}$$

C Detector capacity on pF
 t_p ... Integration time in μs
 R_s ... Series resistor in Ω

Note that, in this noise contribution t_p is inverse, hence a long t_p reduces the noise. The detector capacitance is again responsible for larger noise.

To avoid excess noise the aluminum lines should have low resistance (e.g. thick aluminum layer) and all other connections as short as possible.

Signal to Noise Ratio Summary

To achieve a high signal to noise ratio in a silicon detector system the following conditions are important:

- Low detector capacitance (i.e. small pixel size or short strips)
- Low leakage current
- Large bias resistor
- Short and low resistance connection to the amplifier
- Long integration time

Obviously some of the conditions are contradictory. Detector and front end electronics have to be designed as one system. The optimal design depends on the application.

Example Signal-to-noise ratios

DELPHI Microvertex:

- readout chip (MX6):
 $a = 325 \text{ e}$, $b = 23 \text{ e/pF}$, $t_p = 1.8 \mu\text{s}$
- 2 detectors in series each 6 cm long strips, $C = 9 \text{ pF}$
 - $\text{ENC}_C = 532 \text{ e}$
- typ. leakage current/strip: $I \approx 0.3 \text{ nA}$
 - $\text{ENC}_I = 78 \text{ e}$
- bias resistor $R_p = 36 \text{ M}\Omega$
 - $\text{ENC}_{R_p} = 169 \text{ e}$
- series resistor = 25Ω
 - $\text{ENC}_{R_s} = 13 \text{ e}$
- **Total noise: $\text{ENC} = 564 \text{ e}$ (SNR 40:1)**

CMS Tracker:

- readout chip (APV25, deconvolution):
 $a = 400 \text{ e}$, $b = 60 \text{ e/pF}$, $t_p = 50 \text{ ns}$
- 2 detectors in series each 10 cm long strips, $C = 18 \text{ pF}$
 - $\text{ENC}_C = 1480 \text{ e}$
- max. leakage current/strip: $I \approx 100 \text{ nA}$
 - $\text{ENC}_I = 103 \text{ e}$
- bias resistor $R_p = 1.5 \text{ M}\Omega$
 - $\text{ENC}_{R_p} = 60 \text{ e}$
- series resistor = 50Ω
 - $\text{ENC}_{R_s} = 345 \text{ e}$
- **Total noise: $\text{ENC} = 1524 \text{ e}$ (SNR 15:1)**

Calculated for the signal of a minimum ionizing particle (mip) of 22500 e.

POSITION RESOLUTION

Position Resolution Introduction

The position resolution – the main parameter of a position detector – depends on various factors, some due to physics constraints and some due to the design of the system (external parameters).

- **Physics processes:**
 - Statistical fluctuations of the energy loss
 - Diffusion of charge carriers
- **External parameter:**
 - Binary readout (threshold counter) or analogue signal value read out (CMS case)
 - Distance between strips (strip pitch)
 - Signal to noise ratio

Diffusion

- After the ionizing particle has passed the detector the e^+h^- pairs are close to the original track.
- While the cloud of e^+ and h^- drift to the electrodes, diffusion widens the charge carrier distribution. After the drift time t the width (rms) of the distribution is given as:

$$\sigma_D = \sqrt{2Dt} \quad \text{with:} \quad D = \frac{kT}{e} \mu$$

σ_D ... width “root-mean-square” of the charge carrier distribution

t ... drift time

k ... Boltzmann constant

e ... electron charge

D ... diffusion coefficient

T ... temperature

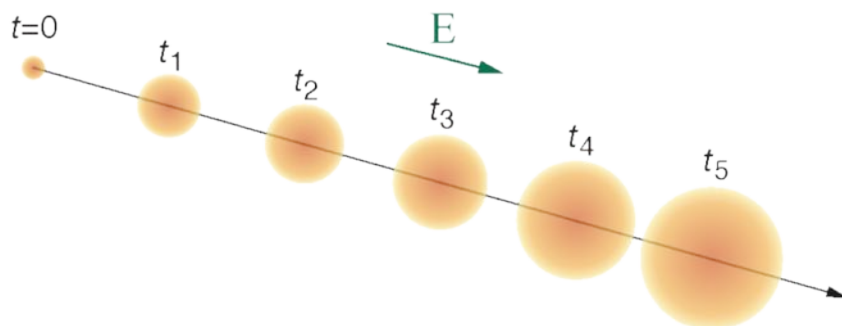
μ ... charge carrier mobility

Note: $D \propto \mu$ and $t \propto 1/\mu$, hence σ_D is equal for e^- and h^+ .

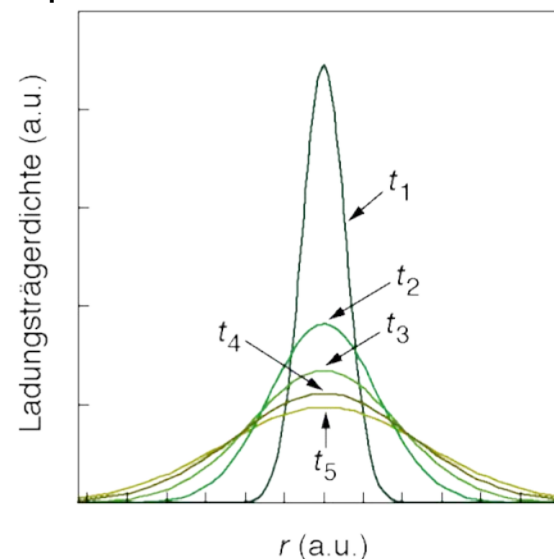
Diffusion (cont.)

- h^+ created close to the anode (i.e. the n^+ backplane) and e^- created close to the cathode (i.e. the p^+ strips or pixels) have the longest drift path. As a consequence the diffusion acts much longer on them compared to $e^- h^+$ with short track paths.
- **The signal measured comes from many overlapping Gaussian distributions.**

Drift and diffusion acts on charge carriers:



Charge density distribution for 5 equidistant time intervals:



Diffusion (cont.)

- Diffusion widens the charge cloud. However, this may have a positive effect on the position resolution!
 - ⇒ charge is distributed over more than one strip, with interpolation (calculation of the charge center of gravity) a better position measurement is achievable.
- This is only possible if analogue read out of the signal is implemented.
- Interpolation is more precise the larger the signal to noise ratio is.
 - ⇒ **Strip pitch and signal to noise ratio determine the position resolution.**
- Larger charge sharing can also be achieved by tilting the detector.

Digital readout

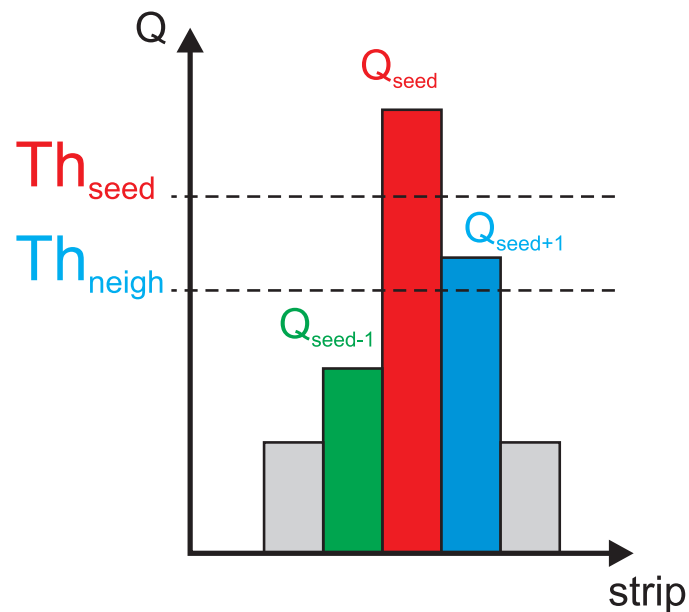
- Position of hit strip
- Resolution proportional strip pitch
 - ATLAS Tracker is working in this way

$$x = \text{strip position}$$

$$\sigma^2 = \frac{1}{p} \int_{-p/2}^{p/2} x^2 dx = \frac{p^2}{12}$$

p ... distance between strips (readout pitch)
 x ... position of particle track

- What happens when more than one strip is hit
 - Cluster



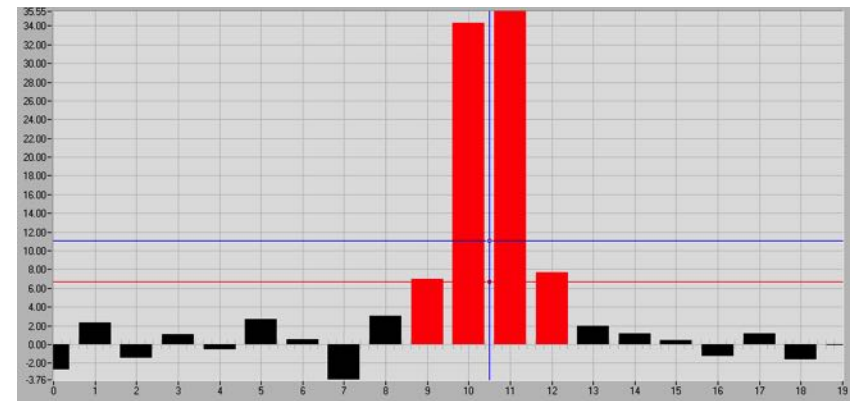
Analogue readout

- Analogue readout allows a much better position resolution than with the simple position of the strip
 - Proportional to signal-to-noise ratio
- Different methods to calculate
 - center-of-gravity
 - interpolation (signal on two strips)

$$x = x_1 + \frac{h_1^2}{h_1 + h_2} (x_2 - x_1) = \frac{h_1 x_1 + h_2 x_2}{h_1 + h_2}$$

$$\sigma_x \propto \frac{p}{SNR}$$

x_1, x_2 ... position of 1st and 2nd strip
 h_1, h_2 ... signal on 1st and 2nd strip
 SNR ... signal to noise ratio



Intermediate strips

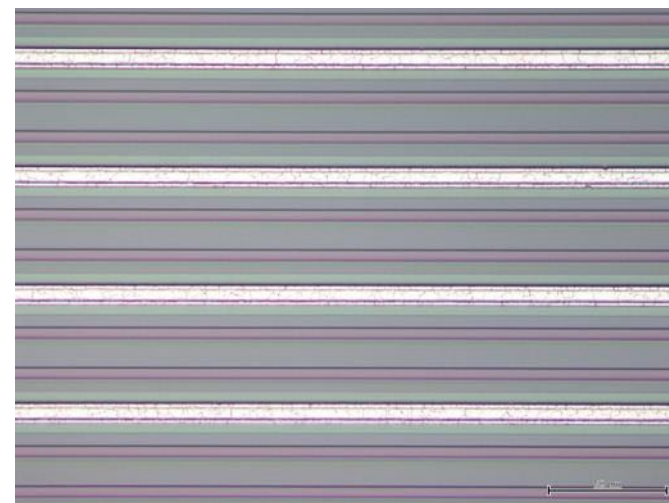
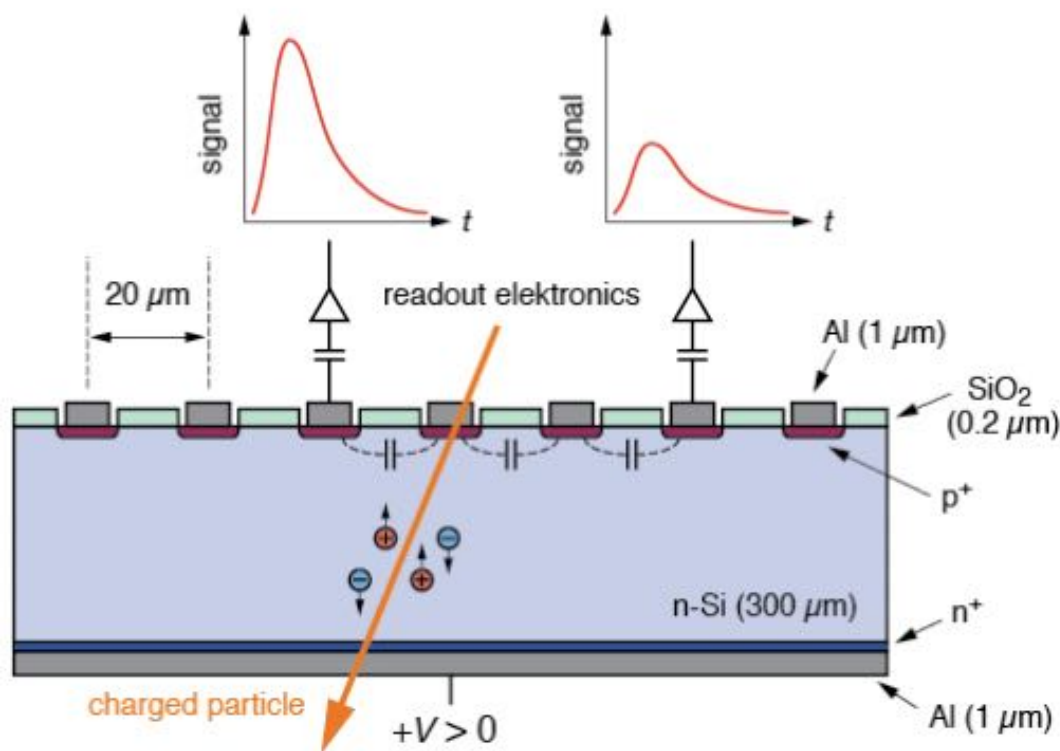
- The **strip pitch determines the position resolution**. With small strip pitch a better position resolution is achievable. Small pitch requires
 - large number of electronic channels
 - cost increase
 - power dissipation increase
- A possible solution is the implementation of intermediate strips. These are **strips not connected to the readout electronics** located between readout strips.

The signal from these intermediate strips is transferred by capacitive coupling to the readout strips.

- more hits with signals on more than one strip
- Improved resolution with smaller number of readout channels.

Intermediate strips (cont.)

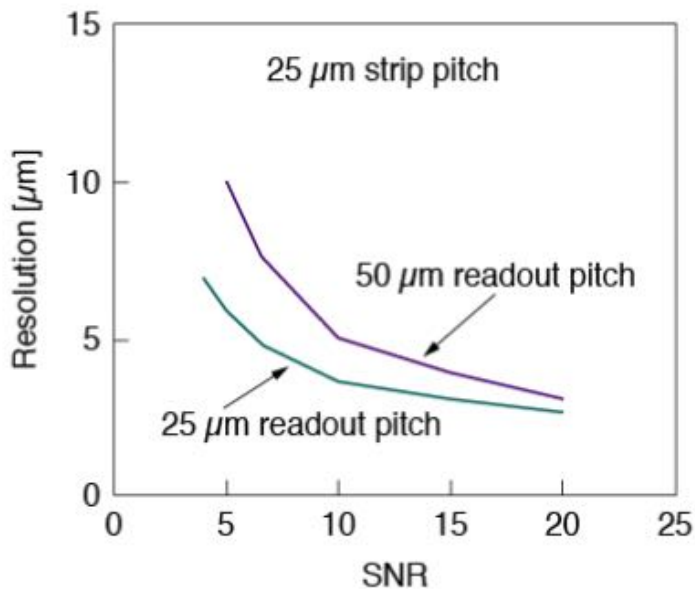
Scheme of a detector with two intermediate strips. Only every 3rd strip is connected to an electronics channel. The charge from the intermediate strips is capacitive coupled to the neighbor strips.



Example – influence of readout pitch and SNR

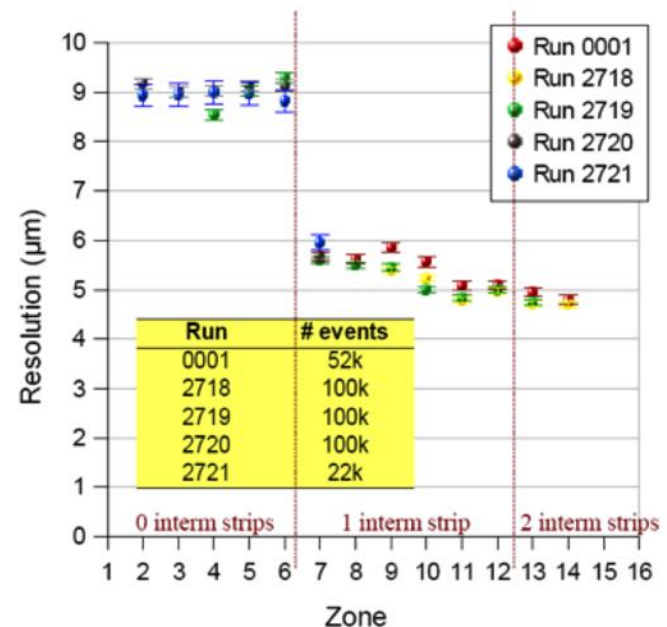
Two examples of a detectors with analogue readout.

Example 1: strip pitch of 25 μm
Binary readout: 7 μm resolution



- Top curve: one intermediate strip
- Bottom curve: no intermediate strips

Example 2: strip pitch of 50 μm
Binary readout: 14 μm resolution

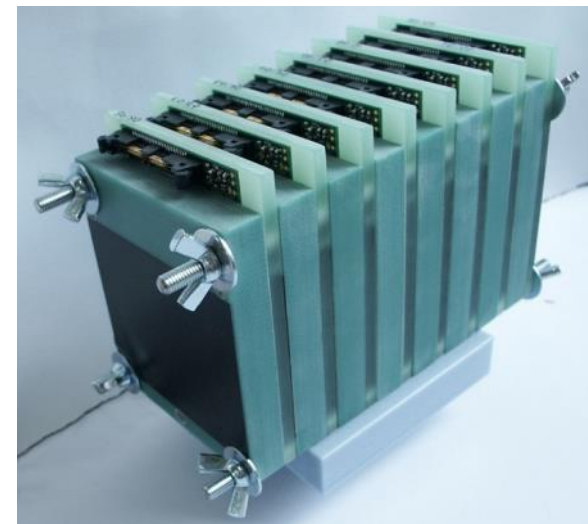
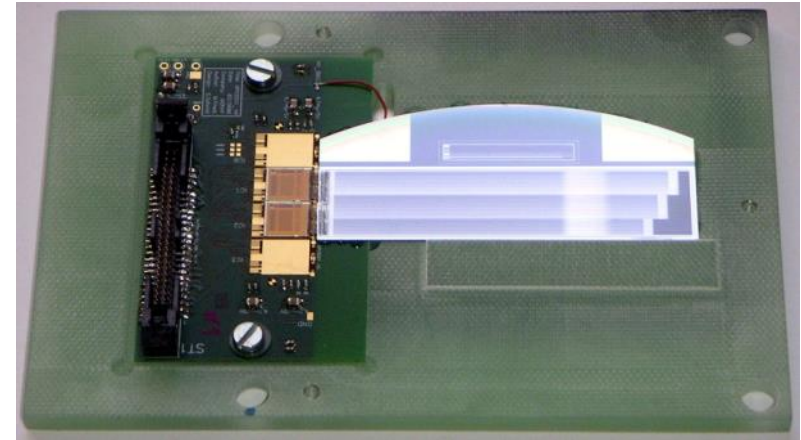


Example: resolution studies

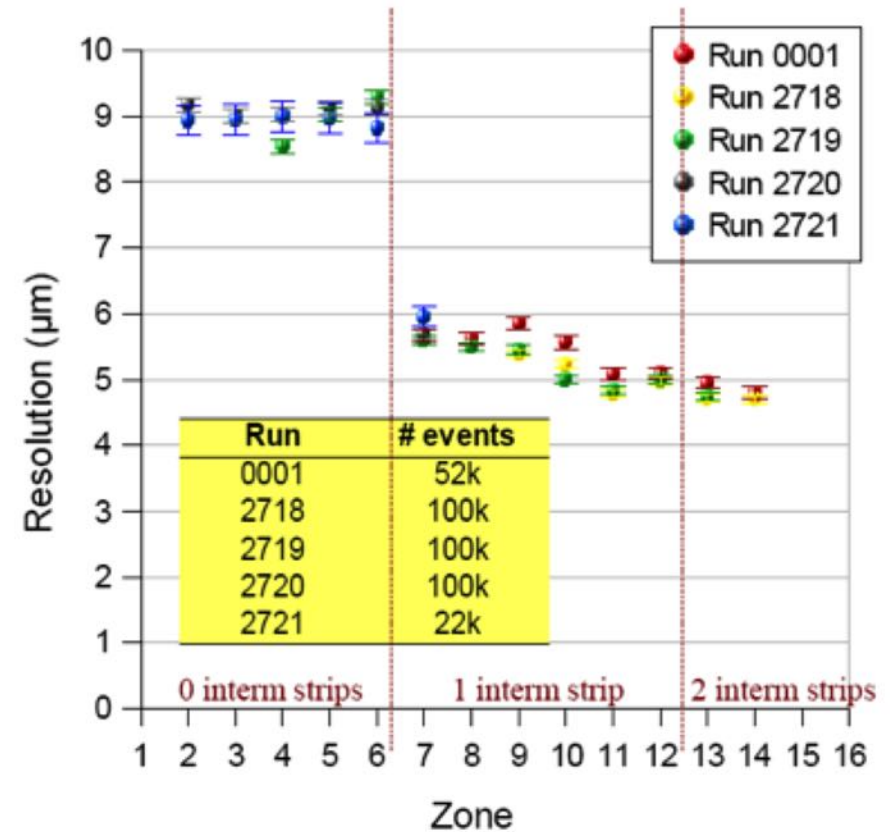
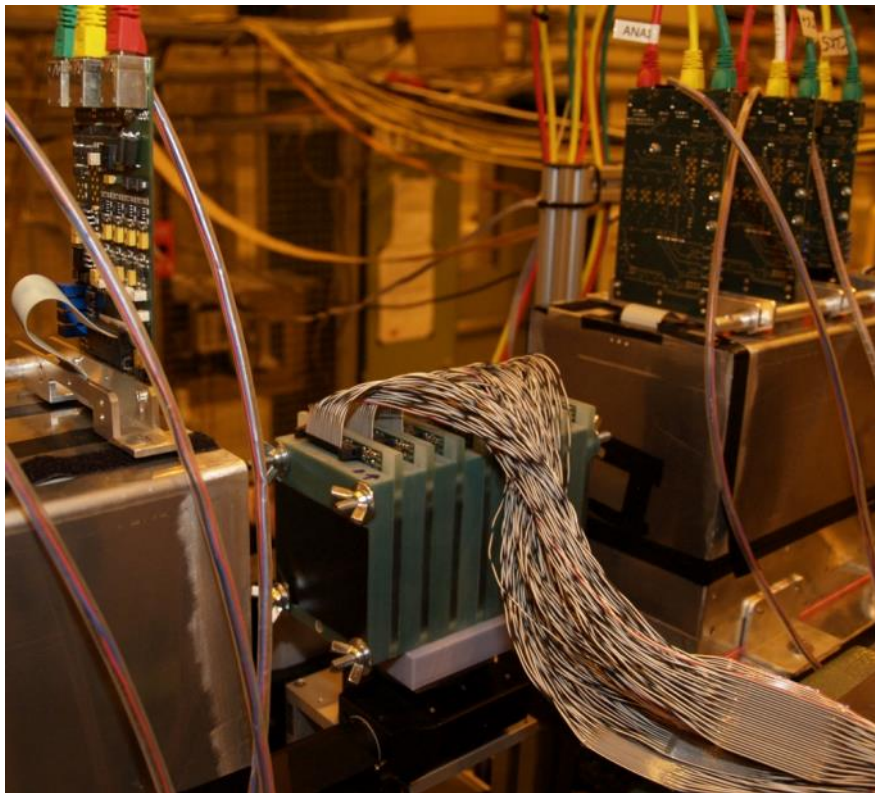


TESTAC:

strip width [μm]	intermediate strips
5	no
10	no
12.5	no
15	no
20	no
25	no
5	single
7.5	single
10	single
12.5	single
15	single
17.5	single
5	double
7.5	double
10	double
12.5	double



Example(cont.): Resolution Studies



RADIATION DAMAGE

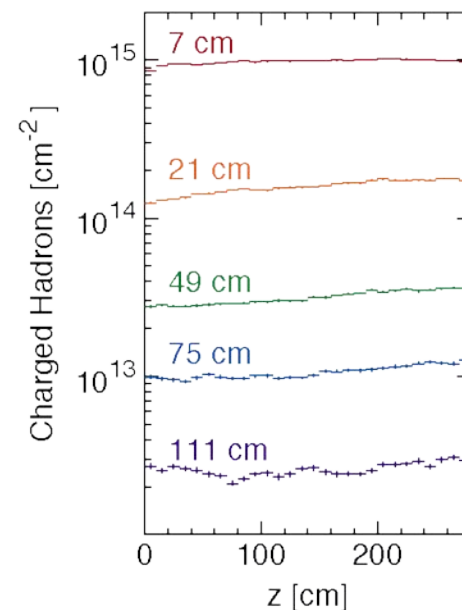
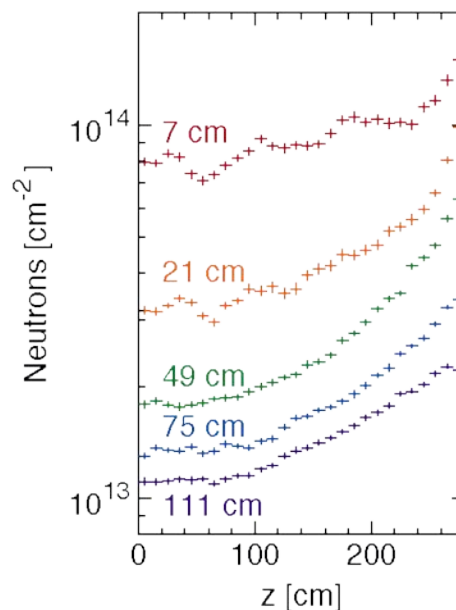
Motivation

- The event rate and as a consequence the irradiation load in experiments at hadron colliders is extreme (e.g. the pp collider LHC, collision energy 14 TeV, event rate 10^9 s^{-1}).
- Understanding radiation damage in silicon detectors is vital for the experiments at LHC and future applications.

Expected particle rates for the silicon detector inner layers in CMS integrated over 10 years as a function of the distance from the vertex point and for various radii.

Left: neutrons

Right: charged hadrons



CERN/LHCC 98-6, CMS TDR 5, 20 April 1998

Introduction

- Particles (radiation) interact a) with the electrons and b) with atoms of the detector material.
 - Case a) is used for particle detection and results in temporarily effects only. Case b) may cause permanent changes (defects) in the detector bulk.
- One distinguishes between damage inside the detector bulk (**bulk damage**) and damage introduced in the surface layers (**surface damage**).

For the readout electronics (also silicon based!) inside the radiation field only surface damage is relevant.

- Defects may change with time. Therefore one distinguishes also between **primary defects** and **secondary defects**. The secondary defects appear with time caused by moving primary defects.

Introduction (cont.)

- Radiation induced damage in the semiconductor bulk are dislocated atoms from their position in the lattice. Such dislocations are caused by massive particles.
 - **Bulk damage** is primarily produced by neutrons, protons and pions.
- In the amorphous oxide such dislocations are not important. The radiation damage in the oxide is due to the charges generated in the oxide. Due to the isolating character of the oxide these charges cannot disappear and lead to local concentrations of these charges.
 - Radiation damage in the oxide (**surface damage**) is primarily produced by photons and charged particles.

Introduction

- **Defects** in the semiconductor lattice **create energy levels in the band gap** between valence and conduction band (see section on doping).
- Depending on the position of these energy levels the following effects will occur:
 1. **Modification of the effective doping concentration**
 - Shift of the **depletion voltage**.
 - caused by shallow energy levels (close to the band edges).
 2. **Trapping of charge carriers**
 - reduced **lifetime** of charge carriers
 - Mainly caused by deep energy levels
 3. **Easier thermal excitement of e^- and h^+**
 - increase of the **leakage current**

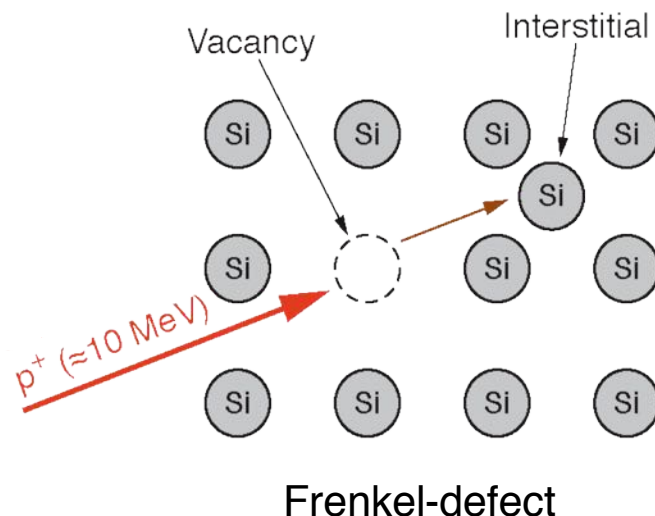
Point defects and cluster defects

- The minimum energy transfer in a collision to dislocate a silicon atom is $E_{min} \approx 15$ eV (depending on the crystal orientation).
- **The energy at which the dislocation probability in silicon is 50% is $E_d \approx 25$ eV (displacement energy).**
- Below E_d only lattice oscillations are excited and no damage occurs.
- Above E_d and below an energy transfer of **1–2 keV** isolated **point defects** are produced.
- At energy transfers **between 2 keV and 12 keV** the hit atom (primary knock-on atom, PKA) can produce additional point defects or **cluster defects**.
- **Above 12 keV several cluster and point defects** are produced.

Point defects

- A displaced silicon atom produces an empty space in the lattice (**Vacancy, V**) and in another place an atom in an inter lattice space (**Interstitial, I**).

A vacancy-interstitial pair is called a **Frenkel-defect**.



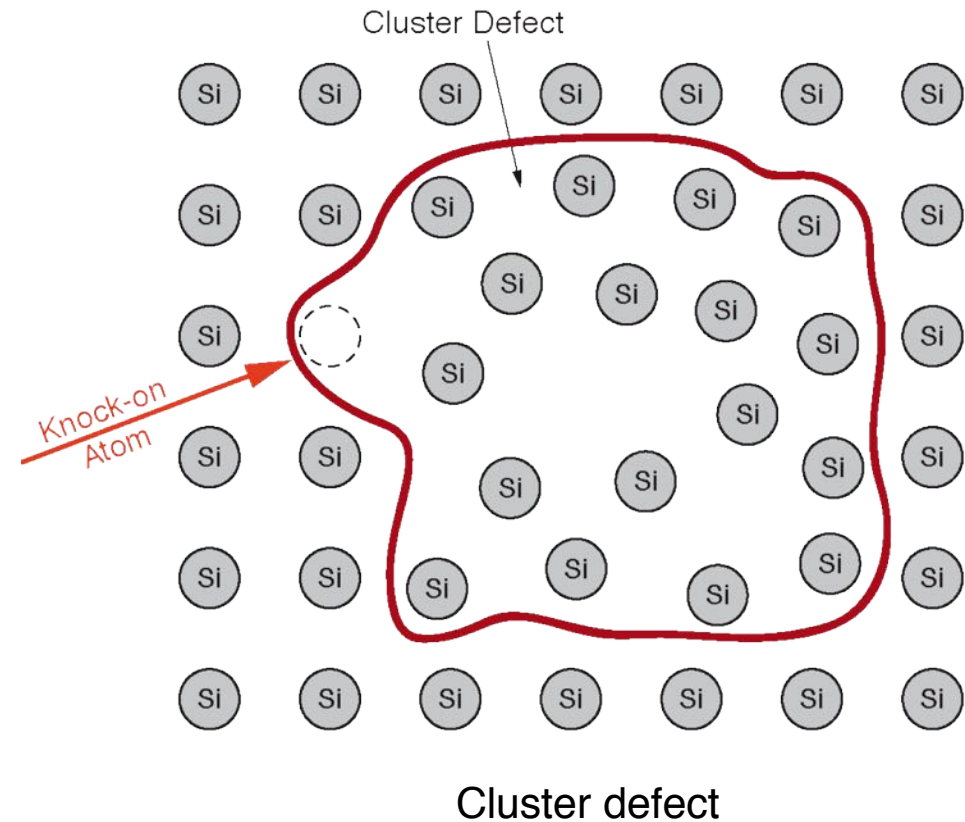
- At room temperature these defects are mobile within the lattice. An interstitial atom may drop into a vacancy and both defects disappear

⇒ **the defects anneal.**

Other defects form stabile secondary defects.

Cluster defects

- In hard impacts the primary knock-on atom displaces additional atoms. These defects are called cluster defects.
- The size of a cluster defect is approximately 5 nm and consists of about 100 dislocated atoms.
- For high energy PKA cluster defects appear at the end of the track when the atom loses the kinetic energy and the elastic cross section increases.



Annealing and secondary effects

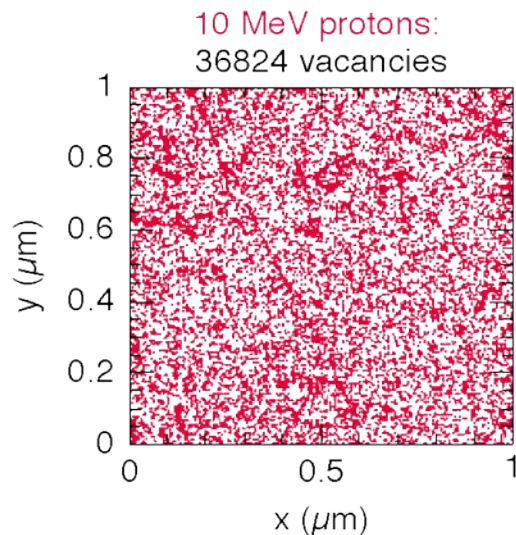
- **Interstitials and the vacancies are moving** inside the crystal lattice and they are not stable defects.
- Some of the dislocated atoms may **fall back into** a regular **lattice position**. This effect is called **beneficial annealing**.
- Some of these primary defects can combine with other defects to immovable, stable secondary defects.

Examples of such secondary defects are:

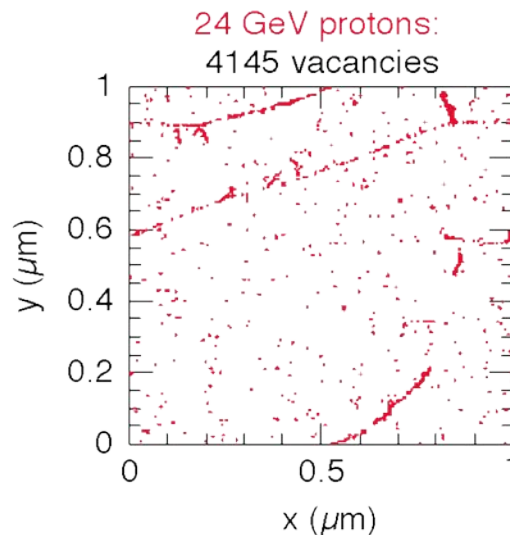
- **E-center (VP_s)**: Vacancy close to a P atom at a regular lattice location. The P atom loses its donor properties.
- **A-center (VO_i)**: Vacancy and an O atom at an interstitial location. O atoms at an interstitial location are electrical neutral. However, together with a vacancy they become an acceptor.
- **Divacancy (V_2), Trivacancy (V_3)**: Double and triple vacancies.
- **Various combinations of interstitials, vacancies, C and O atoms at regular locations or interstitial locations.**

Dependence on type and energy of radiation

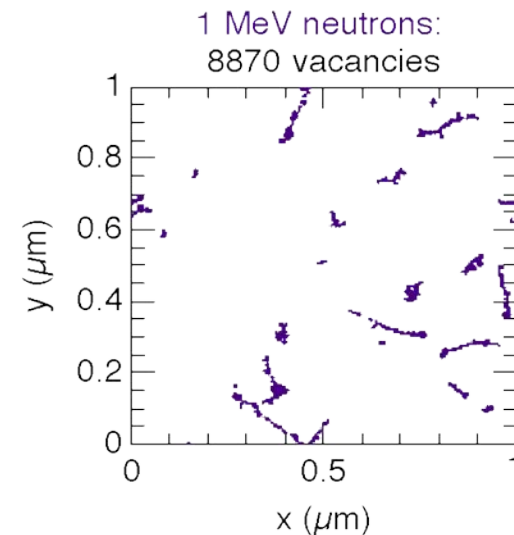
Type and frequency of defects depends on the particle type and the energy. Plots below show a simulation of vacancies in $1 \mu\text{m}$ thick material after an integrated flux of 10^{14} particles per cm^2 :



Many vacancies
produced



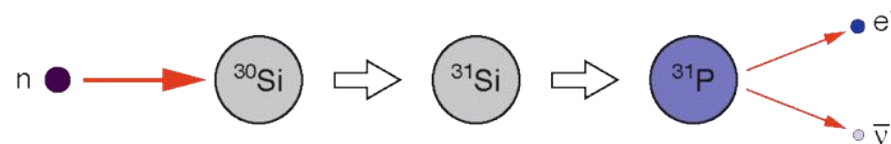
Less vacancies, a significant part of the energy is consumed to produce cluster defects



Very few vacancies, energy of the neutrons is used up to produce cluster defects.

Nuclear Transformations

- Is the strong force responsible for the interaction (rather than the electromagnetic force) an atom might be transformed in another type.
- An example is the transformation of a silicon atom in a phosphor atom with the subsequent beta decay:



- If the transformed atom remains in the correct lattice position this atom acts as a regular dopant – either as donor or acceptor.

Non-ionizing energy loss

NIEL HYPOTHESIS

NIEL Hypothesis - introduction

- According to the **NIEL hypothesis** the radiation damage is
 - linear proportional to the **non-ionizing energy loss** of the penetrating particles (radiation) and
 - this energy loss is again linear proportional to the energy used to dislocate lattice atoms (displacement energy).
- The NIEL hypothesis does not consider atom transformations nor annealing effects and is therefore not exact.
- Nevertheless, it is common to **scale the damage effects** of different particles using the NIEL hypothesis. As normalization one uses **1 MeV neutrons** and instead of using the integrated flux of a particular particle the **equivalent fluence** Φ_{eq} (integrated equivalent flux) of 1 MeV neutrons is used.

Leakage current – damage rate α

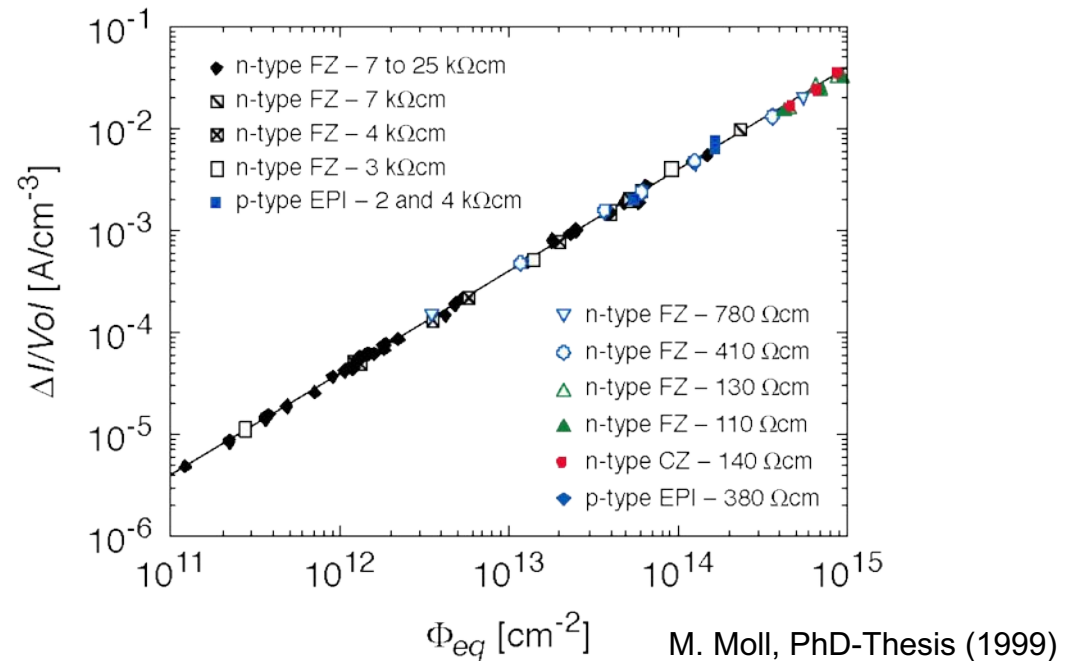
- Irradiation induced leakage current increases linear with the integrated flux:

$$\Delta I = \alpha \cdot \Phi_{eq} \cdot Vol$$

- α is called the **current related damage rate**. It is largely independent of the material type. α depends on temperature $\rightarrow \alpha(T)$

20°C: $\alpha = 4,00 \cdot 10^{-17} \text{ A/m}$

-10°C: $\alpha = 1.86 \cdot 10^{-18} \text{ A/m}$

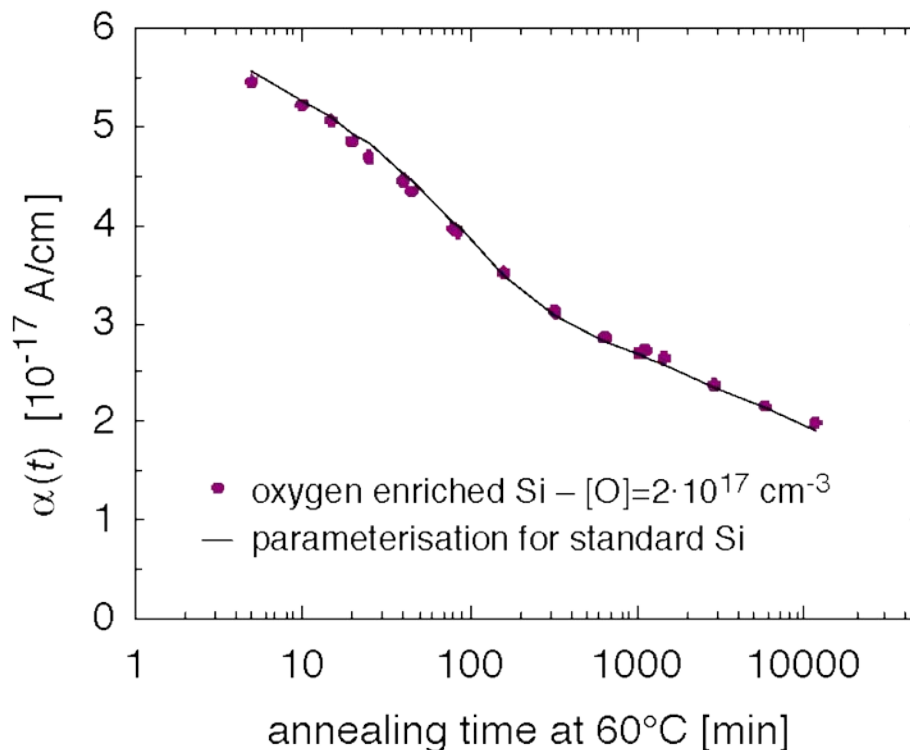


In ten years of LHC operation the currents of the innermost layers increase by 3 orders of magnitude!

Leakage current – annealing

- The damage rate α is time dependent.

The plot shows the development of α for a detector stored at $T = 60^\circ\text{C}$ after irradiation:



G. Lindström, *Radiation Damage in Silicon Detectors*,
 Nucl. Instr. Meth. A **512**, 30 (2003)

Change of effective doping concentration

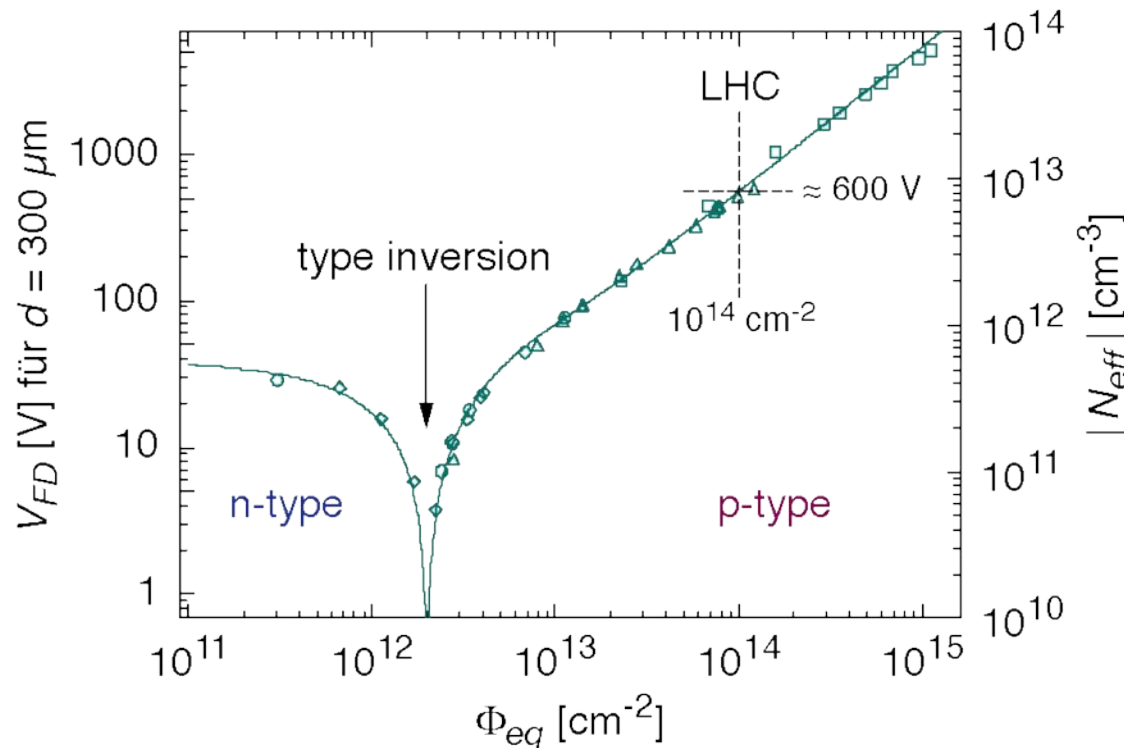
- The irradiation produces mainly acceptor like defects and removes donor type defects. In a n type silicon the effective doping concentration N_{eff} decreases and after a point called type inversion (n type Si becomes p type Si) increases again.
- The voltage needed to fully deplete the detector V_{FD} is directly related to the effective doping concentration:

$$V_{FD} \approx \frac{e}{2\varepsilon_0\varepsilon_r} |N_{eff}| d^2$$

- The depletion voltage and consequently the minimum operation voltage decreases, and after the inversion point increases again.

Change of effective doping concentration (cont.)

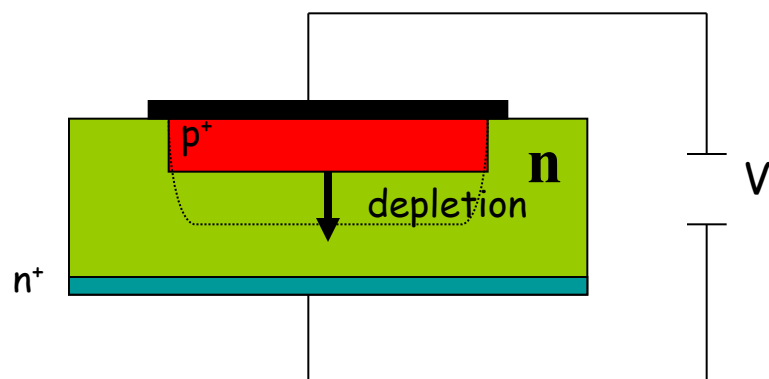
Full depletion voltage and effective doping concentration) of an originally n type silicon detector as a function of the fluence Φ_{eq} :



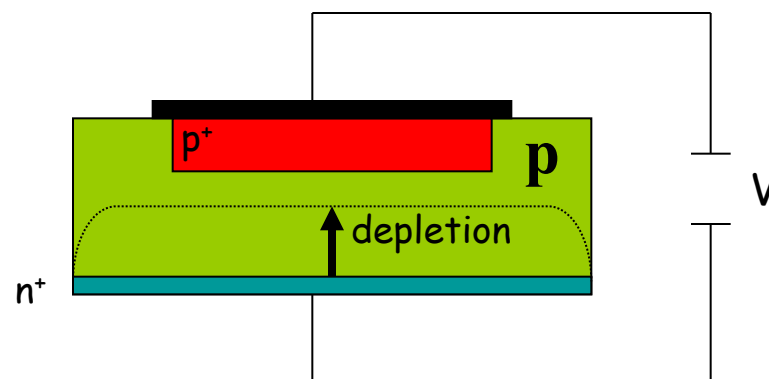
G. Lindström, *Radiation Damage in Silicon Detectors*, Nucl. Instr. Meth. A **512**, 30 (2003)

Depletion Voltage and Type Inversion

Before Inversion:

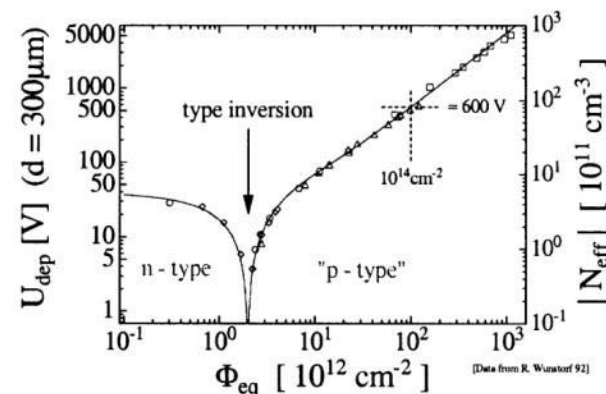


After Inversion:



After “inversion” of bulk-type $n \rightarrow p$:
The depletion region grows from the back

→ Sensor does not work under-depleted anymore



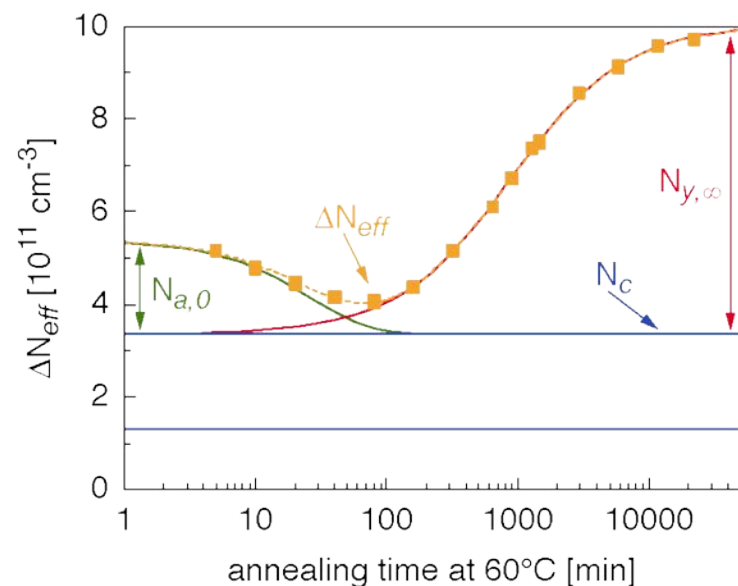
Time Dependence of Radiation Damage

- Defects diffuse with time
- N_{eff} changes:

$$\Delta N_{\text{eff}}(\Phi_{\text{eq}}, t) = \text{stable damage } (N_c(\Phi_{\text{eq}})) \\ + \text{annealing } (N_b(\Phi_{\text{eq}}, t), N_r(\Phi_{\text{eq}}, t))$$

Three Terms:

- constant damage N_c
- Two kinds of Annealing:
 - beneficial annealing:** N_b (short-term)
 - reverse annealing** N_r (long-term)
- Different time-scales:



G. Lindström, Radiation Damage in
Silicon Detectors, NIM A 512, 30 (2003)

$T [^\circ \text{C}]$	-10	-7	0	10	20	40	60	80
τ_b	306d	180d	53d	10d	55h	4h	19min	2min

$T [^\circ \text{C}]$	-10	0	10	20	40	60	80	100
τ_r	516y	61y	8y	475d	17d	1260min	92min	9min

Operating temperature

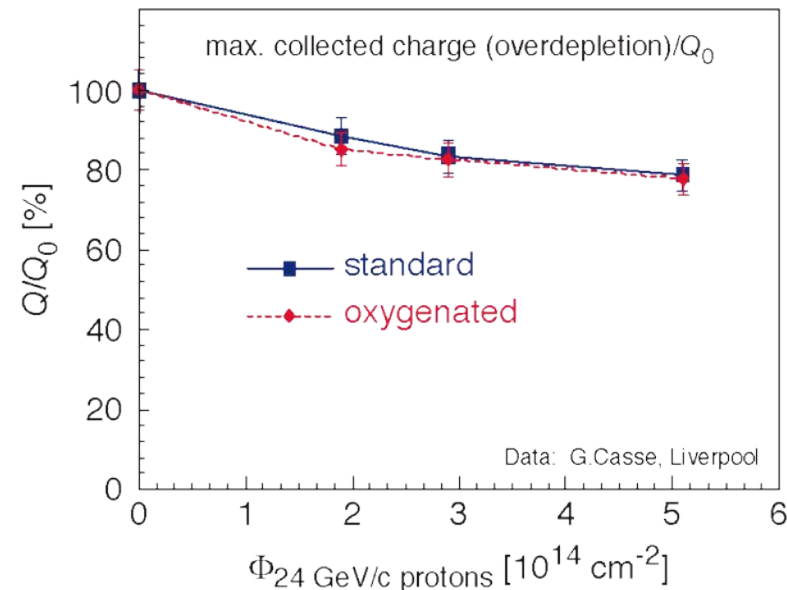
- Annealing and reverse annealing are strongly depending on temperature. Both effects increase with temperature.
- Annealing and reverse annealing overlap in time and develop with different time constants.
 - ⇒ In an operating experiment (detectors under radiation) the operating temperature of the silicon is a compromise between annealing and reverse annealing.
- N_{eff} is relatively stable below a temperature of -10°C .
 - ⇒ The CMS silicon tracker will be operated at a temperature of -20°C .
 - ⇒ An irradiated detector has to remain cooled down even in non operating periods.

Charge collection efficiency

- Irradiation creates defects with energy levels deep inside the band gap. These defects act as **trapping centers**. Charge carriers are trapped in these levels and released after some time (depending on the depth of the energy level). \times charges released with delay are no longer measured within the integration time of the electronics

⇒ detector signal is reduced

Charge collection efficiency, detector irradiated with $5 \cdot 10^{14}$ protons/cm² (24 GeV). Within the readout time of 25 ns only 80% of the signal is observed:



M. Moll, Development of Radiation Hard Sensors for Very High Luminosity Colliders - CERN RD50 Project VERTEX2002, Hawaii (Nov., 2002)

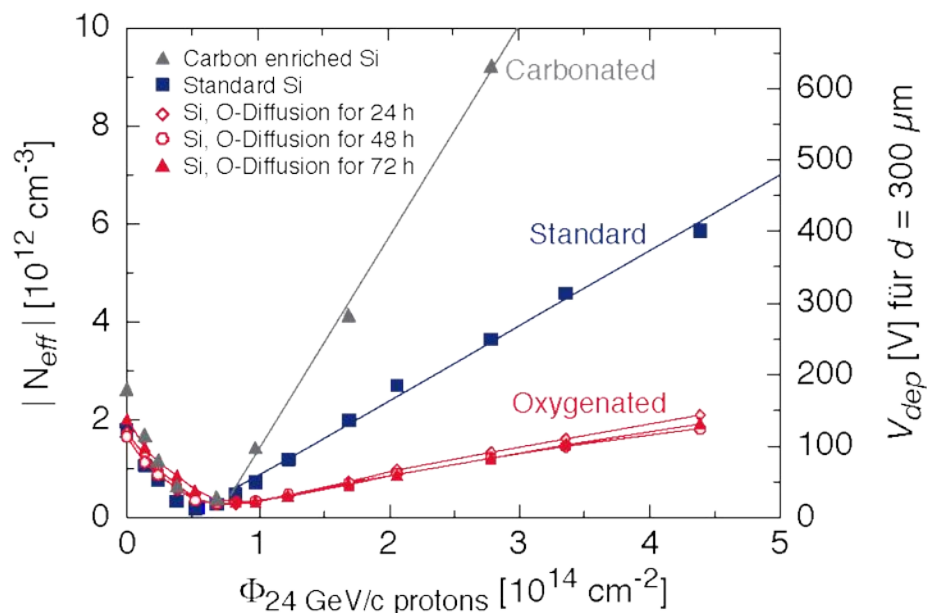
- Irradiated detectors operated with higher bias voltage: over-depletion
⇒ can compensate partly reduced charge collection efficiency

Material engineering

- Introduction of impurity atoms, initially electrically neutral, can combine to secondary defects and modify the radiation tolerance of the material.
- **Silicon enriched with carbon** makes the detector less radiation hard.
- **Oxygen enriched silicon** (Magnetic Czochralski Si) has proven to be more radiation hard with respect to charged hadrons (no effect for neutrons)

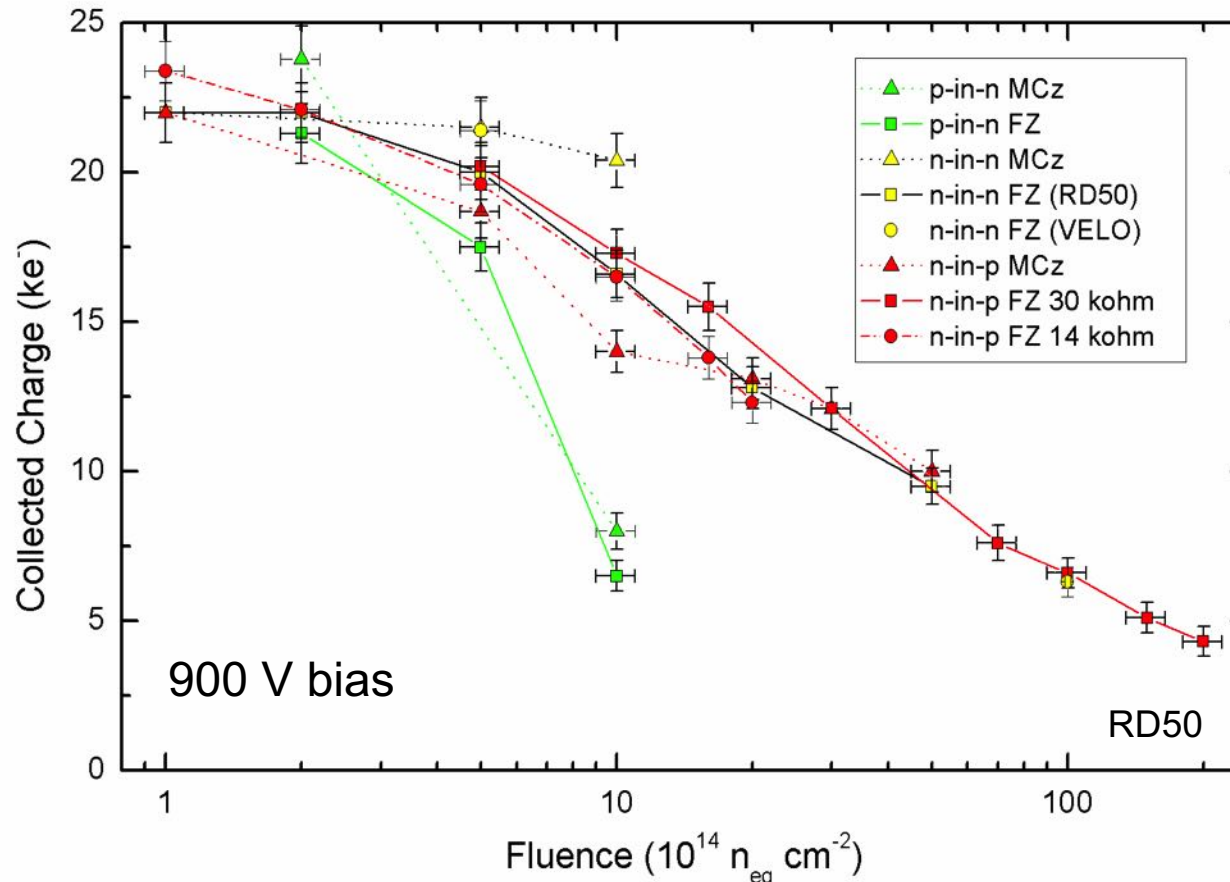
Influence of C and O enriched silicon on the full depletion voltage and the effective doping concentration (Irradiation with 24 GeV protons, no annealing):

Oxygen enriched Si used for pixel detectors in ATLAS and CMS.



G. Lindström, Radiation Damage in Silicon Detectors, NIM A 512, 30 (2003)

Material engineering (2): Other options



- Irradiation Studies show p-in-n FZ Silicon not very radiation hard
- Better: magnetic Czochalski (mCz) or n-in-p FZ
- Needs much higher bias voltages than currently used

Material engineering (3): Diamond

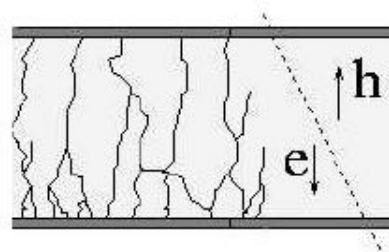
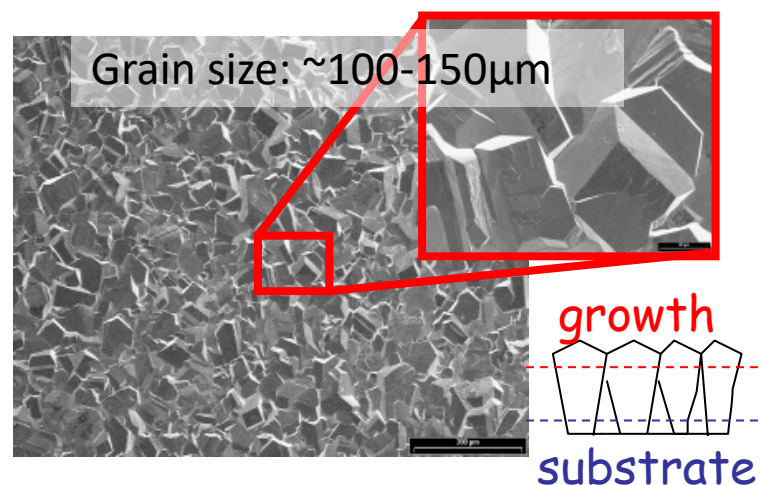
Pro's:

- large band gap and strong atomic bonds give good radiation hardness
- No pn-junction necessary
- low leakage current and low capacitance both give low noise
- 3 (1.5) times better mobility and 2x better saturation velocity give fast signal collection

Con's:

- Small signal:
 - Silicon: 23.500 e⁻ in 300 μm
 - Diamond: ~10.000 e⁻ in 300 μm
- In Polycrystalline Diamond grain-boundaries, dislocations, and defects
- very expensive ☹️

Polycrystalline Diamonds grown by CVD



Surface defects – defects in the oxide

- In the amorphous oxide dislocation of atoms is not relevant. However, **ionizing radiation creates charges in the oxide.**
- Within the band gap of amorphous oxide (8.8 eV compared to 1.12 eV in Si) a large number of deep levels exist which trap charges for a long time.
- The mobility of electrons in SiO_2 is much larger than the mobility of holes
 - ⇒ electrons diffuse out of the oxide, holes remain semi permanent fixed
 - ⇒ **the oxide becomes positively charged due to these fixed oxide charges.**
- **Consequences for the detector:**
 - **Reduced electrical separation between implants (lower inter-strip resistance)**
 - **Increase of inter-strip capacitance**
 - **Increase of detector noise**
 - **Decrease of position resolution**
 - **Increase of surface leakage current**

Surface defects – read out electronics

- The read out electronics is equally based on silicon and SiO_2 structures.

Read out electronics is based on surface structures (e.g. MOS process) and hence very vulnerable to changes in the oxide.

- The front end electronics is mounted close to the detector and experiences equal radiation levels.

⇒ Radiation damage is a very critical issue also for the readout electronics!

Radiation damage Summary

- The defect introduced by radiation change significantly the properties of the detectors
- As long as
 - the bias voltage can follow the development of the full depletion voltage (voltage remains below break down voltage) and
 - the effect of increased leakage current can be controlled (cooling)the detector remains functional.
- Charge trapping, increase of capacitance and leakage current, etc. worsen the performance of the detector gradually.
- The radiation tolerance can be improved by the design of the detector structures, the use of oxygenated silicon, or the development of detectors based on alternative materials (diamond).

Silicon Detectors in High Energy Physics

HISTORY

Early Days till Now

- 1951: First detectors with Germanium pn-Diodes (McKay)
- 1960: working samples of p-i-n-Detectors for α - und β -spectroscopy (E.M. Pell)
- 1964: use of semiconductor detectors in experimental nuclear physics (G.T. Ewan, A.J. Tavendale)
- 1960ies: Semiconductor detectors made of germanium and silicon become more and more important for energy spectroscopy
- **1980: Fixed target experiment with a planar diode (J. Kemmer)**
- 1980-1986: **NA11** and NA32 experiment at CERN to measure charm meson lifetimes with planar silicon detectors
- 1990ies (Europe): LEP Detectors (e.g. **DELPHI**)
- 1990ies and later (US): **CDF** and D0 at Tevatron
- Now: LHC Detectors with up to 200m² active detector area (CMS)

The Birth

- Fixed target experiment with a planar diode
- First use of planar process developed for chip industry

NUCLEAR INSTRUMENTS AND METHODS 169 (1980) 499-502, © NORTH HOLLAND PUBLISHING CO

FABRICATION OF LOW NOISE SILICON RADIATION DETECTORS BY THE PLANAR PROCESS

J KEMMER

Fachbereich Physik der Technischen Universität München, 8046 Garching, Germany

Received 30 July 1979 and in revised form 22 October 1979

Dedicated to Prof Dr H-J Born on the occasion of his 70th birthday

By applying the well known techniques of the planar process oxide passivation, photo engraving and ion implantation, Si pn-junction detectors were fabricated with leakage currents of less than $1 \text{ nA cm}^{-2}/100 \mu\text{m}$ at room temperature. Best values for the energy resolution were 10.0 keV for the 5.486 MeV alphas of ^{241}Am at 22°C using $5 \times 5 \text{ mm}^2$ detector chips.

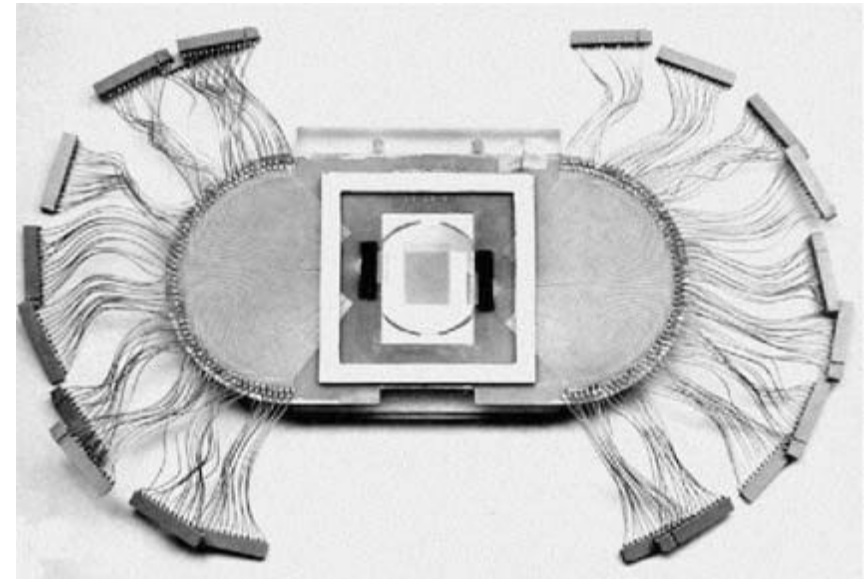
NA11 at CERN

First proof of principle to use a
position sensitive silicon detector in
HEP experiment

- Aim: measure lifetime of charm mesons D^0 , D^- , D^+ , D^+_s , D^-_s (decay length $30\ \mu\text{m}$)
⇒ spatial resolution better
 $10\ \mu\text{m}$ required

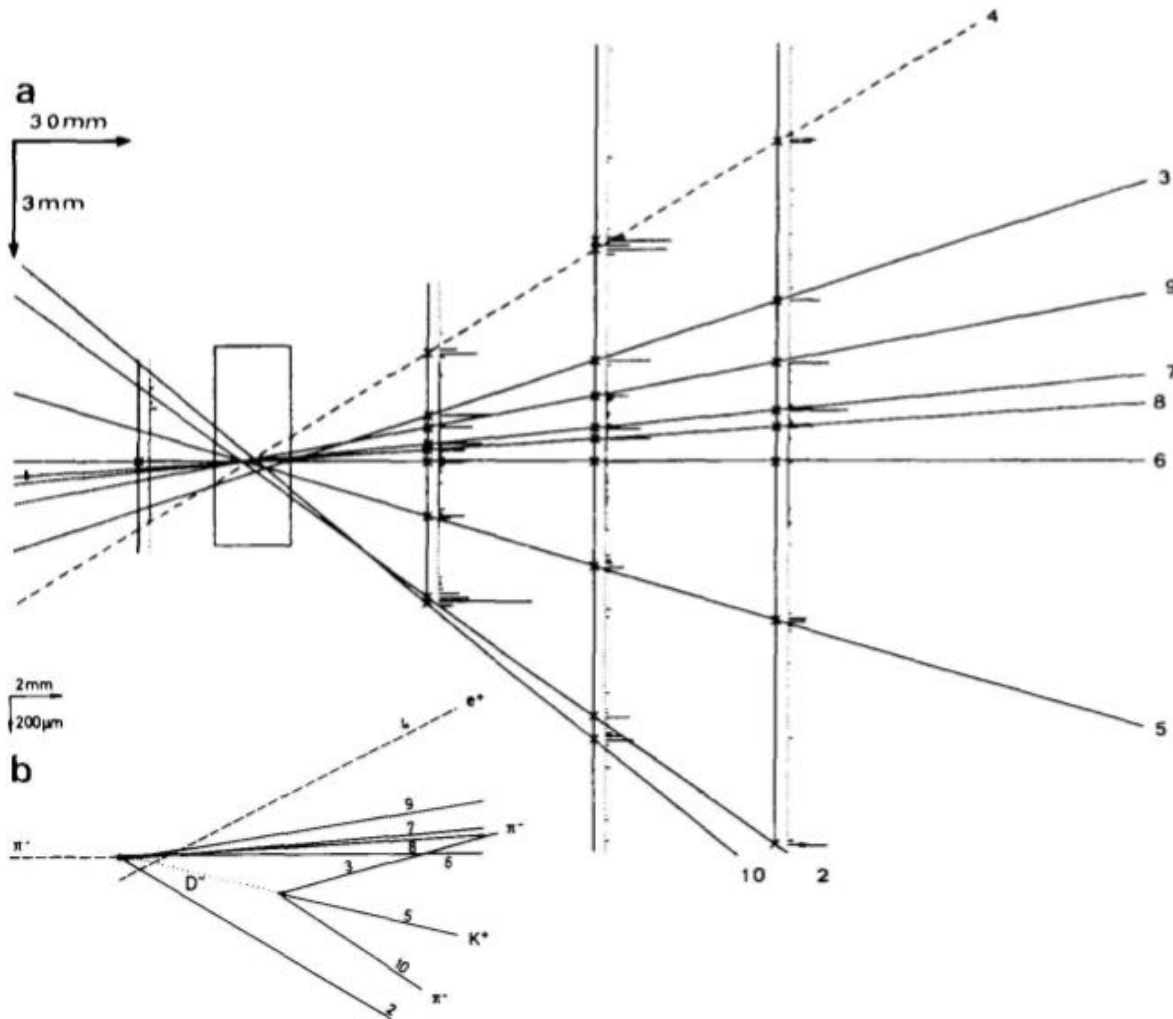
NA11 Detector:

- 1200 diode strips with $20\ \mu\text{m}$ pitch on $24\ \text{cm}^2$ active area (2" wafer)
- 250-500 μm thick bulk material
- 8 silicon detectors (2 in front, 6 behind the Target)
- Resolution of $4.5\ \mu\text{m}$



NA11

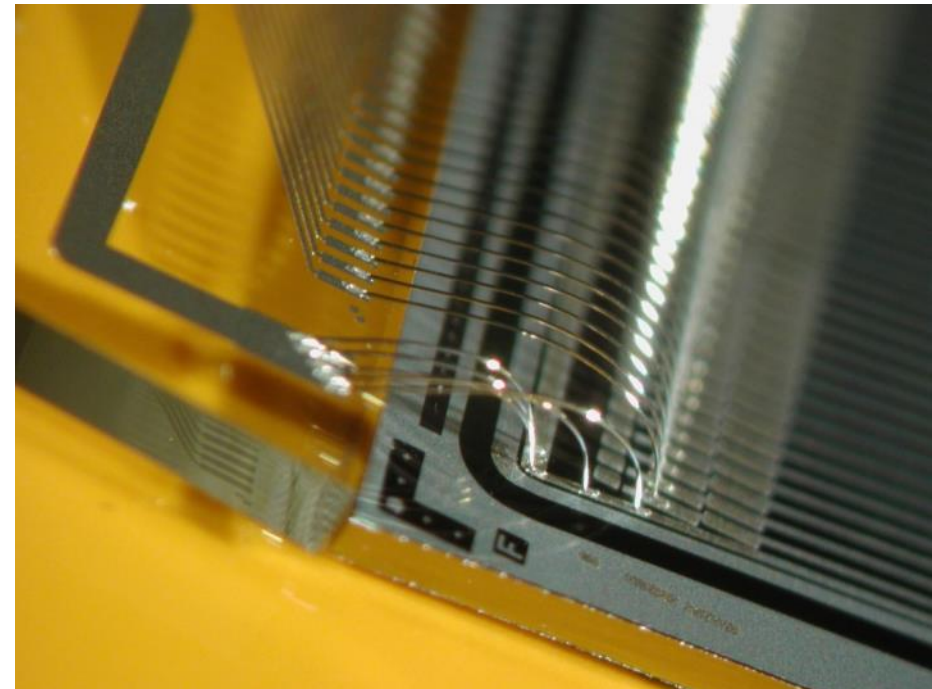
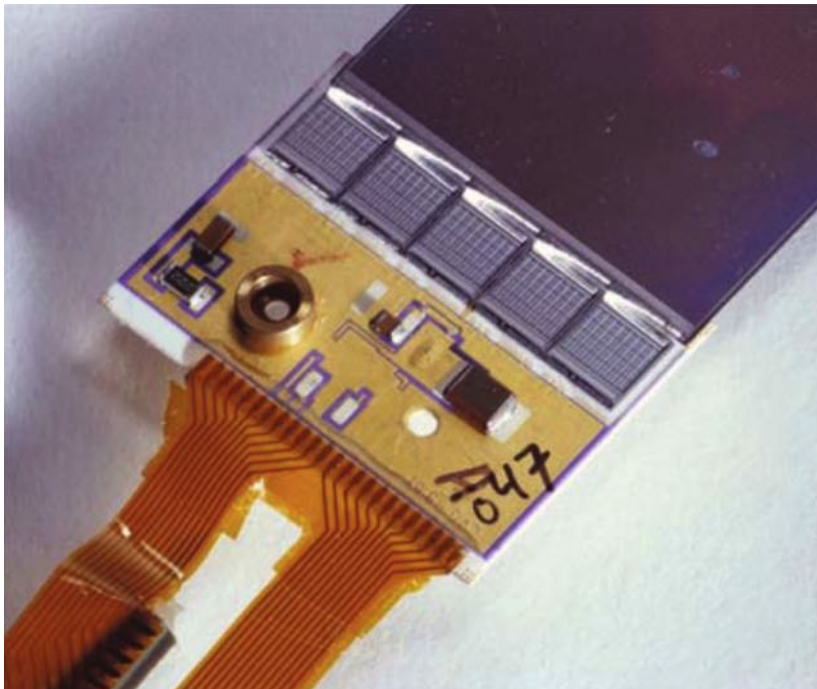
Computer reconstruction of a decay of $D^- \rightarrow K^+ \pi^+ \pi^-$



Flight path length ($c\tau\gamma$)
used to deduce the lifetime
of the particle.

Towards Complex Detectors

- Development of custom designed VLSI chips with up to 128 readout channels.
- Chips containing preamplifier, shaper, pipeline, multiplexer, etc.
- Connection to the strips on the sensors using thin pitch wire bonding



Detail from the DELPHI Vertex detector

Vertex Detectors

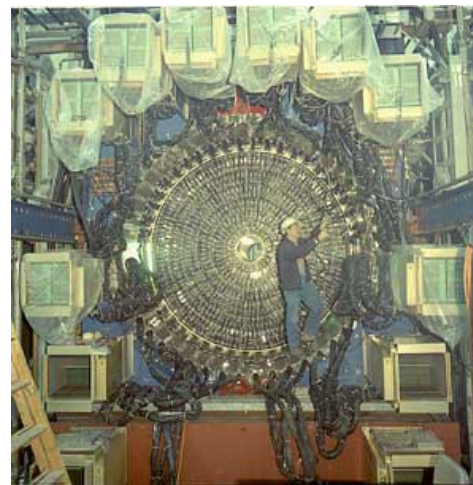
Experiments:

- LEP Detectors at CERN
- SLAC Linear Collider (Mark II experiment)
- Minimize the mass inside tracking volume
- Readout chips at end of ladders
- Minimize the mass between interaction point and detectors
- Minimize the distance between interaction point and the detectors

DELPHI



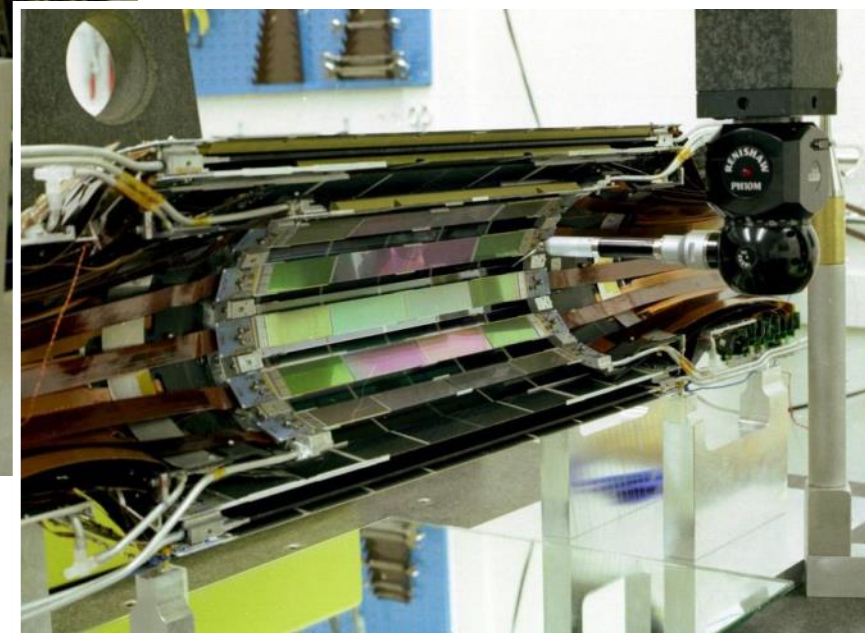
Mark II



DELPHI Microvertex detector



- 888 silicon sensors (surface $\sim 1.5\text{m}^2$)
- 2 silicon layers, 40cm long ladders
- $300\mu\text{m}$ DSSDs with double metal readout



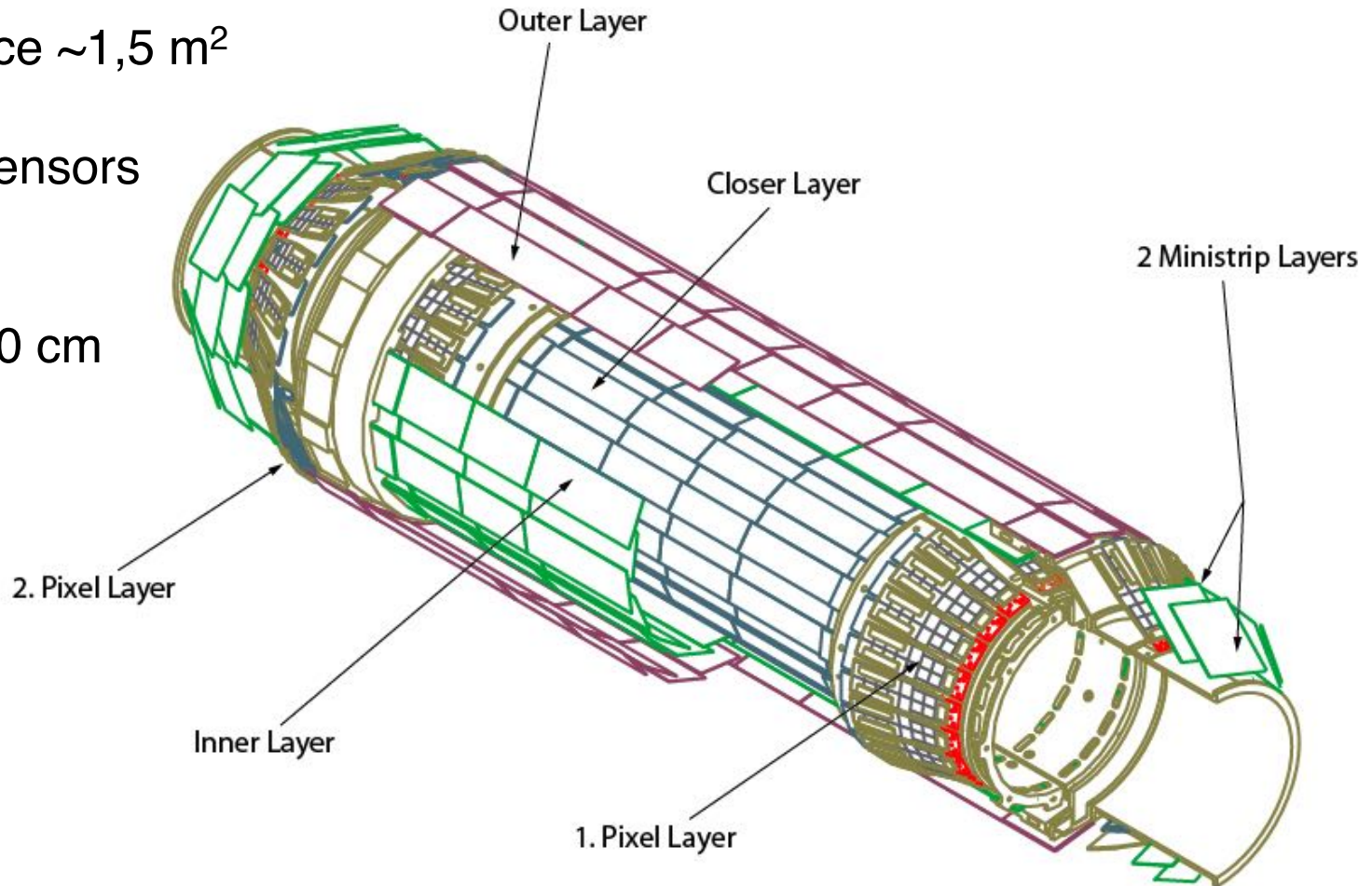
DELPHI Microvertex detector

Sensor surface $\sim 1,5 \text{ m}^2$

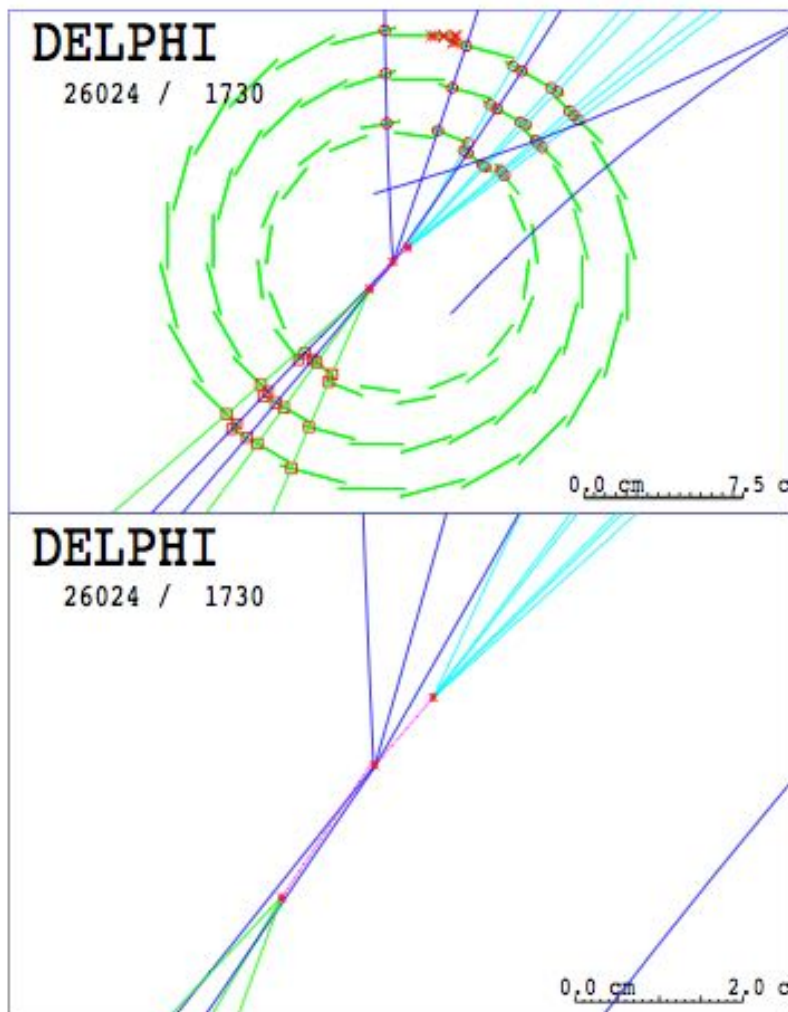
888 Silicon sensors

Length $\sim 1 \text{ m}$

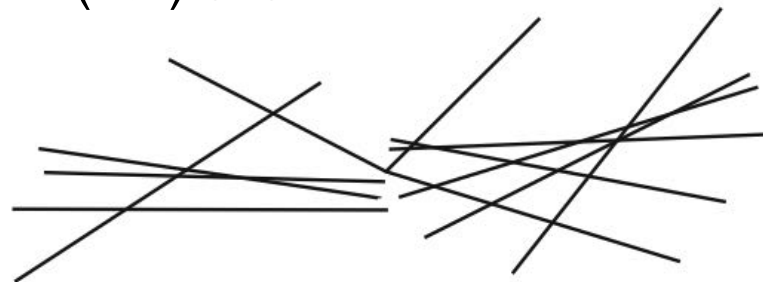
Diameter $\sim 20 \text{ cm}$



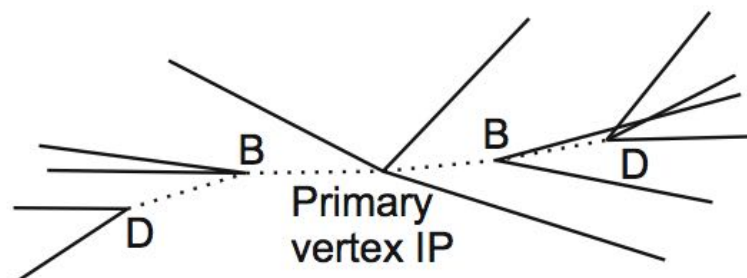
A $b\bar{b}$ event from DELPHI



A $b\bar{b}$ event:



After reconstruction:



**Sophisticated reconstruction
algorithms necessary!**

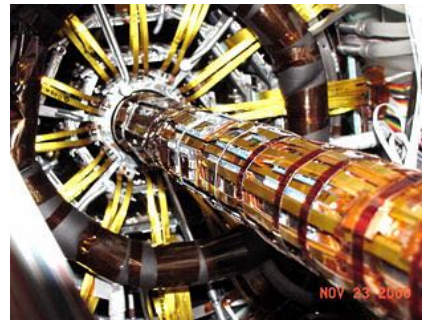
CDF at Tevatron (Fermilab)

Collider Detector at Fermilab (CDF) is one of the two Experiments at the 2x1TeV Tevatron

- Discovery of top-quark (1995)

Tracker:

- Barrel only (no endcaps)
- Different Silicon Layers:
 - L00 (SSSD, $r \sim 1.5$ cm, $l=94$ cm)
 - SVX ($r = 5-10$ cm)
 - ISL (DSSD, $r = 20-29$ cm)
- Total active area: approx. 10 m²



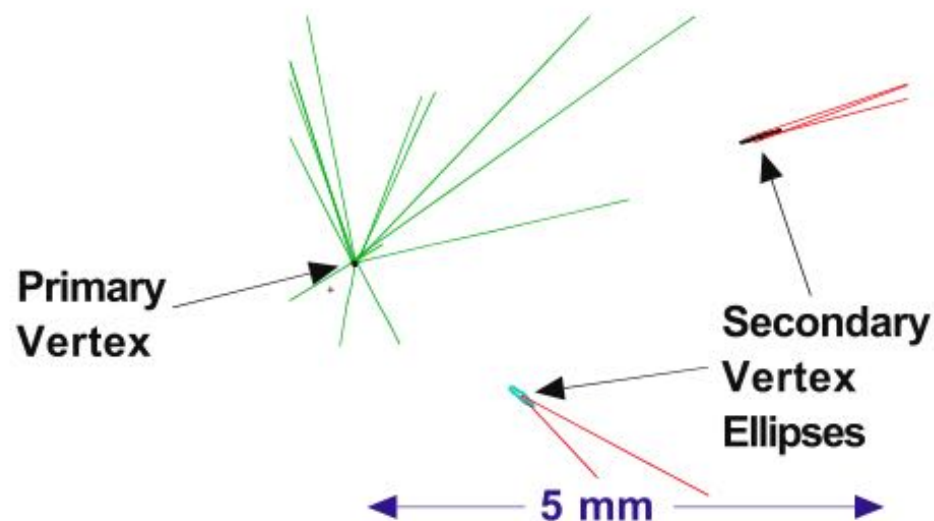
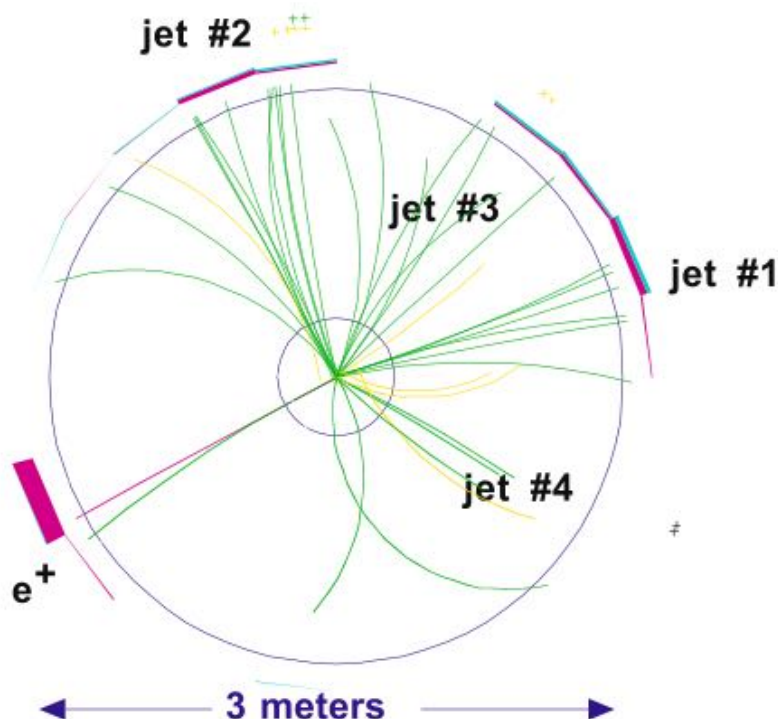
A “golden” top event in CDF

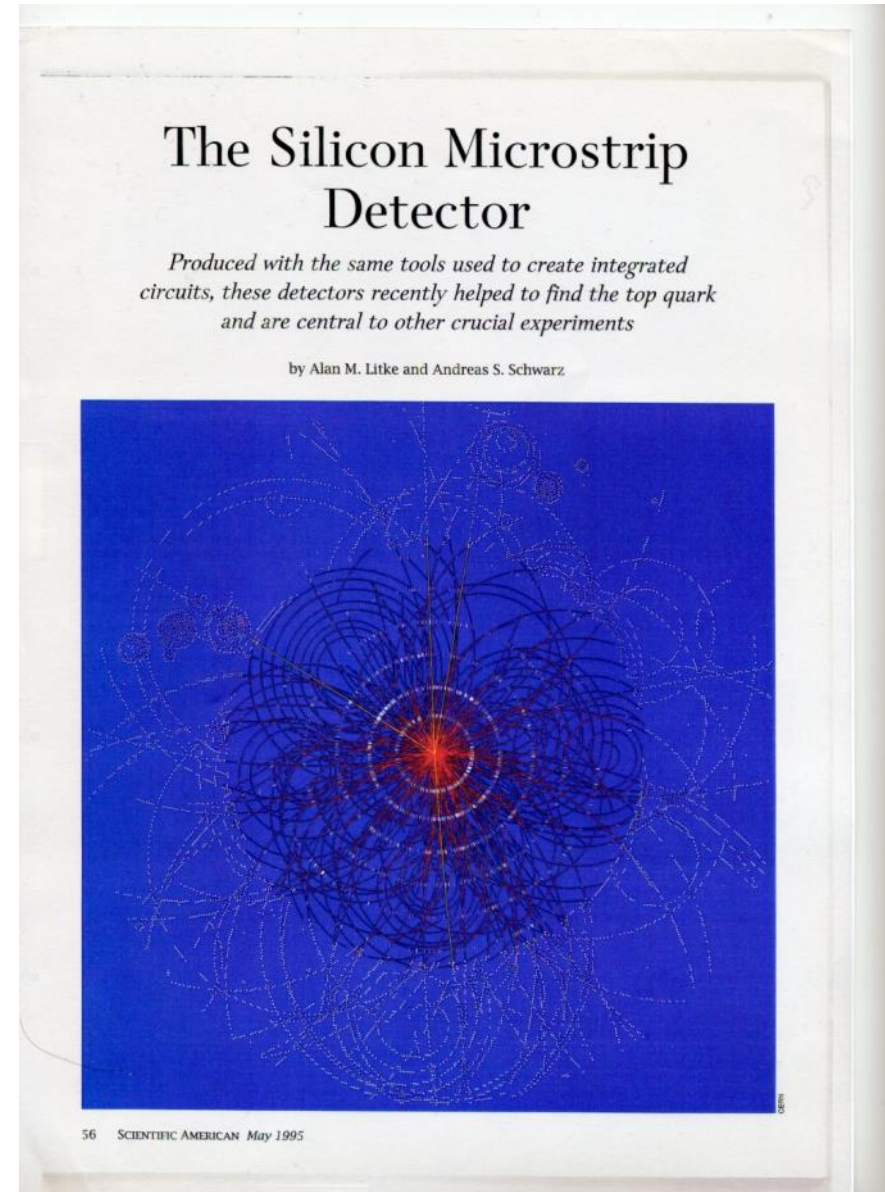
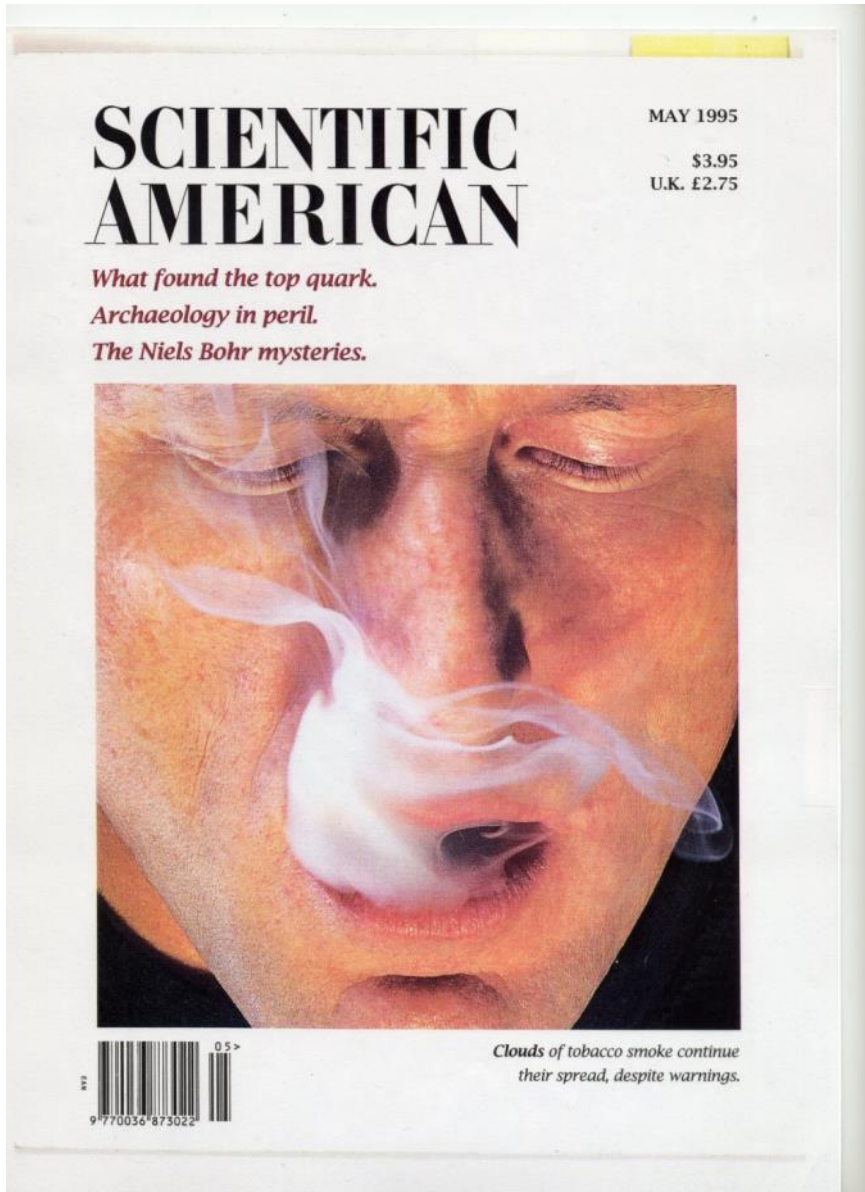
$t\bar{t} \rightarrow W^+b, W^-b\bar{b}$

One W decays leptonically showing one lepton plus missing energy

Second W decays into $q\bar{q}$ producing two jets

Signature: one lepton, four jets of which two tagged b jets and missing energy

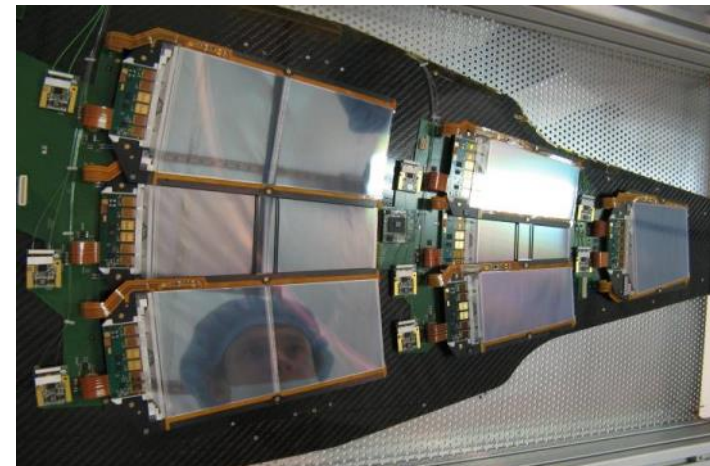




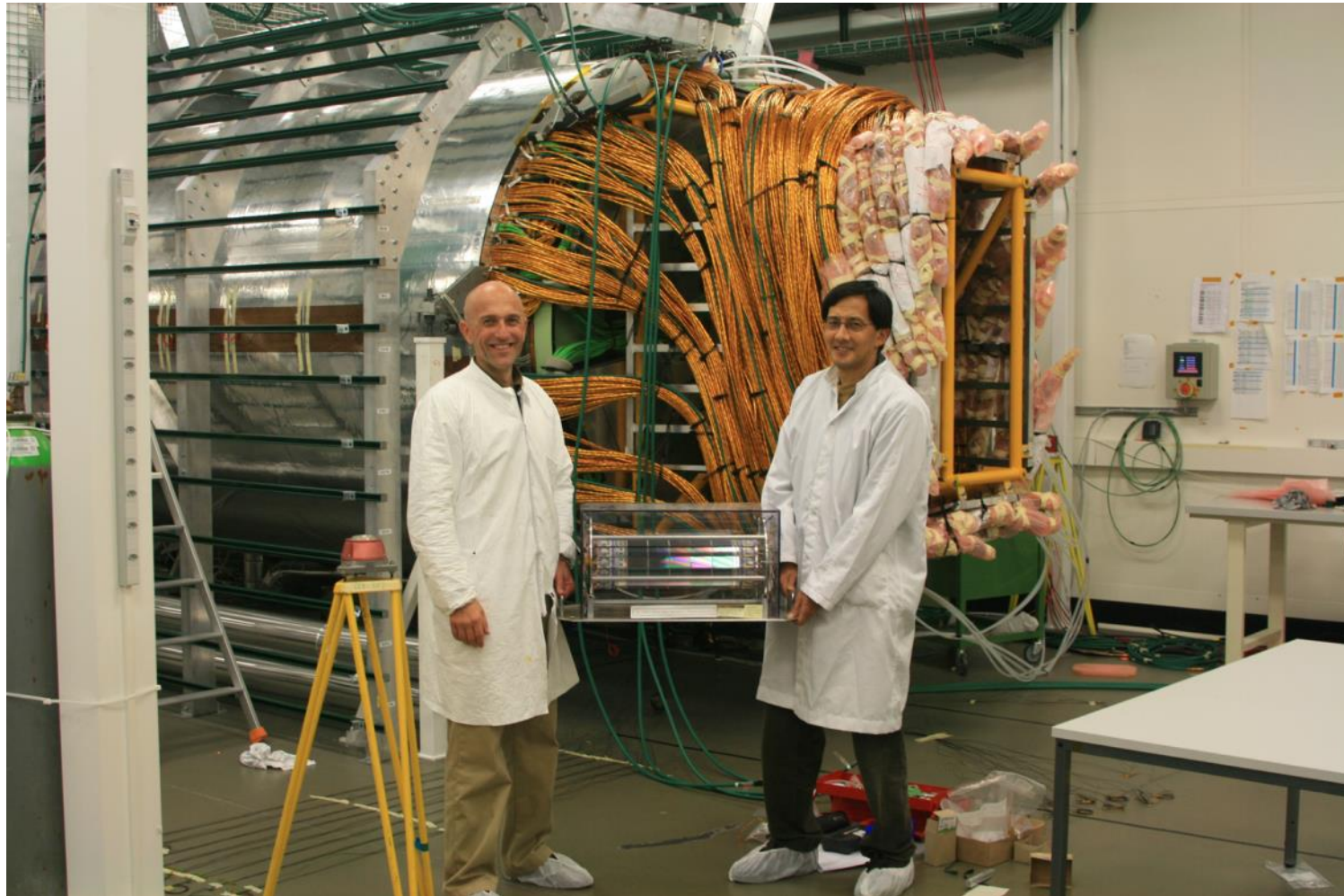
Tracking Paradigm

Tevatron and LHC Experiments:

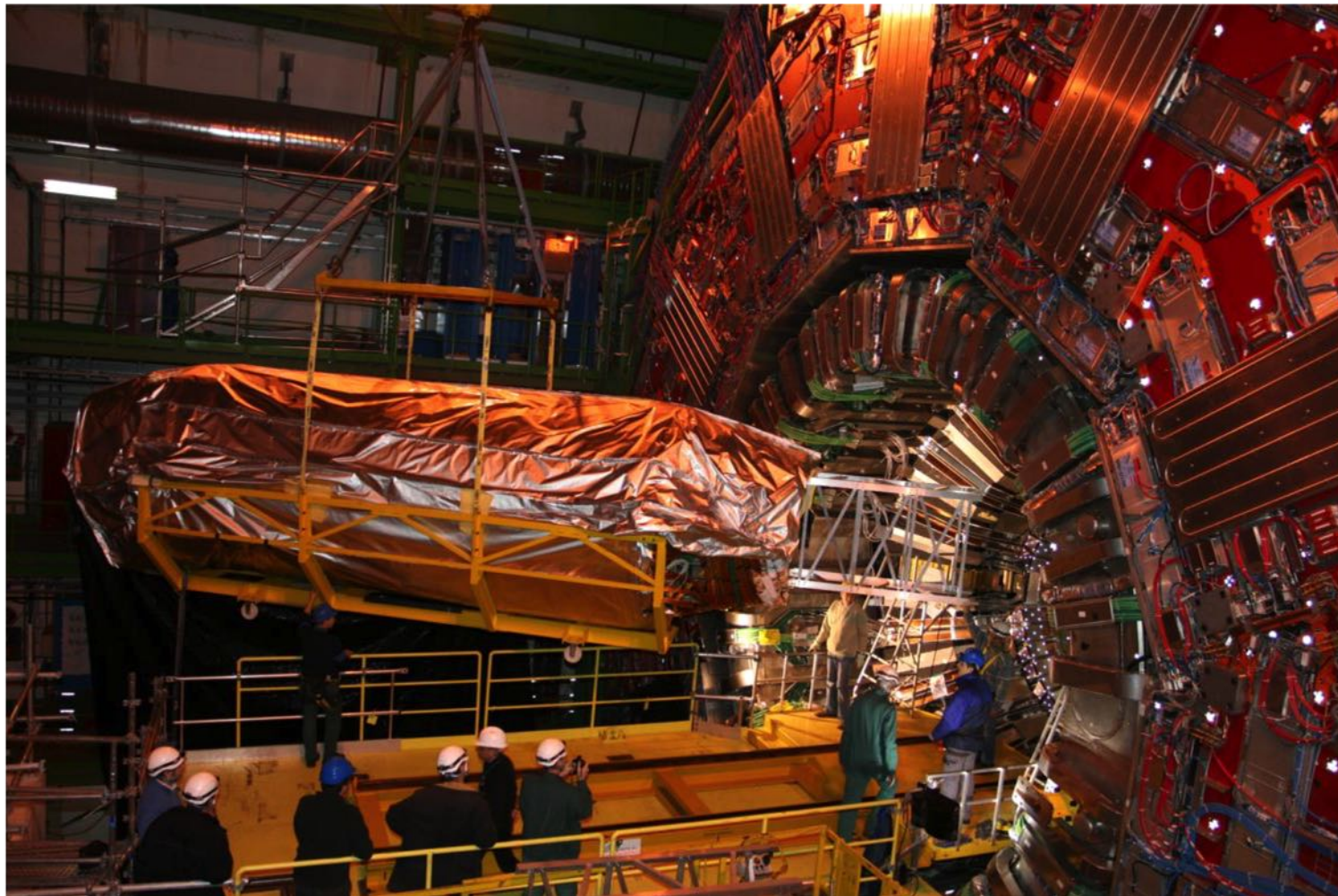
- Emphasis shifted from vertexing to tracking
- Cover large area with many silicon layers
- Detector modules include readout chips and services **inside** the tracking volume
- Large number of layers (redundancy) because of limited access possibilities



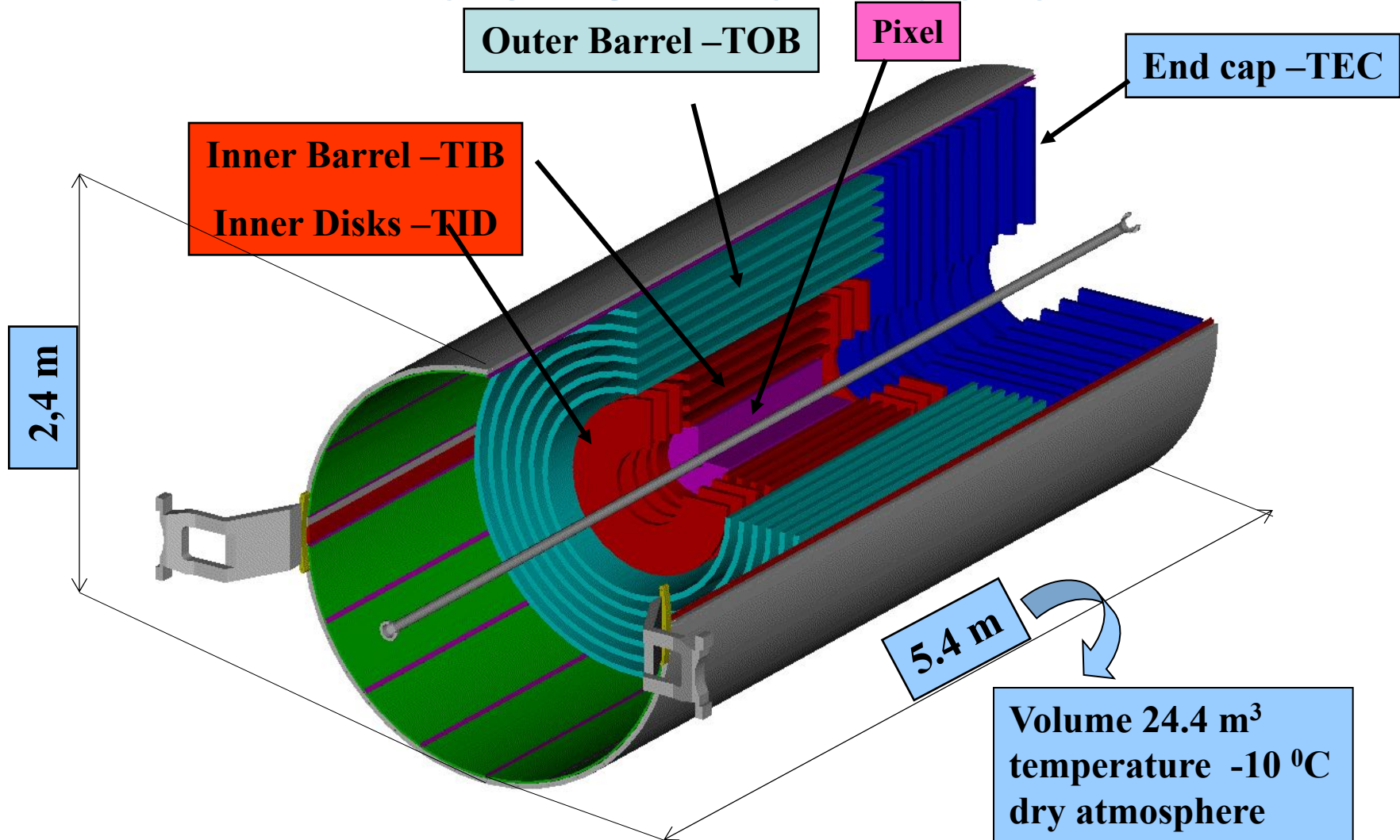
DELPHI vs. CMS Tracker



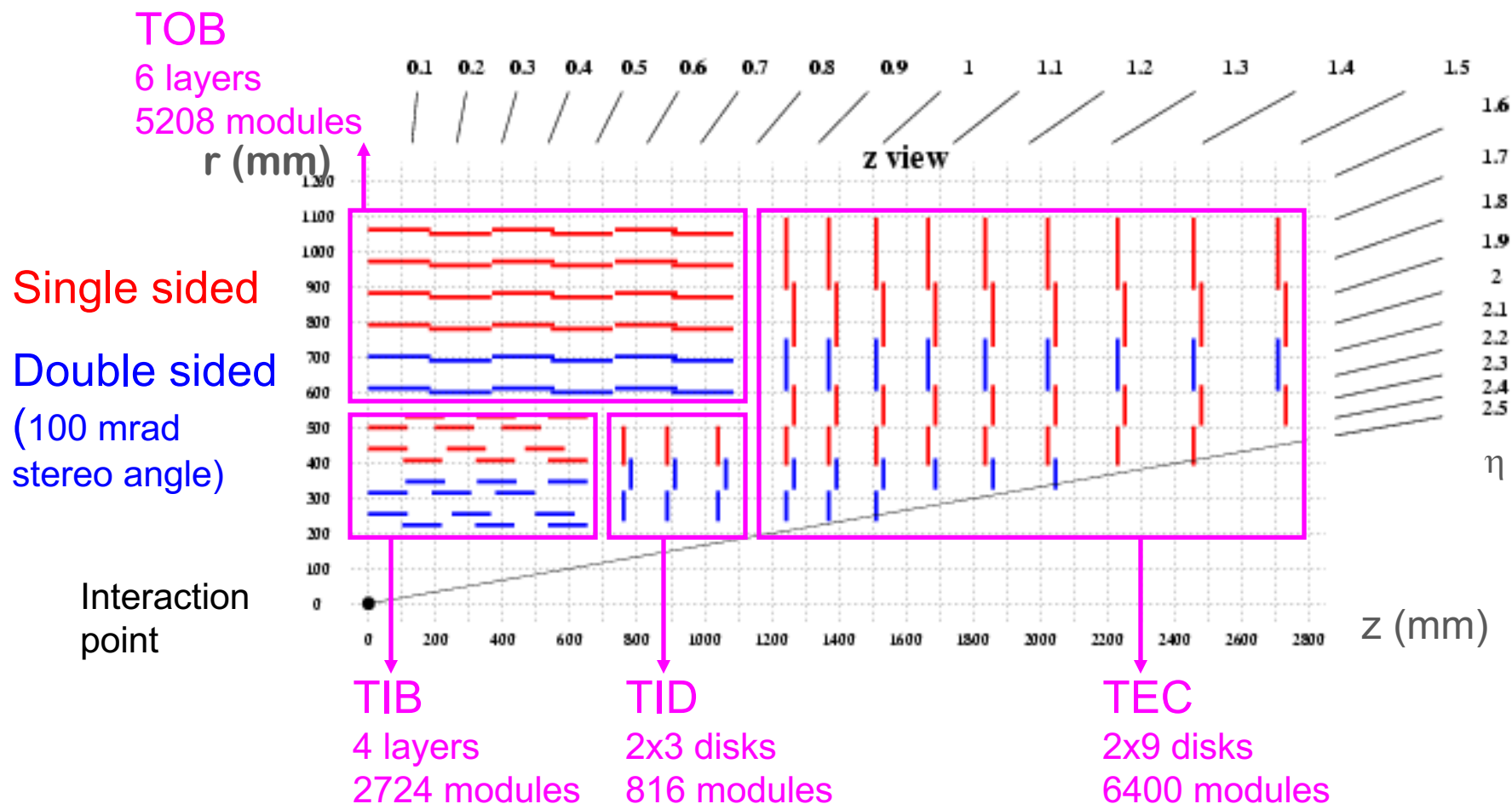
Installation of CMS Tracker



The CMS Inner Tracker



CMS Tracker layout



Barrel: strips parallel to beam
End cap: strips in radial direction

200 m² of silicon sensors

→ Industry involvement + 25 institutes

Complex Logistic & Quality Assurance

CMS Tracker: Some Numbers

Strip detector:

- ~200 m² of silicon sensors
- 24,244 single silicon sensors
- 15,148 modules
- 9,600,000 strips \equiv electronics channels
- 75,000 read out chips (APV25)
- 25,000,000 Wire bonds

Pixel detector:

- 1 m² detector area
- 1440 pixel modules
- 66 million pixels

Industrial type of production in many laboratories worldwide.

Largest Silicon detector built so far !

CMS Tracker Collaboration



55 institutes from 9 countries (Austria, Belgium, Finland,
France, Germany, Italy, Switzerland, UK, USA)

About 500 scientists and engineers involved in the design and construction
of the CMS inner tracker.

Tracker Outer Barrel (TOB)

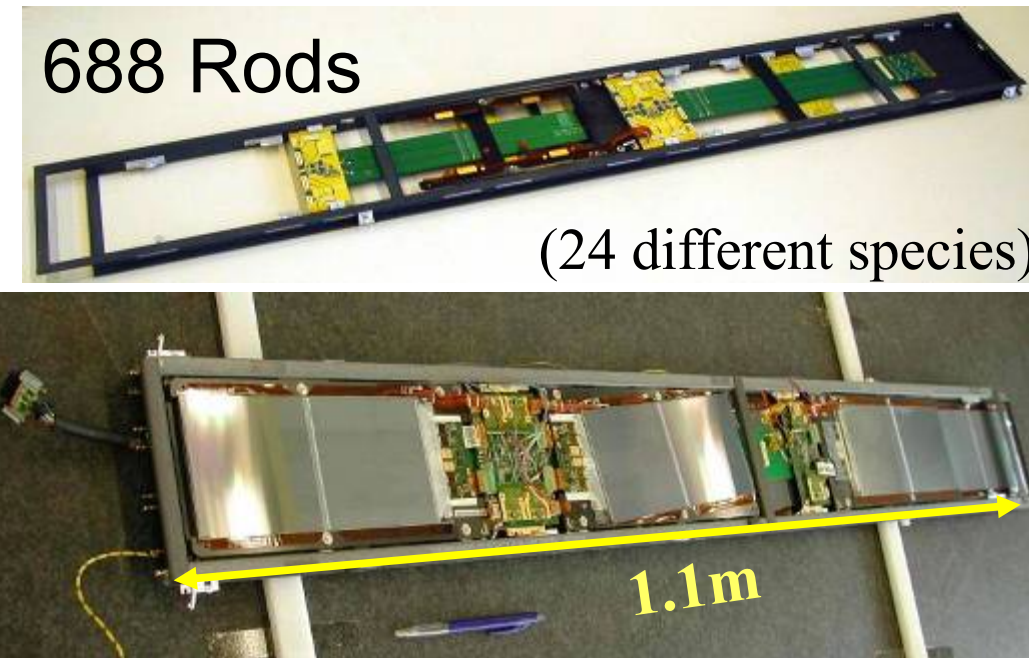
- Tracker Outer Barrel (TOB) mainly produced in US



Tracker Support Tube:

688 Rods

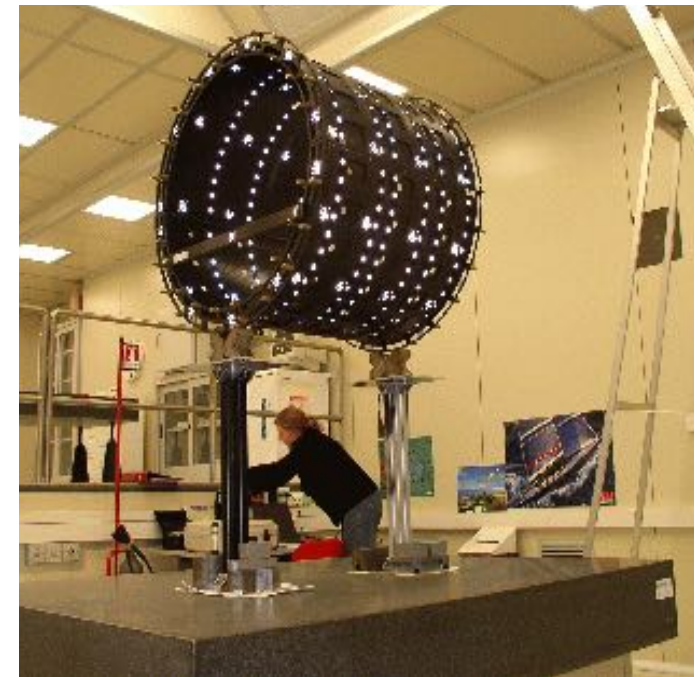
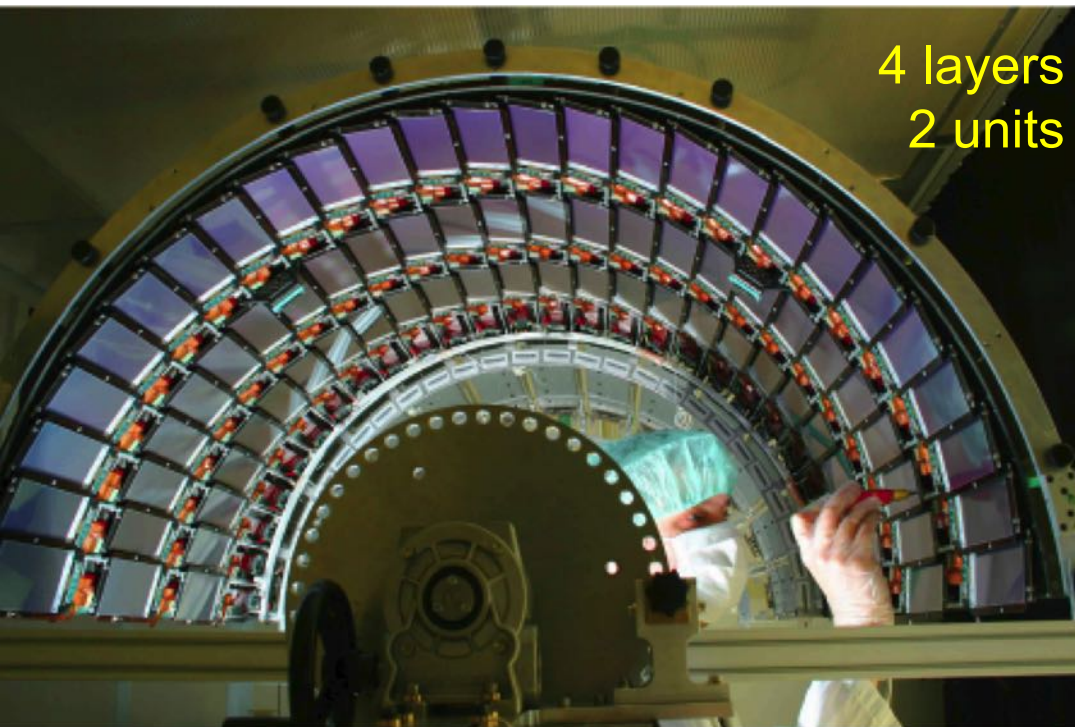
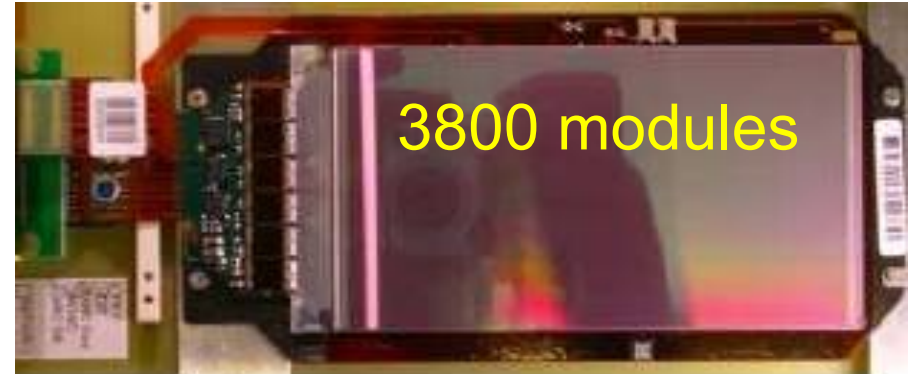
(24 different species)

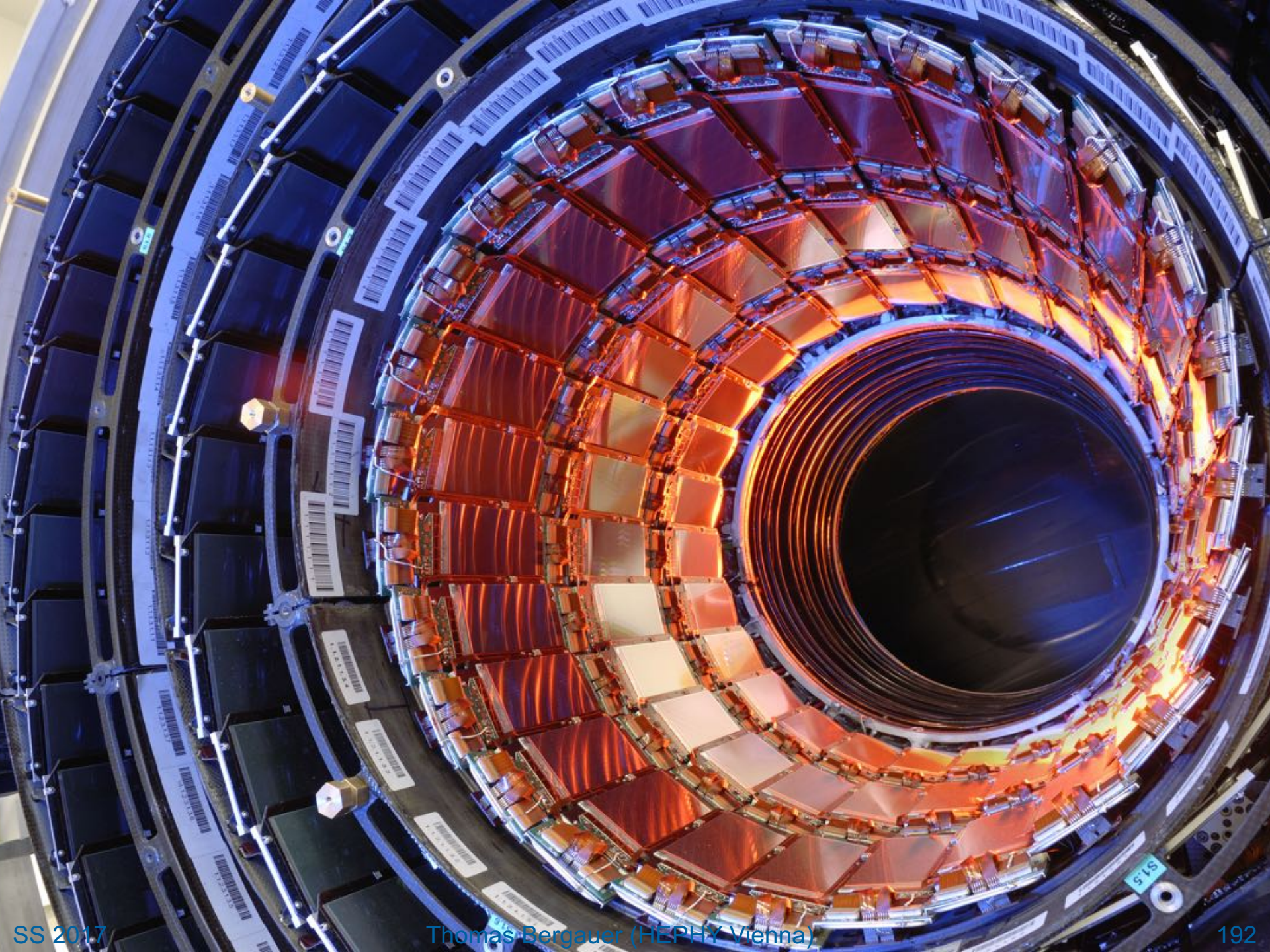


Tracker Inner Barrel (TIB)

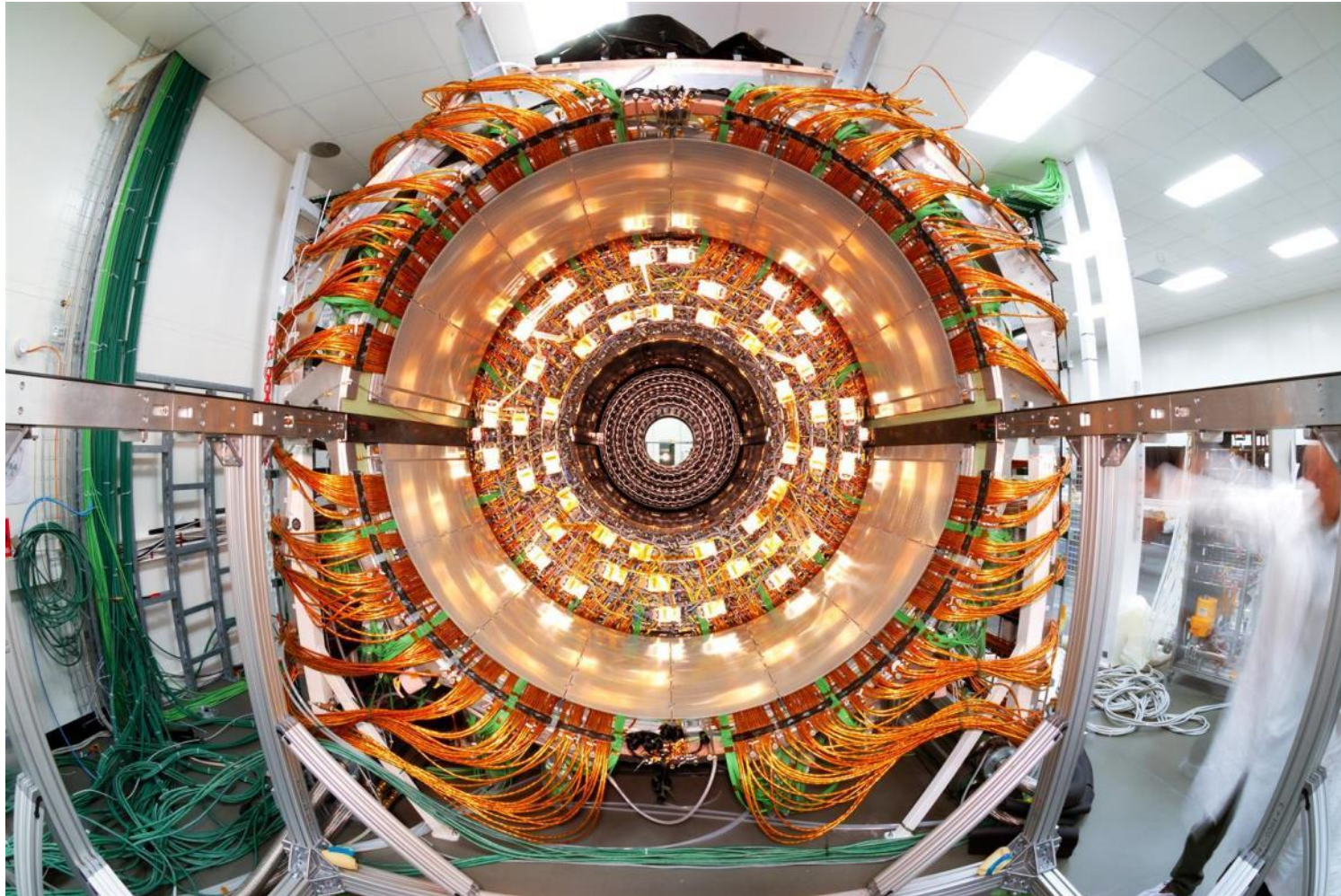
- TIB mainly produced in Italy

16 shells + 6 disks



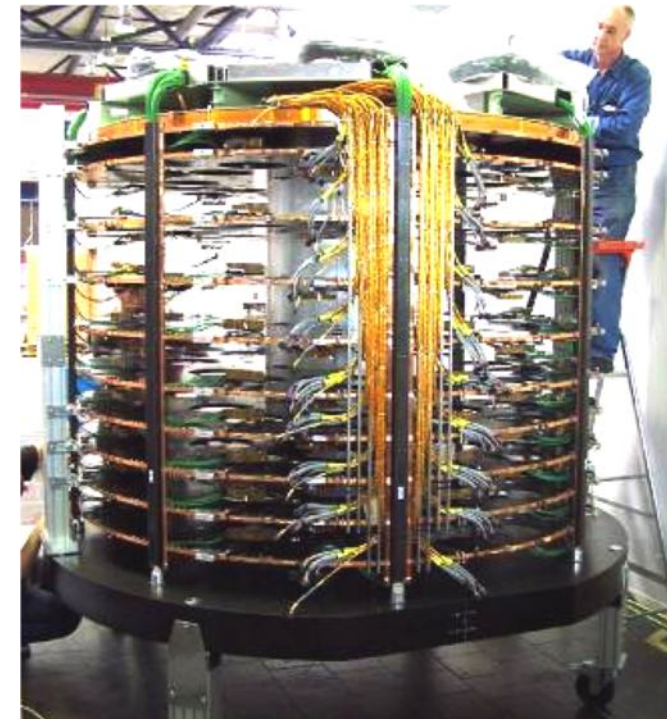
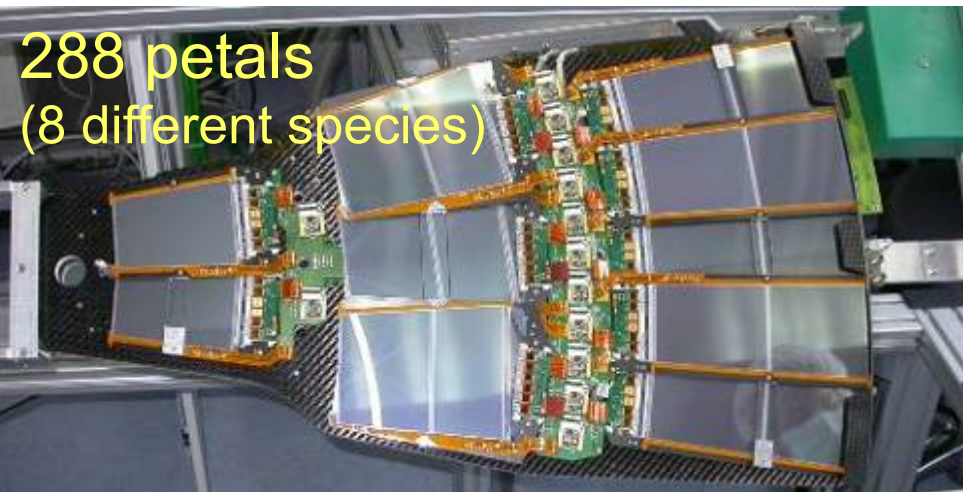
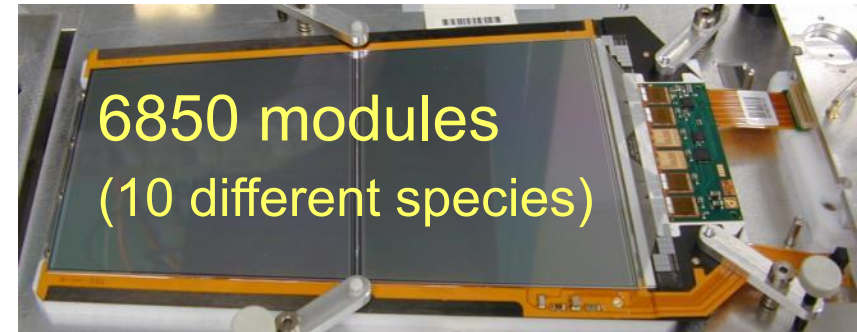


TOB plus TIB/TID



Tracker End Caps (TEC)

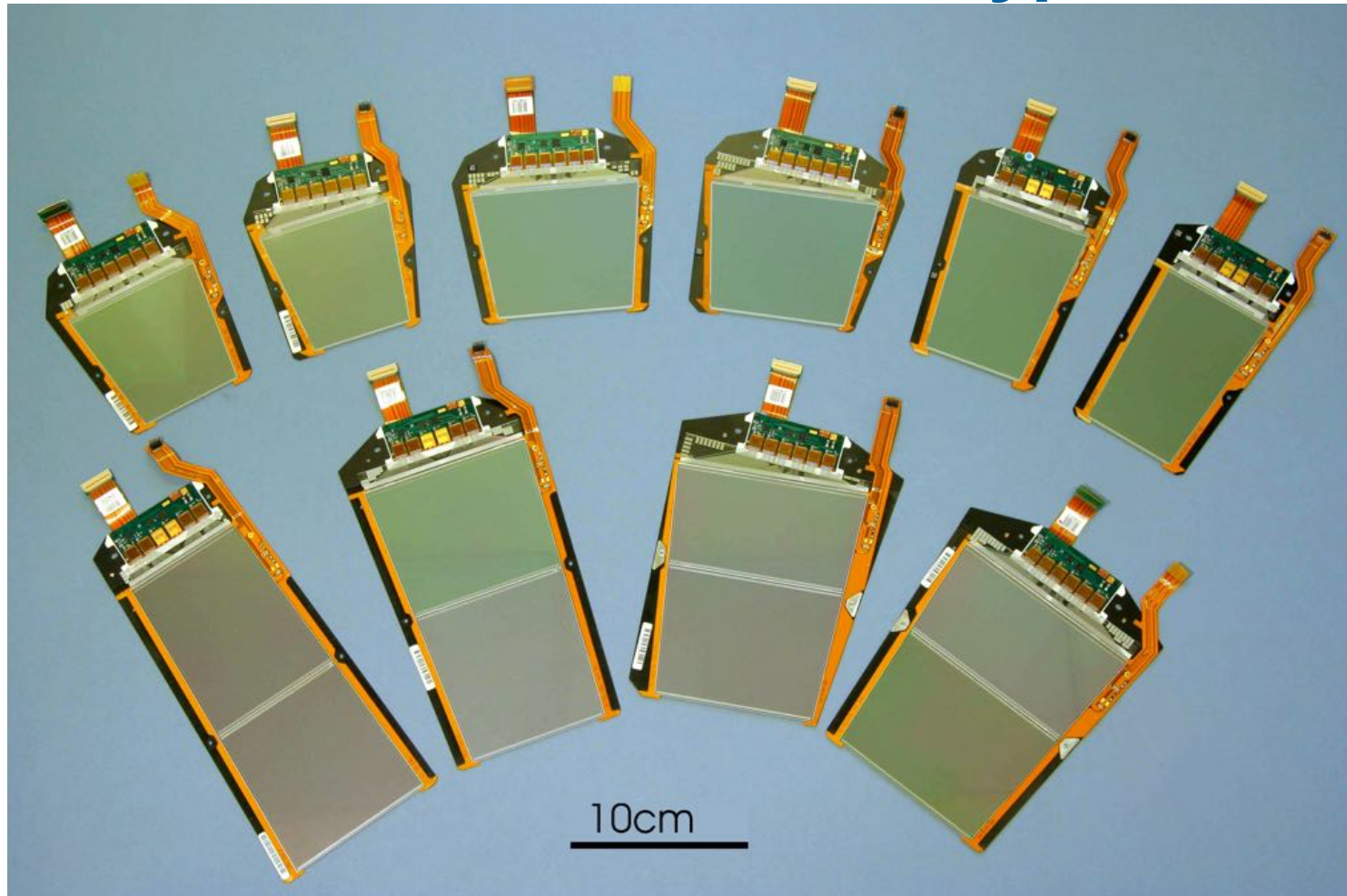
- TEC modules and petals mostly from Central Europe (Belgium, Germany, France, Austria)



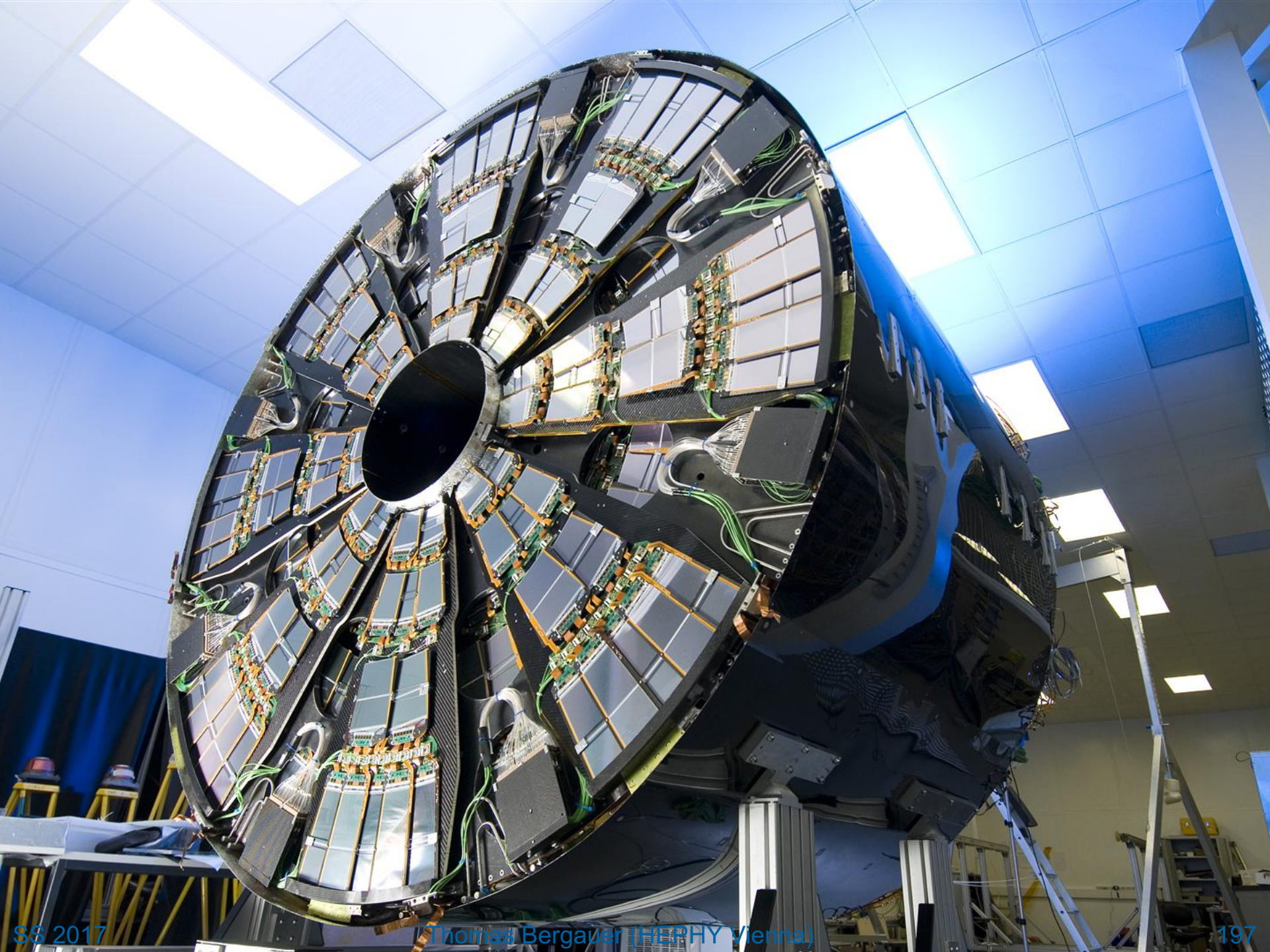
TEC Installation



CMS TEC Module Types



27 mechanical different modules + 2 types of alignment modules

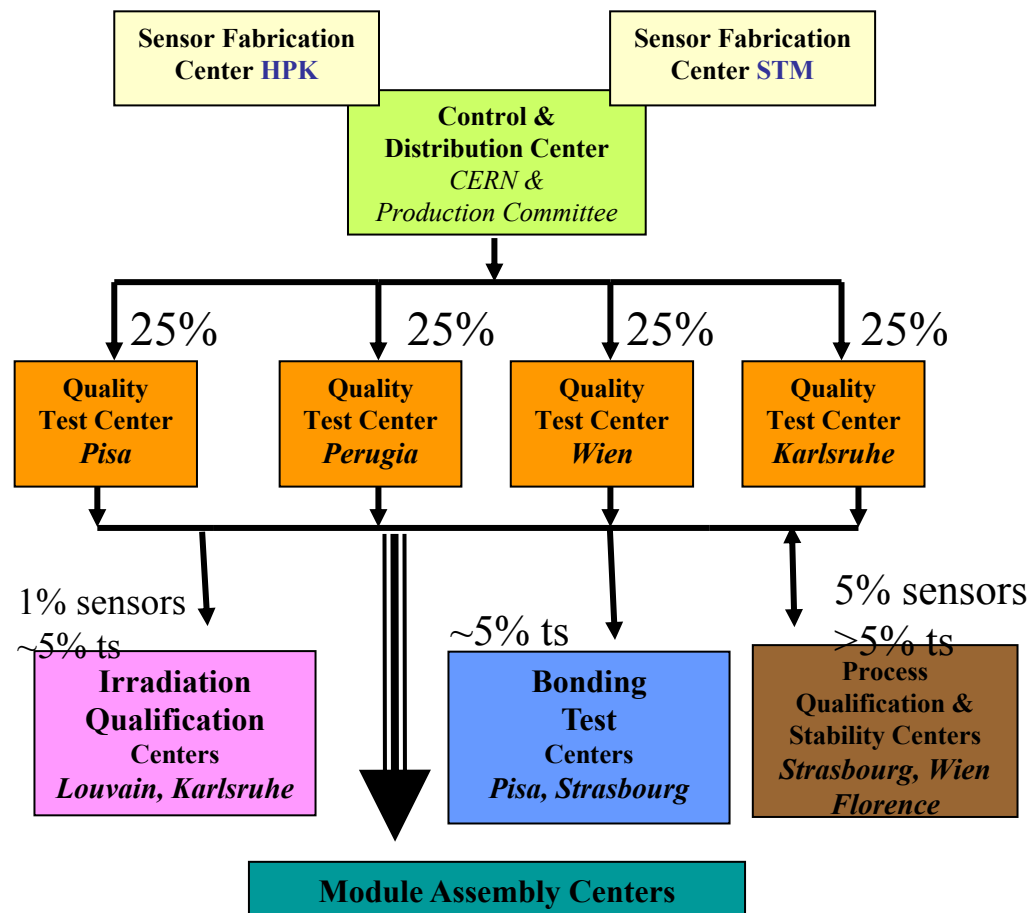


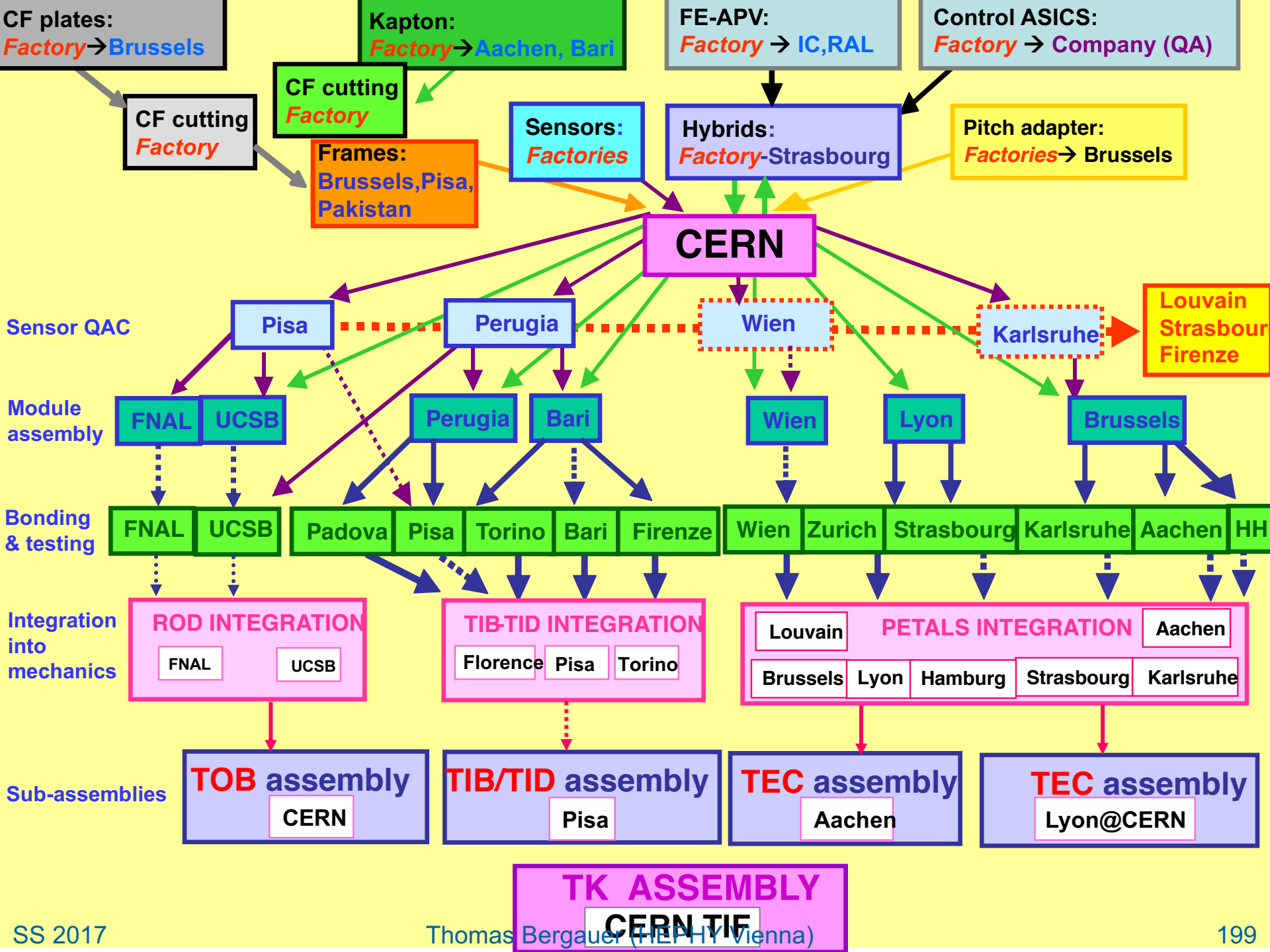
Silicon Sensors

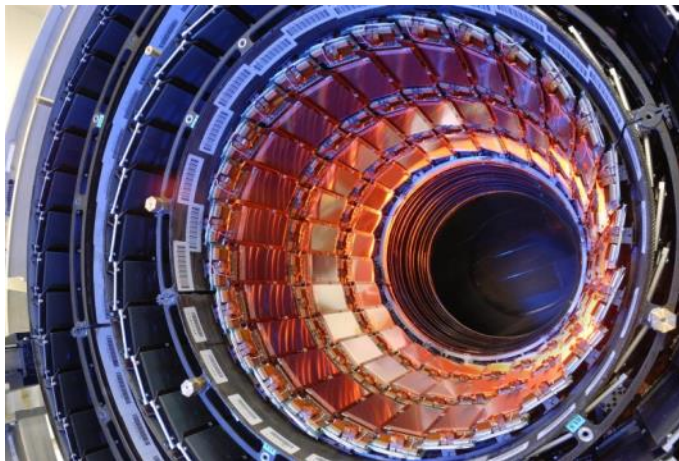
- Two producers:
 - Hamamatsu Photonics (Japan)
 - ST Microelectronics (Italy)
- Four main Test centers
 - Supported by smaller tests in different locations
 - Irradiation
 - Bonding tests
 - Process Qualification & Longterm stability



Complex logistics







CMS Upgrade

Phase I: Pixel upgrade

Phase II: Strip Tracker upgrade

Requirements for Phase II Upgrade

- Cope with 10x irradiation levels

Mostly a sensor issue

- Cope with increased track density per BX (by factor 10-20)

Increase granularity to keep occupancy within few %

Better done reducing strip length than reducing pitch: “strixel”, “stripsel”

- Reduce material budget (limitation today for CMS)

Minimize power density (within requirements)

Balance “optimization” vs “standardization”

Optimize n of layers (material vs robustness)

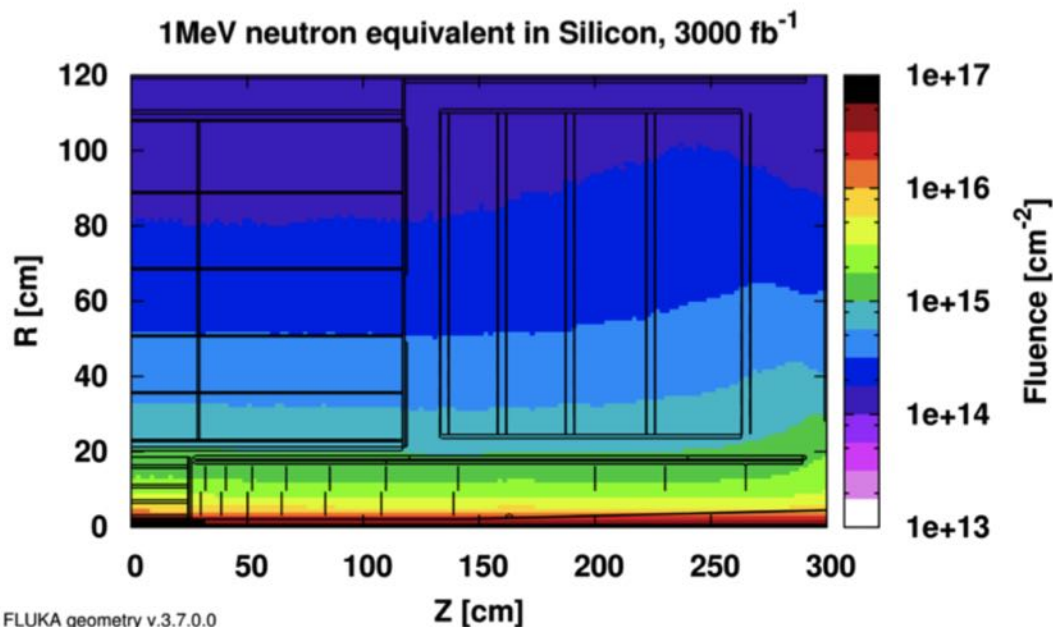
- Maintain CMS trigger performance (cope with 10x luminosity while keeping the output rate)

Provide information from tracker , in the whole rapidity range

Points (or “stubs”) from the tracker used to improve reconstruction or isolation criteria (good progress lately - encouraging results)

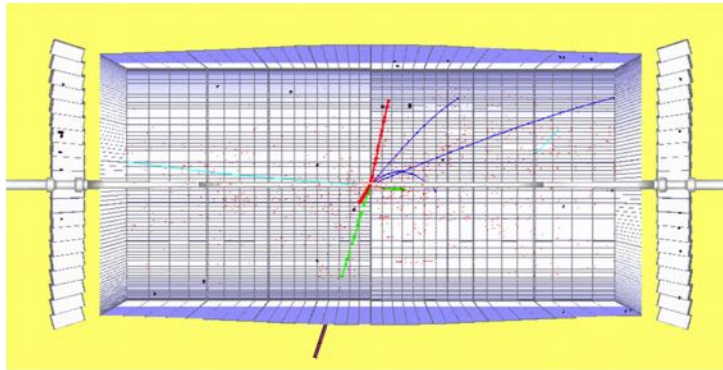
Irradiation Targets

radius	proton Φ_{eq} [cm^{-2}]	neutron Φ_{eq} [cm^{-2}]	total Φ_{eq} [cm^{-2}]
40 cm	$3 \cdot 10^{14}$	$4 \cdot 10^{14}$	$7 \cdot 10^{14}$
20 cm	$1 \cdot 10^{15}$	$5 \cdot 10^{14}$	$1.5 \cdot 10^{15}$

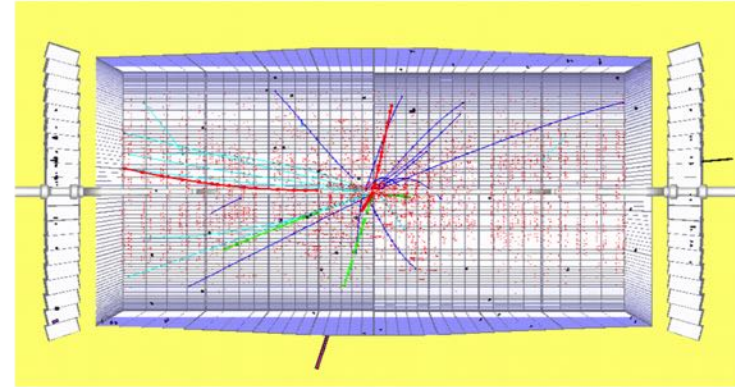


- Fluences target **20** and **40 cm radius** in the outer tracker after 3000 fb⁻¹
- Highest fluence for innermost layers of the outer tracker at **$1.5 \times 10^{15} \text{ n}_{eq} \text{ cm}^{-2}$**

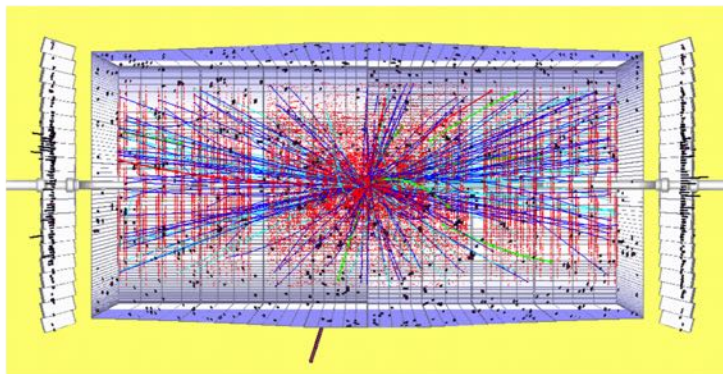
Track density at high Luminosity



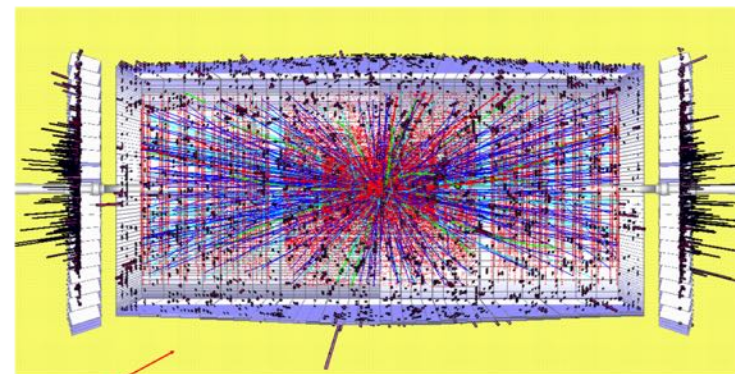
one month: 10^{32}



one year: 10^{33}



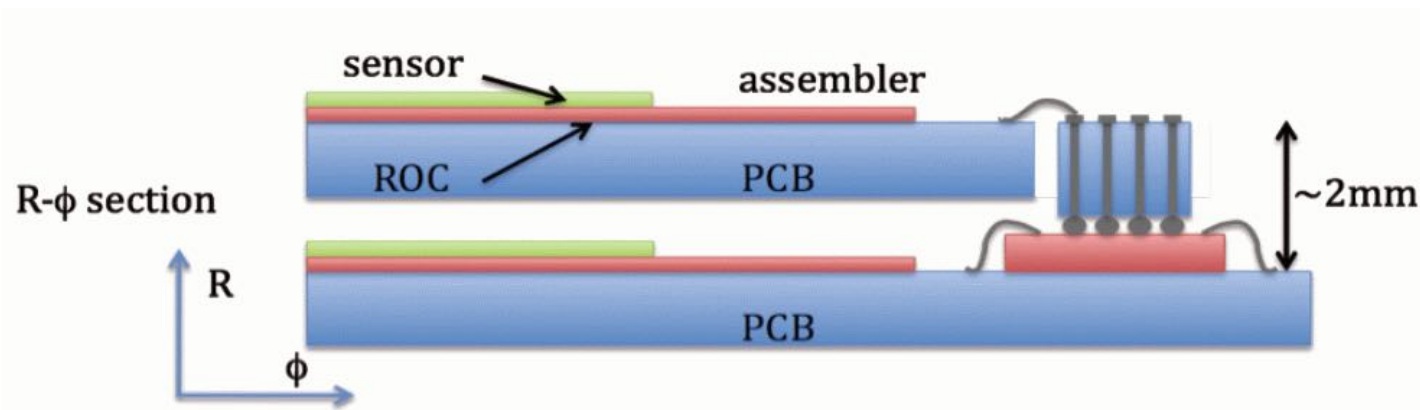
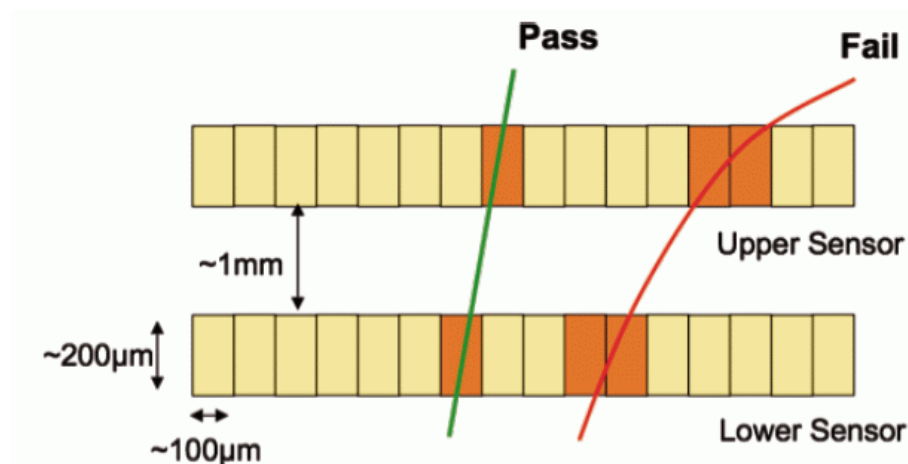
nominal L: 10^{34}



SLHC: 10^{35} => Higher granularity needed

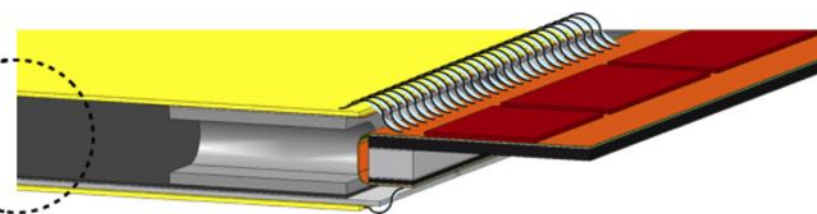
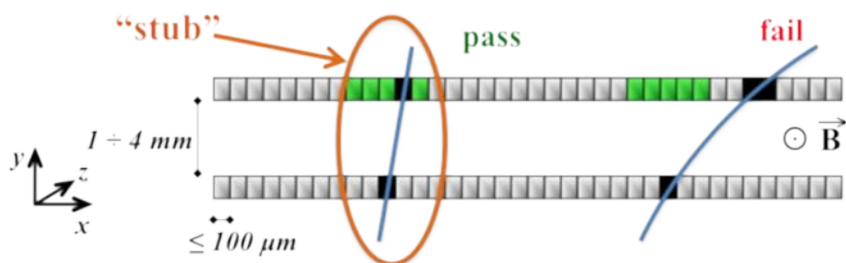
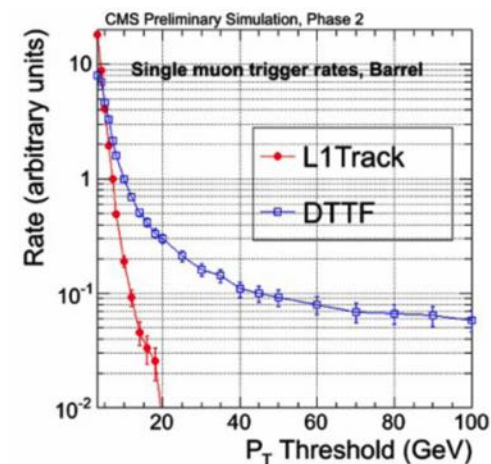
Tracker Trigger (“P_t module”)

- Higgs golden channel: $H \rightarrow ZZ \rightarrow 4\mu$
- Low momentum tracks: not interesting
- High momentum tracks: interesting \rightarrow trigger condition
- Try to deduce particle momentum from track curvature directly in the Tracker

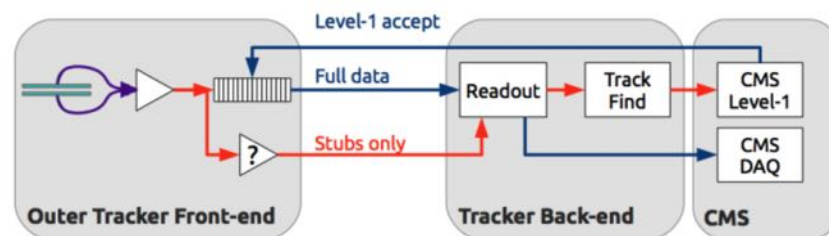


p_T -Module Concept

- Myon and calorimeter-based triggers will not be able to stand the rates due to PU and limited resolution
- Myons: no p_T threshold can limit the rate
 - due to strong magnetic field in the tracker high- p_T tracks can be discriminated

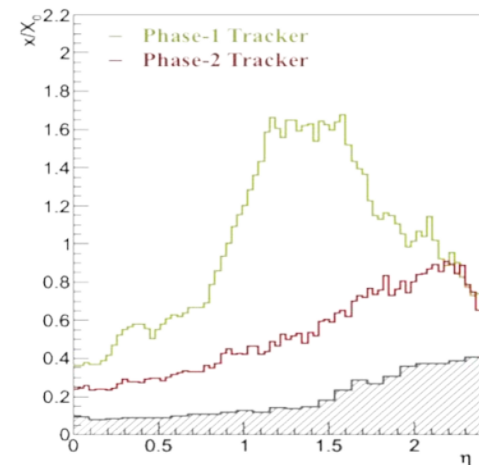
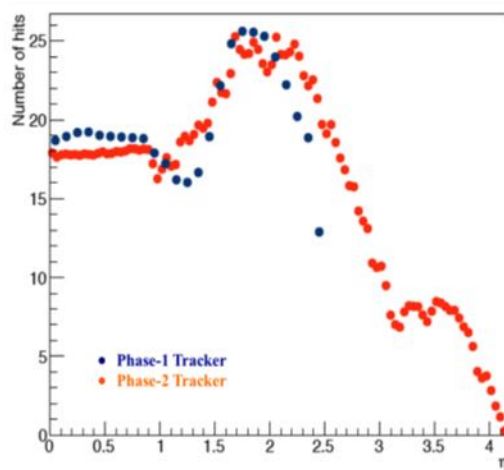
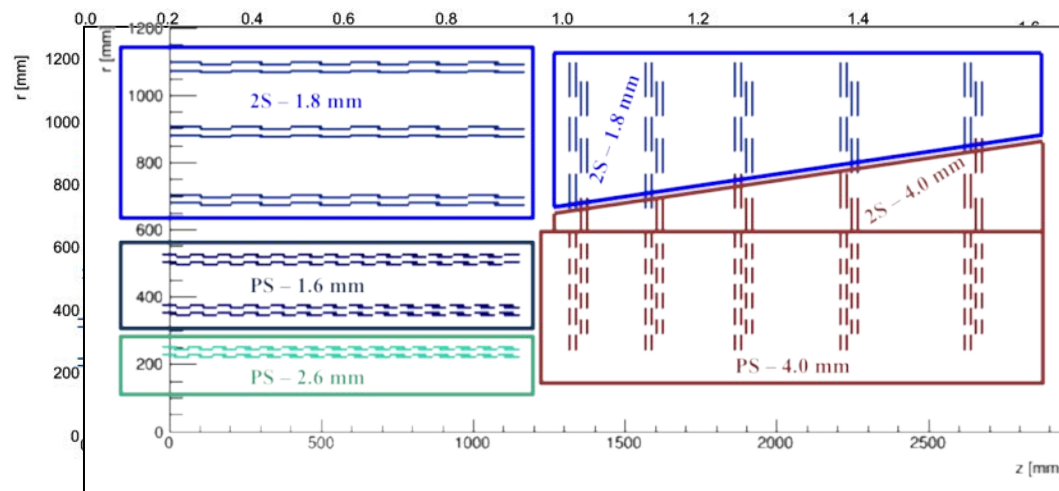


- Stubs will be processed in the back end to build L1A



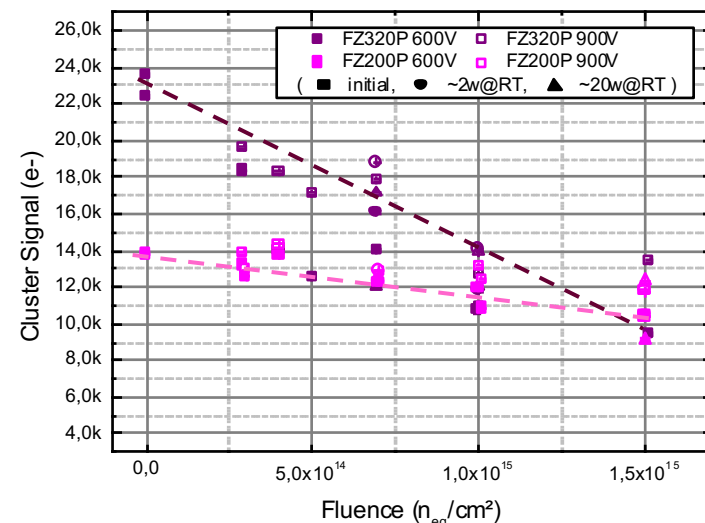
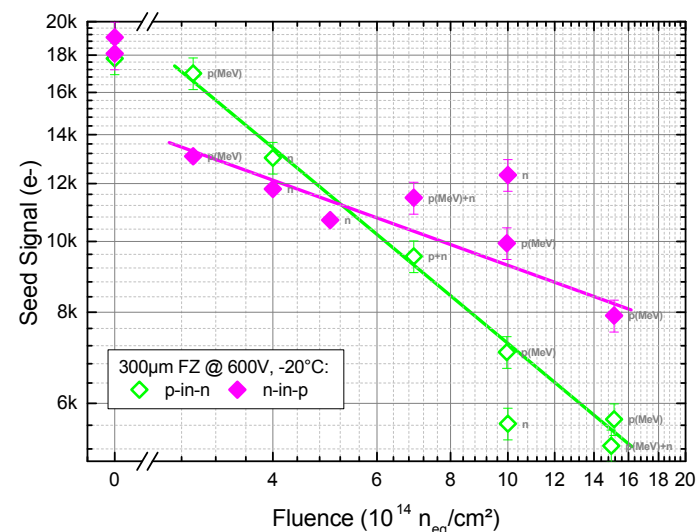
Tracker Layout Baseline

- **2 module types only**, both for barrel and end caps
 - **Pixel-Strip-(PS)-module** ($r < 60$ cm)
 - **2 Strip (2S) modules** ($r > 60$ cm)
- Sensor spacing optimised with 2 (2S) or 3 (PS) groups
- Similar number of hits vs. η
 - Extending coverage to $|\eta| < 4$
- Lower material budget than existing tracker due to
 - CO₂ cooling
 - DC/DC powering
 - No dedicated control electronics



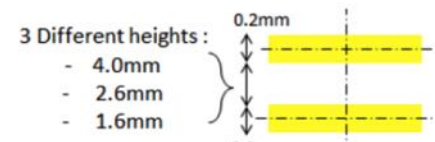
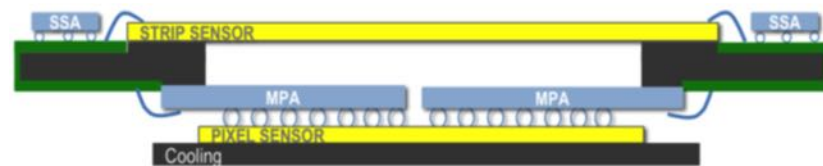
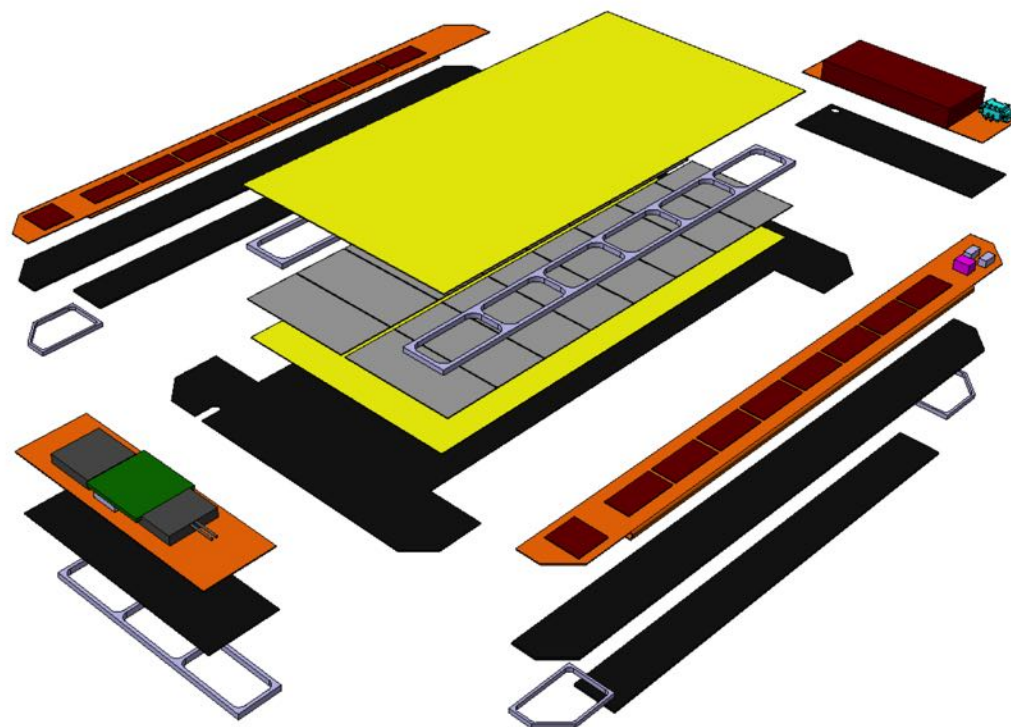
Collected Charge

- N-type sensors (hole collection) show higher signal degradation than p-type
- Beyond $\sim 10^{15} n_{eq} cm^{-2}$ 200 μm of active silicon show a similar signal to 300 μm



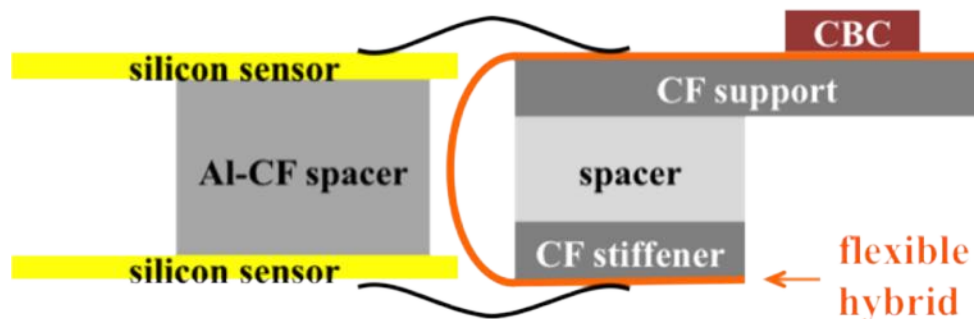
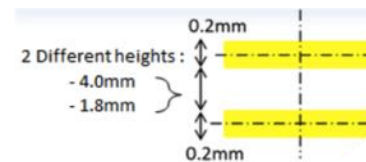
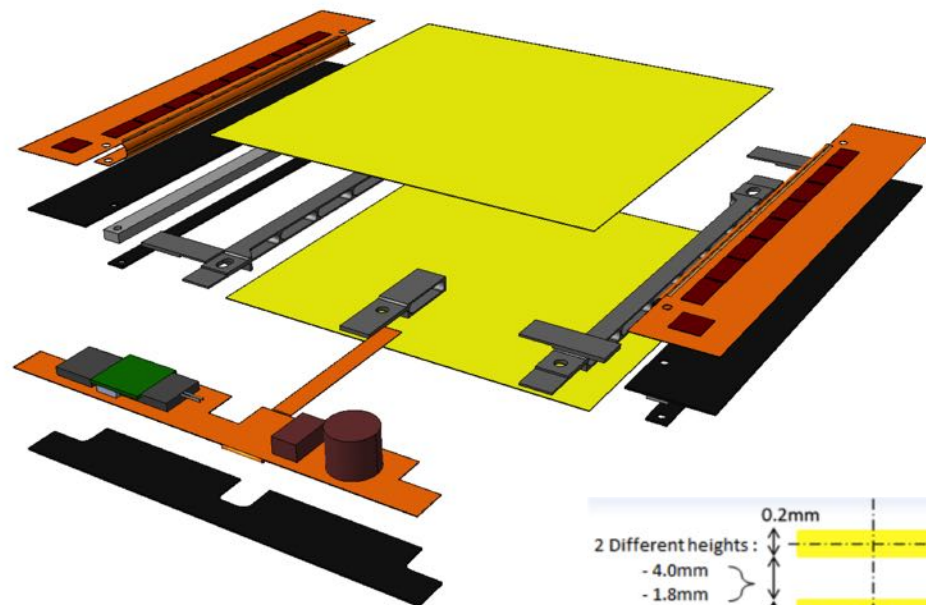
PS Module

- 5 x 10 cm² hybrid module consisting of
 - **one strip sensor (PS-s)** ; 2 x 960 strips of 25mm at p=100µm
 - **one pixelated layer** of 32 x 960 pixels with 1446µm and p=100µm consisting of PS-p sensor with bump-bonded chips
- Readout:
 - Strips: 2x8 **Short Strip ASIC (SSA)**,
 - Pixels read out by 16 **MacroPixel ASIC: MPA**
 - SSA processes strip sensor signals at BX frequency
 - MPA processes signals from each pixel and correlates hits from pixel sensor with data received from SSA and
 - builds stubs ($p_T > 2\text{GeV}/c$)



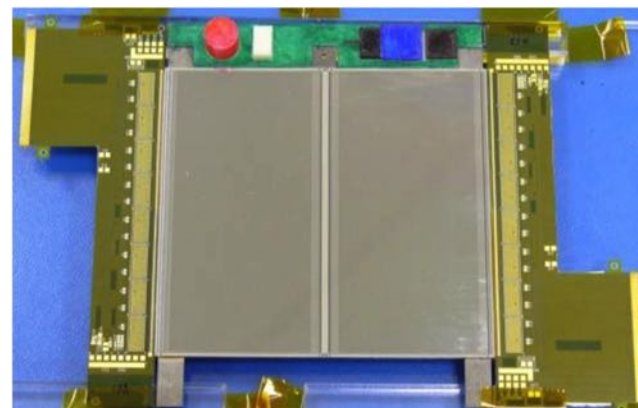
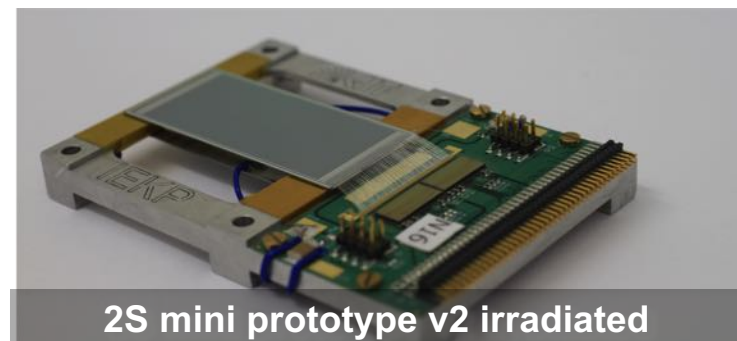
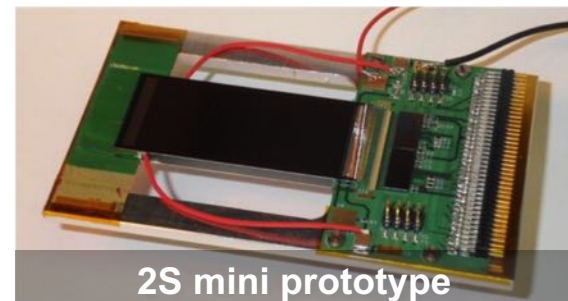
2S Module

- **2 x Strip sensors: 2S sensor**
 - Size: 10 x 10 cm²
 - Pitch: 90 μm
 - Strip length: 5 cm
 - No. of strips per sensor: 2x1016
- **2 x 8 CMS Binary Chips: CBC**
 - 2x127 channels per chip
 - Bump bonded to flexible hybrid
 - Connects to top and bottom sensors
 - Interchip communication via hybrid
- **Concentrator ASIC: CIC**
 - collects data from 8 CBCs (half module)
- **Service Hybrid:**
 - Low Power Gigabit Transceiver
 - 2-stage DC/DC powering

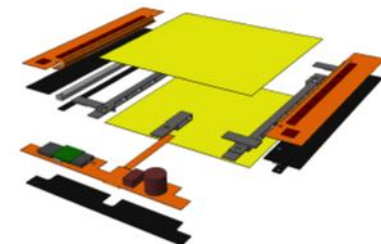


2S prototype modules

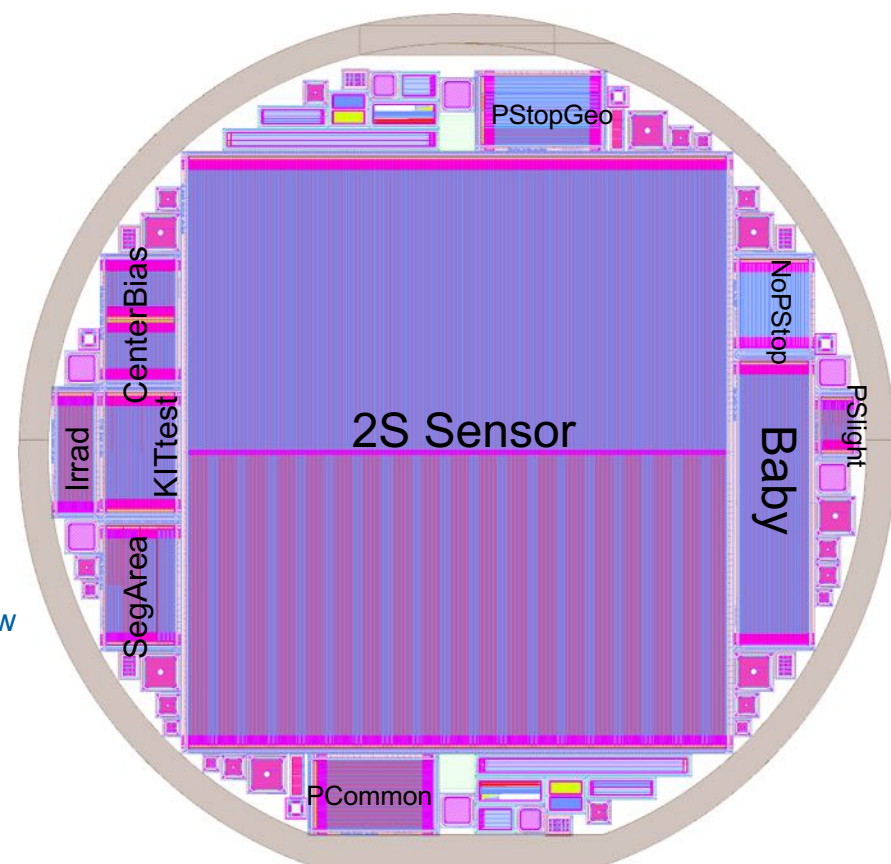
- First mini 2S prototype modules were built in 2013
 - Two $5 \times 2.3 \text{ cm}^2$ sensors with 256 strips from Infineon or CNM
 - 2 x CBC2 readout chips bumped to hybrid
- Beam test at DESY in 2013 and SPS in 2015 (with irradiated modules)
 - Demonstrate stub finding efficiency
 - Show performance of irradiated module
- Full-scale dummy modules built for assembly studies
 - Prototype readout hybrids without chip
 - Inactive dummy sensors



Baseline Design 2S Sensor



- **Wafer**
 - Wafer diameter (6" wafer): **150 mm**
 - Forbidden margin 5 mm -> **140 mm usable**
- **2S Sensor Layout**
 - Strips: **2032** (2 x 8 x 127)
 - Strip Pitch: **90 μmm**, Width/Pitch: ~ **0.25**
- **2S Sensor size**
 - Sensor width: **94.183 mm**
 - Sensor length: **102.7 mm**
- **And more ...**
 - Test sensors to evaluate design options
 - Test structures (Diodes, MOS, Sheet, Van-der-Pauw Cross-Bridge-Kelvin-Resistors, etc ...)
- Ordered from both, HPK and Infineon



2S Sensor (8" version)

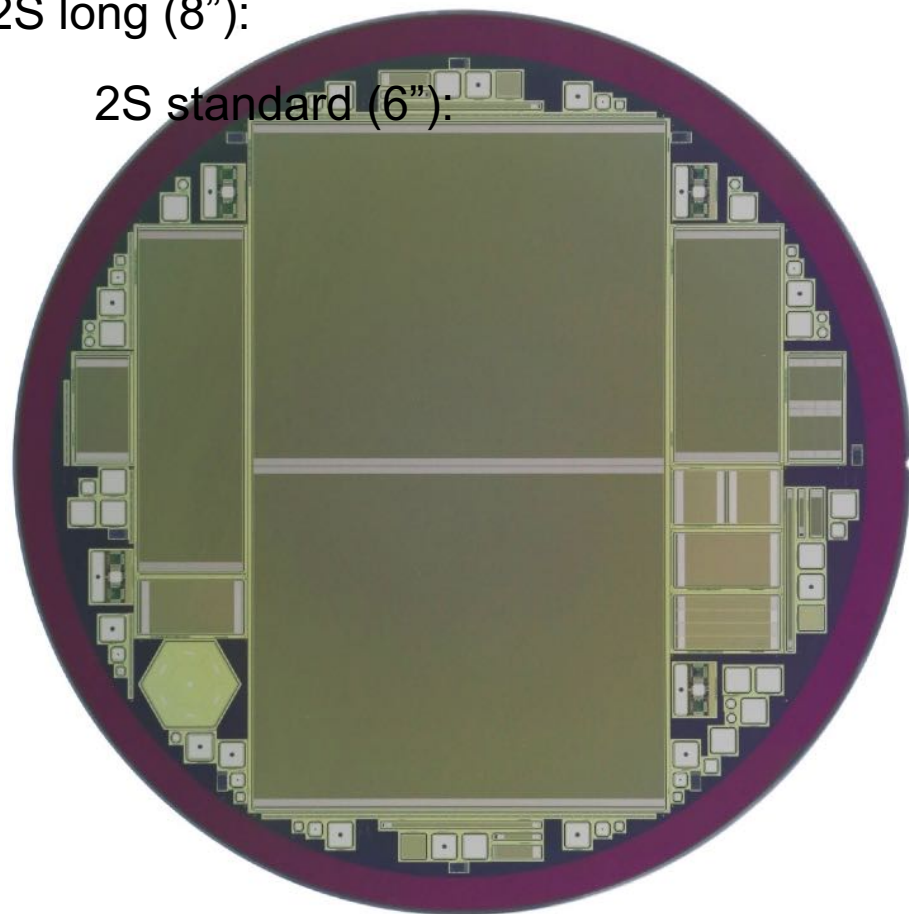
- Wafer:
 - Wafer diameter (8" wafer): **200 mm**
 - Resistivity $\sim 7 \text{ k}\Omega\text{cm}$, n-on-p float zone, orientation $\langle 100 \rangle$
 - **200 μm physical thickness** $\rightarrow V_{fd} \sim 60\text{V}$

- Main Sensor
 - Same as the 6" version but elongated
 - Size: **94.183 x 153.4 mm²**

- Split groups for first batch (25 pcs)
 - P-stop / p-spray
 - implant/p-stop depth and concentration
 - Different R_poly doping

2S long (8"):

2S standard (6"):



First batch produced without any losses at Infineon and is now in Vienna for electrical tests since two weeks!

Silicon Detectors in High Energy Physics

DETECTOR CHARACTERIZATION

Characterization of strip detectors

- Introduction
- Measurement techniques
 - Electrically
 - Optically
 - Mechanically
- Construction of Detector Modules
 - Wire Bonding
- Beam Tests
 - Active operation with particles
 - Beam telescope

What is Quality control?

- Characterize devices
 - **Electrically:** currents, capacitances
 - **Mechanically:** bondability, sag, bow
 - **Optically:** dust, dirt, lithography issues, dimensions if they comply to the specifications
- Define acceptance criteria
 - E.g. CMS: number of non-working strips $< 1\%$
 - non-working strips to be excluded from being used
- What means “not working”?
 - Outside parameter range (e.g. $200\text{pF} < C_{ac} < 220\text{pF}$)

Electrical parameters



- Typical Setup at HEPHY Vienna
 - Light-tight box
 - Instruments
 - Computer running NI Labview

Mechanical parameters

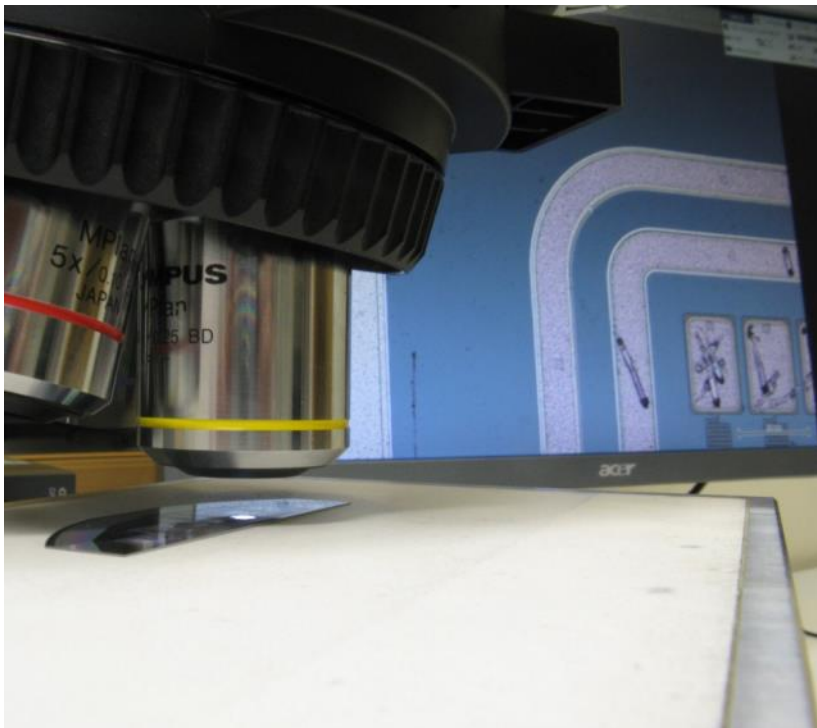
- Measurement of
 - Sag
 - Bow
 - ThicknessUsing 3D mechanical measurement system
- Coordinate measurement machine (CMM)



Optical measurements

Optical microscopy

Olympus BX60+DP21



HEPHY cleanroom

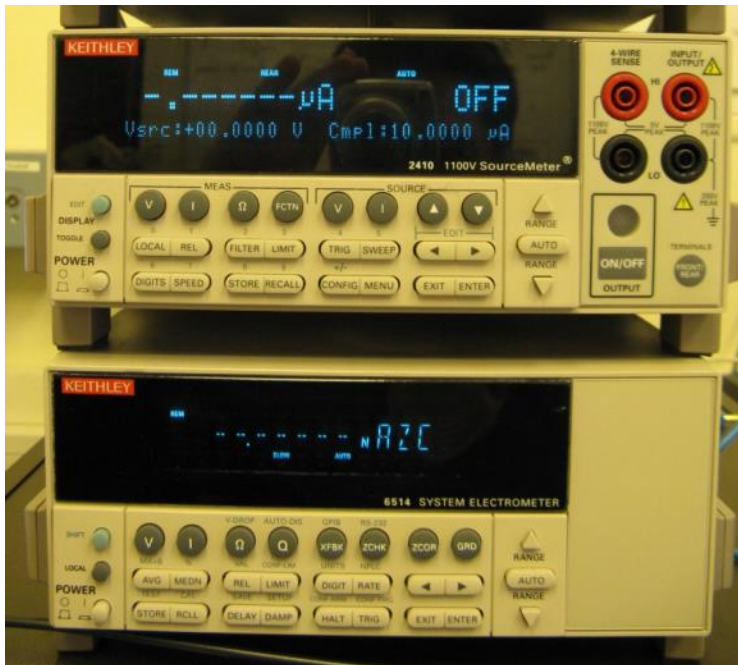
Electron microscopy

FEI Quanta 200 FEG SEM



USTEM Vienna UT

Instruments for electrical measurements



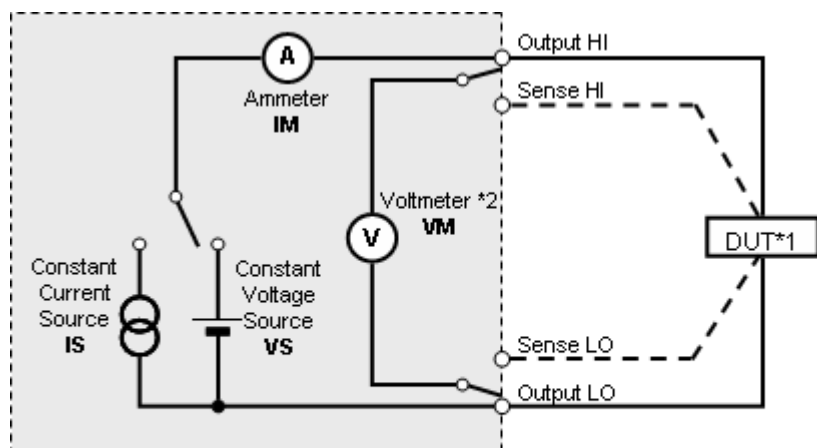
- Electrometer (precise Amp-meter)
- LCR Meter
- Source Measure Unit (SMU)

What is a Source Measure Unit?

- Source
 - Voltage source
 - Constant current source
 - Amp-meter
 - Volt-meter
- in one device



Keithley 237

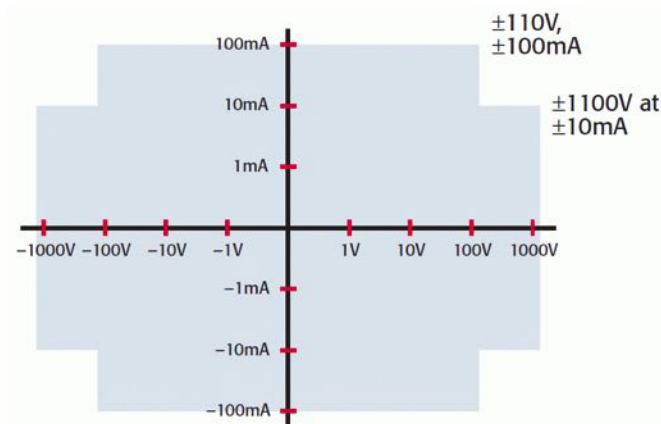


GS610 construction

--- four-wire system

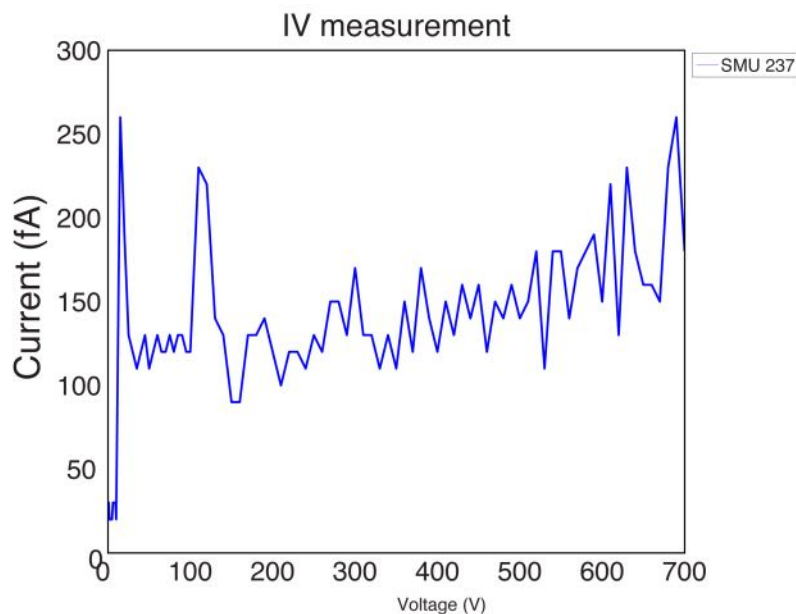
*1 DUT : Device Under the Test

*2 For DUT voltage measurement



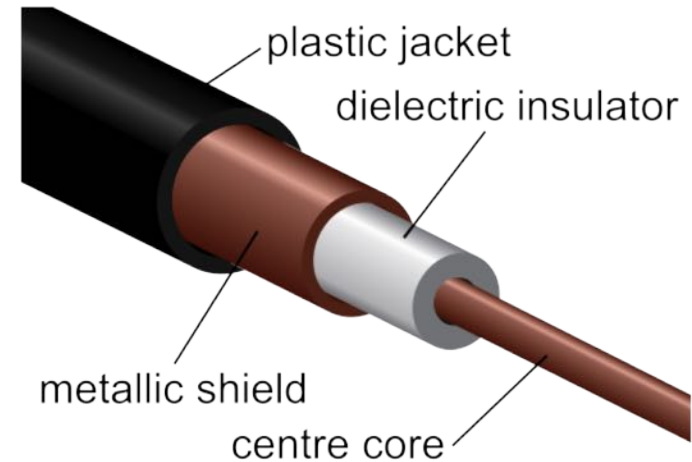
What is a Source Measure Unit? (cont.)

- High precision Amp-meter
- K237: 250fA at 700V
- High precision needs Triax connectors



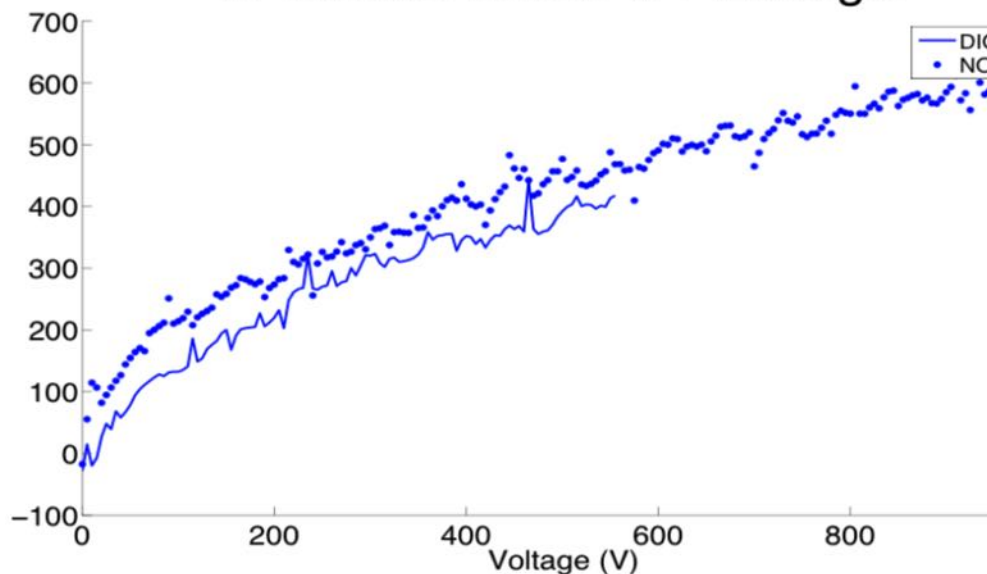
Low noise measurements (2)

- Shielded cables necessary for whole conduction path
- Coax often sufficient
- For extreme sensitive measurements (e.g. pA):
 - Triax cables necessary

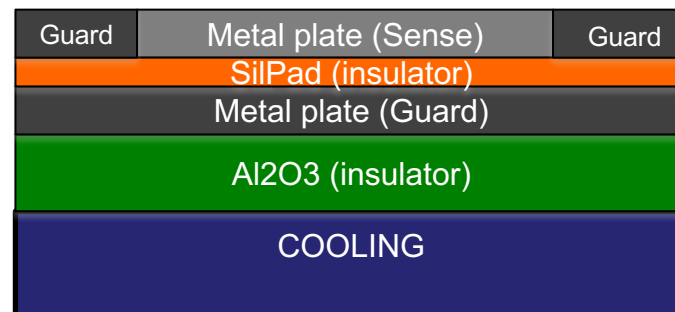
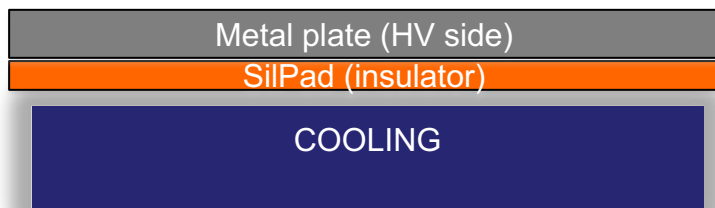
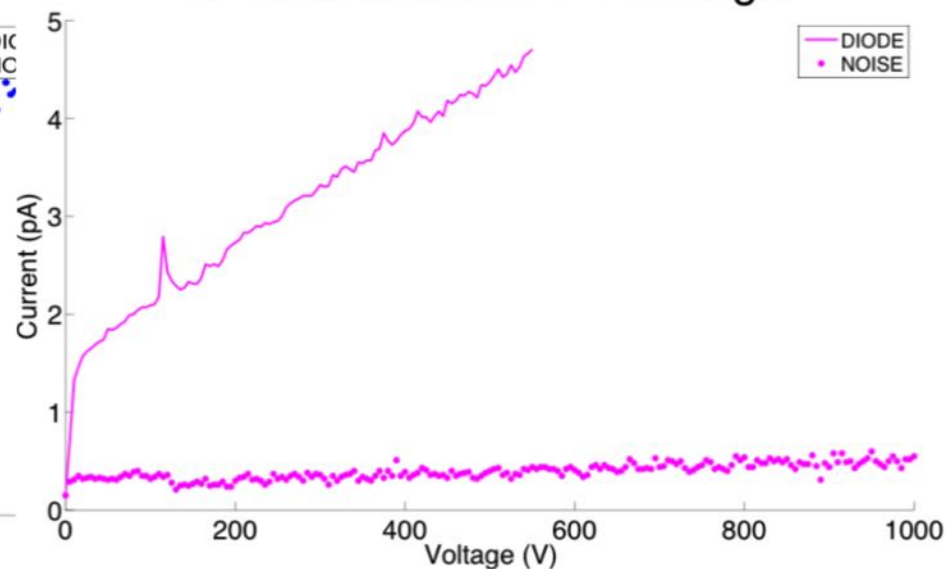


Low noise measurements

IV measurement $T = -20\text{degC}$

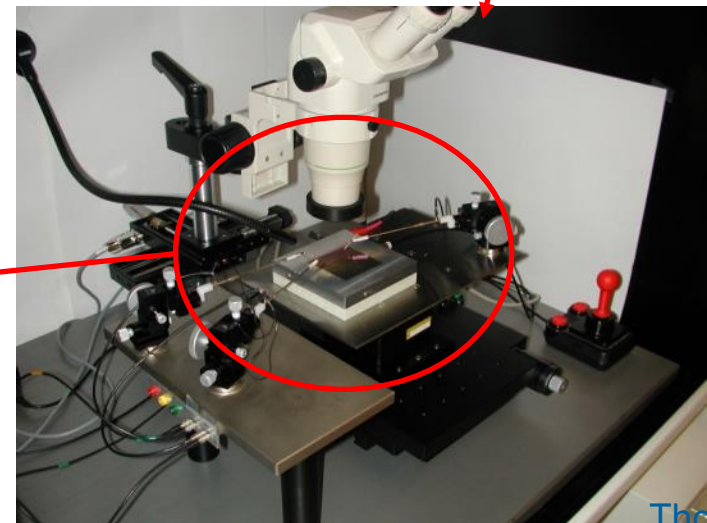
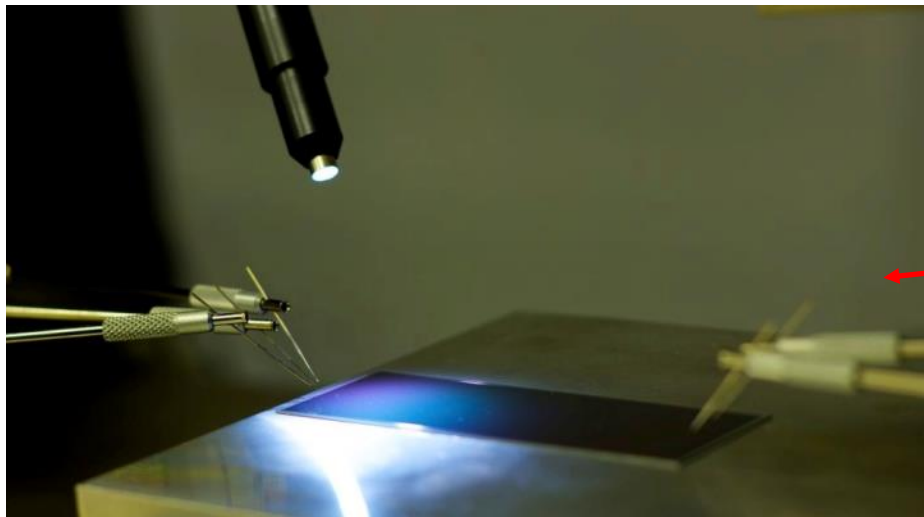


IV measurement $T = -20\text{degC}$



Strip-by-strip Test Setup

- Sensor in Light-tight Box
- Vacuum support jig is carrying the sensor
 - Mounted on movable table in X, Y and Z
- Needles to contact different structures on sensor
- What do we test?
 - Electrical parameters
 - strip failures

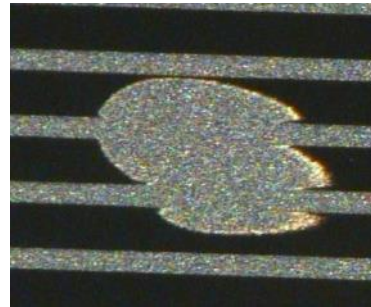


Common strip failures

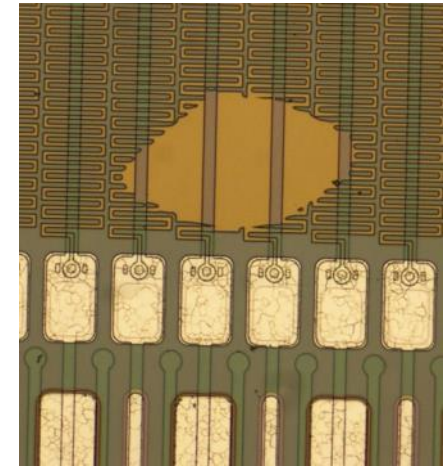
Open Strip:



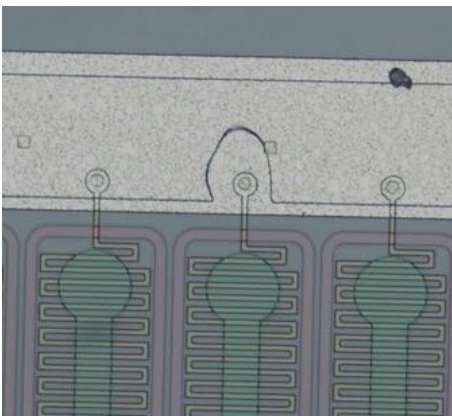
Shorted Strip:



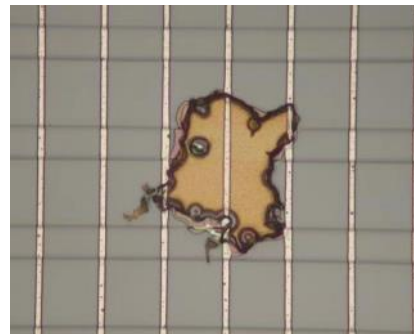
Open bias resistor:



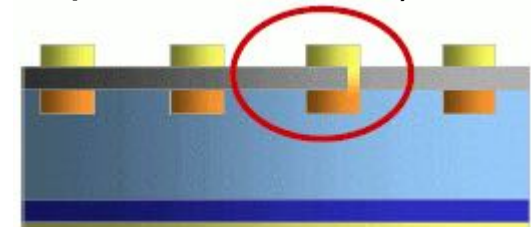
Open implant at via:



Open implant:

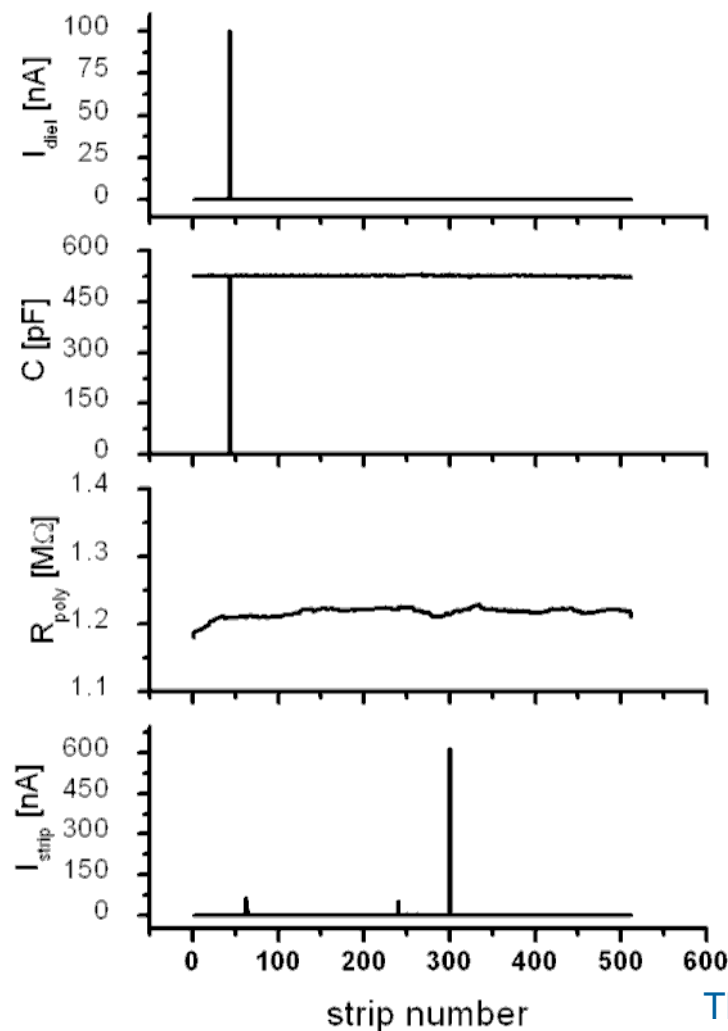
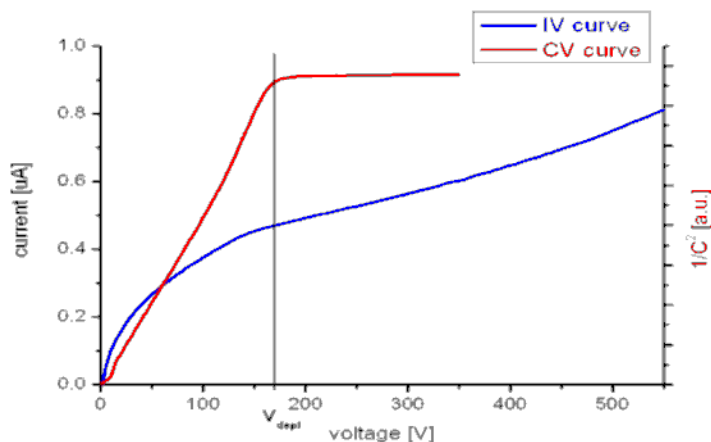


“Pinhole” (short between
implant and metal):

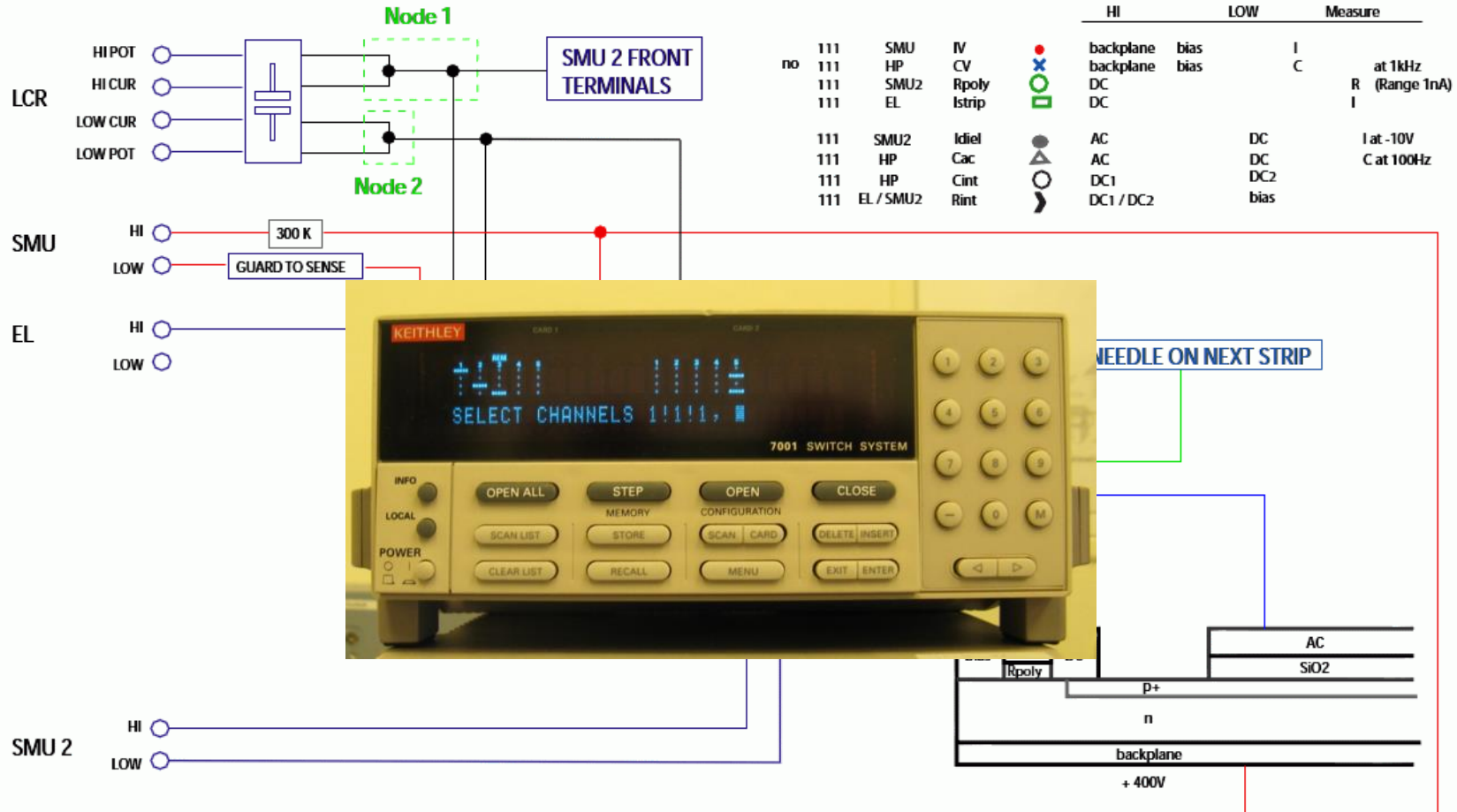


What do we test?

- Global parameters:
 - **IV-Curve:** Dark current, Breakthrough
 - **CV-Curve:** Depletion voltage, Total Capacitance
- Strip Parameters e.g.
 - strip leakage current I_{strip}
 - poly-silicon resistor R_{poly}
 - coupling capacitance C_{ac}
 - dielectric current I_{diel}



Switching Scheme



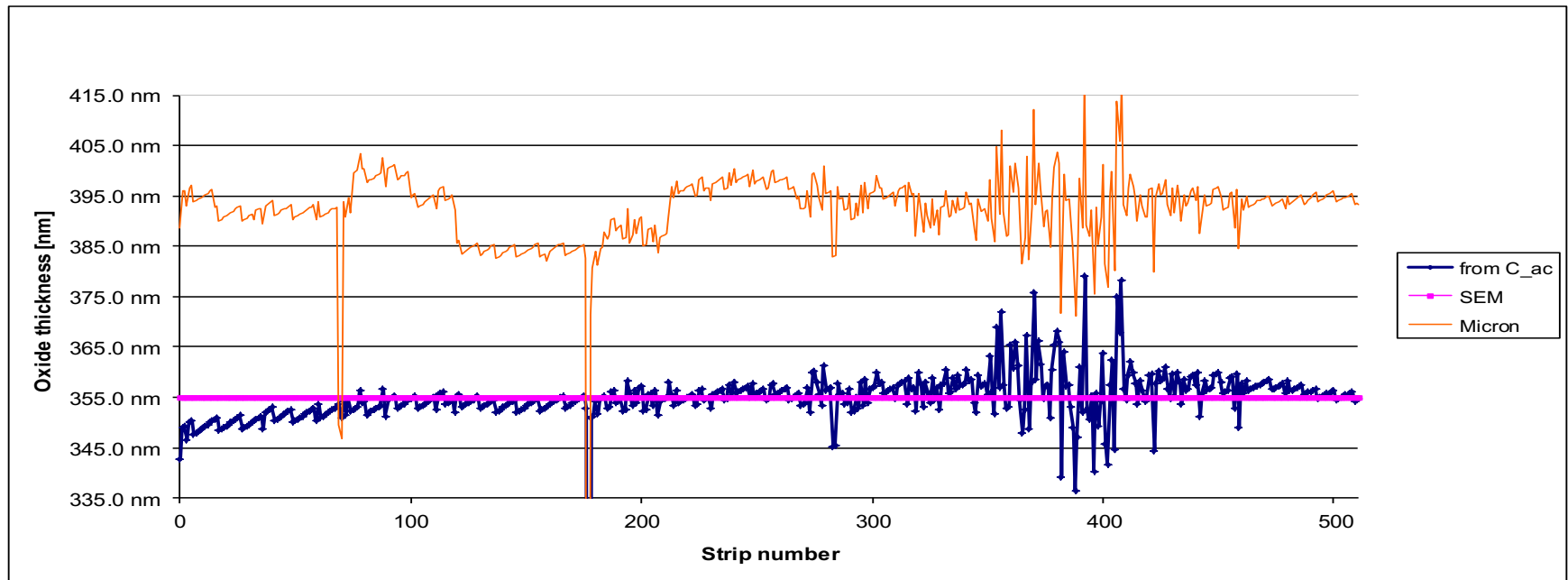
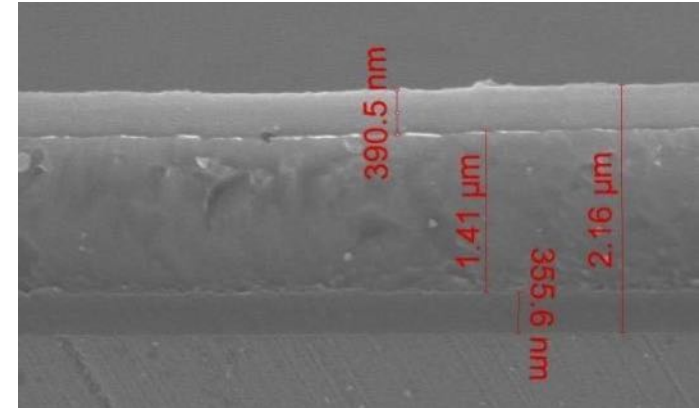
Measurement validation

Direct measurement of oxide thickness by electron microscopy

SEM result: 355nm

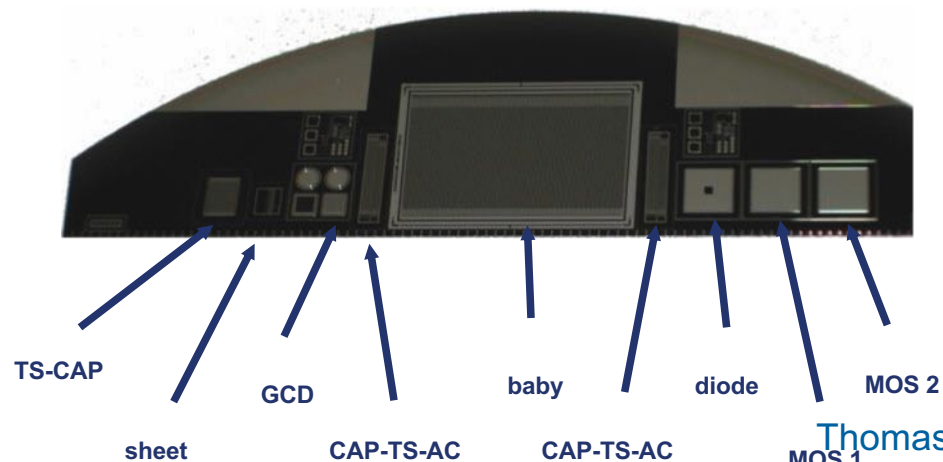
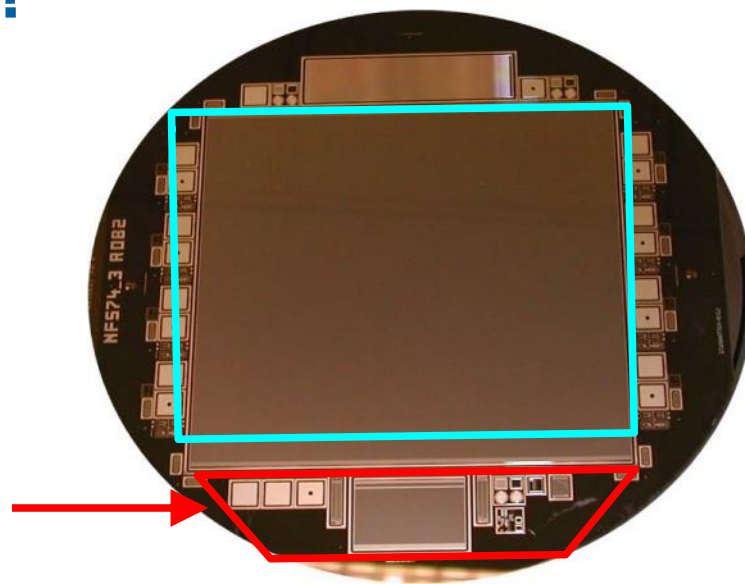
average from C_ac measurement: 354.2 nm

Vendor average: 391.8



What is Process Monitoring?

- Each wafer hosts additional test structures around main detector
- “standard” set of test structures is called “half moon” (because of its shape)
- Test structures used to determine one parameter per structure
- Assuming that sensor and test structures behave identically
- Some parameters are not accessible on main detector (e.g. flatband voltage of MOS), but important for proper operation

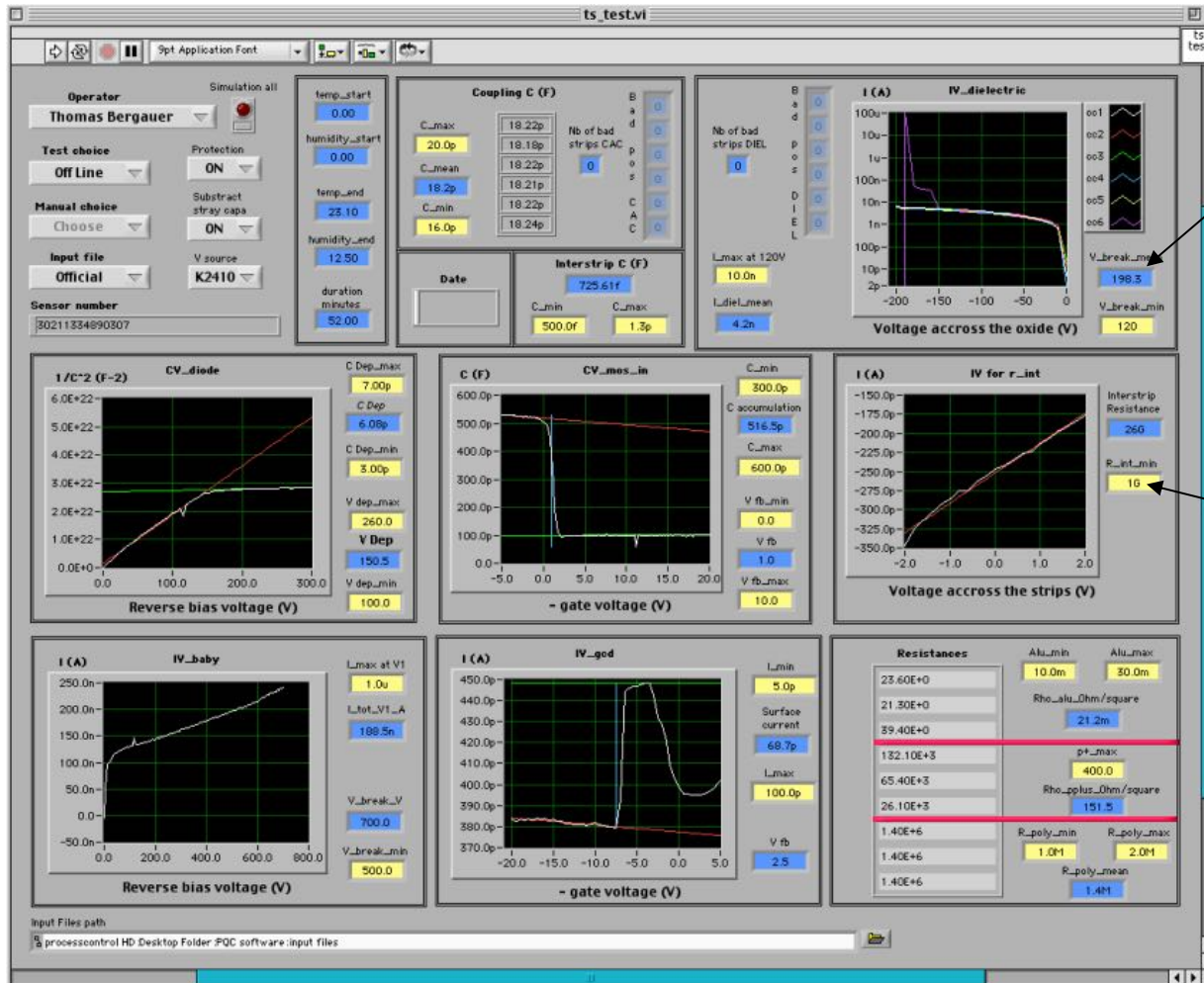


Test Structures Description

- **TS-CAP:**
 - Coupling capacitance C_{AC} to determine oxide thickness
 - IV-Curve: breakthrough voltage of oxide
- **Sheet:**
 - Aluminium resistivity
 - p⁺-impant resistivity
 - Polysilicon resistivity
- **GCD:**
 - **Gate Controlled Diode**
 - IV-Curve to determine surface current $I_{surface}$
 - Characterize Si-SiO₂ interface
- **CAP-TS-AC:**
 - Inter-strip capacitance C_{int}
- **Baby-Sensor:**
 - IV-Curve for dark current
 - Breakthrough
- **CAP-TS-DC:**
 - Inter-strip Resistance R_{int}
- **Diode:**
 - CV-Curve to determine depletion voltage $V_{depletion}$
 - Calculate resistivity of silicon bulk
- **MOS:**
 - CV-Curve to extract flatband voltage $V_{flatband}$ to characterize fixed oxide charges
 - For thick interstrip oxide (MOS1)
 - For thin readout oxide (MOS2)



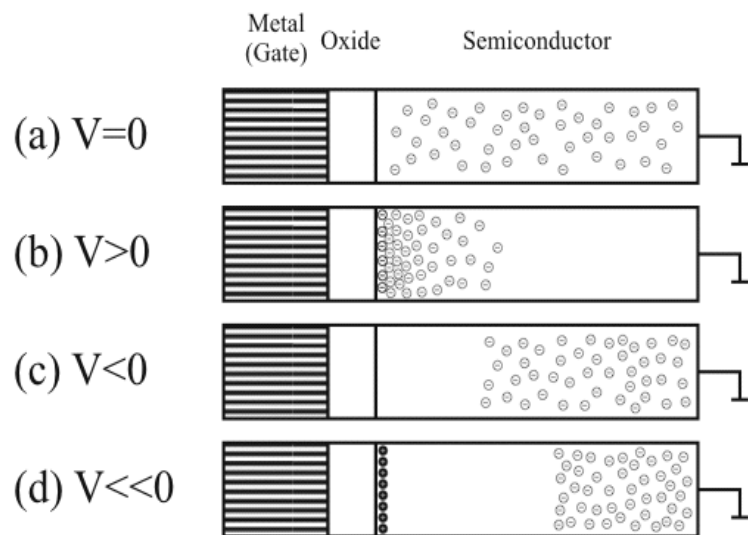
Fully automated Labview Software



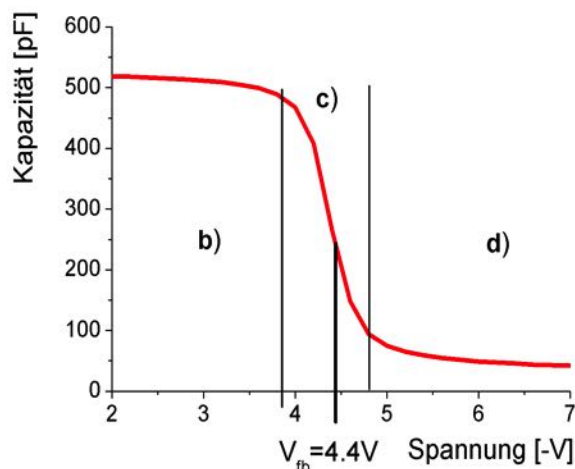
Blue Fields:
Obtained results extracted from graph by linear fits (red/green lines)

Yellow Fields:
Limits and cuts for qualification

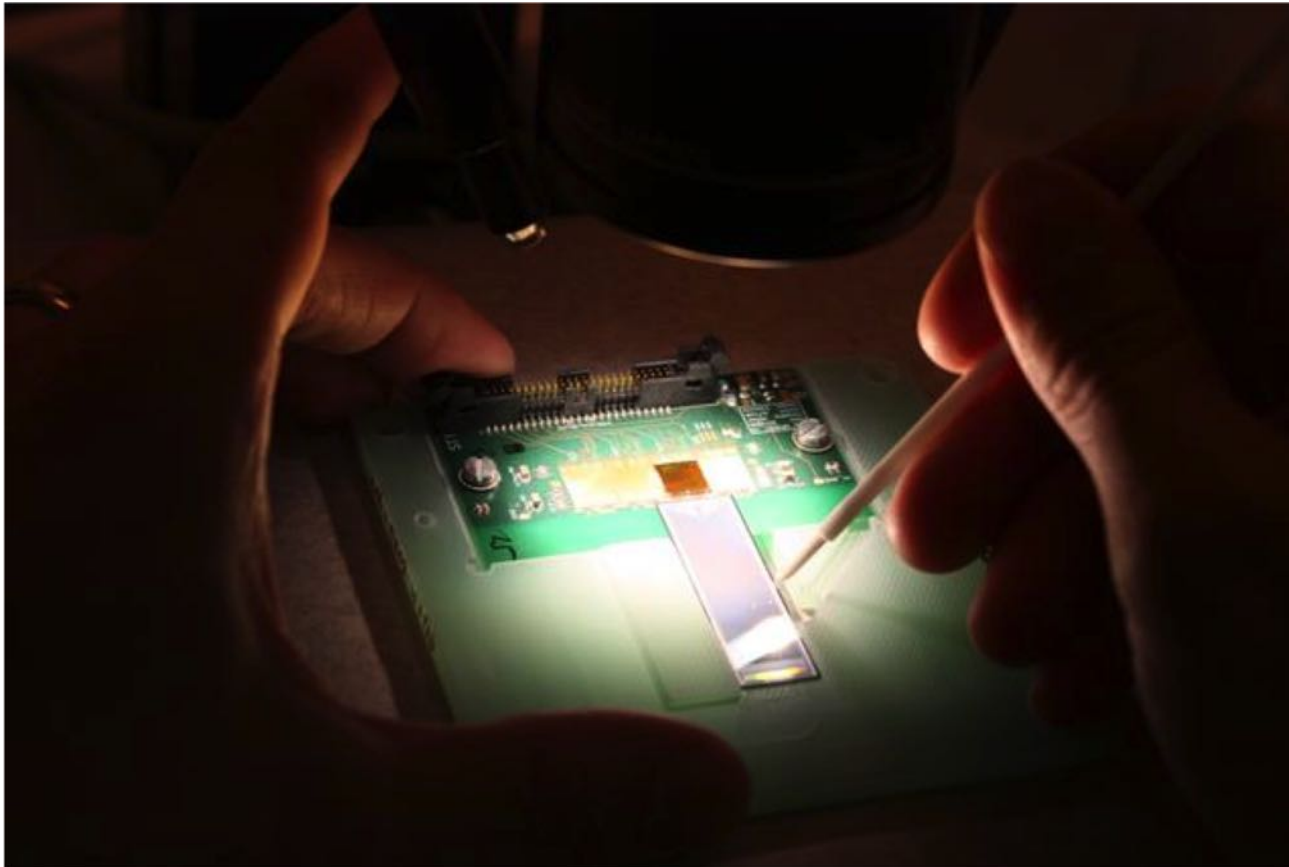
Example measurement: CV on MOS



- Metal Oxide Semiconductor
- Used to determine
 - fixed oxide charges by measuring so-called *flat-band voltage*
 - *Oxide thickness*
- Measurement by taking capacitance vs. voltage
 - $V_{\text{flatband}} = 0$
(Ideal oxide without any charges)
 - Accumulation layer
 - Depletion
 - Inversion



MODULES

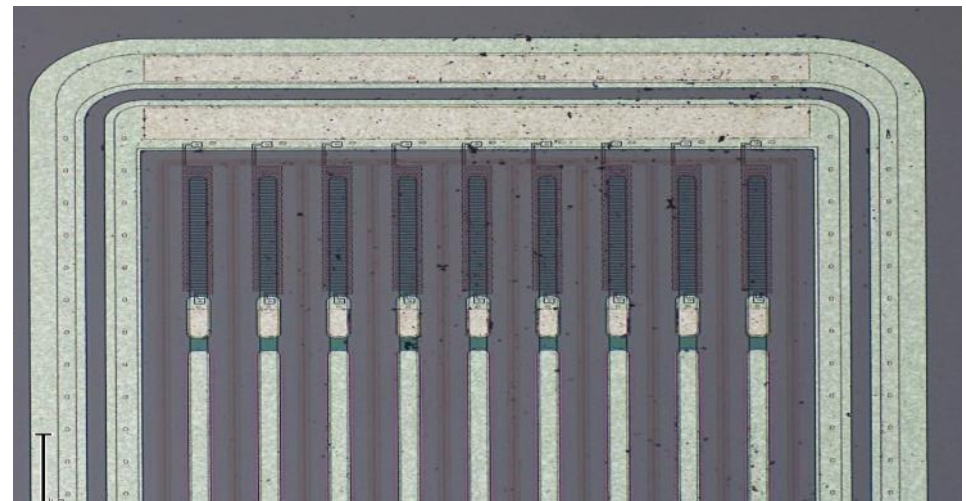


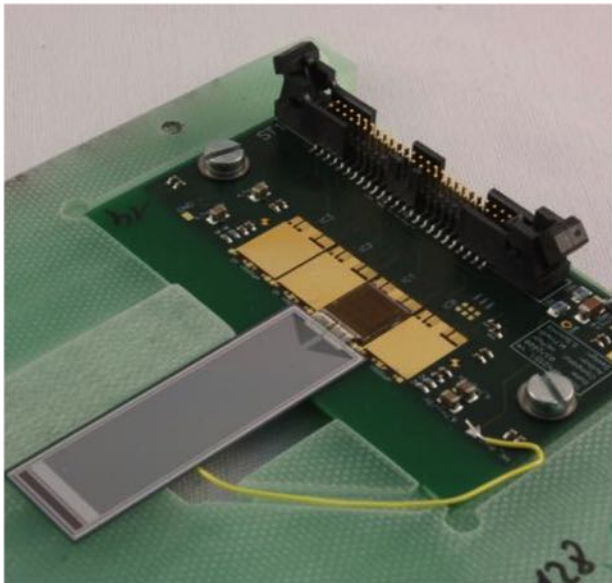
Module Construction

Connecting a bare sensor with a readout chip onto a mechanical support structure

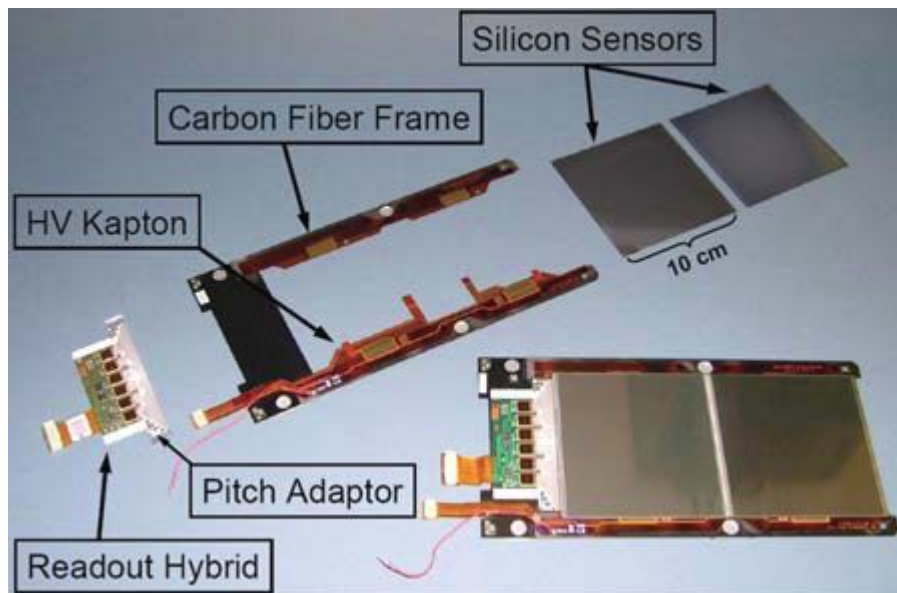
Detector Modules

- A detector module consists of
 - Front-end hybrid containing readout chips (CMS: APV25)
 - Pitch adapter
 - Silicon Sensor
 - frame/support
- Wire bonding for connections





Basic Element of the Tracker: Module

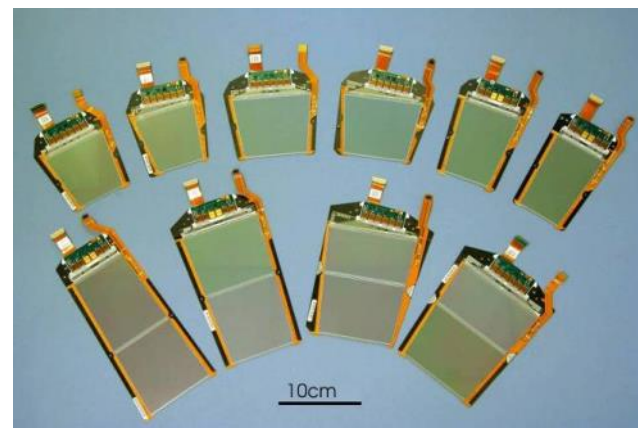


Components:

- Carbon fiber/graphite frame
- Kapton flex circuit for HV supply
- Front End Hybrid housing readout chip
- Pitch Adaptor
- One or two silicon sensors

Total:

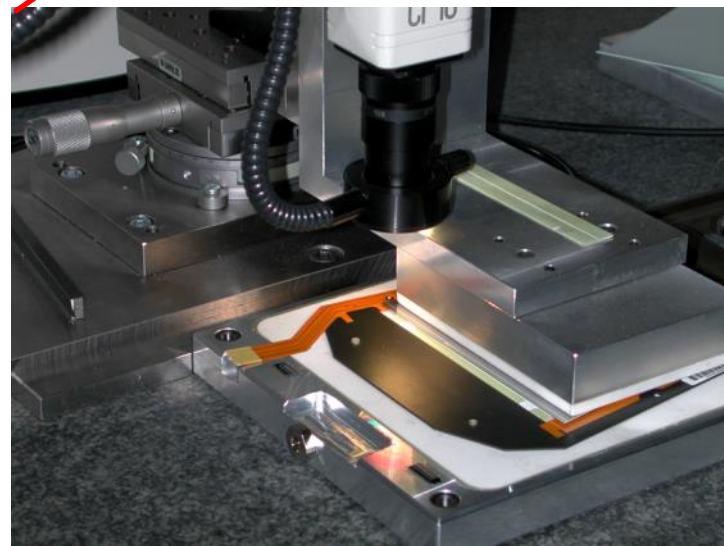
- 29 module designs
- 16 sensor designs
- 12 hybrid designs



Module Assembly

Module assembly for CMS was manual process in Vienna:

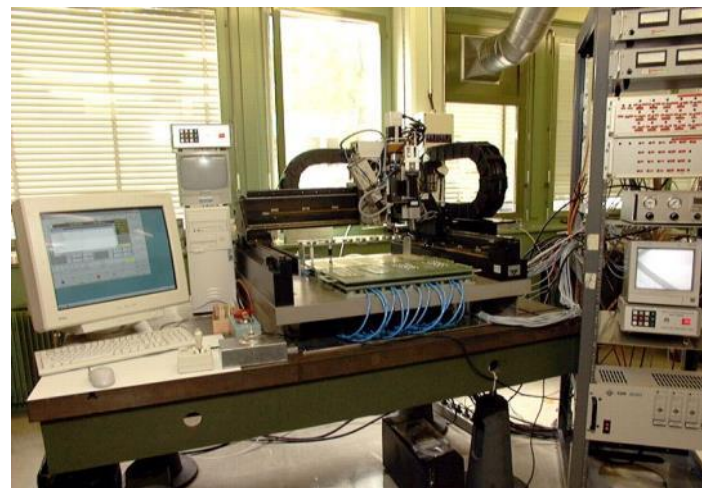
- CF frame was fixed with vacuum support
- Glue dispensed
- Sensor put onto frame using gantry positioning system
- Glue curing
- Using 3D coordinate measurement machine for measurement of assembly precision (<10 micron)
- Throughput: 4 modules per day



Automatic Module Assembly

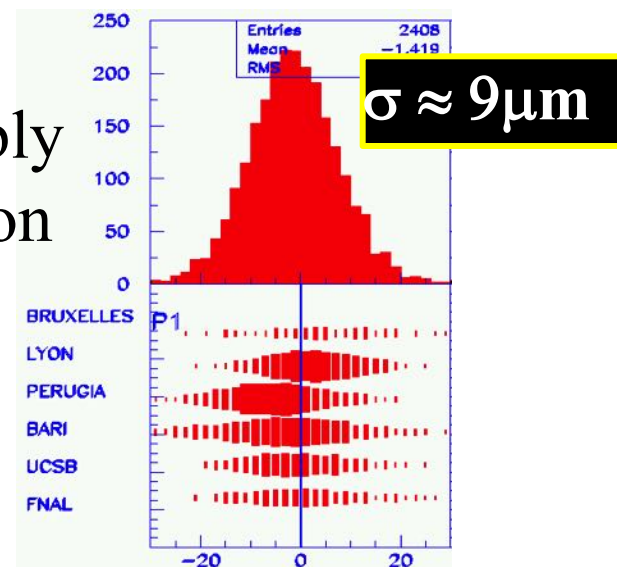
Robotic assembly system which:

1. Apply glue on frame
2. Place hybrid onto frame
3. Place sensor onto frame
4. Optical measurement of placement precision
5. Glue curing
6. Second measurement of alignment precision



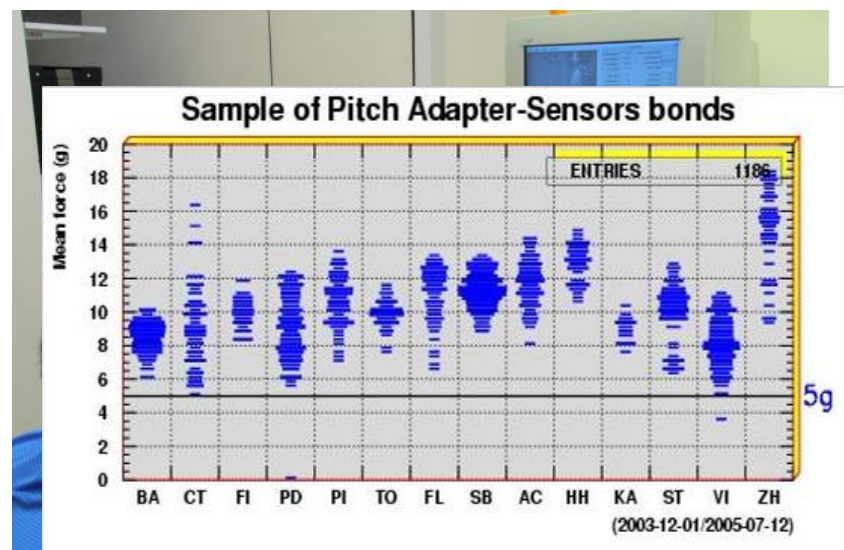
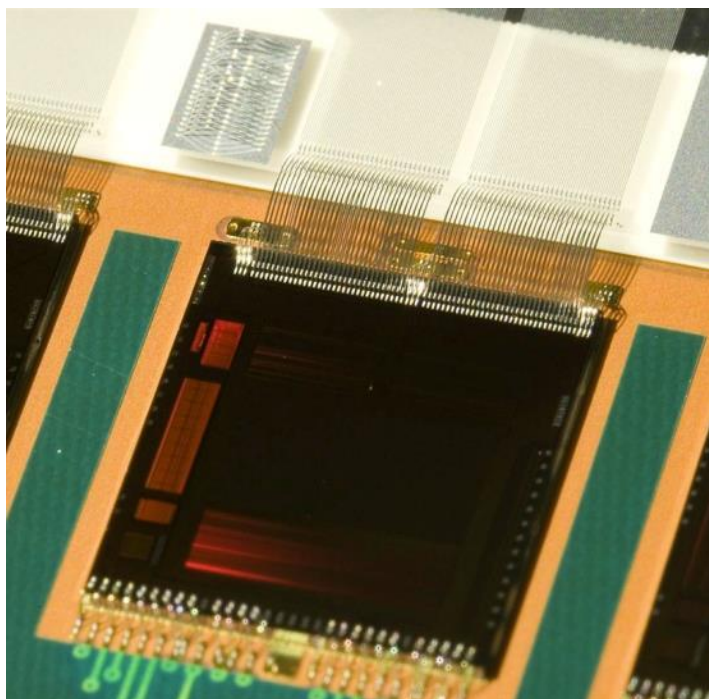
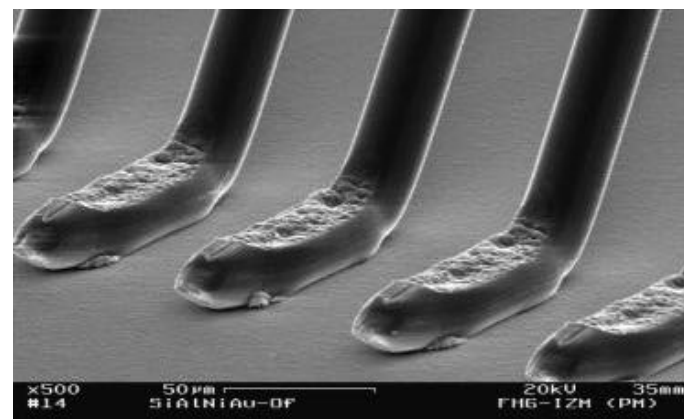
Displacement data entered in TrackerDB and used for correction during track reconstruction (more precise: as starting point of track-based alignment)

Assembly precision



Wire bonding

- Ultrasonic welding technique
- 25 micron bond wire of Al-Si-alloy
- Pull-tests to verify bond quality

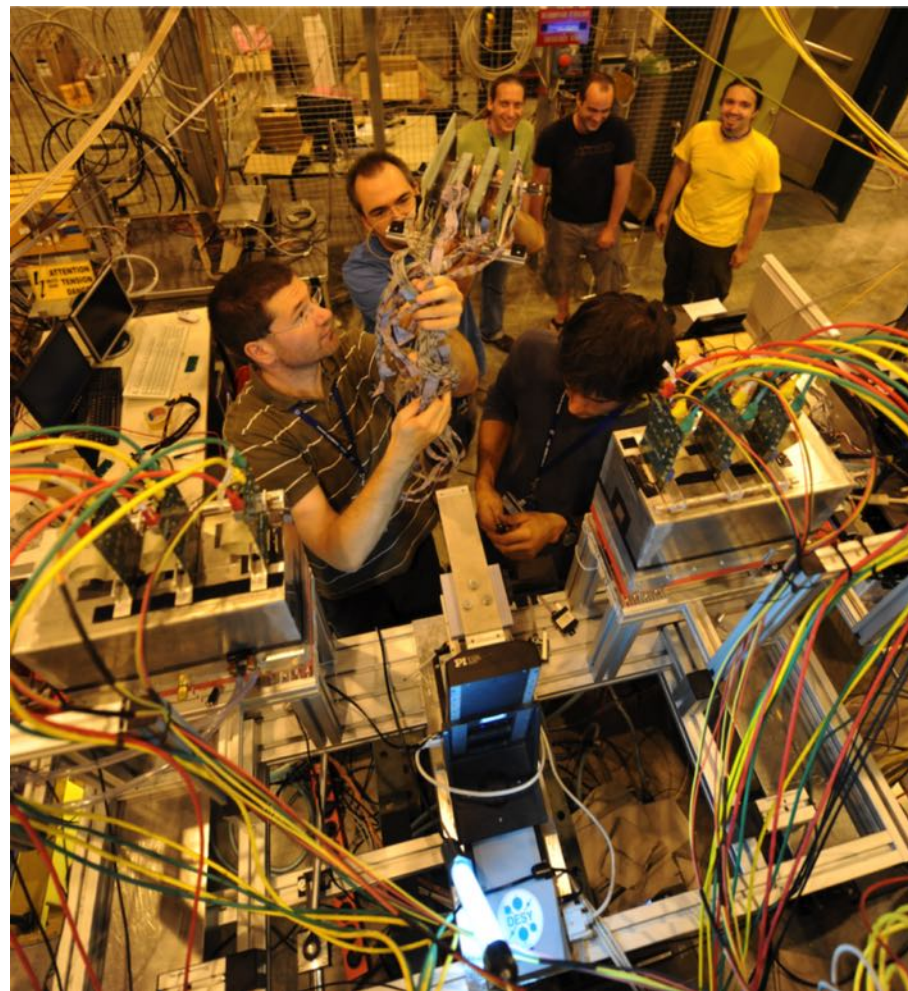


BEAM TESTS

Purpose of beam tests

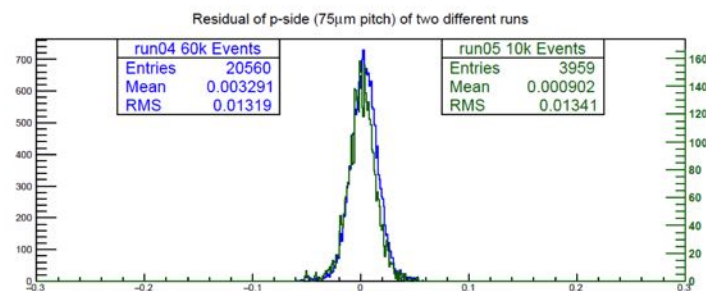
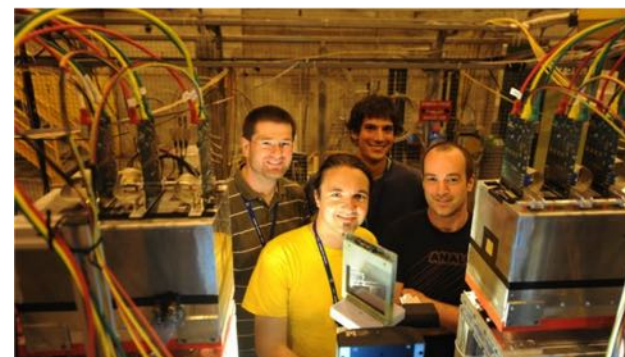
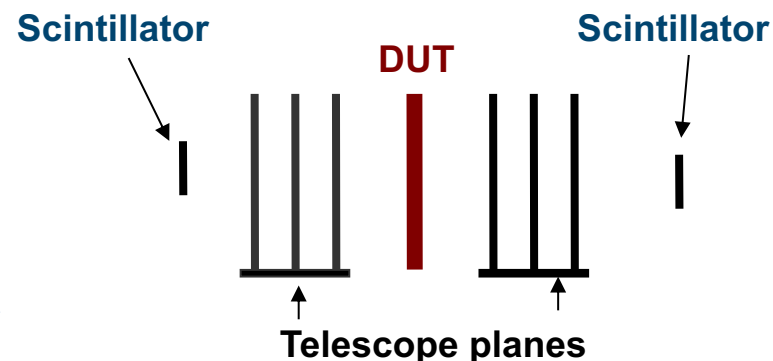
Realistic test of detector plus readout system. Results are:

- **SNR** (could also be obtained with radioactive source on lab test bench)
- **Residuals/resolution** studies only with high-energy beam
 - Multiple scattering at low energy does not allow such measurements
 - Beam telescope needed
- Also realistic test of
 - Cooling system
 - slow control
 - Mechanical stages
 - Data Acquisition



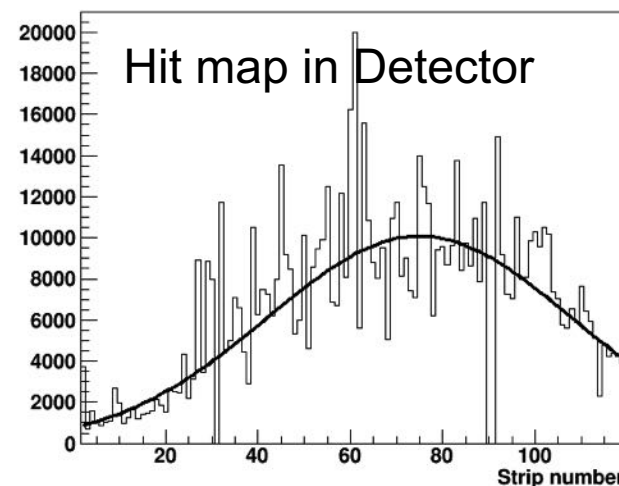
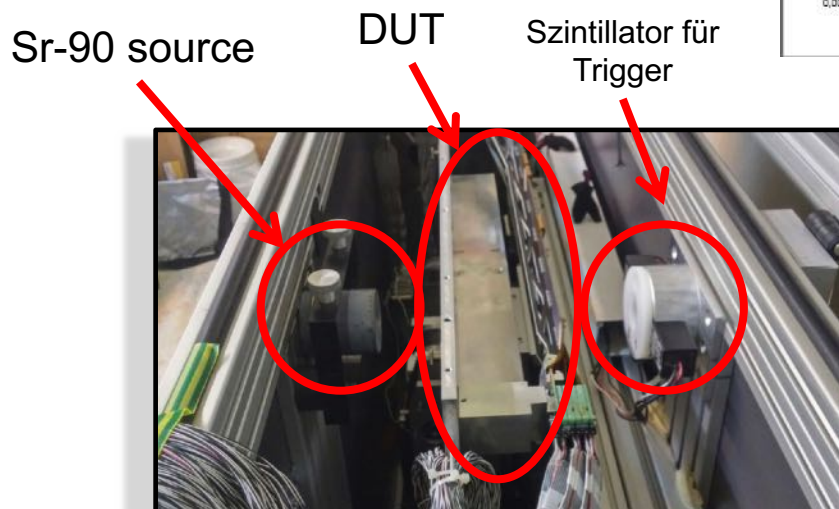
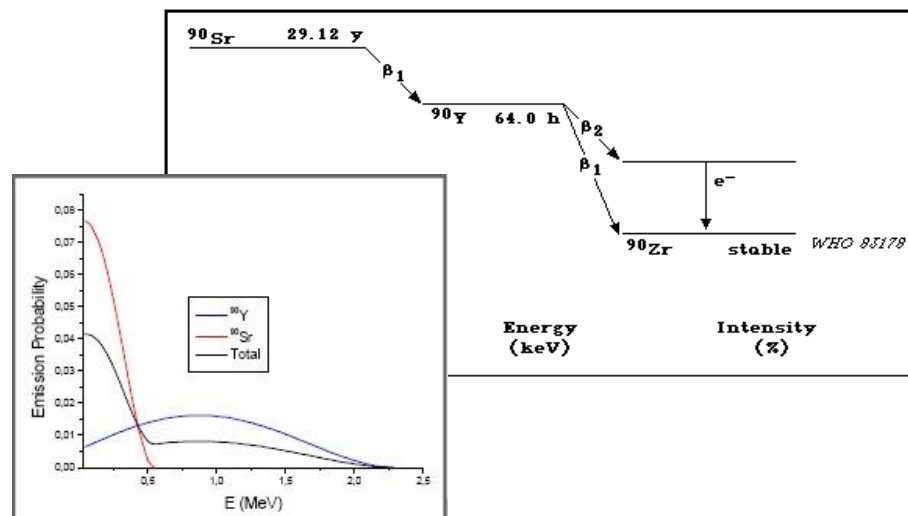
Beam Telescope

- Beam telescope consists of
 - several planes of high-resolution particle detectors (e.g. Si pixel detectors)
 - Scintillators for triggering
- Device under Test (DUT) is placed in center of telescope planes
- It is used for determination of high-precision particle tracks and interpolation of hit position on DUT plane
 - Difference between DUT hit and hit projected by track gives resolution of detector (residual distribution)
 - Only works with high-energetic particle beams where multiple scattering can be neglected
- Result: residual plot (difference between estimated and true hit).
 - RMS of distribution gives resolution of detector



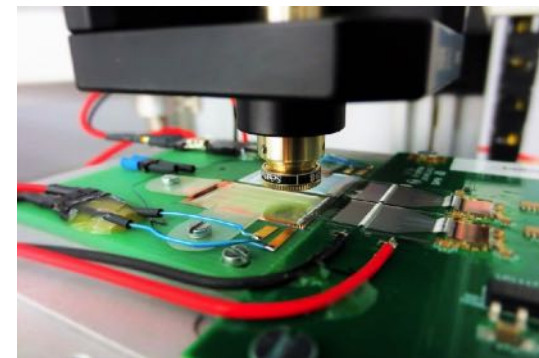
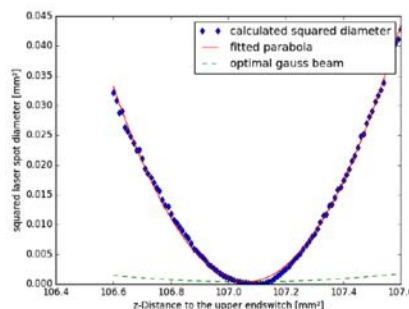
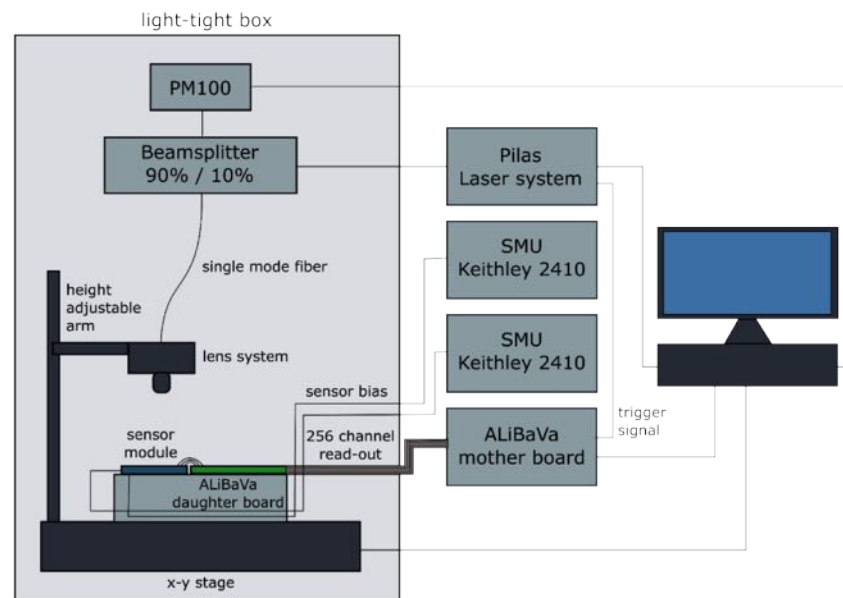
Lab setup using radioactive sources

- Typical source for high-energetic electrons: Strontium-90
 - Electrons with energy up to 2 MeV
 - Test of one plane only due to multiple scattering effects
 - Scintillator detector behind DUT for triggering purposes



Lab setup using laser

- Laser also generates signal in detector → can be used alternatively to particle beam or radioactive sources
- Laser penetration depth:
 - ~1mm for IR laser (1060nm)
→ charge generation in whole bulk
 - ~1 μ m for red laser (630nm)
→ charge generation on surface only
- Advantages:
 - Laser is focused, position is well defined
 - No radioactive source needed
- Disadvantages:
 - Reflections on metal
 - Difficult focusing (IR invisible)
→ sharp edge focussing method



THE END.